Reviews of Geophysics®

Key Points:
- Many tipping elements have uncertain thresholds, which could be crossed this century if human emissions and impacts remain unabated
- Many tipping elements significant to global climate may exhibit slower onset behavior, responding to climate forcing over a century or more
- Emissions pathways and climate model uncertainties may dominate over tipping elements in determining overall multi-century warming

Correspondence to:
S. Wang,
seaver@thebreakthrough.org

Author Contributions:
Conceptualization: Seaver Wang, Zeke Hausfather
Data curation: Seaver Wang, Merritt Turetsky
Formal analysis: Seaver Wang
Methodology: Seaver Wang, Liana O. Anderson, Merritt Turetsky, William R. Boos, Zeke Hausfather
Software: Seaver Wang
Supervision: Seaver Wang, Zeke Hausfather
Visualization: Seaver Wang, John D. Kessler, Julienne C. Stroeve, William R. Boos, Zeke Hausfather
Writing – original draft: Seaver Wang, Adrianna Foster, Elizabeth A. Lenz, John D. Kessler, Julienne C. Stroeve, Liana O. Anderson, Merritt Turetsky, Richard Betts, Sijia Zou, Wei Liu, William R. Boos, Zeke Hausfather
Writing – review & editing: Seaver Wang, Adrianna Foster, Elizabeth A. Lenz, John D. Kessler, Julienne C. Stroeve, Liana O. Anderson, Merritt Turetsky, Richard Betts, Sijia Zou, Wei Liu, William R. Boos, Zeke Hausfather

Mechanisms and Impacts of Earth System Tipping Elements

Seaver Wang[1] [iD], **Adrianna Foster[2]** [iD], **Elizabeth A. Lenz[3]**, **John D. Kessler[4]** [iD], **Julienne C. Stroeve[5,6,7]** [iD], **Liana O. Anderson[8]** [iD], **Merritt Turetsky[9]**, **Richard Betts[10,11]** [iD], **Sijia Zou[12]** [iD], **Wei Liu[13]** [iD], **William R. Boos[14]** [iD], and **Zeke Hausfather[15,16]**

[1]The Breakthrough Institute, Berkeley, CA, USA, [2]Climate and Global Dynamics Laboratory, National Center for Atmospheric Research, Boulder, CO, USA, [3]University of Hawaiʻi Sea Grant College Program, University of Hawaiʻi at Mānoa, Honolulu, HI, USA, [4]Department of Earth & Environmental Sciences, University of Rochester, Rochester, NY, USA, [5]Centre for Earth Observation Science, University of Manitoba, Winnipeg, MB, Canada, [6]Department of Earth Sciences, University College London, London, UK, [7]National Snow and Ice Data Center, University of Colorado, Boulder, CO, USA, [8]National Center for Monitoring and Early Warning of Natural Disasters (CEMADEN), São José dos Campos, Brazil, [9]Department of Ecology and Evolutionary Biology, Institute of Arctic and Alpine Research, University of Colorado Boulder, Boulder, CO, USA, [10]Met Office, Exeter, UK, [11]Global Systems Institute, University of Exeter, Exeter, UK, [12]State Key Laboratory of Marine Environmental Science, College of Ocean and Earth Sciences, Xiamen University, Xiamen, China, [13]Department of Earth and Planetary Sciences, University of California Riverside, Riverside, CA, USA, [14]Department of Earth and Planetary Science, University of California, Berkeley, CA, USA, [15]Berkeley Earth, Berkeley, CA, USA, [16]Stripe, South San Francisco, CA, USA

Abstract Tipping elements are components of the Earth system which may respond nonlinearly to anthropogenic climate change by transitioning toward substantially different long-term states upon passing key thresholds or "tipping points." In some cases, such changes could produce additional greenhouse gas emissions or radiative forcing that could compound global warming. Improved understanding of tipping elements is important for predicting future climate risks and their impacts. Here we review mechanisms, predictions, impacts, and knowledge gaps associated with 10 notable Earth system components proposed to be tipping elements. We evaluate which tipping elements are approaching critical thresholds and whether shifts may manifest rapidly or over longer timescales. Some tipping elements have a higher risk of crossing tipping points under middle-of-the-road emissions pathways and will possibly affect major ecosystems, climate patterns, and/or carbon cycling within the 21st century. However, literature assessing different emissions scenarios indicates a strong potential to reduce impacts associated with many tipping elements through climate change mitigation. The studies synthesized in our review suggest most tipping elements do not possess the potential for abrupt future change within years, and some proposed tipping elements may not exhibit tipping behavior, rather responding more predictably and directly to the magnitude of forcing. Nevertheless, uncertainties remain associated with many tipping elements, highlighting an acute need for further research and modeling to better constrain risks.

Plain Language Summary In recent years, discussions of climate change have shown growing interest in "tipping elements" of the Earth system, also imprecisely referred to as "tipping points." This refers to Earth system components like the tropical rainforests of Amazonia or the Greenland and Antarctic ice sheets which may exhibit large-scale, long-term changes upon reaching critical global warming, greenhouse gas, or other thresholds. Once such thresholds are passed, some tipping elements could in turn produce additional greenhouse gas emissions or change the Earth's energy balance in ways that moderately reinforce warming. In this review, we summarize the current state of scientific knowledge on 10 systems that some have referred to as potential tipping elements of the climate system. We describe the mechanisms important to each system, highlight the response of these systems to climate change so far, and explain the dynamics of potential future changes that these systems could undergo in response to further climate change. Overall, even considering remaining scientific uncertainties, tipping elements will influence future climate change and may involve major impacts on ecosystems, climate patterns, and the carbon cycle starting later this century. Aggressive efforts to stabilize climate change could significantly reduce such impacts.

1. Introduction

Global climate change will intensify over the 21st century if ongoing human emissions of greenhouse gases and human impacts on terrestrial and marine ecosystems remain unabated (Peters et al., 2020; Raftery et al., 2017). In assessments of impacts associated with climate change, increasing focus is centering around "tipping elements"—components of the Earth system that could potentially undergo state shifts triggered at some level of climate forcing by modest levels of additional forcing that exceed critical thresholds or "tipping points" (Armstrong McKay et al., 2022). Examples of large-scale state shifts associated with tipping elements include ecosystem changes, shifts in the frequency or intensity of extreme events, or the atmospheric release of large carbon stocks (Lenton et al., 2008). Research literature and public discourse have at times incorrectly referred to tipping elements as "climate tipping points." Tipping elements of the Earth system could drive significant additional biodiversity loss, alter the distributions of major ecological biomes, compound greenhouse gas emissions and radiative forcing, and produce important consequences for human society via climate impacts such as sea-level rise and severe weather events.

Natural archives provide some evidence for such dynamics during past periods of Earth's history. Reconstructions of past climate show sharp transitions in Earth system components that may suggest rapid shifts to new states over uncertain timeframes (Dakos et al., 2008). Paleoclimate records provide compelling evidence for relatively sudden shifts in the stability of ice sheets and ocean circulation systems on timescales perhaps as short as centuries, that produced major effects on global climate (Brovkin et al., 2021). Paleoevidence also indicates large past releases of carbon to the ocean-atmosphere system on potentially multi-century to multi-millennial timescales, such as at the start of the Paleocene-Eocene thermal maximum 55.5 million years ago (G. J. Bowen et al., 2015). High-latitude tipping elements including ice sheets, boreal forests, and permafrost experienced large-scale changes during the Last Interglacial 129,000–116,000 years ago (Z. A. Thomas et al., 2020).

Discussion of "tipping elements" and "tipping points" in the context of earth and climate science research increased sharply in the mid-2000s (Kopp et al., 2016) with influential work (Lenton & Schellnhuber, 2007; Lenton et al., 2008) proposing formal definitions for tipping elements and calling attention to a number of Earth system components as potential examples. Tipping elements have since become an increasing focus of research and discussion for example, (Armstrong McKay et al., 2022; Cai et al., 2016; Kriegler et al., 2009; Lenton, 2011, 2012). Various classes of tipping elements have been proposed, including classic bifurcations, noise-induced tipping caused by a combination of forcing and natural variability, and "rate-dependent" tipping caused by a high rate of change in a control parameter (Ashwin et al., 2012). Some researchers have also proposed that such tipping elements could dynamically interact with one another, producing compounding effects that could ultimately commit the climate system to several degrees of additional long-term warming beyond the level resulting from anthropogenic factors alone (Steffen et al., 2018), and researchers have since continued to develop tipping cascade theory (Dekker et al., 2018; Lenton et al., 2019; Rocha et al., 2018; Wunderling et al., 2021). Exceeding warming thresholds that could trigger such a cascade has been proposed to carry the potential to alter the long-term climate trajectory of the earth on geologic timescales (Lenton et al., 2019; Steffen et al., 2018). Many tipping behaviors may also be difficult to halt, reverse, mitigate, or adapt to after state shifts have begun in response to climate perturbations.

Evaluating the projected impacts associated with tipping elements of the climate system and their potential interactions has proven challenging for the earth science community. Most of the most frequently cited tipping elements, such as permafrost carbon release (Miner et al., 2022), disruption of the Atlantic Meridional Overturning Circulation (AMOC) (Lynch-Stieglitz, 2017), degradation and deforestation of the Amazon rainforest (Nobre et al., 2016), and large-scale ecosystem shifts within the northern circumpolar boreal forest (Scheffer, Hirota, et al., 2012), involve highly complex physical and biological systems, competing feedbacks in response to climate change, and large uncertainties. Many of these systems are poorly resolved by the current generation of climate models or omitted altogether, making tipping elements—alongside carbon cycle feedbacks—an important source of ambiguity regarding climate predictions and global climate sensitivity.

Definitions of what constitutes a tipping element have varied somewhat in the scientific literature regarding whether tipping behavior is necessarily irreversible, fast-acting once activated, or triggered at a precise threshold. Inconsistency in terminology can produce confusion, particularly regarding the timescales over which climate mechanisms act. As outlined by Kopp et al. (2016), a "tipping point," as invoked in socioeconomic contexts prior

to the term's adoption by climate researchers, referred to a key threshold beyond which a small change could trigger a rapid shift between substantially different system states. In introducing the term in an earth science context (Lenton et al., 2008), interpreted "climate tipping points" as referring more generally to large state shifts in components of the climate system resulting from relatively small forcings, including examples anticipated to take place over longer time scales of centuries or more. This latter, broader definition has become standard within contemporary discussions of tipping points in the earth science community (Armstrong McKay et al., 2022; Lenton et al., 2019; Steffen et al., 2018). Tipping elements therefore do not refer solely to systems capable of exhibiting rapid change within years or decades.

Remarking on the varied terminology employed by current literature, Kopp et al. (2016) identified the need to resolve confusion through improved terminology, proposing the term "tipping elements" to refer to any Earth system components capable of committed nonlinear shifts between states—rapid or gradual—resulting from small changes in climate forcing. Meanwhile, "critical thresholds" refer to the precise level of forcing required to trigger committed system changes. The term "tipping points" would then refer strictly to critical thresholds beyond which tipping elements undergo more rapid state shifts, with little temporal lag separating commitment and realization. However, different authors have alternatively used "tipping points" to refer to critical thresholds for tipping elements that undergo both slow versus abrupt response to threshold transgression, and have proposed spatial and impact-based criteria for classifying an Earth system component as a tipping element, for example, (Armstrong McKay et al., 2022).

This review largely adopts the convention proposed by Kopp et al. (2016) to maximize clarity, characterizing systems as "tipping elements" based on the above definition. Meanwhile, "Non-tipping elements" refer to systems that do not exhibit tipping behavior by committing to new system states after crossing critical thresholds in climate forcing. Non-tipping elements may adopt an effectively continuous range of incrementally different stable states in response to small changes in forcing, at least within reasonable bounds of the physical system. Non-tipping elements would also include monostable systems with a single stable state regardless of the forcing applied. Kopp et al. (2016) further distinguished between tipping elements that show little time lag between the transgression of a critical threshold and the system's subsequent response, versus systems that exhibit considerable lag. With human policy planning timescales in mind, we characterize tipping behaviors as abrupt (time lag of less than two decades between threshold transgression and system response), fast (time lag of several decades), or slow (time lag of a century or longer) throughout this review. We employ the term "tipping point" to refer only to critical thresholds for tipping elements capable of abrupt or fast changes. Further, we use the term "irreversible" to refer only to changes that cannot be halted or returned to the original state on timescales of less than hundreds of years. In contrast, a "reversible" process can undergo more rapid reversion to the original system state in under a century under the right conditions. Note that the terms "tipping elements" and "non-tipping elements" in and of themselves do not imply whether changes are reversible or irreversible.

Given the high importance of tipping elements for informing future risk assessments and determining optimal societal actions, a firmer understanding of potentially abrupt or fast tipping elements and how they may interact holds the potential to greatly benefit assessment of climate risks. This review contributes by synthesizing the latest research on a number of the most frequently discussed candidate tipping elements. Evaluation of the risks posed by tipping elements requires considering their timescales of action, climate impacts, and important uncertainties surrounding triggering thresholds and associated factors.

This review explores each of these aspects for 10 global and regional candidate tipping elements (Figure 1). Our selection considered Earth system components based on a balance of several criteria: (a) strong evidence for or active ongoing debate regarding the risk of tipping behavior, (b) high potential impacts upon climate system feedbacks or ecosystems in the event that a committed change occurs, (c) particularly intense discussion of a system in the context of tipping elements even if said system is not thought to be subject to tipping behavior. We used the list of tipping elements examined in Lenton et al. (2008) and Steffen et al. (2018) as a starting point, adding or removing tipping elements based on these criteria. The selected candidate tipping elements include weakening of the Atlantic Meridional Overturning Circulation (Section 2.1), release of methane from marine methane hydrate deposits (Section 2.2), loss of major ice sheets (Section 2.3), permafrost carbon release (Section 2.4), boreal forest ecosystem shifts (Section 2.5), disruption of tropical monsoons (Section 2.6), stratocumulus cloud deck breakup (Section 2.7), die-off of shallow tropical coral reefs (Section 3.1), Amazon rainforest dieback (Section 3.2), and loss of summer Arctic sea ice (Section 3.3).
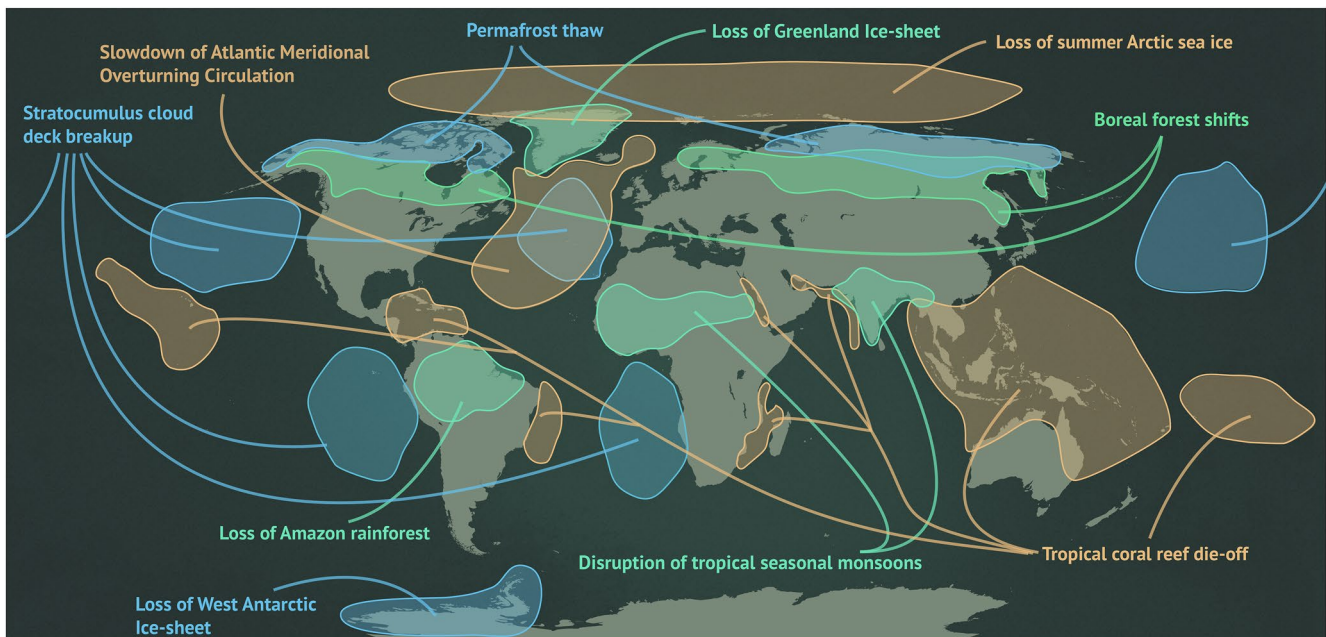
Figure 1. Approximate global geography of the candidate tipping elements covered in this review. Note that boundaries are simplified for visual presentation and do not capture heterogeneity or full spatial extent, such as the complete distribution of shallow tropical coral reefs or of areas with high coverage by marine stratocumulus cloud decks. Marine methane hydrate deposits are omitted for visual simplicity, but are widely distributed along ocean continental margins and are more sensitive to warming in regions with shallow depths and higher warming rates such as the Arctic Ocean, although the Arctic also contains deeper hydrate deposits more protected from destabilization. Figure adapted with permission from McSweeney (2020). Colors are informally assigned for ease of visual interpretation.

We also evaluate scientific discussion of the likelihood of "tipping cascades" in which multiple tipping elements might interact, potentially producing substantial further cumulative global warming. We summarize and quantify the potential future impacts of tipping elements on global temperature and greenhouse gas levels by leveraging a simple climate model (FaIR) (Millar et al., 2017; C. Smith et al., 2017) that was extensively used in developing the assessed warming projections in the IPCC AR6 (J.-Y. Lee et al., 2021) and effectively reproduces the performance of the latest generation of Earth system models (CMIP6) for global mean surface temperature projections (Schwarber et al., 2019). We find the additional global mean surface temperature increase over the 21st century with the inclusion of tipping elements to be around ∼0.21°C (low: 0.10°C, high: 0.36°C) in the high-emissions SSP5-8.5 scenario. We furthermore assess the tipping elements that we consider the highest-risk mechanisms in terms of driving more significant, imminent changes to major ecosystems, global carbon cycling, or climate and circulation patterns.

2. Global Candidate Tipping Elements

2.1. Slowdown or Collapse of the Atlantic Meridional Overturning Circulation (AMOC)

2.1.1. Background

The global Meridional Overturning Circulation (MOC), previously referred to as the thermohaline circulation, is a critical component of the climate system (Stocker, 2013). In the North Atlantic basin, the Atlantic MOC (AMOC) is characterized by warm, saline waters that move northward in the upper ocean by the Gulf Stream and the North Atlantic Current (Buckley & Marshall, 2016). As they travel north along these pathways, these waters become dense due to a loss of buoyancy to the atmosphere, sinking once they reach a critical density threshold relative to underlying waters and becoming North Atlantic Deep Waters (NADW), which then return southward in the deep ocean (Broecker, 1991).

Due to its circulation structure, the AMOC impacts the northern hemisphere weather and climate by redistributing heat between the low and high latitudes (Bryden et al., 2020; Wunsch, 2005). In addition, the AMOC is shown to play a key role in the uptake and export of anthropogenic carbon (Takahashi et al., 2009), and influence

long-term global patterns of ocean circulation and carbon cycling, with important consequences for global warming and oceanic primary productivity (Menviel et al., 2008; Muglia et al., 2018).

On interannual timescales, AMOC variability is shown to be driven by large-scale wind patterns across the North Atlantic according to observations at 26.5°N (Moat et al., 2020; C. D. Roberts et al., 2013) and model simulations (Biastoch et al., 2008; Zhao & Johns, 2014). Over decadal timescales and beyond, temperature and salinity anomalies exert a stronger influence (Biastoch et al., 2008; Buckley & Marshall, 2016; Buckley et al., 2012).

Ongoing climate change has sparked concerns that this important feature of the ocean circulation could be disrupted by rising water temperatures, melting ice-sheets (Böning et al., 2016; Rahmstorf et al., 2015; Stocker & Schmittner, 1997) and Arctic sea ice (W. Liu & Fedorov, 2022; W. Liu et al., 2019) and enhancing poleward atmospheric moisture transport (Held & Soden, 2006; Zhang et al., 2013). A slowdown or shutdown of the AMOC system would significantly affect regional and global climate patterns (L. C. Jackson et al., 2015; W. Liu et al., 2020). Paleoclimate evidence and numerical simulations have identified AMOC transitions and/or latitudinal shift of deep-water formation sites as potential drivers of multiple large, rapid shifts in past climate, including fast or abrupt changes occurring on timescales as short as a few decades (Alley et al., 2001; Bozbiyik et al., 2011; Brovkin et al., 2021; Clark et al., 2001; Ganopolski & Rahmstorf, 2001; Rahmstorf, 2002). The impacts of past AMOC shifts affected climate globally, significantly altering tropical rainfall patterns and causing heat redistribution between the northern and southern hemispheres (S. Li & Liu, 2022; Masson-Delmotte et al., 2013). Changes to the overturning circulation could also affect the ocean's strength as a heat and carbon sink (X. Chen & Tung, 2018; Fontela et al., 2016; Nielsen et al., 2019; Romanou et al., 2017) and heat redistribution (S. Li & Liu, 2022; W. Liu & Fedorov, 2019; X. Ma et al., 2020).

Model simulations of the abovementioned paleoclimate changes indicate that the AMOC may have transitioned rapidly between different modes during past climates, including potentially bistable behaviors. Driven by the salt-advection feedback (Stommel, 1961), the AMOC could switch between "on" and "off" states under natural perturbations such as deglacial meltwater pulses when the ocean system passes certain tipping points. These sudden AMOC changes have been suggested as one of the main mechanisms explaining the climate changes during the Heinrich events (Broecker et al., 1985; Clark et al., 2002; Rahmstorf, 2002; Stocker, 2000; Stocker & Wright, 1991). The AMOC also may have shifted between different modes during Dansgaard-Oeschger events in response to changes in freshwater forcing, rapidly transitioning to a marginally unstable "warm" mode associated with a northward shift of the deep-water formation site and more intense convection, in contrast to flipping between an "on" and "off" state (Ganopolski & Rahmstorf, 2001). Moreover, based on an AMOC stability indicator (de Vries & Weber, 2005; W. Liu & Liu, 2013; Rahmstorf, 1996), analyses of modern observations suggest that the current AMOC resides in a bi-stable regime. The circulation may be at risk of an eventual collapse under future anthropogenic warming, as the possibility of an AMOC collapse could be downplayed currently by most coupled climate models due largely to a ubiquitous model bias toward AMOC stability (W. Liu et al., 2014, 2017). Models with eddy permitting or resolving oceans seem to serve as a promising approach potentially to reduce or eliminate this AMOC stability bias (L. C. Jackson & Wood, 2018), yet the limited length of simulations (a few centuries) with these models is insufficient to confirm that the AMOC has transitioned to a new equilibrium after perturbations (Hirschi et al., 2020; Weijer et al., 2019).

Increasing temperatures in combination with heightened meltwater fluxes from the Greenland Ice-sheet (GIS), intensification of the hydrological cycle, and enhanced poleward atmospheric moisture transport could warm and freshen surface waters. As the twin factors of temperature and salinity play key roles in the buoyancy loss process responsible for driving the overturning circulation, warming and freshening of surface waters may inhibit the sinking process that drives NADW formation from taking place (Bakker et al., 2016; Drijfhout et al., 2015; Durack et al., 2012; Stocker & Schmittner, 1997). The slowdown of NADW formation may be further reinforced by a positive advective-convective feedback in association with the subpolar gyre circulation, according to coupled climate models (Born et al., 2013, 2016). A reduced NADW formation decreases the density contrasts between the buoyant boundary current and the convective interior, resulting in a weakened baroclinic gyre circulation. The weakened baroclinic gyre and eddy activities cause a salt divergence at the convective site, further inhibiting NADW formation. The coupling between the subpolar gyre circulation and AMOC may even trigger abrupt warming and cooling events that resemble the Dansgaard-Oeschger events without external freshwater forcing (Klockmann et al., 2020), underlining the important role of internal ocean dynamics in determining the AMOC variability. Consequently, the climate and oceanographic research communities are devoting considerable

attention toward determining whether the AMOC is currently weakening and assessing its risk of weakening or collapse in response to future warming beyond a certain threshold.

2.1.2. Evidence for a Weakening AMOC Warrants Concern Given Uncertainties in Response to Climate Change

Assessments of whether the AMOC is weakening or has weakened since the pre-industrial era are complicated by a relative paucity of direct measurements of the AMOC's transport strength. Mathematically, AMOC transport strength is quantified as the total northward component of the zonally integrated volume flux (unit: Sverdrup or Sv, 1 Sv = 10^6 m³/s) along a zonal section with closed boundaries. The first continuous, basin-wide observations of the AMOC transport strength only became available with the installation of the RAPID-MOCHA instrument array at 26.5°N since 2004, where mean AMOC was estimated to be ∼18 Sv (Cunningham et al., 2007; McCarthy et al., 2020). A relatively new monitoring array, OSNAP, was installed in the subpolar North Atlantic at approximately 52°–60°N in 2014 (Lozier et al., 2017, 2019). At 34.5°S, moored arrays SAMBA were deployed in 2009–2010 and since 2013 to understand the overturning variability in the South Atlantic (Kersalé et al., 2018). Consequently, direct measurements of the overturning circulation have only been available for less than 18 years, precluding a robust detection of AMOC's long-term trend.

Other studies seek to reconstruct AMOC variability using hydrographic sections, satellite altimetry measurements and reanalysis products. With five transatlantic sections along 25°N, Bryden et al. (2005) reported a decline of the AMOC transport strength by 30% or 8 Sv between 1957 and 2004. At similar latitude, Frajka-Williams (2015) constructed AMOC transport strength back to the mid-1990s using altimetry and cable measurements and found a slight decrease of the AMOC. The AMOC decline was also simulated at subpolar latitudes in an ocean reanalysis product (L. C. Jackson et al., 2016). Contrastingly, a reconstructed AMOC at a mid-latitude (41°N) was found to exhibit a slight increase since the early 1990s (Willis, 2010). The discrepancy is possibly attributed to the sensitivity of reconstructed AMOC to different calculation and assimilation procedures (Karspeck et al., 2017), as well as the latitudinal dependence of AMOC strength variability (Biastoch et al., 2008; Bingham et al., 2007). Furthermore, estimates of the AMOC state since the 1990s using model-based reanalysis and data from hydrographic sections show considerable interannual to decadal variability, such that a distinct trend in AMOC strength over recent decades remains unclear (Y. Fu et al., 2020; L. C. Jackson et al., 2019).

To assess the impact of anthropogenic climate forcing upon AMOC strength over the past century and beyond, scientists have leveraged proxy data to estimate historical changes in the AMOC. Several proxy-based studies have presented evidence that the AMOC's strength has fallen over time since the onset of the industrial age. One analysis utilized silt grain size in sediment cores taken offshore of North Carolina as a proxy for bottom current flow speed and found that the AMOC's near-bottom flow speed over the past 150 years has been weak relative to the preceding 1,500 years in association with weakened Labrador Sea convection (Thornalley et al., 2018). Uncertainty associated with precisely dating the age of silt grains as well as potential sediment mixing from physical or biological activity represent potential sources of error, although estimates of AMOC strength from sediment cores do demonstrate good agreement with temperature-based reconstructions. Furthermore, this study suggests that an AMOC weakening may have begun early in—if not prior to—the industrial era, and the authors note that the degree to which the potential weakening is associated with anthropogenic forcing remains an open question.

A 20th century AMOC decline is consistent with a number of other proxy records, including the North Atlantic SST and subsurface temperature, and $\delta^{18}O$ in benthic foraminifera (Rahmstorf et al., 2015). The decline accelerated around 1970, followed by a partial recovery in the 1990s before rapidly accelerating again in the mid-2000s (Caesar et al., 2018, 2021; Rahmstorf et al., 2015). A more recent publication used 11 proxies, including reconstructed SST, $\delta^{18}O$, and $\delta^{15}N$ and found a consistent rapid decline of the AMOC in the mid-20th century (Caesar et al., 2021). However, some researchers have pointed to data limitations and uncertainties that could affect this assessment (Kilbourne et al., 2022). SST indices may exhibit an uncertain relationship with historic AMOC variability and change (Menary, Robson, et al., 2020). Strong internal SST variability also influences 20th century trends in AMOC strength, making the anthropogenic signal in AMOC slowing difficult to ascertain at present (Latif et al., 2022).

Such considerations emphasize the importance of interpreting hydrographic and proxy-based reconstructions in concert with direct observational measurements, which, albeit limited in time, have revealed a number of

unprecedented aspects of the AMOC and its variability. For example, observations from the RAPID monitoring array at 26.5°N have revealed significant daily to inter-decadal AMOC variability, with the AMOC transport strength varying from 4 to 35 Sv over 1 year (Srokosz & Bryden, 2015), implying the inadequacy of inferring AMOC changes from hydrographic snapshots that were collected in different seasons and/or years. Additionally, the first several years of OSNAP observations have suggested that the AMOC strength is mostly explained by conversion of warm, salty, upper layer waters into cold, fresh, deep waters in ocean basins east of Greenland, instead of in the Labrador Sea west of Greenland as suggested by historical paradigm (F. Li et al., 2021; Lozier et al., 2019; Menary, Jackson, & Lozier, 2020). The minimal contribution of the Labrador Sea to the AMOC is further attributed to the compensating effects of cold and fresh anomalies on density in the basin's boundary current (Pickart & Spall, 2007; S. Zou et al., 2020), highlighting the equally important role of heat and freshwater flux in determining the AMOC strength.

These results suggest that proxy records for either temperature or salinity alone may not be adequate to reconstruct overturning variability and highlight the importance for climate models to accurately simulate the water mass transformation/formation process, including when, where and how deep waters are produced, mixed, and exported (Heuzé, 2017; Lozier et al., 2019). Refining computations of seawater density and the pressure gradient force in ocean and climate models can also reduce uncertainty in AMOC simulations (L. Ma et al., 2020) Yet at the same time, the strong agreement across such models that AMOC strength is expected to decline under continuing emissions scenarios (Collins et al., 2019; J.-Y. Lee et al., 2021; Menary & Wood, 2018) emphasizes that continued efforts to refine existing models and re-assess risks would be prudent.

Whereas assessments of whether the AMOC is currently weakening remain subject to some uncertainty, the research community stands largely in agreement that a complete collapse of the AMOC in the near term is a low-probability event. The IPCC's Special Report on Oceans and the Cryosphere in a Changing Climate concluded that an AMOC collapse in the 21st century was "very unlikely," with only one of 27 models producing an AMOC collapse by 2100, and even then only under the worst-case RCP8.5 high-emissions scenario (Collins et al., 2019). However, the IPCC AR6 WG1 report revised this assessment of unlikelihood downward to "medium confidence" (Fox-Kemper et al., 2021). Modeling results from a 2016 study concluded that the likelihood of an AMOC collapse under RCP8.5 was 44% by 2290–2300, while AMOC collapse was averted altogether under the RCP4.5 pathway (∼2.5°C warming in 2100) (Bakker et al., 2016). However, current coupled climate models exhibit biases in surface ocean climatology that favor greater AMOC stability (W. Liu et al., 2014). A modeling analysis correcting for these biases and assuming a CO_2 doubling approximately between the RCP4.5 and RCP6.0 scenarios produced an AMOC collapse 300 years after the CO_2 perturbation (W. Liu et al., 2017), emphasizing a need to improve model physics to allow for more realistic AMOC predictions. An analysis of Earth system models uncovered one instance in which the AMOC declines in strength and then collapses during the 21st century (Drijfhout et al., 2015). More recently, early warning indicators for a collapse were identified from a suite of AMOC temperature and salinity indices since the late 1800s, suggesting that the AMOC might be close to a critical transition point from relatively stable conditions to a weakening mode (Boers, 2021). High natural AMOC variability close to the critical threshold could in turn cause initiation of a transition toward a weak AMOC state, a pattern identified in earlier work (Aeberhardt et al., 2000). For historical CMIP5 model simulations, the same indicator only increases in a subset of models, underlining concerns regarding models' ability to predict AMOC transitions (Boers, 2021).

Troublingly, defining particular critical temperature thresholds expected to contribute to committed weakening of the overturning circulation also represents a challenge (Weijer et al., 2019). Hoegh-Guldberg et al. (2018) determined a higher likelihood of more intense weakening for >2°C of warming based on model predictions. Committed loss of the GIS is more likely than not to occur beyond a 2°C warming threshold (Pattyn et al., 2018), with the IPCC expressing medium confidence regarding long-term near-complete loss of Greenland ice for sustained warming of 3°C or more (IPCC, 2021). As loss of significant volumes of Greenland ice carries important implications for buoyancy dynamics in deep water formation regions, the IPCC's assessment of a 2°C threshold seems a plausible lower bound above which the risks of significant weakening of the AMOC increase. A recent paper suggests that even small, incremental changes in freshwater forcing could drive AMOC collapse if the rate of forcing is sufficiently rapid (Lohmann & Ditlevsen, 2021). However, the current ability of models to accurately represent the AMOC and predict its response to climate change remains low, leaving the proximity of today's AMOC to potential critical thresholds uncertain (Weijer et al., 2019).
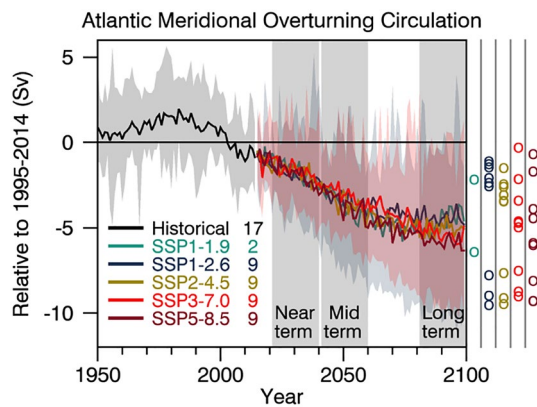
Figure 2. Historical and scenario simulations of maximum annual mean AMOC strength at 26°N in CMIP6 models. Ensemble averages are shown via colored curves, while shaded areas show the 55%–95% ranges for SSP1-2.6 through SSP3-7.0 ensembles. Averaged 2081–2100 anomalies for individual model simulations are shown to the right as open colored circles. The number of model simulations for each group of scenarios is given to the right of the legend. Figure reproduced with permission, originally published as Figure 4.6 in the IPCC AR6 WG1 Ch 4 (J.-Y. Lee et al., 2021).

Some researchers have suggested that the response of the AMOC to climate forcing may depend not only on the transgression of a freshwater forcing threshold but also upon the duration of such an overshoot. Early work by Stocker and Schmittner (1997) suggested that AMOC weakening would depend not only on the magnitude of climate forcing but also the rate of anthropogenic emissions. Ritchie et al. (2021) utilized a simplistic model of the AMOC to illustrate how a sufficiently short overshoot of a climate threshold followed by a rapid reversion in forcing strength to below the critical level could allow the system to return to the original state, while a longer overshoot would lead to committed, long-term system state change. Studies using coupled climate models and ocean box models have shown this varying pattern of recovery for the AMOC in response to freshwater hosing perturbations of different strengths and lengths of time (Alkhayuon et al., 2019; L. C. Jackson & Wood, 2018).

Taken together, the possibility that the overturning circulation is currently weakening and may weaken further with continuing warming is sufficiently backed by recent research to justify the degree of past and ongoing attention devoted to this potential tipping element.

2.1.3. Projected Magnitude of AMOC Weakening and Resulting Impacts

Multimodel analyses of new CMIP6 models have found a potential for stronger decreases in the AMOC over the 21st century than in previous CMIP5 climate models (M. J. Roberts et al., 2020; Weijer et al., 2020), with mean declines of 6–8 Sv by 2100 at 26.5°N and, for the upper-end RCP8.5 scenario, a mean decline of 8 Sv (range of 6–11 Sv) in strength (Weijer et al., 2020). CMIP6 simulations under low to moderate warming scenarios now estimate declines in AMOC strength of a similar magnitude as CMIP5 simulations using the high-end RCP8.5 scenario, which previously produced declines of 5.5 ± 2.7 Sv by 2100 (Figure 2) (Collins et al., 2019; J.-Y. Lee et al., 2021). Overall, the IPCC AR6 WG1 estimated that for end-of-century warming levels of 1.5–2°C, 2–3°C, and 3–5°C, AMOC strength in 2100 would decline by 29%, 32%, and 39% relative to pre-industrial levels (Ranasinghe et al., 2021). At the same time, concern exists that current climate models still overestimate the stability of the AMOC in response to warming, while computational and cost limitations prevent assessment of AMOC stability over millennial timescales using high-resolution ocean models, as reviewed by Weijer et al. (2019).

The consequences of an AMOC collapse would be of substantial magnitude and global in scale. Paleoclimate evidence and numerical simulations have shown that a complete shutdown of the overturning circulation could cause significant North Atlantic cooling (3–8°C), South Atlantic warming (0–3°C), reduced North Atlantic rainfall (−0.5 to −2 mm/d), and a southward shift of the tropical rain belt (by ~10° latitude) (L. C. Jackson et al., 2015; Lynch-Stieglitz, 2017). In contrast to total collapse, however, weakening of the AMOC results in more moderate impacts. Modeling a freshwater-induced reduction in AMOC strength from 16 to 9 Sv yielded North Atlantic subpolar gyre cooling of 2°C (Haarsma et al., 2015). A modeling exercise isolating the climate impacts resulting from a weakening AMOC under future warming produced similar findings, including North Atlantic cooling, shifts in rainfall and atmospheric circulation, and deceleration of Arctic sea ice loss (W. Liu et al., 2020). An analysis of CMIP6 AMOC modeling results found an inverse relationship between modeled historical AMOC strength and global climate sensitivity to greenhouse gas forcing, with models simulating a weaker AMOC exhibiting lower climate sensitivity (Weijer et al., 2020).

Changes in the AMOC may also alter storm tracks and intensities in the North Atlantic (Gastineau et al., 2016) as well as Arctic sea ice patterns (Delworth & Zeng, 2016; W. Liu & Fedorov, 2022; Yeager et al., 2015). Evidence of sea-level changes along parts of the eastern coast of North America linked to AMOC variability (Ezer et al., 2013; Goddard et al., 2015; Little et al., 2019) also suggests that a weakened AMOC may have implications for adaptation to sea-level rise in this region. Climate modeling supports a potential for AMOC weakening to drive accelerated sea-level rise in the North Atlantic basin (Levermann et al., 2005; Yin & Goddard, 2013; Yin et al., 2009) with a follow-up study predicting meaningful regional sea-level impacts even under lower emissions scenarios (Schleussner et al., 2011). Some of the most acute AMOC-induced impacts for human communities

Table 1
Section Summary Box Synthesizing the Forcing Mechanism, Response Behavior, Reversibility, and Classification of AMOC Weakening and Collapse

	Classification	Mechanism	Irreversibility
AMOC weakening/collapse	Tipping element Nonlinear state shift in response to small forcing changes (e.g., Alkhayuon et al., 2019; Drijfhout et al., 2015; Lohmann & Ditlevsen, 2021; Stocker & Schmittner, 1997)	Freshwater and seawater temperature forcing, preventing surface waters from sinking to form deep water	Potentially irreversible Apart from short transgressions of forcing thresholds, may require a century or more to return to original state (e.g., L. C. Jackson & Wood, 2018; J.-Y. Lee et al., 2021; Ritchie et al., 2021)

include substantial potential reductions in rainfall in the Sahel region, negatively impacting crop yields (Defrance et al., 2017). Other global-scale interactions with the Pacific Ocean and the Antarctic remain uncertain but are the subject of continuing research (Collins et al., 2019).

A slowdown of the AMOC is also theorized to potentially contribute to positive carbon cycle feedbacks due to reduced ocean carbon uptake (Joos et al., 1999) and possible wetland methane-related interactions (Parsons et al., 2014). The concern also exists that an AMOC slowdown may interact with other potential tipping elements within the climate system, such as the potential for Amazon forest dieback or the acceleration of ice loss from the West Antarctic Ice-sheet (Brovkin et al., 2021; Dekker et al., 2018; Rocha et al., 2018; Steffen et al., 2018; Wunderling et al., 2021). Particularly given these broader implications, further improvements to our understanding of the AMOC and additional advances in model complexity and computing power will prove crucial for better constraining potential long-term outcomes, both with respect to the AMOC and to the global climate system (Table 1).

2.2. Large-Scale Release of Methane From Destabilization of Marine Methane Hydrate Deposits

2.2.1. Background

Methane (CH_4) is a potent greenhouse gas. The majority of atmospheric methane is biological in origin, often the product of methane-emitting microorganisms undergoing respiration under low or no-oxygen conditions (Dean et al., 2018). Wetlands, inundated rice fields, biomass burning, and gases released from the gastrointestinal tract of ruminant herbivores like cows, for instance, all represent significant fluxes of methane globally. The remainder of atmospheric methane is of fossil origin, released by activities such as oil, gas, and coal extraction and production.

The global warming potential of methane has been revised slightly upwards over the last few decades to a current figure of 83 CO_2-eq (CO_2 equivalents) over a 20-year time horizon (GWP-20), 30 CO_2-eq over a 100-year time horizon (GWP-100), and 10 CO_2-eq over a 500-year horizon (GWP-500) (IPCC, 2021). These time horizons incorporate the differences in the atmospheric lifetimes of CH_4 and CO_2 along with differences in their respective radiative forcing contributions. Note that a 100-year time horizon does not capture the full climate impact of atmospheric CO_2, which produces warming effects that persist for thousands of years.

Estimates of methane fluxes exhibit uncertainty, with emissions estimates for some methane sources differing considerably between "top-down" and "bottom-up" methods (Table 2). "Bottom-up" methods estimate methane fluxes associated with a source using small-scale measurement data, emissions records, and land surface modeling. In contrast, "top-down" methods use observed atmospheric methane measurements and inverse-modeling techniques to attribute fluxes to different sources (Saunois et al., 2020). New research continues to update and refine the global methane budget, with one recent study finding that a proportion of methane emissions previously attributed to natural geological sources are actually of anthropogenic fossil origin, thus reapportioning estimated methane fluxes from these two sources (Hmiel et al., 2020). In the future, the global methane budget will evolve further in response to climate change and human activities, and investigations are currently being conducted into methane emissions from sources that are currently minor or negligible that may increase significantly due to warming. One of the currently minor sources of atmospheric methane with the potential for substantially increased emissions is methane clathrate hydrates.

Significant deposits of methane are currently sequestered in ocean sediments as methane clathrates or methane hydrates, a solid, ice-like form of methane stable at high pressures, low temperatures, and high methane

Table 2
Current Estimates for Sources of Atmospheric Methane in Mt CH$_4$ yr^{-1} Based on Hmiel et al. (2020), Kirschke et al. (2013), Saunois et al. (2020), and Schwietzke et al. (2016)

	Emission rate (Mt CH$_4$ per year)			
Methane source	Kirschke et al. (2013) (bottom-up estimates)	Schwietzke et al. (2016)	Saunois et al. (2020) (full range of reported top-down and bottom-up estimates, 2000–2017)	Hmiel et al. (2020)
Wetlands	217 (177–284)		100–217	
Agriculture*	200 (187–224)		178–246 (includes landfills and waste)	
Fossil fuels*	96 (85–105)	145 ± 23	71–164	177 ± 37
Geological	54 (17–97)	51 ± 20	18–65	1.6
Freshwater	40 (8–73)		117–212	
Biomass burning*	35 (32–39)		22–46	
Wild animals	15 (15–15)		1–3	
Termites	11 (2–22)		3–15	
Methane hydrates	6 (IPCC AR5 estimate for methane hydrate release)		0	
Wildfires*	3 (1–5)		1–5 (estimate from Saunois et al. (2016), possible double-counting with biomass burning)	
Permafrost	1 (0–1)		0–1	

Note. Asterisks denote anthropogenic methane sources, including wildfires. When combining a range of multiple estimates, uncertainties are not shown.

concentration conditions. Hydrate deposits form at these pressure and temperature conditions when methane molecules are encapsulated in water molecule cages. While the methane contained in hydrate deposits may originate from either the microbial decomposition of organic matter in ocean sediments (Claypool & Kvenvolden, 1983) or geological/thermogenic processes (Sassen et al., 1999), all hydrate deposits measured to date have been shown to be devoid of natural radiocarbon, suggesting that clathrate methane carbon is older than 60,000 years (Kessler et al., 2008 and references therein; Sparrow et al., 2022). Typically, water depths of greater than 500 m are necessary to establish the pressure/temperature conditions for marine methane hydrates to form; yet in colder Arctic waters, only around 300 m in depth is required (Ruppel & Kessler, 2017). Combining the higher methane abundances found in continental margin sediments with these depth requirements for hydrate stability indicates that the majority of hydrates are found globally on and at the base of continental slopes (Figure 3) (Ruppel, 2011).

Estimates of total carbon contained within marine methane hydrates globally vary widely, but have largely fallen since the 1990s as important assumptions used in early estimates were overturned by field sampling (Ruppel & Kessler, 2017). Calculations range between ~1,100 Gt C (K. Kretschmer et al., 2015) and ~12,400 Gt C (G. R. Dickens, 2011), with numerous studies converging on values toward the lower end of this range (<2,000 Gt C) (Archer et al., 2009; Boswell & Collett, 2011; Milkov, 2004; Piñero et al., 2013). Nonetheless, even the lower end of this range places hydrates as one of the largest organic carbon reservoirs on Earth (Ruppel & Kessler, 2017). Since much of the methane hydrate carbon pool globally is located at greater depths in bottom ocean sediments with higher pressures, large amounts of this carbon (95%) are not considered to be vulnerable to dissociation or release due to projected ocean warming (K. Kretschmer et al., 2015; Ruppel, 2011). However, methane clathrates can co-occur with free methane trapped below this largely impermeable barrier. Thus in regions vulnerable to dissociation, the quantity of free methane at risk of release may be up to two-thirds higher than the local methane hydrate pool (Hornbach et al., 2004).

2.2.2. Methane Hydrate Dissociation Would Act as a Slow Process With Correspondingly Gradual Impacts

A significant time lag separates atmospheric warming due to climate change and the much longer timescales required for transport and diffusion of heat anomalies into the ocean and sediment. As sediment warming is required for methane hydrate instability, dissociation may not be initiated until centuries to millennia after the requisite warming spike (Archer, 2015; Archer et al., 2009; K. Kretschmer et al., 2015; Ruppel, 2011). For deep ocean sediments, tens of millennia might be required for the methane hydrate zone to begin appreciably
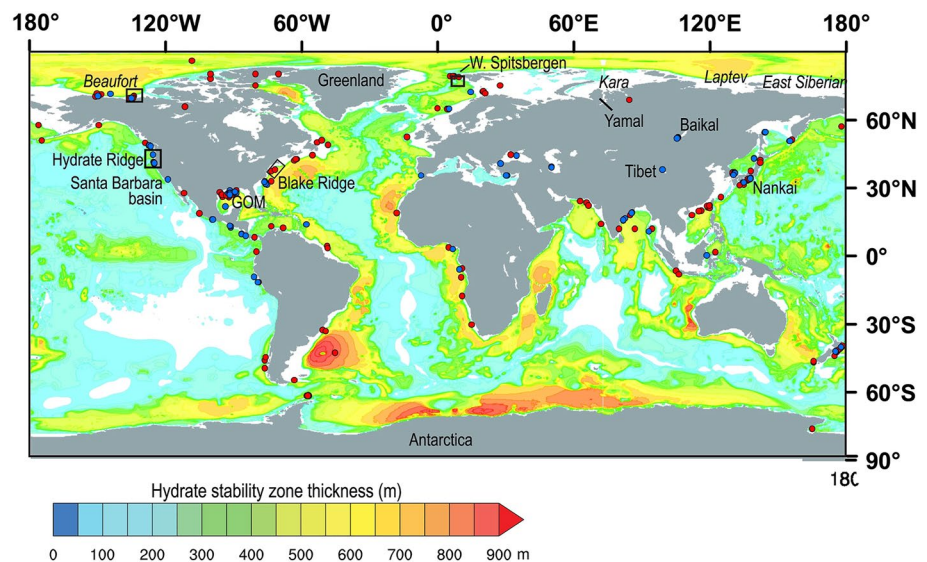
Figure 3. Theoretical gas hydrate stability zone (GHSZ) thickness calculated by K. Kretschmer et al. (2015), with locations of known gas hydrate (recovered samples/photographs; blue circles) and inferred gas hydrate (based on well logs or geophysical markers; red circles). GOM refers to the Gulf of Mexico. Boxes on the Canadian Beaufort margin (Paull et al., 2015), northwest U.S. Pacific margin (Johnson et al., 2015), northern U.S. Atlantic margin (Skarke et al., 2014), and West Spitsbergen margin (Westbrook et al., 2009) show locations where upper continental slope methane seeps may be linked to gas hydrate dissociation processes. Figure reproduced with permission, originally published as Figure 3 in Ruppel and Kessler (2017).

warming, let alone for hydrate to begin dissociating (Archer et al., 2009; Ruppel, 2011). This factor does not preclude eventual significant release of carbon from methane hydrate, but does mean that this climate feedback occurs with a very substantial delay between commitment and realization.

Several further factors probably ensure that future methane release from hydrate deposits will occur as a gradual emission rather than an abrupt spike. In particular, some physical mechanisms will act to greatly slowdown the rate of methane escaping from sediments into the water column. Hydrate dissociation is an endothermic process (heat is consumed by the thaw process), limiting the rate at which methane hydrates respond to increased heat flux (Circone et al., 2005; Gupta et al., 2008; Ruppel & Waite, 2020). Hydrate deposits are also generally expected to thaw first at greater depths in the sediment column. This is because the stability of frozen methane hydrates is greatest at the seafloor, with hydrates becoming less stable as sediment temperature increases with depth due to geothermal heating from below (Zatsepina & Buffett, 1998). Consequently, a "cold trap" exists for destabilized methane migrating upwards to shallower, colder depths in sediment, encouraging reformation of methane hydrate (National Research Council, 2013). Field observations have also found marked declines in methane seepage from marine sediments during the cold season, an effect that may be leading to overestimation of methane release rates calculated only from warm season measurements (Ferré et al., 2020).

Physical barriers can significantly slow or halt the release of methane from sediments. These include factors such as low permeability and barriers to upward migration. At the same time, other physical features such as faults may facilitate the delivery of released methane to the water column (Kessler et al., 2005). Abrupt physical events such as submarine landslides could also destabilize hydrate deposits, although even the large Storegga landslide (8,150 years ago, 5 Gt C released) did not release sufficient methane to measurably affect climate (Archer, 2007). Such considerations as well as significant limitations of the bubble volume threshold and other important parameters considerably limit the ability of models to confidently predict methane release in response to warming.

Current models also do not explicitly account for a number of chemical, physical, and biological methane sinks within both sediments and ocean waters which can greatly limit the atmospheric emission of liberated methane (Figure 4). Microbial activity within the sediment column can consume a significant percentage of escaping methane gas (variable by site but up to 80%–90%) (Reeburgh, 2007). Even for methane that escapes methane oxidation in sediments, a significant fraction dissolves in the overlying waters and is oxidized prior to atmospheric
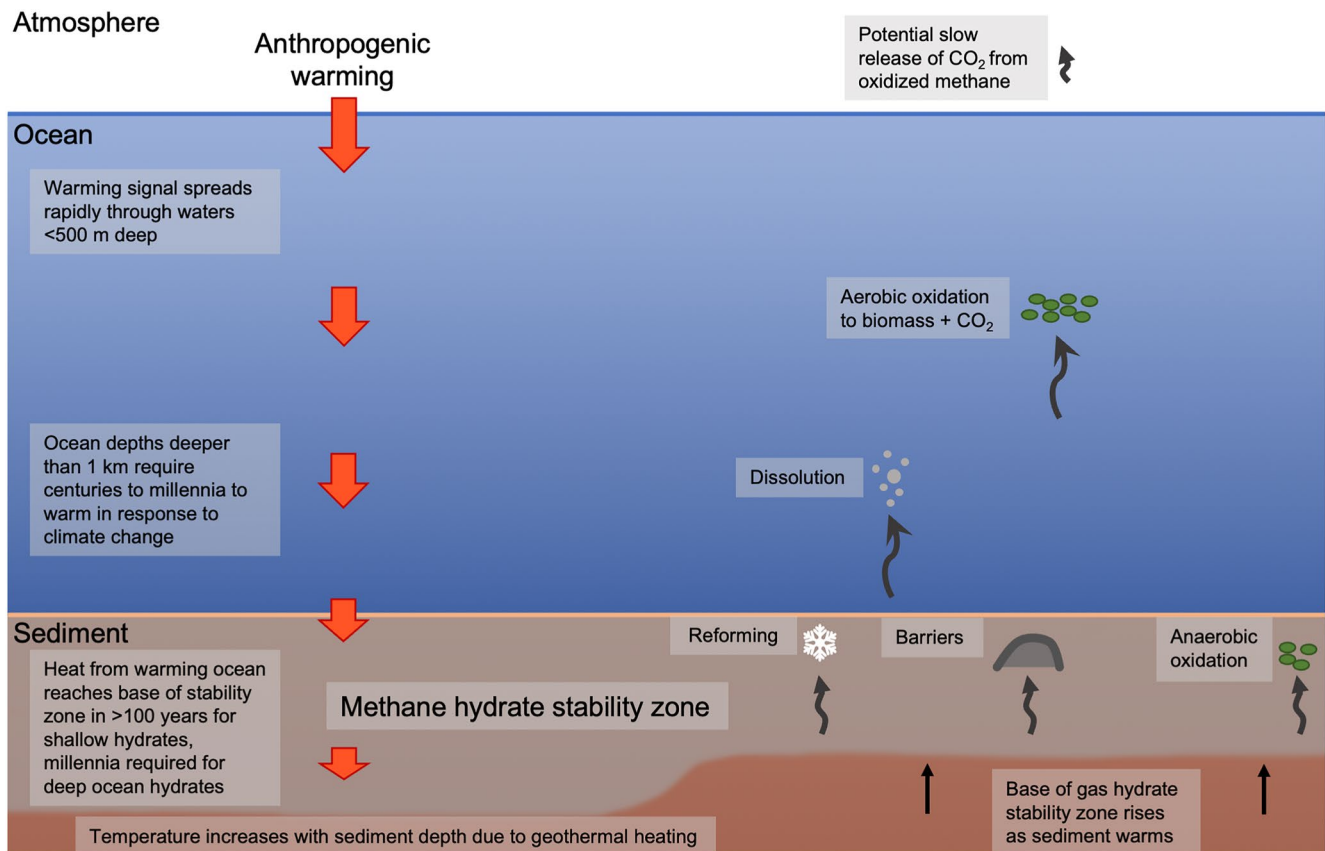
Figure 4. Schematic diagram of marine and sedimentary sources and sinks for methane and carbon dioxide derived from gas hydrate deposits, along with timescales required for warming to reach effective depth within methane hydrate stability zone.

emission. McGinnis et al. (2006) determined that for 50% of methane within a bubble escaping from the seafloor to reach the atmosphere from a depth of 100 m, the bubble must be 2 cm in diameter. However, since methane hydrates are stable below approximately 500 m depth, even larger bubbles are required to drive substantial methane fluxes. B. Wang, Jun et al. (2020) determined that most bubble diameters range from 2 to 6 mm and dissolve prior to any atmospheric emission. Following this physical sink, microbial activity within the water column will also oxidize escaping methane to CO_2 (Chan et al., 2019; Elliott et al., 2011; Kessler et al., 2011; Leonte et al., 2020; Mau et al., 2013; National Research Council, 2013; Valentine et al., 2001). Both the sediment and water column biological sinks would strengthen slightly with increasing temperatures due to the favorable effect of temperature upon microbial metabolic processes, acting as a negative feedback. Transformation of methane to CO_2 represents a tradeoff, where methane emitted to the atmosphere results in larger immediate climate impacts while CO_2 dissolved in seawater may contribute to ocean acidification (Garcia-Tigreros et al., 2021). Also, CO_2 derived from oxidized hydrate methane could be emitted to the atmosphere as a longer-lived greenhouse gas with a lower radiative forcing than methane. However this has not been directly measured and would require this CO_2 to escape the ocean's biological pump. Overall, such factors greatly limit the potential magnitude and rate of any atmospheric release of methane from dissociating hydrates.

Recent modeling analyses suggest that the climate impacts of methane hydrate release would be gradual and moderate if not minimal. For a 3°C level of warming, one study calculated, over multiple millennia, an additional 0.4–0.5°C temperature increase as a result of methane hydrate destabilization of 940 Gt C (Archer et al., 2009). However, the quantity of carbon released in response to warming is overwhelmingly driven by the choice of key parameters governing the migration of methane through seafloor sediment and the water column, making modeled climate impacts highly uncertain. Simulating more limited passage of methane through sediment led to insignificant quantities of released carbon for negligible climate impact. Further, for a total anthropogenic CO_2 forcing of 1,000 Gt C resulting in 2°C of warming, methane hydrate dissolution was modeled to contribute

less than an additional 0.5°C warming even assuming that all dissociated methane reached the atmosphere. In contrast, an assumption of total conversion of escaping methane to CO_2 only extended the duration of 2°C warming, without producing an additional temperature increase (Archer et al., 2009).

A near-term modeling study (K. Kretschmer et al., 2015) determined that relative to current annual anthropogenic methane emissions of 335 Mt C per year, warming caused by doubling CO_2 concentrations over the 21st century would release a total quantity of just 473 Mt of methane from destabilized hydrates over a 100-year period. A more recent modeling analysis similarly concluded that the quantity of methane within shallower, more vulnerable hydrate deposits and the likely rates of dissociation were too low to impart a significant climate impact within the next few centuries under current climate change (Mestdagh et al., 2017). Although the last deglaciation does not represent a perfect analog to contemporary warming, analysis of atmospheric concentrations from 18,000 to 8,000 years ago suggest that release of ancient methane from permafrost and seafloor hydrates in response to past warming events may have been small (<19 Mt CH_4/yr) (Dyonisius et al., 2020; Petrenko et al., 2017). Isotopic analysis of ice core records for three past glacial terminations corroborates the conclusion that methane hydrates have not significantly influenced atmospheric methane concentrations during deglaciations (Bock et al., 2017).

As a result of being positioned at shallower depths and the significant warming currently experienced at high latitudes, Arctic methane hydrate deposits are thought to be the most vulnerable pool of marine methane hydrates to warming-induced thaw. With the Arctic Ocean containing a large percentage of the planet's total continental shelf area, a significant inventory of marine hydrate (~116 Gt C) exists across this basin at relatively modest depths (K. Kretschmer et al., 2015). Consequently, the scientific community is actively assessing the potential for a large-scale thaw and release of methane hydrate from the Arctic seafloor. Early estimates of high rates of methane emissions from hydrate dissociation on the East Siberian Arctic Shelf (Shakhova et al., 2014) have been revised substantially downwards by numerous subsequent studies (Berchet et al., 2016; Thornton et al., 2016, 2020; Tohjima et al., 2020). Present-day marine methane release from Arctic hydrate dissociation is probably primarily of natural origin, resulting from the pressure decrease associated with isostatic uplift following the last glacial maximum, rather than a response to anthropogenic forcing (Wallmann et al., 2018). And in the Beaufort Sea, fossil methane possibly from hydrate emissions was observed in deeper waters but was removed, likely via oxidation, prior to atmospheric emission (Sparrow et al., 2018).

In conclusion, while levels of warming exist beyond which large quantities of methane in hydrate deposits may eventually become destabilized, numerous physical, thermodynamic, chemical, and biological factors combine to substantially limit the rate at which this methane might escape to the atmosphere. For more moderate warming of ~2°C, methane hydrates might well exert a negligible overall impact on atmospheric temperatures. Methane hydrate dissociation would additionally take place on extremely long timescales of millennia, rather than over abrupt or fast timescales that would produce an acute warming spike. This review primarily focuses on the impact of radiative forcing caused by the release of methane and CO_2 to the atmosphere associated with dissociating methane hydrates. It does not comment on other consequences of hydrate dissociation such as ocean acidification or the decrease in the ocean's ability to be a sink of anthropogenic CO_2, both of which are caused by the increase in dissolved CO_2 concentration from methane oxidation. While these processes are less studied than the direct emission of methane to the atmosphere, some preliminary investigations show that it could be important over longer timescales similar to the invasion of anthropogenic CO_2 into surface seawater (Biastoch et al., 2011; Boudreau et al., 2015; Garcia-Tigreros & Kessler, 2018; Garcia-Tigreros et al., 2021). With all of this in mind, in relation to other candidate tipping elements covered within this review, marine methane hydrates represent a relatively lower-impact climate feedback especially for warming in the Anthropocene (Table 3).

2.3. Multi-Meter Sea-Level Rise From Loss of Major Greenland and Antarctic Ice-Sheets

2.3.1. Background

Currently, the majority of sea-level rise (~3.69 mm/yr) (Fox-Kemper et al., 2021; Global Sea Level Budget Group, 2018) is driven by thermal expansion of ocean waters in response to rising temperatures (~1.39 mm/yr) as well as water inputs from melting glaciers (~0.62 mm/yr) outside of the major Greenland and Antarctic ice-sheets (Figure 5). By contrast, since the onset of the industrial era the GIS and the Antarctic Ice-sheet (AIS) have been responsible for relatively little sea-level rise to date, but their contribution to sea-level rise has accelerated over the past four decades (currently ~1.44 mm/yr—(Bamber et al., 2018a; Fox-Kemper et al., 2021; Oppenheimer

Table 3
Section Summary Box Synthesizing the Forcing Mechanism, Response Behavior, Reversibility, and Classification of Marine Methane Hydrate Destabilization

	Classification	Mechanism	Irreversibility
Marine methane hydrate destabilization	Non-tipping element Unclear that nonlinear state shift in hydrate stability occurs in response to small forcing changes (e.g., Archer et al., 2009; K. Kretschmer et al., 2015; Mestdagh et al., 2017; Minshull et al., 2016)	Diffusion of anthropogenic warming into the ocean and marine sediments, leading to hydrate dissociation	Irreversible Reversal of warming in marine sediments and reformation of methane hydrate deposits would require multi-millennium timescales

et al., 2019; The IMBIE Team, 2018)), increasing by more than 700% relative to the 1992–2001 period (Bamber et al., 2018a; Bevis et al., 2019; Fox-Kemper et al., 2021; Meredith et al., 2019; Rignot et al., 2019; The IMBIE Team, 2018). With continued warming, the potential for significant acceleration of sea-level rise due to ice loss from these two regions poses a large threat to coastal regions globally. While thermal expansion and loss of glaciers outside the GIS and AIS cause irreversible sea-level rise on human timescales due to the ocean's gradual response to warming (Ehlert & Zickfeld, 2018; Solomon et al., 2009; Zickfeld et al., 2017) and to shifts away from climate conditions that permit mountain glaciers to persist (Lenaerts et al., 2013), their relative contribution to future sea-level change will diminish (Clark et al., 2016). Mass losses from the Greenland and Antarctic ice sheets are similarly irreversible on these timescales and will contribute the majority of expected future sea-level changes.

The GIS and the AIS would drive multi-meter increases in sea-level over future centuries in the event of significant ice-sheet loss (Pattyn et al., 2018). At the same time, ongoing research into ice-sheet dynamics has focused on concerns that air and sea temperature increases may initiate feedback mechanisms leading to uncontrolled, irreversible ice-sheet collapse over a timescale of centuries (DeConto et al., 2021; Fox-Kemper et al., 2021; Gregory et al., 2020). Climate change is expected to cause large-scale losses from the GIS and the West Antarctic Ice-sheet (WAIS) at lower levels of climate forcing, followed by further Antarctic ice loss as vulnerable basins of the East Antarctic Ice-sheet (EAIS) retreat under higher levels of warming (Fox-Kemper et al., 2021). Given the high concentration of vulnerable human populations and infrastructure in coastal regions worldwide, the risk of crossing critical thresholds for major polar ice-sheets represents a particularly high-priority topic in terms of research, planning, and climate mitigation (Pörtner et al., 2022).

2.3.2. Powerful Feedback Mechanisms Suggest a Real Possibility for Irreversible Ice-Sheet Collapse

Major ice-sheet processes have exerted a dominating influence on sea-levels over the geologic past due to the tremendous quantities of ice contained within the GIS, WAIS, and EAIS. Global sea levels may have been 6–9 m higher than the present day during the Eemian (125,000 years ago, 1°C warmer than present day) (Dutton et al., 2015), although recent research points to uncertainty in sea-level reconstructions (Austermann et al., 2021) and proposes that sea levels in this period may have been lower than previously assumed (Dyer et al., 2021). A reduced EAIS during the Pliocene (5.33–2.58 million years ago, 2–3°C warmer than present day) may have contributed to global sea level rise of 3–12 m, in addition to up to 12 m of sea level contribution from the GIS and WAIS (C. P. Cook et al., 2013). Full loss of the current GIS would raise global mean sea-level by 7.42 ± 0.05 m (Morlighem et al., 2017); collapse of the WAIS would yield a global increase of as much as 5.08 m (mean estimate 3.16 m) (L. Pan et al., 2021; Sun et al., 2020). While the EAIS may only begin to lose significant ice mass for higher thresholds of warming, vulnerable marine-terminating basins of the EAIS contain sufficient mass to potentially raise sea-levels globally by up to 19.2 m (Fretwell et al., 2013).
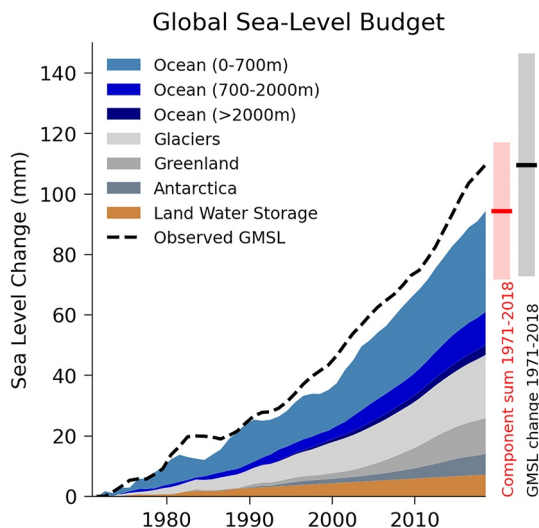

Figure 5. Budget showing changes in components of global mean sea-level rise for 1971–2018. The observed global mean sea-level change from tide gauge reconstructions (1971–1993) and satellite altimeter measurements (1993–2018) is shown for comparison (dashed line) as a 3-year running mean. Closure of the global sea-level budget is indicated to the right (red bar = component sum central estimate; black bar = total sea level central estimate; red or gray sharing = very likely range). Figure adapted with permission, originally published as Cross-Chapter 9.1, Figure 1 in the IPCC AR6 WG1 Chapter 9 (Fox-Kemper et al., 2021).

However, the stability of portions of the EAIS may depend on the integrity of relatively small volumes of ice at the margins of features such as the Wilkes marine ice-sheet, which could impart tipping behavior leading to large-scale ice loss over centuries (Mengel & Levermann, 2014).

The magnitude of future sea-level rise resulting from ice-sheet loss depends on climatic and topographic factors as well as differences in glacier characteristics that may trigger ice-sheet destabilization at different critical temperature thresholds for different ice-sheet regions. Generally, ice basins of the GIS and WAIS are more sensitive to current and projected climate change and are hypothesized to reach key critical thresholds first, while the EAIS region responds more to higher intensities of warming (Golledge et al., 2015; Robinson et al., 2012). This is because temperatures across Antarctica are much lower than in Greenland, greatly reducing surface melt, but the WAIS is more vulnerable to ocean warming. Significant ice loss is already occurring for both the GIS and WAIS in the present day, with an ongoing sea-level rise contribution of 1.44 mm/yr (Bamber et al., 2018a; Fox-Kemper et al., 2021; Oppenheimer et al., 2019; The IMBIE Team, 2018). The EAIS is potentially at a mass balance currently (no net sea-level contribution) (B. Smith et al., 2020) thanks to increased snowfall caused by a warming-induced increase in atmospheric moisture poleward transport, although this balance is subject to considerable temporal variability and uncertainty that do not rule out the possibility of net loss since observations began (Bamber et al., 2018a; Boening et al., 2012; Martin-Español et al., 2017; The IMBIE Team, 2018; Velicogna et al., 2014).

Ongoing field and satellite studies have confirmed or even revised upward earlier findings that vulnerable ice-sheets are already feeling the effects of climate change (Hamlington et al., 2020). Mass loss from Greenland has continued, with the pace of its contribution to sea-level having accelerated over time in recent decades (McMillan et al., 2016). The current total contribution of ice-sheet loss to sea-level rise is following that predicted by upper-end IPCC AR5 emissions scenarios, although this results from a combination of observed surface mass balance losses that have exceeded the range of modeled losses and observed losses via ice dynamics that have fallen largely in the mid-to-lower range of model projections (T. Slater et al., 2020). Recent observational evidence also suggests that the EAIS may be worryingly more vulnerable to ocean heating than assumed previously (Silvano et al., 2016). New research has also pointed to a potentially longer-term natural trend of ice-sheet thinning for parts of the EAIS over the past 300 years, potentially predisposing the region to some vulnerability to future ice loss (W. A. Dickens et al., 2019).

The feedbacks affecting the major ice-sheets and the patterns and timeframes of their physical responses to climate change differ markedly between regions. In contrast to the WAIS, Greenland ice is exposed to higher temperatures and more glaciers terminate on land prior to reaching the sea, particularly to the southwest. Consequently, surface melt in response to rising air temperatures that greatly outpaces new ice-sheet accumulation represents the primary cause of ongoing and projected ice loss for the GIS (Bevis et al., 2019). Surface ablation and snow melt can result in the formation of meltwater pools or exposure of darker ice that reduce surface reflectivity, further intensifying melt through a melt-albedo feedback (MacFerrin et al., 2019; Ryan et al., 2019). Refreezing of meltwater also warms adjacent ice. At the same time, meltwater can percolate through holes and crevasses through to the foot of the glacier, lubricating the glacier where it meets the bedrock and accelerating the speed of ice flow toward the sea (Bell, 2008). Warming glaciers also exhibit lower viscosity, further increasing their rate of flow. As glaciers move seawards, their altitude falls, bringing them into lower, warmer layers of air—another positive feedback known as the melt-elevation feedback or height-mass-balance feedback (Huybrechts & De Wolde, 1999). A recent study using ice core reconstructions to compute early warning signals for committed regional ice loss based on past melt rates and a simple melt-elevation feedback model found evidence that the central-western GIS may currently be close to a critical threshold (Boers & Rypdal, 2021). While approximately half of Greenland ice loss is being driven by such atmospheric effects upon surface mass balance (Enderlin et al., 2014; van den Broeke et al., 2016), marine-terminating Greenland basins are also subject to ocean-driven forcing (Carroll et al., 2016) and such discharge-driven losses remain significant at the scale of the GIS as a whole (Choi et al., 2021; Enderlin et al., 2014). Ocean forcing is a focus of ongoing efforts to improve projections of the GIS's future sea-level contribution (D. A. Slater et al., 2020).

In contrast, marine warming represents the primary driver of Antarctic ice loss. Many sectors of the Antarctic Ice-Sheet are marine-based, sitting on bedrock beneath sea-level and forming ice shelves and marine-terminating ice streams at their margins. Consequently, such marine-based ice is at risk of mass loss from processes that result from oceanic warming (Shepherd et al., 2004) in addition to atmospheric warming (Figure 6) (DeConto
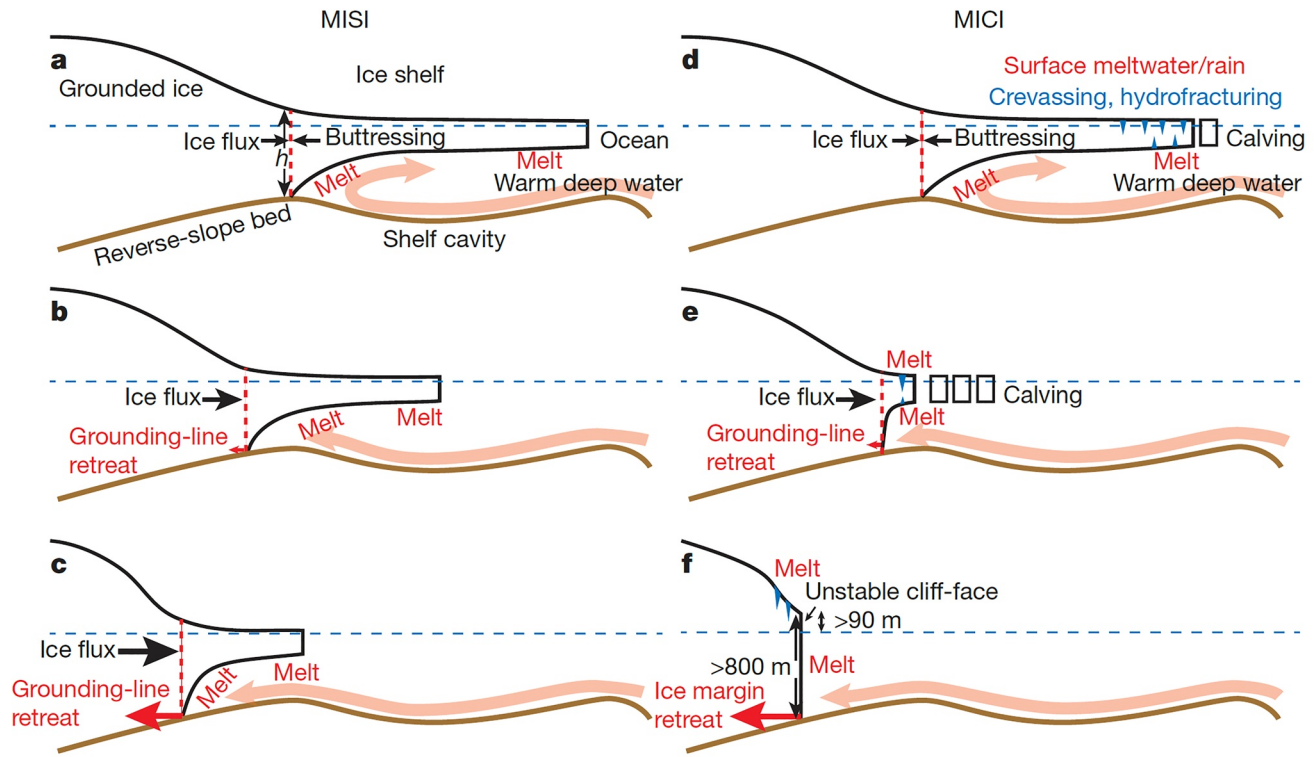
Figure 6. Schematic diagram of the (a–c) marine ice shelf instability (MISI) and (d–f) marine ice cliff instability (MICI) processes. In MISI, (a) ocean and atmospheric heating induce melt proceeding from ice shelf edges, (b) causing the ice-sheet's grounding line to retreat onto reverse-sloping bedrock. (c) As the thickness of the glacier at the grounding line grows, the ice-sheet flows out to sea faster in a positive feedback. According to the MICI hypothesis, (a) loss of ice shelves due to iceberg calving and surface and subsurface heating leads to (b) retreat of the ice-sheet onto reverse-sloping bedrock, followed by (c) exposure of progressively higher ice cliff faces that unstably collapse, driving rapid retreat. Figure originally published in DeConto and Pollard (2016).

et al., 2021). The observational record has established the predominant role of ocean-driven subsurface melt at the base of ice shelves, leading to the thinning and retreat of Antarctic ice shelves (Khazendar et al., 2016; Y. Liu et al., 2015; Wouters et al., 2015). Shifts in atmospheric circulation have driven increased intrusions of warm Circumpolar Deep Water (CDW) onto the continental shelf at depths of several hundred meters, promoting the melt of basal ice (Jenkins et al., 2016). As ice shelves also provide a supportive "buttressing" effect that opposes and slows the rate of ice flux to sea, loss of ice shelf mass itself accelerates flow from ice streams and enhances discharge of ice into the ocean (Schoof, 2007). Ocean warming in combination with physical stresses can also drive an ice shelf damage feedback in which crevasses and fractures develop within the ice shelves buttressing outlet glaciers of the AIS, accelerating ice loss and further exacerbating damage (Lhermitte et al., 2020). Patterns of ice loss have been influenced partly by natural tropical variability (Jenkins et al., 2016) but are also driven by anthropogenically forced shifts in regional winds and positive feedbacks from the ungrounding of ice sheets (P. R. Holland et al., 2019).

Much of the WAIS lies on reverse-sloping (retrograde) bedrock well below sea-level (Le Brocq et al., 2010), leading to greater instability of the WAIS under modest warming scenarios relative to the EAIS (Pattyn et al., 2018). For marine-terminating ice-sheets, the rate at which ice flows out to sea is proportional to the thickness of the glacier at the grounding line, the boundary between grounded and floating ice, where the ice begins to float. On reverse slopes where the bedrock becomes deeper toward the interior of the ice-sheet, the thickness of the ice at the grounding line increases as the grounding line retreats (Schoof, 2007). Warming subsurface waters can increase melt beneath ice shelves, causing inland retreat of the grounding line and thus accelerating the rate at which the glacier flows out to sea. This irreversible positive feedback mechanism for ice loss is called Marine Ice Shelf Instability (MISI) (Shepherd et al., 2004; R. H. Thomas & Bentley, 1978; Weertman, 1974).

While not all vulnerable Antarctic glaciers terminate on reverse slopes or are currently thought to be undergoing MISI today, several major basins are currently retreating thanks to processes that may indicate MISI dynamics

(Favier et al., 2014; Joughin et al., 2014; Rignot et al., 2014). In particular, individual ice shelves on the West Antarctic Peninsula, the Southern Antarctic Peninsula, and in the Bellingshausen and Amundsen seas are experiencing losses via behavior potentially consistent with irreversible onset of MISI (Paolo et al., 2015; Rignot et al., 2014; Wouters et al., 2015). Buttressing from ice shelves and/or low driving stress may permit or restore grounding line stability even on reverse slopes (Gudmundsson, 2013; Gudmundsson et al., 2012; Sergienko & Wingham, 2019). Local bed topography in combination with driving stress and the ice thickness gradient at the grounding line can also produce more complex stability behavior in which stable positions can occur on reverse slopes and vice versa (Sergienko & Wingham, 2022). But as a whole, should grounding lines retreat beyond forward slopes and onto reverse-sloping topography, as is the potential case for many major Antarctic basins (Ross et al., 2012), the process of MISI could begin rapidly accelerating ice loss from many major glaciers.

Warmer waters and thinning and hydrofracturing of ice shelves due to surface melt from atmospheric heating can also cause overlying ice shelves to shrink. In the event that ice shelves disappear completely, a feedback mechanism known as Marine Ice Cliff Instability (MICI) may be triggered at locations where the height of cliffs at an exposed ice-sheet's edge exceeds critical thresholds. Beyond such heights, the shear strength of ice would be insufficient to withstand longitudinal stress at the cliff face, causing progressive collapse via iceberg calving (Bassis & Jacobs, 2013; Bassis & Walker, 2012). Since the thickness of ice shelves often increases further inland, MICI could represent a strong positive feedback for ice-sheet loss. Furthermore, unlike MISI, MICI may be capable of occurring on flat or forward slopes so long as the ice cliff threshold is exceeded (Pollard et al., 2015). A recent modeling study suggests that over realistic timescales of ice shelf collapse, physical stress and deformation are more evenly distributed across the cliff face, potentially preventing widespread cliff failure as proposed by the MICI hypothesis (Clerc et al., 2019). This does assume that the ice shelf is not otherwise damaged or compromised, in which case thresholds for stable cliff heights may decrease significantly (Crawford et al., 2021; DeConto et al., 2021). At the same time, calving from ice cliffs can also cause accumulation of ice mélange, particularly in more constricted bays or fjords, that may act as a source of physical resistance (Bassis et al., 2021; Crawford et al., 2021).

Currently, no evidence indicates that MICI is occurring on Antarctic ice-sheets, and deep uncertainty remains concerning the potential importance of MICI for projections of future ice loss (Fox-Kemper et al., 2021; Meredith et al., 2019). However, seafloor geological evidence from iceberg-keel plow marks suggest that MICI processes may have taken place in Pine Island Bay in West Antarctica between 12,300 and 11,200 years before the present (Wise et al., 2017). Overall, projecting ice-sheet losses from MICI remains a contentious topic given its significant impact on near-term and long-term sea-level rise estimates. While studies incorporating MICI dynamics perform well in reproducing past ice sheet retreat under warm paleoclimates (DeConto et al., 2021), researchers have not yet fully validated the physical mechanisms involved using field observations (Edwards et al., 2019).

Some negative feedbacks may slow rates of Antarctic ice-sheet loss. For instance, increasing ice congestion in restricted bays may provide added resistance, buttressing some glaciers and inhibiting ice movement out to sea (Seneca Lindsey & Dupont, 2012), although this does not protect basins that terminate in the open sea, such as the Thwaites (DeConto et al., 2021). Increased snowfall over portions of Antarctic ice have also provided mass inputs that offset a portion of ice loss (Boening et al., 2012). These factors only represent relatively minor influences upon the ice-sheets' mass balance as a whole. More significantly, uplift of the land surface beneath retreating ice-sheets as the weight of the overlying ice is reduced has been suggested to act much faster than previously assumed, potentially providing a negative feedback (Barletta et al., 2018) and slowing the multicentennial rate of ice loss from the Thwaites (Larour et al., 2019). One modeling study suggests that weaker, more responsive Earth structure beneath the WAIS could delay its collapse by millennia or even prevent full collapse in some RCP2.6 and RCP4.6 scenarios (Coulon et al., 2021). However, uplift may also accelerate meltwater flux into the ocean and further amplify global sea level rise over coming centuries (L. Pan et al., 2021). Further study will help resolve remaining uncertainties regarding the relative importance of such processes. Overall, however, modeling suggests that negative feedbacks will exert limited impact in slowing Antarctic ice sheet retreat (DeConto et al., 2021).

2.3.3. Commitment to Loss of the Greenland and West Antarctic Ice-Sheets Causes Accelerated, Multi-Meter Sea-Level Rise Over Centuries and Millennia

Initiation of irreversible ice-sheet collapse would bring about serious long-term consequences for global sea-level (Figure 7). For summer warming of more than 2°C, the GIS has been assessed as more likely to reach a critical
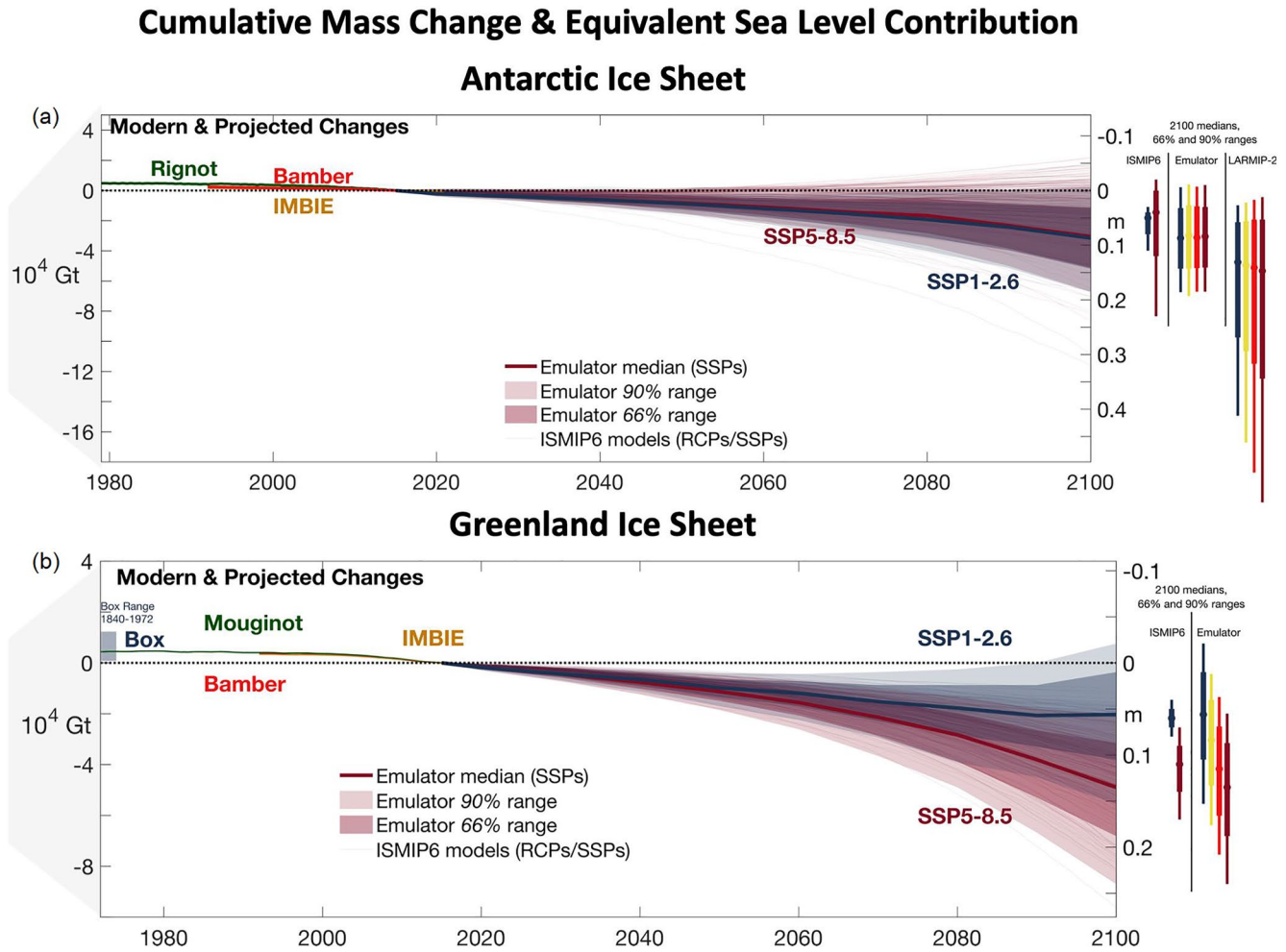
Cumulative Mass Change & Equivalent Sea Level Contribution

Antarctic Ice Sheet

Greenland Ice Sheet

Figure 7. (a) Antarctic Ice sheet cumulative mass loss and sea level equivalent since 2015, with satellite observations shown from 1993 (Bamber et al., 2018b; The IMBIE Team, 2018; WCRP Global Sea Level Budget Group, 2018) and observations from 1979 (Rignot et al., 2019), ISMIP6 projected changes by 2100 under RCP8.5/SSP5-8.5 and RCP2.6/SSP1-2.6 scenarios (thin lines from Edwards et al. (2021), Payne et al. (2021), Seroussi et al. (2020) and 17–83‰, 5–95‰ ranges of the ISMIP6 emulation (shaded line, Edwards et al., 2021)). Right, 17–83‰, 5–95‰ ranges for ISMIP6, emulator, and LARMIP-2 including SMB at 2100. (b) Greenland Ice Sheet cumulative mass loss and sea level equivalent from 1972 (Mouginot et al., 2019) and 1992 (Bamber et al., 2018a; The IMBIE Team, 2020), the estimated mass loss from 1840 (Box & Colgan, 2013; Kjeldsen et al., 2015) indicated with a shaded box and projections from ISMIP6 by 2100 under RCP8.5/SSP5-85 and RCP2.6/SSP1-26 scenarios (thin lines from Edwards et al. (2021), Goelzer et al. (2020), and Payne et al. (2021)) and likely range of the ISMIP6 emulation (shades and bold line (Edwards et al., 2021)) are shown in time. Figure adapted with permission, originally published as Figure 9.18b and Figure 9.17b in the IPCC AR6 WG1 Chapter 9 (Fox-Kemper et al., 2021).

threshold than not (Pattyn et al., 2018). Local annual mean warming of 3°C could be attained this century and would eliminate nearly all Greenland glaciers, raising seas by 7 m over approximately 1,000 years (Gregory et al., 2004; Huybrechts et al., 1991). A recent paper calculating the GIS's geometric instability relative to current climate forcing suggests that the GIS could already be committed to long-term loss of 3.3% ± 0.9% of its present volume irrespective of future 21st century scenarios (Box et al., 2022). Central-western Greenland may already be approaching a critical transition (Boers & Rypdal, 2021). However, a new study coupling an ice-sheet model with an atmospheric general circulation model has produced results suggesting that the Greenland Ice Sheet may not exhibit bistable behavior in response to transgression of a critical threshold (Gregory et al., 2020). While further research is required to verify the existence of intermediate diminished states of the Greenland Ice Sheet under steady-state warmer climates, this result leaves open a possibility that the Greenland Ice Sheet may exhibit stable states between its modern extent and complete loss.

For the Antarctic ice sheet, a modeling analysis utilizing extremely gradual temperature forcing to investigate the system's critical thresholds, stability, and hysteresis (see Rahmstorf & England, 1997) observed strong retreat of

grounding lines in the WAIS for global temperatures 1–2.5°C above pre-industrial, producing a partial collapse of the WAIS at a critical threshold around 2°C warming (Garbe et al., 2020). One recent study assuming a worst-case RCP8.5 emissions scenario and incorporating a strong but uncertain MICI feedbacks (DeConto & Pollard, 2016) calculated a potential for Antarctic ice loss to contribute 34 cm (17–83‰: 20–53 cm) of sea-level rise by 2100, with an eventual sea-level increase of 9.57 m (6.87–13.55 m) by 2300 (DeConto et al., 2021). 3°C pathways result in significant WAIS ice loss within 500 years, driven strongly by intense retreat of the Thwaites Glacier, yielding 15 cm (8–27 cm) of sea-level rise from Antarctica by 2100 and an eventual total Antarctic contribution of 1.54 m (1.04–2.03 m) by 2300 (DeConto et al., 2021). However, modeling of MICI processes is highly sensitive to the chosen regional climate forcing and differences in ice-sheet modeling, as such factors influence surface melt, hydrofracturing, and the subsequent collapse of ice shelves required for the exposure of tall ice cliffs (DeConto et al., 2021). Other modeling results produce somewhat more conservative sea-level changes, with an Antarctic contribution to sea-level rise of 22 cm of sea-level rise by 2100 (5–95‰: 8–43 cm) estimated using pessimistic assumptions under the high-emissions RCP8.5 pathway (Edwards et al., 2021). Newer ISMIP6 ice-sheet model simulations using CMIP5 model outputs have thus far yielded a similar range of −6.7 to 35 cm of sea-level rise contributed by the Antarctic Ice Sheet by 2100 under RCP8.5 (Seroussi et al., 2020). One modeling study assessed a cumulative contribution from Greenland and Antarctica of 25 cm of sea-level rise by 2100 under RCP8.5 (Golledge et al., 2019). Overall, total predicted sea-level rise by 2100 ranges between 0.63 and 1.02 m for SSP5-8.5 (Fox-Kemper et al., 2021).

Projections of future sea-level rise from ice-sheet losses remain highly uncertain, primarily due to limited observational records, incomplete understanding of ice-sheet dynamics, and model limitations. Changes to buttressing from ice shelves and the dependence of mass losses upon sliding and basal friction physics will strongly determine sea level contributions from Antarctica (Gudmundsson et al., 2019; Sun et al., 2020). Such uncertainty poses a significant challenge to governments and planners' attempts to assess adaptation needs (Rasmussen et al., 2020).

Antarctic ice-sheet collapse would be irreversible absent substantial cooling that would permit reformation of buttressing ice shelves. Otherwise, retreat may continue until topography that halts MISI/MICI is reached. Greenland melt is theoretically reversible to a point, with the ice sheet regrowing to its present-day extent upon a modeled restoration of late 20th-century climate provided ice loss is confined to a magnitude of 4.0 m sea-level equivalent or less (Gregory et al., 2020). Beyond this threshold, the retreat of ice from northern Greenland reduces regional snowfall, preventing regrowth of ice around 2.0 m of sea-level equivalent in total. The albedo of the ice sheet's surface remains a relatively uncertain factor in modeling the surface mass balance of the GIS, with higher recovery of the ice sheet possible if surface albedo remains high but improbable at lower albedo values.

Timescales of collapse depend strongly on climate forcing and bed topography and can require centuries to millennia. The Thwaites glacier may already have reached the early stages of irreversible mass loss, although its rate of reduction may remain moderate over the 21st century, with collapse potentially occurring over a period of 200–500 years (Cornford et al., 2015; DeConto et al., 2021; Golledge et al., 2015). EAIS basins may take more than a century under high warming scenarios to begin shedding substantial mass, with multi-meter contributions to sea-level rise over the course of several millennia (Golledge et al., 2015). As mentioned above, reduction of the GIS will likely require a millennium. Yet the weakening of ice shelf buttressing directly accelerates ice flow and discharge independent of MISI and MICI processes, with immediate implications for observed rates of sea-level rise. Consequently, under our current best understanding, Greenland and Antarctic ice-sheet collapse cannot be considered an abrupt or fast phenomenon in which most sea level impacts manifest within decades. Nevertheless, ice-sheet losses may contribute to regional sea level rise under RCP8.5 and worst-case scenarios that reaches 1–2 m for many cities globally by 2100, seriously threatening existing communities and infrastructure (Trisos et al., 2022). Over longer timescales, sustained high rates of global sea-level rise (>1 cm/yr by 2200, with further acceleration to up to a couple centimeters per year beyond) may broadly strain coastal adaptation efforts (Oppenheimer et al., 2019).

At the same time, models indicate that strong climate mitigation may avert significant fractions of potential sea-level rise and prevent ice-sheet collapse across large regions. In several modeling studies the RCP2.6 scenario prevents collapse of the WAIS (Bulthuis et al., 2019; DeConto & Pollard, 2016) and may reduce the Antarctic contribution to global sea level rise by 2100 to 13 cm (Edwards et al., 2021). The IPCC AR6 WG1 suggests total sea-level rise by 2100 under RCP2.6 would range between 0.33 and 0.61 m (Fox-Kemper et al., 2021). However, current global climate efforts are currently not on track for these relatively more optimistic scenarios,

Table 4
Section Summary Box Synthesizing the Forcing Mechanism, Response Behavior, Reversibility, and Classification of Major Mass Loss From the Greenland and West Antarctic Ice Sheet and Shelves

	Classification	Mechanism	Irreversibility
Mass losses from the Greenland and Antarctic ice sheets	Tipping element Large committed mass losses from ice sheets in response to small forcing and stability changes (e.g., Boers & Rypdal, 2021; DeConto et al., 2021; Edwards et al., 2021; Garbe et al., 2020; Gregory et al., 2020; Mengel & Levermann, 2014; Pattyn et al., 2018)	Rising air and ocean temperatures, leading to increased surface melt and loss of ice shelves, which in turn intensify physical feedbacks promoting ice sheet retreat	Irreversible for millennia

with end-of-century warming of ∼3–4°C still quite possible (Hausfather & Peters, 2020). Although significant uncertainties remain regarding the precise temperature thresholds that could trigger ice-sheet collapse, research to date suggests that aggressive climate mitigation could limit risks from ice-sheet instabilities (Table 4).

2.4. Carbon Release From Thawing Permafrost

2.4.1. Background

Permafrost is any earth material (soil, sediment, and rock) that remains below freezing temperatures for at least several consecutive years, with many permafrost regions worldwide having remained predominantly frozen over the past several thousand years. Due to minimal rates of decomposition at such low temperatures, considerable quantities of organic matter have accumulated and become incorporated in these frozen soils. Consequently, sizable stocks of carbon lie contained within permafrost soils globally. Today permafrost covers ∼23 million km^2 of the planet, with $13–18 \times 10^6$ km^2 in the Arctic, 1.06×10^6 km^2 in the Tibetan plateau and $16–21 \times 10^6$ km^2 in subsea and Antarctic regions (Chadburn et al., 2017; Gruber, 2012; Sayedi et al., 2020; D. Zou et al., 2017). Total organic carbon content of all permafrost soils in the Northern Hemisphere is assessed to range between 1,460 and 1,700 Gt C, nearly twice the amount of carbon currently in the atmosphere (Olefeldt et al., 2016; Schuur et al., 2018). On a worldwide scale, permafrost carbon represents about one-third of all global soil carbon within the upper 3m (Jobbágy & Jackson, 2000; Schuur et al., 2015).

Rising global temperatures are causing permafrost to warm (Biskaborn et al., 2019; Lewkowicz & Way, 2019; S. L. Smith et al., 2022). Temperatures at permafrost depths 10–20 m below the ground surface are now 2–3°C higher than those observed 30 years before (Figure 8) (Romanovsky, Isaksen, et al., 2017; Romanovsky, Smith, et al., 2017). While rates of permafrost warming are impacted by surficial geology, landscape morphology, and ground ice content, warming is occurring even in deep permafrost boreholes across the circumpolar region (Biskaborn et al., 2019). Over the past two decades, the climate community has devoted serious efforts toward assessing how widespread permafrost thaw will stimulate organic matter mineralization and C emissions, a potential positive climate feedback termed the permafrost carbon feedback to climate (PCF). This feedback depends on understanding how much of the permafrost carbon pool is vulnerable to mineralization, how quickly permafrost carbon losses will occur over time, whether these emissions will be released as CO_2 versus CH_4, and the degree to which permafrost carbon loss can be offset by increasing plant biomass post-thaw.

In addition to warming, changes in weather patterns such as elevated precipitation rates also influence rates of permafrost thaw (Douglas et al., 2020; Kokelj et al., 2015; Neumann et al., 2019). Observations indicate that high-latitude rainfall may already be increasing (J. E. Walsh et al., 2011), and climate models predict a strong likelihood for future high-latitude precipitation to increase with climate change (Overland et al., 2011). Higher temperatures in permafrost regions could also boost the frequency of wildfires, both releasing significant carbon and transferring heat to deeper permafrost layers (Goetz et al., 2007; J. E. Holloway et al., 2020; Mack et al., 2011; Randerson et al., 2006; X. J. Walker et al., 2019). Strong evidence points toward an increasing frequency and severity of wildfires throughout the arctic and boreal north (Flannigan et al., 2009; Hanes et al., 2019; Kasischke & Turetsky, 2006; McCarty et al., 2020). Field observations have demonstrated that wildfire can act as a major driver of regional permafrost thaw, with fire contributing toward the expansion of thermokarst (areas where thaw leads to ground subsidence) area in western Canada (Gibson et al., 2018), Alaska (Y. Chen et al., 2021), and Siberia (Yanagiya & Furuya, 2020).
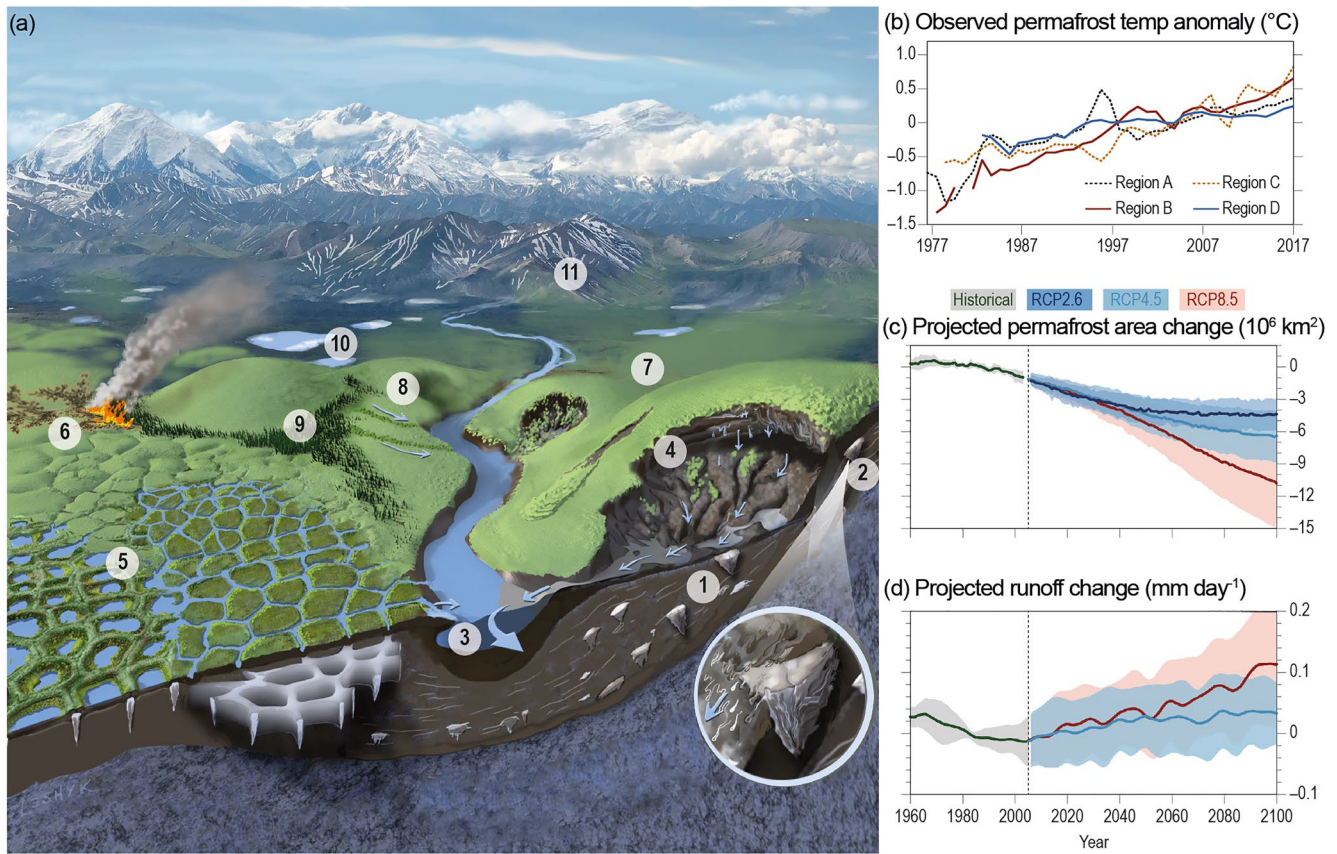
Figure 8. (a) Diagram illustrating components of the circumpolar Arctic terrestrial landscape potentially sensitive to climate change, including (1) permafrost, (2) ground ice, (3) river flow rates, (4) abrupt thaw via landslides and small-scale processes, (5) surface water accumulation, (6) wildfires, (7) tundra biome shifts, (8) shrub vegetation, (9) boreal forests, (10) lake ice, and (11) seasonal snow cover. (b) Observed permafrost temperature anomalies (relative to the 2007–2009 International Polar Year baseline) over time (Romanovsky, Isaksen, et al., 2017; Romanovsky, Smith, et al., 2017). (c) global area of near-surface permafrost soils and (d) projected change in surface runoff to the Arctic Ocean under low (RCP2.6), middle-of-the-road (RCP4.5), and worst-case (RCP8.5) emissions scenarios. Figures adapted with permission from Figure 3.10 in the IPCC SROCC Ch 3 (Meredith et al., 2019).

Permafrost thaw—and resulting carbon emissions—has sometimes been characterized as a fast-acting tipping element with tipping points which, once crossed, would trigger abrupt and severe warming. On the other hand, permafrost is still perceived as a relatively stable component of the climate system on century or possibly millennial times scales. Thus, whether permafrost carbon will or will not be an important factor in abrupt carbon cycle shifts in addition to the other components reviewed here is contentious (Dyonisius et al., 2020; Petrenko et al., 2017).

The majority of permafrost thaw will occur via thickening of the active layer, often referred to as gradual permafrost thaw because it affects centimeters of surface permafrost relatively slowly on a time scale of decades to centuries (McGuire et al., 2018; Schneider Von Deimling et al., 2015). Abrupt thaw processes—the collective term for rapid erosion, thermokarst (thaw that leads to subsidence, land slumping, and erosion), and similar phenomena—lead to more abrupt exposure and thaw of permafrost on time scales of days to years (Abbott & Jones, 2015). Thermokarst can locally affect meters of permafrost over such timescales. Thermokarst-prone landscapes can occur in both discontinuous and continuous permafrost (Fraser et al., 2018; Lewkowicz & Way, 2019; Olefeldt et al., 2016; Rudy et al., 2017) and are often associated with surface water accumulation and/or melting ground ice that triggers sudden landslides, crevasses, or subsidence. Abrupt thaw represents an important ecosystem state change (M. G. Turner et al., 2020) and has the potential to impact <20% of the Arctic region (Olefeldt et al., 2016; Turetsky et al., 2020). Such processes carry implications not just for susceptibility to thaw but also for subsequent rates of carbon release. Carbon mobilized by thermokarst events particularly in Yedoma permafrost soils (a type of Pleistocene aged permafrost) has demonstrated rapid rates of biodegradation, underlining the potential for significant carbon release from thermokarst features (Vonk et al., 2013). On the other hand, other

types of permafrost carbon, such as Holocene aged permafrost soils in some peatlands, have been found to be relatively resistant to degradation post-thaw (Heffernan et al., 2020).

Beyond carbon and climate feedbacks, permafrost thaw also has important consequences for local communities, infrastructure, and ecosystems ranging from structural damage and loss of life caused by unstable ground to an elevated risk of infectious disease outbreaks at the hands of live pathogens liberated from thawed permafrost (Hjort et al., 2022; Meredith et al., 2019; Miner et al., 2021; M. G. Walsh et al., 2018). For example, abrupt thaw was associated with the majority of hazards experienced by land users in Alaska, impacting the way northerners can hunt or travel over land or rivers (Gibson et al., 2021). Consequently, limiting the extent of climate change can both limit climate risks associated with permafrost thaw and reduce impacts upon northern communities (Pörtner et al., 2022).

2.4.2. Cumulative Methane and CO_2 Release From Abrupt and Gradual Permafrost Thaw Manifests Over a Century or More

It is highly likely that a sizable fraction of permafrost area globally will thaw by end-of-century, though estimates of the extent of loss range widely from 5% to 70% (Koven, Lawrence, & Riley, 2015; Koven, Schuur, et al., 2015; Lawrence et al., 2012; McGuire et al., 2018; Schaefer et al., 2011; Schuur & Abbott, 2011; Schuur et al., 2015; Wisser et al., 2011). Some permafrost can persist even in the face of disturbance and 1.5–2°C of observed regional warming (J. E. Holloway & Lewkowicz, 2020; James et al., 2013). For example, lowland permafrost associated with thick peat layers persisted as relict patches of permafrost remnant from the Little Ice Age in North America (Halsey et al., 1995). In large part due to ecosystem protection of permafrost created by vegetation, peat, and snow characteristics, thermal modeling also suggests that permafrost in the southern margins of the permafrost zone may be more resilient than previously assumed (Way et al., 2018). However, such findings also emphasize that substantial permafrost degradation at regional to continental scales has already occurred to date and will continue under high and mid-range emissions scenarios.

From a carbon emission perspective, both gradual and abrupt thaw will contribute to climate change slowly over a century or longer rather than being released all at once (Turetsky et al., 2019, 2020).

Projections for emissions from thawed permafrost by 2100 are quantitatively large (range of 37–174 Gt C, with two recent estimates of 57 and 87 Gt C under a worst-case RCP8.5 emissions scenario) (Koven, Schuur, et al., 2015; Meredith et al., 2019; Schneider Von Deimling et al., 2015). A multi-model mean of 92 Gt C released from gradual thaw by 2100 under RCP8.5 (Meredith et al., 2019) would represent about a decade of present-day emissions (~10 Gt C/yr) (Peters et al., 2020). The IPCC AR6 WG1 assessed the strength of the permafrost feedback to be 18 (3.1–4.1, 5–95‰ range) and 2.8 (0.7–7.3) Gt C of CO_2 and CH_4, respectively, per 1°C of global mean warming, implying a middle figure of 90 Gt C of CO_2 and 14 Gt C of CH_4 under RCP8.5-like warming of ~5°C globally (Canadell et al., 2021). Over longer multi-century timescales, models demonstrate higher uncertainty, with estimates for carbon release from gradual thaw by 2300 under RCP8.5 ranging between 167 Gt C absorbed to 641 Gt C released (mean of 208 Gt C released) (McGuire et al., 2018).

Abrupt thaw could produce CH_4 and CO_2 fluxes of 38–104 Mt CH_4/yr and 0.01–0.45 Gt C/yr of CO_2 through 2300 under an RCP8.5 scenario (McGuire et al., 2018; Schneider von Deimling et al., 2012; Schneider Von Deimling et al., 2015; Turetsky et al., 2020). One modeling study suggests thermokarst processes could cumulatively emit an additional 60–100 Gt C by 2300 under RCP8.5, although associated climate impacts could vary depending on the proportion of methane emissions (Turetsky et al., 2020). Methane fluxes from abrupt thaw will induce a moderate additional climate forcing relative to anthropogenic methane emissions today (335 Mt C/yr). Cumulative carbon release from abrupt thaw is anticipated to be less than 50% of that stemming from gradual thickening of the active layer, yet due to higher CH_4:CO_2 ratios the climate impact of abrupt thaw via radiative forcing are projected to be similar to that of gradual thaw (McGuire et al., 2018; Schneider von Deimling et al., 2012; Schneider Von Deimling et al., 2015; Turetsky et al., 2020). Climate mitigation could significantly preserve existing permafrost carbon, with the modest-mitigation RCP4.5 scenario significantly minimizing permafrost carbon release from both abrupt and gradual thaw (McGuire et al., 2018; Turetsky et al., 2020).

Currently, permafrost carbon emissions are characterized by high CO_2:CH_4 ratios (Miner et al., 2022). Empirical and modeling studies agree that permafrost C emissions currently are dominated by CO_2 fluxes in oxic soil environments, with much smaller fluxes of CH_4 occurring in anoxic conditions (Schädel et al., 2016; Walter Anthony et al., 2018). However, particularly in lowland regions prone to abrupt thaw, the contribution of CH_4 to total

permafrost C release is expected to increase in the future (Turetsky et al., 2020; Walter Anthony et al., 2018). Increasing methane emissions from saturated thawing soils in these northern lowlands often is driven by modern carbon assimilated recently by the ecosystem rather than older carbon that previously resided in permafrost layers (Estop-Aragonés et al., 2020) highlighting the important connection between permafrost thaw, land cover change, and ecosystem carbon emissions. The role of methane oxidation has been shown to be important in some thaw environments (Abbott et al., 2015) but requires more study to determine its overall significance to permafrost carbon emissions as well as its sensitivity to future changes in permafrost, climate, and biophysical conditions. Beyond microbial transformations of methane, natural methane stores trapped under currently frozen soil layers may also be released thanks to permafrost thaw, although this source is not currently anticipated to be climatically significant (Petrenko et al., 2017).

Emissions of nitrous oxide—another potent greenhouse gas—from permafrost also may be non-negligible (Voigt et al., 2020; Wilkerson et al., 2019) and require further study. In general, improved projections of hydrological changes within the permafrost region (Andresen et al., 2020) and better quantification of the rates of permafrost organic carbon mineralization into CO_2 versus CH_4 (or other greenhouse gases such as N_2O), and the fate of permafrost C exported as dissolved organic matter in aquatic environments remain active areas of study with major climate implications (J. C. Bowen et al., 2020; Laurion et al., 2020; Zolkos & Tank, 2020).

Patterns of vegetation and biomass recovery patterns post-thaw also are important to ecosystem C balance including the potential for new peat accumulation post-thaw. At least some portion of permafrost C release is likely to be offset by increased plant growth and new accumulation of biomass (Koven, Lawrence, & Riley, 2015; McGuire et al., 2018; Turetsky et al., 2019, 2020). Landscape to regional vegetation shifts are occurring as a result of permafrost thaw (Baltzer et al., 2014) but may in turn also carry important consequences for permafrost carbon cycle feedbacks. In particular, the large-scale expansion of shrubs across the circumpolar north (Bjorkman et al., 2018; Tape et al., 2006) may accelerate the seasonal timing of snow melt due to albedo effects from protruding branches, acting as a positive feedback upon permafrost thaw (Wilcox et al., 2019). Plant roots can further stimulate the decomposition of organic carbon in thawed permafrost, exerting a potentially large impact on regional scales as warming and enhanced nitrogen availability promotes vegetation growth (Albano et al., 2021; Keuper et al., 2020). Simulations focused on permafrost thaw show that enhanced plant carbon uptake can entirely offset permafrost carbon emissions under the RCP4.5 emissions scenario (McGuire et al., 2018). The future of Arctic vegetation and CO_2 uptake depends on patterns of regional wetting versus drying in combination with disturbances like fire regimes. It seems likely that ecosystem carbon balance in the northern permafrost region will be strongly affected by the strength of plant CO_2 fertilization in combination with vegetation response to climate, which need better mechanistic representation in most large scale models. The response of different landscapes and vegetation types to warming, changes to nutrients, increased CO_2, precipitation, and fire will generally drive large-scale ecosystem changes across the circumpolar north, with important implications for not only permafrost but also northern boreal forests (see Section 2.5).

Efforts to assess the climate implications of future permafrost thaw are complicated by the limitations of current models (Bonnaventure et al., 2018). CMIP5 models produce a wide range of estimates due to differences in modeled transfer of warming to permafrost and to varying model treatment of surface factors such as snow and hydrology (Koven et al., 2013). Models' limited ability to account for ground ice represents a particularly important challenge, as ground ice may slow rates of permafrost warming over coming decades (H. Lee et al., 2014) but ultimately increase landscape susceptibility to thermokarst over longer timescales (Nitzbon et al., 2020). CMIP6 models generally yield similar projections for future changes in permafrost area and volume, but still do not incorporate important factors including ground ice (E. J. Burke et al., 2020). Land surface models continue to exhibit widespread in estimates of soil carbon stocks and in the response of soil carbon dynamics to changing temperature and moisture (Huntzinger et al., 2020). The use of high-resolution regional permafrost models forced by the results of GCM runs may enable improvements in model performance, by better capturing landscape heterogeneity (Lara et al., 2020).

Overall, added inputs of atmospheric carbon (worst-case estimates equivalent to up to ~400 Gt C by 2300) (Turetsky et al., 2019) would be climatically significant, further incentivizing climate change mitigation to a level that would minimize the impact from this feedback. Abovementioned uncertainties concerning feedbacks between temperature, ground ice, precipitation, permafrost thaw, local landscape and vegetation changes, and the response of microbial communities and biomass (Bonnaventure et al., 2018; Jorgenson et al., 2010; Kokelj

Table 5
Section Summary Box Synthesizing the Forcing Mechanism, Response Behavior, Reversibility, and Classification of Carbon Release From Thawing Permafrost

	Classification	Mechanism	Irreversibility
Carbon release from thawing permafrost	Tipping element Committed declines in frozen carbon and subsequent long-term carbon release to atmosphere in response to forcing, with potential local or regional threshold-like behavior (e.g., Drijfhout et al., 2015; Koven, Schuur, et al., 2015; McGuire et al., 2018; Schneider Von Deimling et al., 2015; Turetsky et al., 2020; Walter Anthony et al., 2018)	Warming temperatures, precipitation shifts, wildfires, and changes to vegetation and surface albedo drive permafrost warming and thaw, followed by carbon release from decomposing organic matter	Irreversible for centuries or longer (e.g., Boucher et al., 2012; de Vrese & Brovkin, 2021; M. C. Jones et al., 2017; H. Lee et al., 2019; Schaefer et al., 2011)

et al., 2015; McGuire et al., 2018; Rivkina et al., 2004; Shur & Jorgenson, 2007) also leave considerable uncertainty associated with net CO2 and methane emissions estimates (Dean et al., 2018). Together, emissions associated with permafrost thaw and increasing Arctic fires will reduce the amount of greenhouse gases that humans can emit to remain below policy targets (Natali et al., 2021) (Table 5).

2.5. Large-Scale Boreal Forest Ecosystem Shifts

2.5.1. Background

The northern boreal biome has felt the effects of climate change to a substantial degree, with decades of observations highlighting rapid regional temperature increases, more frequent occurrence of wildfires, and intensification of pest-driven tree mortality. Near-surface fall and winter air temperatures within the band of latitudes from 70° to 90°N rose by 1.6°C per decade over the 1989–2008 period, with summer temperatures rising at a rate of 0.5°C per decade (Screen & Simmonds, 2010). Increasing temperatures have resulted in substantial greening overall within boreal North America (Figure 9) and Eurasia (Ju & Masek, 2016; Piao et al., 2020). Despite overall greening trends, the observational record has seen a marked increase in the extent, frequency, and severity of browning events from boreal wildfires, with this increasing trend predicted to continue with further warming (De Groot et al., 2013; Flannigan et al., 2009; Seidl et al., 2020; Veraverbeke et al., 2017). Higher temperatures have additionally been linked to acute outbreaks of insects leading to large-scale tree mortality events in Alaska, Canada, and Siberia (Boyd et al., 2021; Kharuk et al., 2020; Kurz et al., 2008; Sherriff et al., 2011; US Forest Service, 2019), sparking concern that similar pest invasions could occur more often in the future, infecting new tree species and expanding pest ranges northward (de la Giroday et al., 2012). These differential impacts of climate change on greening and browning trends occur continentally—for example, areas with browning trends are much more prevalent and stronger in boreal North America versus Eurasia (Bi et al., 2013)—as well as regionally, with browning from fires and drought much more prevalent in the southern margins of the North American boreal forest (Hogg et al., 2008) in contrast to greening trends at the northern margins (C. T. Maher et al., 2021).

Between the biomass in soil, permafrost, and living and dead vegetation, boreal forests represent a significant pool of terrestrial organic carbon (30% of global soil carbon) (Mcguire et al., 2009; Turetsky et al., 2019), and constitute 30% of global forest area (Kasischke, 2000). Of this fraction, two-thirds of boreal forest are found within Russia, with Russia's boreal forests estimated to contribute around half (0.6 Gt C/yr) of the total global terrestrial carbon sink (Dolman et al., 2012; Schaphoff et al., 2013). Recent research has proposed that boreal forest carbon stocks could be underestimated, with updated calculations suggesting that boreal regions hold more terrestrial carbon (Bradshaw & Warkentin, 2015) than tropical areas, which have been previously suggested to harbor the largest stock of carbon among all terrestrial biomes (Y. Pan et al., 2011).

It is important to note that 95% of boreal zone carbon is stored in peatlands and soils (Bradshaw & Warkentin, 2015), and an uncertain proportion of this underground carbon stock overlaps with the stock of permafrost carbon (Section 2.4). Boreal vegetation and permafrost soils also interact with one another (Carpino et al., 2018),
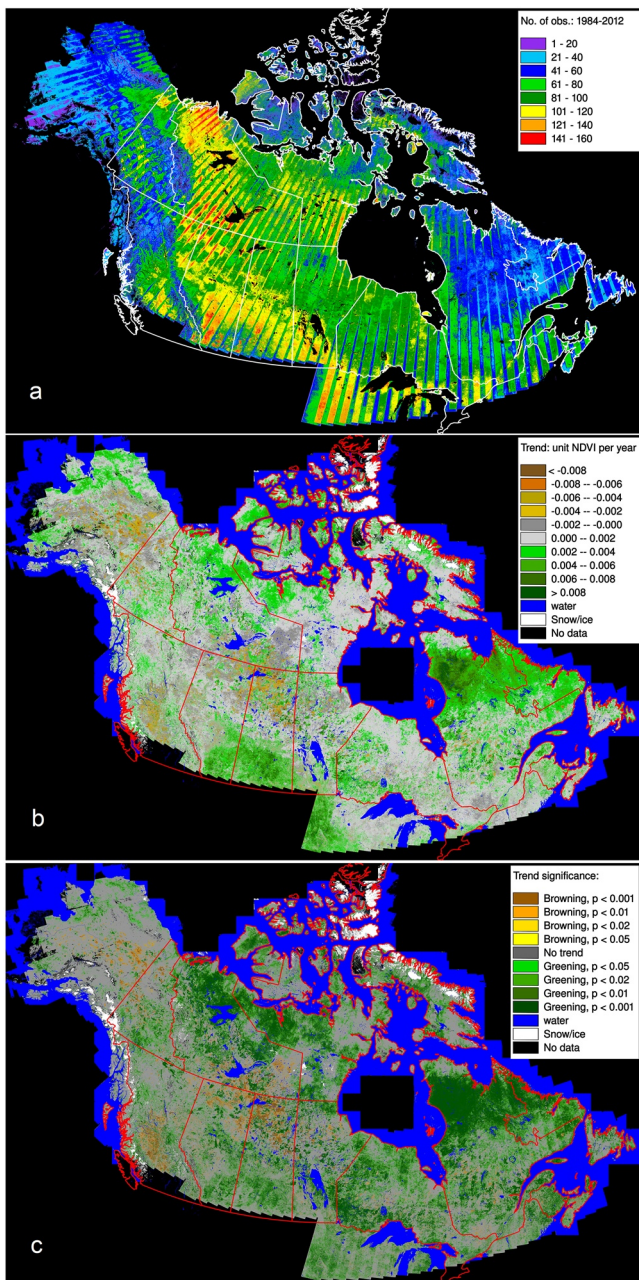
Figure 9. Maps of Landsat-based greenness trends for Canada and Alaska from 1984 to 2012. (a) Counts of Landsat observations from 1984 to 2012. (b) Greenness trends expressed in units of Normalized Difference Vegetation Index (NDVI) change per year. (c) Statistical significance of the calculated greenness trends. Figure reproduced with permission from Ju and Masek (2016).

complicating attempts to disentangle potential carbon fluxes associated with changes in the vegetation and soil systems. Regardless, boreal forests make up an important component of the terrestrial and global carbon cycles, with changes in this biome potentially acting as large climate feedbacks.

A growing number of research studies over the past 25 years have provided increasing evidence for the possibility of region- (e.g., North America vs. Siberia) and landscape- (e.g., upland vs. lowland) specific shifts within the circumpolar boreal biome, with potentially significant climate implications (Chapin et al., 2005; Foley et al., 1994; Lenton et al., 2008; X. Lin et al., 2020; Scheffer, Hirota, et al., 2012). This hypothesis theorizes that a landscape-dependent mix of temperature, moisture, and precipitation changes, shifts in wildfire regimes and soil conditions, greater vulnerability to pest insect outbreaks, and a lengthening of the growing season may all combine to drive acute mortality of boreal forest vegetation in drier, upland areas and at the southern margins of boreal zones and its replacement by more open deciduous woodlands and grasslands, as reviewed by Gauthier et al. (2015) and predicted in forest modeling studies (Foster et al., 2019; Mekonnen et al., 2019). In contrast, increasing boreal forest productivity in wetter ecosystems and at latitudinal and elevational range boundaries is also possible (Foster et al., 2019; Pastick et al., 2019). Region-specific differences in wildfire regimes and permafrost dynamics (Baltzer et al., 2021; Rogers et al., 2015) may also lead to diverging responses to climate change. X. Lin et al. (2020) found that the net sink of atmospheric carbon in Siberia has increased by 18 Tg/year since 1980, while the carbon flux over the North American boreal and arctic biomes has remained relatively constant. Such ecosystem- and continental-scale shifts could represent a climatically significant tipping element with the potential to change land surface albedo (Beck, Juday, et al., 2011; Bonan et al., 1992) over large areas and release a considerable pool of carbon to the atmosphere, in addition to altering the strength of an important terrestrial organic carbon sink.

2.5.2. Boreal Forests Worldwide Are Experiencing Rapid Changes With the Potential for Northward Expansion and Southern Margin Shifts to Deciduous Forest or Grasslands

Observations of ongoing changes in boreal ecosystems worldwide provide abundant evidence of increasing climate impacts, particularly within southern and interior boreal regions. As mentioned above, temperatures for the Arctic north are rising at two to four the global mean rate of warming (Rantanen et al., 2022; Screen & Simmonds, 2010). Tree mortality across the Russian boreal forest has increased over the late 20th and early 21st centuries (Allen et al., 2010). The same region has also seen a substantial intensification in fire occurrence, with the fire return interval falling from 101 years in the 19th century to 65 years in the 20th century for larch-dominant forest stands (Kharuk et al., 2008). Increased recurrence of wildfires is reducing the carbon stocks of affected boreal forest sites (Palviainen et al., 2020), altering soil and permafrost regimes (Gibson et al., 2018), changing dominant species compositions (Baltzer et al., 2021; Mack et al., 2021), and in some cases leading to post-fire "regeneration failure" (Burrell et al., 2021). Forest area burned has correspondingly increased across Siberia based on data from multiple sources (Soja et al., 2007). The extent of wildfires in boreal environments is widely anticipated to continue increasing in the future (Balshi et al., 2009; Kloster et al., 2012; Shuman et al., 2017; Wotton et al., 2017). Satellite data also highlight decreases in forest productivity across Alaska since 1982 (Beck, Goetz, et al., 2011). With regional warming, Alaska has also begun to see large-scale forest mortality events driven by previously cold-limited spruce beetles, as reviewed in Soja et al. (2007). For example, an ongoing spruce beetle outbreak in south-central Alaska has affected ~0.5

million ha since 2016 (US Forest Service, 2019). The North American boreal forest is also exhibiting an increase in the proportion of deciduous tree cover (J. A. Wang et al., 2019).

Replacement of boreal forest by grasslands and deciduous forest is expected to continue based on the response of vegetation models to climate forcing (Foster et al., 2019; J. A. Wang et al., 2019). Together with climate-driven changes to precipitation and soil moisture, increasing insect outbreaks and more frequent and intense wildfires may drive declines in boreal forest productivity within the interior of boreal regions (Boyd et al., 2021; Foster et al., 2019; J. A. Wang et al., 2019). Region-specific modeling studies focusing on Alaska (Foster et al., 2019; Mann et al., 2012), Siberia (Shuman et al., 2015), and China's boreal forests (Wu et al., 2017) support the potential for future climate-induced shifts in vegetation consistent with such patterns.

Yet while boreal forest productivity and tree cover are on the decline at the southern edge of the boreal zone and within interior regions, 30-year data sets of satellite and observational evidence also point toward ongoing expansion of boreal forests northwards into area previously occupied by tundra thanks to higher temperatures (Figure 9) (Beck, Juday, et al., 2011; Ju & Masek, 2016; Pastick et al., 2019; Pearson et al., 2013). Since 1960, the growing season across the boreal zone has lengthened by 3 days/decade (Euskirchen et al., 2006). Expansion of trees into the tundra biome has implications for regional and global climate, as the albedo of forests is lower than that of tundra, leading to warmer winter conditions with greater tree cover (Bonan et al., 1992). The spatial extent and speed of boreal treeline migration is dependent on a number of factors (Rees et al., 2020), including nutrient and permafrost conditions and wildfire. However, increasing temperatures are likely to drive boreal expansion, leading to cascading impacts on soil, disturbance, and climate regimes.

The accelerated pace of boreal climatic shifts relative to the rest of the world is likely to continue over the 21st century. Warming of 3–5°C globally by end-of-century would imply average temperature increases of 7–10°C for large parts of Russia, with regional warming of up to 12°C (Schaphoff et al., 2016). Such warming would probably exacerbate the abovementioned climate impacts upon the boreal environment. For example, one study predicts that the probability and intensity of Canadian boreal forest fires might more than double across large areas by 2080–2100 under an RCP8.5 scenario (Wotton et al., 2017), while another recent analysis modeled mean potential increases in burned area of 29%–35% for the Northwest Territories and 46%–55% for interior Alaska by 2050–2074 under RCP8.5, driven predominantly by more frequent occurrence of lightning (Veraverbeke et al., 2017).

The rapid pace of such observed and predicted patterns, which in some cases exceed older predictions, raises the possibility that future change and warming-induced feedbacks within the boreal biome may proceed non-linearly rather than linearly (Foster et al., 2019; Johnstone et al., 2010; Soja et al., 2007). An extensive survey of forest cover across the boreal environment has indicated that intermediate states of landscape tree cover are rare and potentially unstable, suggesting that forested areas may transition to systems with sparse tree cover more abruptly than previously thought (Scheffer, Hirota, et al., 2012). Shifts toward more prevalent fires potentially play a major role in driving a transition toward more deciduous tree cover (Johnstone et al., 2010). Decades of remote sensing data from North American boreal forests suggest that current CMIP6 models are failing to account for notable impacts from disturbances like fire and insects, while overestimating additional biomass accumulation from CO_2 growth enhancement (J. A. Wang et al., 2021). Paleoclimate evidence of boreal forests responding strongly to temperature changes suggests that large shifts in boreal biome extent have occurred within the past 10,000 years, potentially acting as a large-scale climate feedback (Bigelow et al., 2003; Foley et al., 1994; MacDonald et al., 2000, 2008).

Ecosystem changes for the boreal forest may take place within decades to a century. A multi-region model analysis found that for large portions of all major boreal regions with the exception of Eastern North America, projected temperature changes under worst-case emissions would alter local climatic conditions to resemble current woodland/shrubland climates by 2090 (Gauthier et al., 2015). Mann et al. (2012) in fact suggest that a transition to mixed woodlands has already begun for the Alaskan boreal region and is anticipated to reach completion by mid-century. Projections for Siberia also indicate a relatively rapid shift, with dark and light-needled forest declining from ~60% of the modeled area to ~40% and ~24% for a 720 ppm and >800 ppm end-of-century emissions scenario, respectively (Shuman et al., 2015).

2.5.3. The Importance of Boreal Forest Regions for Global Climate

The potential for boreal forests to exhibit tipping element behavior remains uncertain, but troubling (Table 6). The recent pace of change witnessed in the boreal north clearly points to the potential for large-scale transitions.

Table 6
Conceptual Outline of Changes Within Different Regions of the Boreal Zone Organized by Their Anticipated Impacts Upon Climate

	Boreal forest zone		
	Southern margins	Boreal zone interior	Northern margins
Warming feedbacks in response to warming	Soil organic matter decomposes at higher rates	Soil organic matter decomposes at higher rates	Soil organic matter decomposes at higher rates
	Increased wildfire impacts	Increased wildfire impacts	Increased wildfire impacts
	Increased boreal tree mortality from pests	Increased boreal tree mortality from pests	Expansion of boreal conifers into previously bare ground darkens land surface
Cooling feedbacks in response to warming	Carbon storage eventually shifts aboveground into more robust deciduous vegetation	Carbon storage eventually shifts aboveground into more robust deciduous vegetation	Faster vegetation growth due to warmer temperatures stores more carbon
	Replacement of dark-leaved boreal conifers increases land surface reflectivity	Replacement of dark-leaved boreal conifers increases land surface reflectivity	
Net effects	Highly uncertain, but with a considerable possibility for net warming due to increased carbon release from decomposition and burning of organic matter in boreal forest soils.		
	Climate impacts may also differ by region (i.e., E. Siberia vs. W. Siberia vs. N. Canada vs. Alaska)		

Projections for such a transition, however, remain based on models that must make simplifying assumptions about complex mechanisms such as precipitation, fire, and soil moisture availability and their effects on needle-leaved trees. These processes as well as differential responses of tree species to environmental changes (Dusenge et al., 2020) and competitive interactions between individual trees and species are important factors for modeling the response of boreal regions to climate forcing (Foster et al., 2019; Shugart et al., 2015). Due to landscape and ecological heterogeneity, some boreal areas may prove relatively more resilient to climate change thanks to favorable terrain or ecosystem conditions (Stralberg et al., 2020). Nevertheless, parallel findings from a growing number of analyses predicting major vegetation shifts across the biome region underline the real possibility for a boreal transition beginning later this century.

Uncertainty continues to surround the critical thresholds, extent of change, and climatic impacts of large-scale boreal ecosystem shifts. Polling of expert researchers produces a wide range of increases in global mean temperature relative to pre-industrial temperature (3–4°C) for intensifying boreal forest transitions (Kriegler et al., 2009). Comparisons of vegetation shifts under multiple climate scenarios suggest that boreal forest changes may be strongly mitigation-dependent, with more limited impacts for more moderate emissions pathways (Lucht et al., 2006). Loss of boreal forest in southern regions may also be partially compensated by afforestation along the northern boundaries of the boreal biome as warmer, less-frozen tundra gives way to forested landscapes (Scheffer, Hirota, et al., 2012). Existing large-scale vegetation models also remain limited in their ability to replicate complex terrestrial ecosystem dynamics and produce confident estimates for changes in biomass carbon (Schaphoff et al., 2016). Finally, the future of boreal forests will also strongly depend on human management practices.

One of the most worrying aspects of a potential boreal tipping element involves the difficulty of quantifying the climatic impact of replacement of boreal forests by deciduous woodlands or shrublands. Boreal forests contain 30% or more of global soil carbon, and up to 95% of organic carbon within boreal forest ecosystems may be stored belowground (Bradshaw & Warkentin, 2015; Flannigan et al., 2009). Small-scale processes triggered by warming, hydrological changes, and permafrost thaw may precipitate the release of some of this large carbon pool via decomposition (Turetsky et al., 2019), while fire and post-fire mortality have the potential to emit considerable carbon from both forest biomass as well as upper soil organic layers (Brando et al., 2014; De Groot et al., 2013; Dieleman et al., 2020; Shvidenko et al., 2011). At the same time, projections for potential carbon release from boreal soils are complicated by a high degree of overlap with estimates for permafrost carbon release (Bradshaw & Warkentin, 2015), as the northern boreal and permafrost zones partially coincide. A potential also exists for interactions between permafrost thaw and vegetation shifts. For instance, observations in Canada suggest that permafrost thaw may push boreal landscapes toward wetland-like conditions, resulting in declines in forest cover

Table 7
Section Summary Box Synthesizing the Forcing Mechanism, Response Behavior, Reversibility, and Classification of Boreal Forest Ecosystem Shifts

	Classification	Mechanism	Irreversibility
Boreal forest ecosystem shifts	Tipping element Large-scale changes in boreal forest distribution and vegetation patterns induced by climate forcing, with potentially abrupt local/regional ecosystem shifts (e.g., Beck, Juday, et al., 2011; Carpino et al., 2018; Foster et al., 2019; Lucht et al., 2006; Mekonnen et al., 2019; Scheffer, Hirota, et al., 2012; Shuman et al., 2015)	Regional warming and climate change drive changes in fire regime, growing season, permafrost zone, weather patterns, and insect outbreaks, promoting interior vegetation shifts and shifting the geographic range of the circumpolar boreal forest	Uncertain

(Carpino et al., 2018). Warming additionally affects carbon gains and losses in boreal vegetation thanks to shifts in productivity and respiration, with potentially opposing seasonal effects (Z. Liu et al., 2020).

Some research from a set of Alaskan studies suggests that after wildfires, a shift in vegetation from needle-leaved trees to deciduous forest would not substantially change the total pool of organic carbon, and would potentially increase the storage lifetime of carbon due to the greater resistance of deciduous biomass to fire and decay (Alexander & Mack, 2016; Mack et al., 2021). Biotic feedbacks such as vegetation shifts toward hardwoods during post-fire succession may also improve resilience to fire (Hansen et al., 2020) and reduce the future frequency of wildfires relative to model projections that predict fire activity from changes in climate alone (Marchal et al., 2020).

Apart from implications for fire and carbon storage, a shift in vegetation from darker coniferous species to lighter deciduous trees would increase regional reflectivity of the southern and interior areas of the boreal zone, acting as a negative feedback on warming (R. A. Betts, 2000; Z. Liu et al., 2019; Mykleby et al., 2017; Piao et al., 2020). As boreal forests expand northwards into current tundra biomes, however, the same research suggests that the darker surface of boreal vegetation—particularly as it overtakes treeless ground previously snow-covered in winter—will act as a positive feedback reinforcing climate change. This albedo-driven effect will likely overcome any positive benefits from added carbon sequestration from northwards expansion of boreal vegetation.

Overall, the climatic impact of worldwide changes to the boreal biome under expected future emissions remains challenging to assess. Reductions in boreal forest area in southern and upland boreal regions combined with fire regime changes and the predicted northward treeline expansion in response to higher temperatures produce multiple competing, complex climate impacts (Beck, Goetz, et al., 2011; Foster et al., 2019; Ju & Masek, 2016; Pastick et al., 2019; Pearson et al., 2013). Calculations of changes to carbon stocks, regional albedo, carbon sinks, and the timescales involved even at local or regional scales remain imprecise and depend upon multiple complex processes and feedbacks (Foster et al., 2019; Shuman et al., 2015). Ultimately, current research cannot eliminate the possibility that changes across the boreal zone due to a warming climate could act as a net positive climate feedback, thanks to the potential for permafrost thaw and wildfires to liberate the soil carbon that makes up the majority of stored carbon across this ecosystem. Consequently, boreal forest dieback and shifts represent one of the more potentially immediate and significant climate system tipping elements (Table 7).

2.6. Disruption of Tropical Seasonal Monsoons

2.6.1. Background

Seasonal monsoon precipitation is the primary source of water for nearly all tropical land, governing water availability and agricultural yields for billions of people in much of Africa and Asia, the tropical Americas, and northern Australia (Christensen et al., 2013). Furthermore, extreme precipitation in these regions typically results from storms embedded within the continental-scale monsoon winds, causing flooding and landslides that often inflict significant loss of life and property. Given the importance of monsoons to food security, water availability, and natural disaster risk, researchers worldwide have devoted sizable effort to predicting changes in monsoon seasonality and intensity that might result from anthropogenic climate change.

Although monsoons are sometimes viewed as regional phenomena, they are part of the global circulation of the atmosphere, with warm air rising over tropical continents in the summer hemisphere, flowing across the

equator, and sinking as it cools in the winter hemisphere (Fasullo & Webster, 2003). During solstice seasons, the sum of all the regional monsoons constitutes a large fraction of the global Hadley circulation, with South Asian monsoon winds alone constituting about half the global cross-equatorial mass flux in boreal summer (Boos & Emanuel, 2009; Findlater, 1969; Trenberth et al., 2000; P. J. Webster, 2004). The seasonal cycle of monsoons and the Hadley circulation is driven by the seasonality of solar radiation, with the energy of intense summer sunlight transferred rapidly to the overlying atmosphere due to the low heat capacity of land. The vertical transport of this energy from the thin layer of near-surface air into the bulk of the overlying atmosphere is performed primarily by precipitating clouds, yielding monsoon precipitation (Biasutti et al., 2018). Changes in monsoon precipitation thus involve planetary-scale atmospheric flow, comparatively small-scale clouds, surface and atmospheric absorption of solar radiation, and the properties of land and ocean surfaces.

Because of difficulties in understanding and simulating (e.g., in global climate models) the multi-scale, coupled monsoon systems described above, many studies have turned to the historical record for indications of ongoing shifts in monsoon rainfall; a repeating theme is the identification of large-scale changes in seasonal mean monsoon rainfall in many regions over the last century, with some reversal of those changes in recent decades. For example, monsoon rainfall over central India decreased about 10% between 1950 and 2000, with that trend attributed to various possible causes such as atmospheric aerosols (Bollasina et al., 2011; Ramanathan et al., 2005), Indian Ocean warming (Roxy et al., 2015), land use change (Paul et al., 2016), and irrigation (Niyogi et al., 2010; Shukla et al., 2014). However, that decrease in central Indian rainfall ended around the year 2000 and the negative rainfall anomaly has since almost completely recovered in most observational records (Q. Jin & Wang, 2017). When averaging over the larger region of the whole country of India, precipitation shows no detectable trend in rain gauge data sets extending back in time more than a century, for both summer and the full calendar year (Saha et al., 2018). In Africa's Sahel, monsoon-season rainfall decreased about 40% from the 1950 to the mid-1980s, then partially recovered over the next 20 years (Held et al., 2005). Remote SST variations are strongly associated with this decadal variability in Sahel rainfall (Folland et al., 1986; Giannini et al., 2003), with possible roles for anthropogenic aerosols and natural ocean-atmosphere variability in causing those SST changes (Biasutti & Giannini, 2006; Rotstayn & Lohmann, 2002). Turning from the seasonal mean to the temporal characteristics of rain events within the monsoon season, studies have found evidence for Sahel precipitation becoming increasingly extreme and erratic (Biasutti, 2019). For example, 35 years of satellite imagery showed an increase in the number of intense mesoscale convective systems just south of the Sahara (Taylor et al., 2017). In central India, some studies have found an intensification of rainfall in wet periods and a reduction in the intensity of dry spells (Singh et al., 2014, 2019).

This section does not seek to synthesize all historical and projected future trends in monsoon rainfall, but asks whether monsoons constitute a tipping element of the climate system (other reviews, such as (Hoell et al., 2016; Pascale et al., 2019; A. G. Turner & Annamalai, 2012; B. Wang, Jin, & Liu, 2020) summarize the regionally disparate observed trends in monsoon rainfall). Is it reasonable to expect abrupt changes in monsoon characteristics in response to anthropogenic climate forcings, and if so would such changes be reversible? Studies have indeed suggested that anthropogenic forcings might cause a sudden reduction in South Asian monsoon strength and an abrupt increase in West African monsoon intensity in the next century (Bathiany et al., 2018; Lenton et al., 2008; Levermann et al., 2009; Schewe et al., 2012; Zickfeld et al., 2005). However, these studies have relied on highly idealized and simplified sets of differential equations, often distinct from the formal primitive equations of fluid motion that form the basis of global climate models, and their relevance to monsoons has been disputed (Boos & Storelvmo, 2016a; Seshadri, 2017). The majority of research to date, including the ensemble of CMIP5 and CMIP6 models (Figure 10), suggests that the global monsoon domain will experience a gradual increase of seasonal mean precipitation and a gradual weakening of low-level mean winds in response to warming, albeit with many uncertainties and caveats involving model bias (Z. Chen et al., 2020; Christensen et al., 2013; Hill, 2019; Hoegh-Guldberg et al., 2018; C. Jin et al., 2020; Ranasinghe et al., 2021). Yet, the great importance of monsoons for billions of people living in the tropics justifies continued study of even a slim chance of abrupt change (Shaw et al., 2022; Trisos et al., 2022), especially given the existing evidence for some abrupt variations in both paleo monsoons and the seasonal cycle of modern-day observed monsoons. The rest of this section examines the possibility of abrupt changes in monsoons that might occur in response to comparatively steady global or regional forcings, then closes with a very brief summary of projected future trends in regional monsoons that may be unrelated to tipping elements.
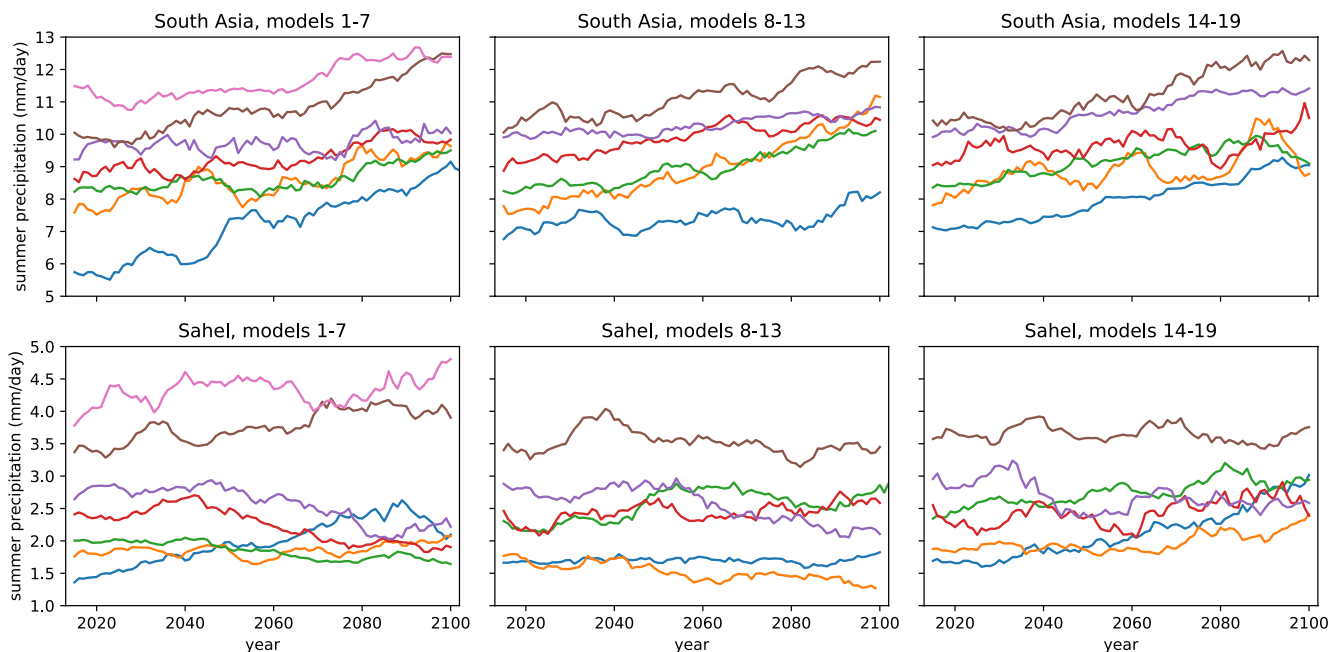
Figure 10. Time series of June–September precipitation averaged over a South Asian monsoon (top row) and Sahel domain (bottom row) from the first ensemble member of 19 CMIP6 models in the SSP5-8.5 future projection (Eyring et al., 2016), showing the absence of modeled abrupt shifts to a much wetter or drier regime in either domain. The time series are split across three panels for ease of visibility. A 10-year moving average has been applied to each time series to filter out shorter timescales of interannual variability. A table of the analyzed models and their associated institutions is available for download on Zenodo at https://doi.org/10.5281/zenodo.7038980.

2.6.2. Evidence for Abrupt Transitions in the Modern-Day Seasonal Cycle and Paleo Monsoons

Multiple regional monsoons exhibit threshold-like transitions in early summer, switching abruptly from a dry, winter-like state to a wet summer state. In early summer, precipitation and continental-scale atmospheric flow in the South Asian monsoon intensify more rapidly than can be explained by a linear response to the seasonal change in solar forcing (Boos & Emanuel, 2009; D. Halpern & Woiceshyn, 1999; Krishnamurti et al., 1981; Murakami et al., 1986). The transition from wintertime trade winds (directed westward) to eastward monsoon flow occurs rapidly -over a time scale of a few days--in the Australian monsoon, although with perhaps greater association with intrinsic intraseasonal variability and less association with the solar forcing than other monsoons (Wheeler & McBride, 2005). Convective cloud activity over the Sahel shifts rapidly from 5° to 10°N during the onset of the West African monsoon (Fontaine et al., 2011; Sultan & Janicot, 2003).

Given this observed behavior in the seasonal cycle, is it reasonable to expect that monsoons might abruptly shift into a much drier or wetter state as a long-term climate forcing is applied? If one could reduce the effective solar forcing below the level needed to produce the observed seasonal onset of the summer monsoon in a region, say by increasing the concentration of reflective atmospheric aerosols, one would expect the summer monsoon to fail to begin. However, such a forcing would need to be very large: insolation increases by about 250 W m^{-2} between winter and summer solstices at 30°N, while regional aerosol radiative forcings typically peak around 10 W m^{-2} or less (Ramaswamy et al., 2001; Takemura et al., 2005). Changes in radiative forcing due to historical changes in land use and land cover (including deforestation, cropland expansion), are of similarly small magnitude (C. J. Smith et al., 2020). Furthermore, monsoons have more degrees of freedom than an idealized mathematical step function, and are known to exhibit changes in intensity, onset and withdrawal dates, and spatial structure in response to a variety of forcings. For example, the well-known reduction in Indian monsoon rainfall that occurs during El Niño events has been shown to be associated with a shortening of the rainy season (Goswami & Xavier, 2005), and one of the most common patterns of interannual variability in the West African monsoon consists of a north-south shift of the rainfall maximum (Nicholson & Grist, 2001). Some of the simple models used to argue that an abrupt failure of monsoons will occur in response to climate forcings can only represent changes in monsoon intensity, and fail to include such well-observed spatial shifts or changes in duration (Bathiany et al., 2018; Levermann et al., 2009).

Paleoclimate proxies provide abundant evidence for sudden changes in annual mean rainfall in several monsoon regions, although the meaning of "abrupt" and the drivers of these changes require careful consideration before they can be used as analogs for future climate change. These proxies include not only stable isotopes, but easier to interpret quantities such as pollen concentrations, lake levels, sediment deposition rates, and macrofossils (COHMAP Members, 1988). The West African monsoon is a well-studied example, with many proxies indicating a step-like beginning and end to the African Humid Period, which comprised a large expansion of rainfall across the Sahara concurrent with the changes in Earth's orbit that brought more intense boreal summer insolation roughly 6,000 to 15,000 years ago (deMenocal et al., 2000; Gasse, 2000). Compared to some anthropogenic forcings, such as increases in greenhouse gas concentrations which exert an order 4 W m^{-2} radiative forcing that is relatively uniform in space, this mid-Holocene insolation anomaly was large in magnitude and non-uniform, peaking at 30 W m^{-2} near the North Pole but absent at the South Pole, thus likely more efficiently driving thermally direct circulations such as monsoons by enhancing the meridional gradient of insolation. This insolation forcing intensified and then decayed over thousands of years, while proxy time series show North African hydrology responding over centuries or even decades, which is comparatively fast (Adkins et al., 2006). However, it remains unclear whether these potentially abrupt changes manifested simultaneously over most of North Africa or occurred sequentially at different latitudes as the narrow summer-mean monsoon rain band gradually shifted north-south in response to the insolation forcing. McGee et al. (2013) found that past changes in dust deposition off Africa's west coast were consistent with synchronous changes in dust across all of northern Africa, suggesting a truly rapid expansion and contraction of the West African monsoon. In contrast, Shanahan et al. (2015) found that hydrogen isotopes in leaf waxes indicated precipitation changes that were only locally abrupt at the end of the African Humid Period, occurring at progressively later times at lower latitudes as the rain belt presumably withdrew gradually toward the equator.

Potentially abrupt changes exist in the proxy records of other paleo monsoons, with related questions regarding locality and relevance for future climate change. For example, high-resolution time series of isotopes in cave deposits extend the record of the East Asian monsoon hundreds of thousands of years into the past, showing step-like responses over many cycles of the smooth, sinusoidal insolation forcing (Y. Wang et al., 2008). However, the East Asian monsoon is distinct from the tropical monsoons discussed in this section, being governed by midlatitude jet stream dynamics (Liang & Wang, 1998; Sampe & Xie, 2010); changes in cave isotopes in East Asia may furthermore indicate changing isotopic fractionation in remote regions thousands of kilometers away, or changes in the source regions of water vapor fluxes (J.-E. Lee et al., 2012; B. A. Maher, 2008; Pausata et al., 2011). Another example is the abrupt change in the South Asian monsoon argued to have occurred in response to geologic uplift of the Tibetan Plateau, with the forcing evolving over millions of years and much debate about the physical meaning of proxies (Molnar, Boos, & Battisti, 2010).

2.6.3. Proposed Mechanisms for Abrupt Changes in Monsoons

Although mechanisms for the abrupt seasonal onset of monsoons have been studied for decades (Numaguti, 1995; Plumb & Hou, 1992; Xie & Saiki, 1999), most recent arguments for monsoons being a tipping element of the climate system have focused on a particular moisture-advection feedback (Zickfeld et al., 2005). In this feedback, water vapor is transported from ocean to warmer and drier land in the thermally direct monsoon circulation; as the water vapor condenses in rising air over land, the latent heat release reinforces the existing land-sea temperature contrast, strengthening the circulation in a self-reinforcing dynamic (Levermann et al., 2009). Anthropogenic aerosol emissions or land use shifts could increase regional albedo, causing cooling over land that weakens the temperature gradient and disrupts the moisture-advection feedback, causing the monsoon to abruptly shift into a dry state (Zickfeld et al., 2005). This tipping point was proposed to exist at a regional albedo of 0.5, with land use change and aerosol emissions over South Asia possibly increasing albedo to that threshold (Lenton et al., 2008; Zickfeld et al., 2005). Studies have explored potential humidity thresholds for this feedback, arguing that past variations in humidity over ocean allowed the feedback to cause abrupt changes in paleo monsoons (Schewe et al., 2012).

The existence of this moisture-advection feedback on monsoon strength has been disputed, because the simple box model used to mathematically formulate the feedback omitted the fact that atmospheric temperature drops as air rises along an adiabat (Seshadri, 2017). Other authors made a consistent criticism (Boos & Storelvmo, 2016b), noting that the moisture-advection feedback model omits the static stability of the troposphere; adding that stabilizing term to the model equations resulted in a continuous and nearly linear response

to forcings. Although (Levermann et al., 2016) asserted in response that this static stability is insufficient to counteract the moisture-advection feedback, pointing to paleoclimate evidence of abrupt monsoonal transitions, static stability has been shown in decades of research to balance high-amplitude atmospheric heatings (Boos & Storelvmo, 2016a), and the occurrence of abrupt shifts in paleo monsoons does not imply the existence of a moisture-advection feedback (see previous subsection). Setting aside arguments about the formulation of simple box models, Boos and Storelvmo (2016b) showed that, in an ensemble of global climate model simulations, no abrupt transitions, hysteresis, or other behavior characteristic of tipping points occurred when the South Asian monsoon was subject to a wide range of greenhouse gas, surface albedo, and aerosol forcings. Furthermore, the proposed moisture-advection feedback for abrupt monsoon transitions is similar in formulation to the moisture-convergence feedback proposed as the cause of hurricanes in the 1960s (Charney & Eliassen, 1964) and later shown to fail in producing realistic simulations of those storms by unrealistically producing the most rapid amplification at the smallest length scales (Yanai, 1964). A review of tropical atmospheric dynamics called the idea that low-level moisture convergence causes precipitation and latent heating "an influential and lengthy dead-end road in atmospheric science" (Emanuel et al., 1994). This does not mean that atmospheric moist dynamics are incapable of causing nonlinear, abrupt changes: Dixit et al. (2018) used idealized heatings in a global climate model to argue that dry air advection from the Sahara suppresses West African rainfall in the modern climate, and that a northward shift of that rainfall in response to the mid-Holocene insolation forcing might have shutdown that dry air advection and produced nonlinear intensification of the West African monsoon. Seshadri (2017) found bifurcations indicative of tipping points when varying the parameters of a simple box model of monsoons, but noted that it was important to determine whether those parameter values were realistic.

Although recent discussion of monsoon tipping points has focused on a moisture-advection feedback (Lenton et al., 2008), the most well-known mechanism for abrupt monsoon change may be the desert-albedo feedback proposed by Charney (1975) in the context of intense drought in the Sahel that started in the late 1960s. That feedback is biogeophysical in nature, with reduced rainfall causing drying and vegetation destruction over land with a consequent increase in land surface albedo, which in turn reduces absorbed sunlight and thus the radiative forcing for monsoon rainfall (Charney, 1975). This idea led to the Sahel and other drylands being thought of as fragile systems prone to nonlinear feedbacks, with modest degradation in vegetation cover prone to push those systems into a new, desert equilibrium (Biasutti, 2019). However, observed association of the Sahel drought of the 1970s and 1980s with decadal variations in SSTs, together with global climate model simulations, led to remote ocean temperature variations now being widely regarded as the cause of that drought (Folland et al., 1986; Giannini et al., 2003). Feedbacks between vegetation and precipitation are now regarded as a possible amplifier of the remote oceanic forcing of the 1970s–1980s drought and are thought to be critical for producing the vast expansion of precipitation across the Sahara during the African Humid Period roughly 6,000 years ago (Biasutti, 2016, 2019; Boos & Korty, 2016; Hopcroft & Valdes, 2021). Quantitative understanding of such biogeophysical feedbacks remains a research frontier (National Research Council, 2013), with parameterization of the vegetation component in climate models being a major area of research and development (Fisher et al., 2018). Although some have argued that a feedback between vegetation and precipitation may create a tipping point in the West African monsoon that would cause grasslands to reduce the area of the Sahara desert at a rate of 10% per decade (Claussen et al., 2003; Lenton et al., 2008), the state of both knowledge and numerical model representations of such feedbacks provides low confidence in such claims.

2.6.4. Monsoon Response to Abrupt Changes in Other Earth Systems

Monsoons might undergo abrupt changes not because of their own internal, nonlinear dynamics, but because they are forced by large amplitude, abrupt changes in some other element of the Earth system. A canonical example is the abrupt variation of monsoons during the last ice age, thought to occur synchronously across multiple continents in response to rapid temperature variations in the Northern Hemisphere that took place during Dansgaard-Oschger events and also during Heinrich events (Dansgaard et al., 1993; Heinrich, 1988; Schulz et al., 1998; Y. J. Wang et al., 2001). In Heinrich events, for example, large discharges of fresh ice from the Laurentide ice sheet into the North Atlantic are hypothesized to have been associated with slowing of the AMOC and cooling of the entire northern hemisphere, resulting in a shift of tropical precipitation maxima southward to dry and weaken the West African and South Asian summer monsoons while enhancing South American monsoon precipitation (Chiang & Bitz, 2005; Deplazes et al., 2013; Schneider et al., 2014; X. Wang et al., 2004). In these sorts of scenarios, monsoons may be responding predictably and even linearly to the abrupt forcing of extratropical climate; synchronous changes in insolation may "pace" or "trigger" these changes (Cheng et al., 2016), but

Table 8
Section Summary Box Synthesizing the Forcing Mechanism, Response Behavior, Reversibility, and Classification of Tropical Seasonal Monsoon Regime Shifts

	Classification	Mechanism	Irreversibility
Tropical seasonal monsoon regime shifts	Non-tipping element Some research has proposed abrupt monsoon regime shifts via moisture-advection and desert-albedo feedbacks (e.g., Charney, 1975; Levermann et al., 2009; Schewe et al., 2012; Zickfeld et al., 2005). However, majority of research suggests gradual increase in seasonal mean rainfall in response to increasing climate forcing (e.g., Boos & Storelvmo, 2016a; Z. Chen et al., 2020; C. Jin et al., 2020; Ranasinghe et al., 2021; Seshadri, 2017). Biogeophysical feedbacks remain an area of uncertainty (Fisher et al., 2018)	Changes in land use and anthropogenic aerosol emissions over land proposed to affect land-sea temperature contrast, disrupting water vapor transportation (e.g., Levermann et al., 2009; Schewe et al., 2012; Zickfeld et al., 2005), but omits key stabilizing factors (Boos & Storelvmo, 2016a, 2016b)	Reversible (Ranasinghe et al., 2021)

the nonlinear response may originate in midlatitude ocean-atmosphere dynamics. Such scenarios bear important lessons for the possible response of monsoons to abrupt changes in the Greenland or Antarctic ice sheets or the Atlantic Meridional Overturning Circulation.

2.6.5. Synthesis and More General Projections of Monsoon Change

Overall, mechanisms for abrupt monsoon regime change in response to global warming remain a topic of active discussion, in part because such changes, even if extremely unlikely, could have catastrophic societal impact. Nevertheless, definitive evidence for the abrupt response of monsoons to gradual forcings remains elusive (Table 8). This is not to imply that large, gradual, and high-impact changes in monsoons are unlikely to occur; many analyses of the CMIP model projections that are performed periodically for IPCC reports indicate coming changes in many regional monsoons (Douville et al., 2021; Ranasinghe et al., 2021). In the latest collection of such models (CMIP6), there is general agreement that annual mean rainfall will very likely increase over most of the Asian and African monsoon domains over the next century, but will likely decrease in the core North American monsoon region (C. Jin et al., 2020; B. Wang, Jin, & Liu, 2020). Future changes in South American and Australian monsoon precipitation are of lower confidence in these models. Projected changes in seasonal-mean precipitation generally increase in magnitude with the strength of the greenhouse gas forcing (Z. Chen et al., 2020; C. Jin et al., 2020), providing no obvious indication of strongly nonlinear or tipping element behavior in the models. Subseasonal variability in precipitation is also expected to increase in nearly all monsoon regions, with an increase in the intensity and frequency of precipitation extremes accompanying enhanced drought risk in some areas (B. Wang, Jin, & Liu, 2020). Such changes will cause large socio-economic impacts even in the absence of tipping points (Shaw et al., 2022; Trisos et al., 2022).

2.7. Catastrophic Warming Due To Breakup of Stratocumulus Cloud Decks

2.7.1. Background

Stratocumulus cloud decks are horizontally extensive layers of shallow clouds, covering some 20% of low-latitude oceans (Eastman et al., 2011) and playing an important role in the global energy balance. These wide swaths of cloud cover reflect 30%–60% of incoming shortwave solar radiation (Wood, 2012), in contrast to the high absorptivity of exposed open ocean waters. Accurate representation of cloud dynamics have remained a weakness of large-scale climate models, resulting in uncertainties arising from parameterizations of cloud processes (Lin et al., 2014; Nam et al., 2012). Such challenges have persisted despite the considerable importance of clouds to Earth's radiative balance. Clouds' relatively fast response to CO_2 effects and rising temperatures could potentially drive large changes in radiative forcing (Caballero & Huber, 2013).

One recent paper proposed that under high CO_2 emissions scenarios (1,200 ppm CO_2-equivalents in radiative forcing terms), a climate feedback may occur in which stratocumulus cloud decks disintegrate, triggering rapid and substantial warming of 8°C globally (Schneider et al., 2019). Stratocumulus cloud decks are maintained by temperature and moisture-driven mechanisms that are in turn affected by atmospheric radiative forcing and surface
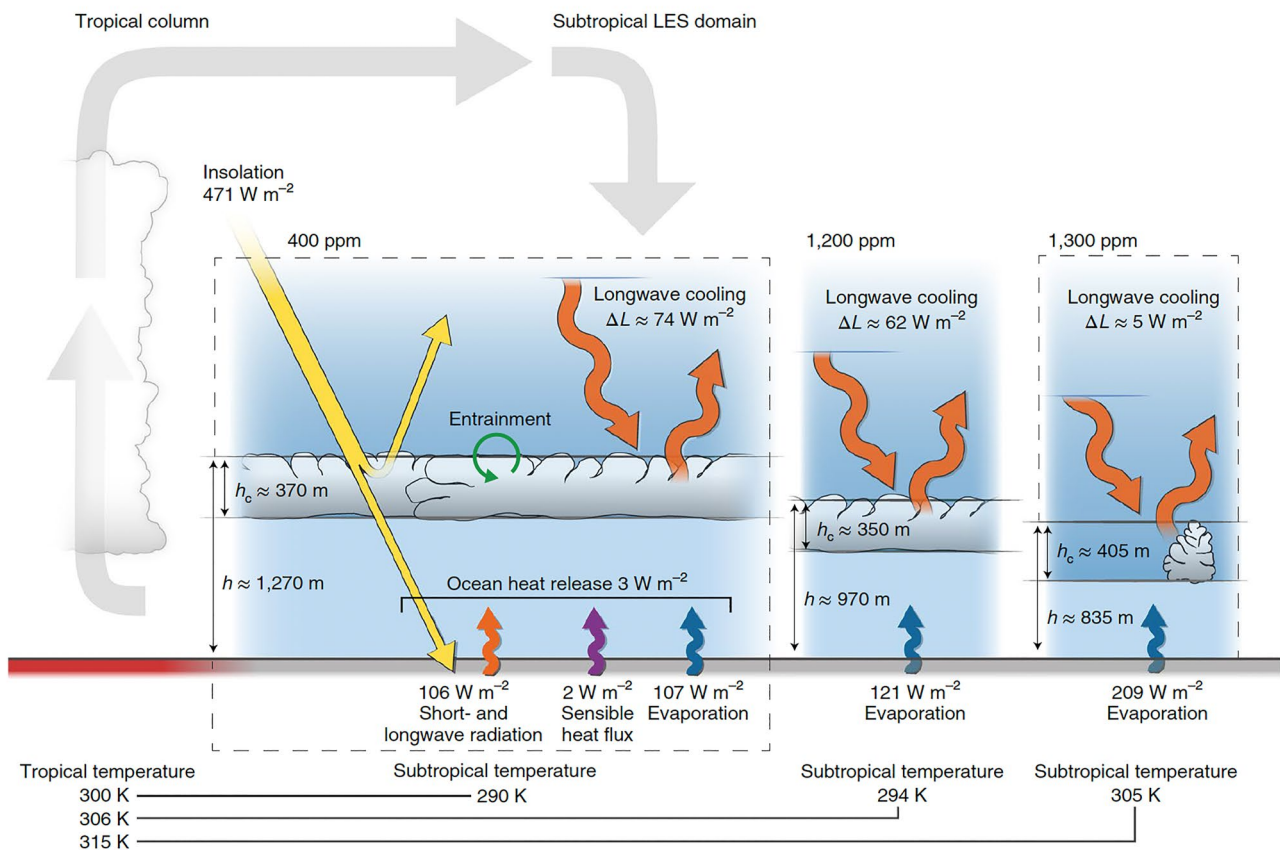
Figure 11. Schematic diagram illustrating mechanisms of stratocumulus cloud deck collapse and resulting consequences upon net radiative energy balance. Under present-day conditions (400 ppm), stratocumulus cloud decks are sustained by longwave radiative cooling at their topmost extents, which drives convective circulation that resupplies moisture to the cloud layer from the ocean's surface. Increasing greenhouse gas concentrations (1,200 ppm) increase the input of longwave radiation to stratocumulus clouds from above, reducing the strength of longwave cooling. Beyond a certain threshold of greenhouse gas levels (1,300 ppm), longwave cooling weakens to the point where cloud decks are cut off from surface moisture, leading to their disintegration and abrupt, acute surface warming from increased absorption of sunlight. Figure originally published in Schneider et al. (2019).

warming. Stratocumulus cloud deck breakup has been proposed to occur when greenhouse gas-induced weakening of radiative cooling at the top of cloud layers disconnects cloud decks from their surface moisture supply, which in combination with elevated fluxes of warm, dry air across the temperature inversion at the top of the boundary layer causes cloud deck evaporation and breakup.

This climate feedback remains an emerging theory, presented in just a couple research publications to date. At this time of publication, virtually no follow-up research has robustly explored this hypothesis under different model conditions. The underlying principles of the mechanisms involved, in which weakened radiative cooling decouples clouds from moisture inputs, are well-established (Bretherton & Wyant, 1997), providing some theoretical grounding for this hypothesis. Nevertheless, the significant temperature increase that would accompany stratocumulus cloud deck evaporation justifies further research attention to this potentially abrupt tipping element.

2.7.2. Mechanisms of Stratocumulus Cloud Deck Evaporation

Stratocumulus cloud decks over the subtropical ocean are maintained thanks to a self-sustaining feedback in which emission of longwave radiation from cloud tops plays an important role (Figure 11). Clouds have a high ability to absorb longwave radiation relative to free air. Consequently, re-emission of longwave radiation from cloud tops cools stratocumulus cloud banks from above, fueling convective circulation that supplies these cloud formations with moisture from near-surface air over the ocean (Wood, 2012). Using a high-resolution large-eddy simulation of a representative summertime subtropical ocean region, Schneider et al. (2019) determined that a sufficiently high concentration of atmospheric greenhouse gases could induce rapid disintegration of stratocumulus cloud

decks by upsetting this self-sustaining feedback, potentially over short timescales. However, the authors did not directly model this mechanism in action at the global scale.

A high greenhouse gas concentration increases the opacity of the air above stratocumulus cloud decks to longwave radiation. This effect increases the downwelling longwave radiative flux from the overlying atmosphere, reducing the difference between this flux and the stronger upwelling radiative flux from the cloud heights. Radiative cooling at the cloud tops weakens with increasing CO_2 concentrations, potentially losing the strength required to drive convection of air parcels to the ocean's surface. At the same time, increased surface evaporation due to GHG-induced warming strengthens turbulence generated by latent heat release from condensation in clouds. This drives greater turbulent entrainment of warm, dry air across the tropospheric temperature inversion (the altitude at which temperature stops decreasing with increasing height in the lower atmosphere, beyond which temperatures warm with altitude) (Mellado, 2017). This second feedback could also reduce the stability of stratocumulus decks at higher CO_2 concentrations.

Together, these two factors drive observed breakup of stratocumulus cloud decks today (Bretherton & Wyant, 1997), and both mechanisms are expected to intensify with continued CO_2 emissions. Schneider et al. (2019) found that cloud deck collapse for the modeled domain occurred at >1,200 ppm CO_2-eq (in radiative forcing terms), with continuous cloud banks replaced by scattered cumulus clouds. At larger scale, breakup of stratocumulus cloud decks could remove significant cloud cover over some ocean regions, increasing marine absorption of solar radiation and triggering substantial warming. The authors estimated that resulting changes to the Earth's energy balance could increase global surface temperatures by 8°C, with warming of up to 10°C in subtropical regions.

At lower CO_2-eq concentrations of 400–800 ppm, cloud cover remained dense at present levels, albeit with reduced water content. Once collapse was initiated, however, the abovementioned feedbacks rapidly self-amplify with the loss of cloud cover, perhaps starting from the edges of stratocumulus regions where cloud decks are closer to stability thresholds. However, because of the limited model scope, and since cloud decks in different regions do not share the same proximity to the stability threshold, it remains unclear how abrupt a process cloud deck breakup would be at a global scale.

The authors further highlight a potential mediating mechanism reducing the likelihood of collapse in which weakening of large-scale subsidence in the troposphere with continued warming may somewhat buttress the effect of increasing cloud deck instability (Blossey et al., 2013; Bretherton, 2015; Held & Soden, 2006; Tan et al., 2017).

Schneider et al. further modeled a lagging, hysteresis-like recovery pattern for stratocumulus decks. Cloud banks may only re-form after CO_2 levels drop significantly below the original triggering threshold to nearly pre-industrial levels (<300 ppm CO_2-eq). A subsequent analysis by the same group suggests even sustained large-scale solar geoengineering would not fully prevent stratocumulus cloud deck evaporation from taking place, merely raising the requisite critical threshold to 1,700 ppm CO_2-eq (Schneider et al., 2020).

This hypothesized tipping element remains a novel problem that has only been identified recently by a single research group. The greenhouse gas concentrations required to initiate stratocumulus cloud deck evaporation (~1,200 ppm CO_2 equivalent) are high, at the upper limit of potential greenhouse gas concentrations in 2100 under RCP8.5. Concentration thresholds required to trigger the stratocumulus cloud deck phenomenon may not be reached this century. However, potential uncertainty regarding critical CO_2 thresholds reinforces the need for additional research.

The response of stratocumulus cloud decks also represents just one of several potential interactions between clouds and climate forcing, including Hadley circulation-driven changes to cloud cover and shifts in midlatitude storm tracks (Bender et al., 2012; Caballero & Huber, 2013). Further efforts are required to investigate this potential climate feedback in detail and better assess the conditions that may trigger cloud deck disintegration or other large-scale changes in cloud forcing (Table 9).

Table 9
Section Summary Box Synthesizing the Forcing Mechanism, Response Behavior, Reversibility, and Classification of Stratocumulus Cloud Deck Breakup

	Classification	Mechanism	Irreversibility
Stratocumulus cloud deck breakup	Proposed tipping element with critical threshold behavior and hysteresis (Schneider et al., 2019). Remains a novel hypothesis in need of further substantiation	Increased greenhouse gas concentrations weaken radiative cooling at the top of cloud layers, causing threshold-like decoupling of cloud decks from surface moisture	Irreversible

3. Regional Candidate Tipping Elements

3.1. Continued Die-Off of Tropical, Shallow-Dwelling Coral Reefs

3.1.1. Background

Coral reefs are among the most productive and ecologically diverse marine ecosystems worldwide, with their biodiversity collapse potentially driving further uncertainty and unanticipated shifts in regional marine ecology, function and resources. Strong scientific evidence points toward critical temperature tipping points beyond which tropical coral reefs undergo severe ecosystem shocks. Shallow, tropical scleractinians (hard, reef-building corals) demonstrate high sensitivity to temperatures outside of their accustomed range, and are additionally under stress due to increasing trends in overexploitation of resources, land-based pollution (i.e., effluence, agricultural run-off, and microplastics), ocean acidification, and deoxygenation (Bindoff et al., 2019). Temperature anomalies are a very strong predictor of coral bleaching (Sully et al., 2019), a phenomenon in which the obligate symbiosis between corals and its photosynthetic dinoflagellate microalgae decouples. As these photosynthetic dinoflagellates of the *Symbiodiniaceae* family provide corals with up to 90% of their energy requirements, the loss of these symbionts for a prolonged period can lead to starvation, reproductive impairment, susceptibility to diseases, and death.

While shallow tropical corals undergo daily environmental fluctuations and have survived substantial evolutionary pressures over the course of geologic history, the current rate of ecosystem change presents a serious threat. As marine heatwaves affect tropical coral reefs worldwide (Baker et al., 2008; Heron et al., 2016; M. D. Spalding & Brown, 2015), coupled with the increasing rate of mean ocean temperature rise (Bindoff et al., 2019), the outlook for functional coral reefs appears grim. Along with more frequent localized events in response to particularly high sea temperature anomalies, researchers have documented three large global-scale coral bleaching events since the 1980s (1998, 2010, and 2014–2017) driven heavily by El Niño events (Eakin et al., 2019; Heron et al., 2016) with a fourth global bleaching event likely to occur within the next decade or two (Hughes et al., 2017). Notably, the 2014–2017 event began with heat stresses that preceded the arrival of El Niño in 2015 and ultimately coincided with negative and neutral phases of the El Niño–Southern Oscillation as well, indicating that large bleaching could occur outside of El Niño conditions (Eakin et al., 2019).

Even for a relatively moderate warming scenario, reef organisms would need to demonstrate the ability to acclimatize and adapt to a temperature change of more than 2°C by the late 21st century, a pace of adaptation likely too extreme for these ecosystems to match (Donner et al., 2005; Laufkötter et al., 2020; Putnam, 2021). The current body of research consequently shows strong agreement that the majority of tropical coral reef ecosystems will see sharp declines in biodiversity within the coming decades (Bindoff et al., 2019; Descombes et al., 2015).

The economic and societal impacts of coral reef loss to Indo-Pacific, Caribbean, and other communities can be expected to be substantial as an estimated 500 million people rely on coral reef ecosystems. Coral reefs serve as critical factors for fishery productivity that sustains island communities and fisheries, hold cultural significance, and provide shoreline fortification from coastal erosion (Ferrario et al., 2014; Storlazzi et al., 2019). Many small island nations have become dependent upon economic activity provided by coastal tourism, which existing reef ecosystems play a strong role in attracting (M. Spalding et al., 2017; Weatherdon et al., 2016). Degradation of warm-water coral ecosystems thus represents a direct threat to island nations and coastal communities across the Asia-Pacific region, endangering their food security, economic well-being, and resilience to sea-level rise and extreme weather events (Shaw et al., 2022).

3.1.2. Ongoing and Projected Temperature Stresses and Amplified Ocean Acidification Will Drive Major Loss of Coral Reefs Within This Century

Coral bleaching events in response to elevated temperatures have been repeatedly documented (Hughes et al., 2017; Wernberg et al., 2015). Four to six week-long periods where water temperature remains +1°C warmer than the average long-term summer maximum can cause bleaching and high mortality (Jokiel & Coles, 1990). Significant long-term declines in coral abundance have already occurred in tropical coral regions, including the Caribbean (Gardner et al., 2003; J. B. C. Jackson et al., 2014), the Indo-Pacific region (Bruno & Selig, 2007), and the Great Barrier Reef (De'Ath et al., 2012) due to overfishing, hurricanes, disease outbreaks, and severe bleaching events. The severity of bleaching events is further observed to be increasing over time, becoming the most prevalent threat to coral reefs (De'Ath et al., 2012; Hughes et al., 2018).

Coral reef ecosystems have demonstrated a limited ability to adapt to temperature stress and rebound once conditions improve (Brown et al., 2002; Coles & Brown, 2003; Jury & Toonen, 2019), with observations of subsequent coral bleaching events being triggered at higher temperatures than previous bleaching episodes (Ritson-Williams & Gates, 2020; Sully et al., 2019). In the geologic record, dominant reef-building corals have shown variable responses to previous mass extinction events, with numerous genera going extinct while some remained resilient and survived substantial extinctions of marine life (Birkeland, 2019). Past histories of thermal stress, the influence of non-thermal factors, and spatial and temporal heterogeneity of temperature deviations from mean local conditions may also make coral bleaching behavior more complex than predictions based on metrics using temperature exposures above a threshold (McClanahan et al., 2019). Coral reef ecosystems can recover following mass mortality events, replacing the loss of coral cover and diversity in a decade or more (M. D. Spalding & Brown, 2015). However, further warming is strongly anticipated to outpace the adaptive capacity of corals and time required for recovery (Frieler et al., 2013; Hoegh-Guldberg et al., 2007; Hughes, Kerry, Baird, et al., 2019; Veron et al., 2009). Furthermore, the capacity to adapt may be limited to just a small subset of coral species and associated marine organisms, severely thinning the biodiversity commonly found in coral reef ecosystems (Heinze et al., 2015; Hughes, Kerry, Connolly, et al., 2019; van der Zande et al., 2020).

The pace of current and future ocean warming will intensify pressures on corals. Over the past 30 years, global mean sea surface temperatures have risen by 0.015°C per year, with this rate projected to accelerate to an average of 0.027°C per year between 1990 and 2090 (Bopp et al., 2013). Under a mean temperature increase of 3°C globally, modelers anticipate bleaching occurring as often as annually or biannually for most reef ecosystems within 30–50 years (Donner et al., 2005; Laufkötter et al., 2020). The potential for warmer waters to alter hurricane intensity and frequency also carries implications for coral ecosystems that can suffer physical destruction, particularly if already under physiological stress (Steneck et al., 2019).

Ongoing ocean acidification represents another important stressor, with mean surface ocean pH declining at a rate of 0.018 units per decade across 70% of ocean biomes (Lauvset et al., 2015). The IPCC assigns near-certainty to the likelihood of continued surface ocean acidification, with a decline in pH of 0.287–0.29 pH units by 2081–2100 relative to 2006–2015 under the RCP8.5 emissions pathway (Bindoff et al., 2019). Even under the more optimistic RCP2.6 scenario, marine pH declines over the same period by 0.036–0.042. Lower pH requires higher energetic costs for reef-building corals to build their calcium carbonate skeletons, while also subjecting dead corals that serve as the foundation for living reef structure to accelerated dissolution and erosion (DeCarlo et al., 2015; Silbiger et al., 2014). While not within the scope of this review, ocean acidification also impacts the physiology of other marine calcifying organisms (e.g., Beaufort et al., 2011; de Moel et al., 2009; Mostofa et al., 2016; Moy et al., 2009; Wittmann & Pörtner, 2013). Numerous observational studies have confirmed the ongoing negative impacts of ocean acidification upon reef habitats and project continued deterioration of corals with further increases in atmospheric CO_2 concentration (Bove et al., 2019; Jiang et al., 2018; Kroeker et al., 2010; Mollica et al., 2018; Orr et al., 2005). Continued ocean acidification in conjunction with marine heatwaves is anticipated to further degrade reef function due to declines in coral photosynthesis, calcification, reproduction, and overall survival (Klein et al., 2022).

Simultaneously, sea-level rise presents an additional threat to shallow-dwelling reefs through inundation, as waters rise faster than the reefs can grow upwards toward light (Perry et al., 2018). Paleo-evidence shows that some reefs were unable to keep pace with rising seas and "drowned" during past de-glacial periods with rapid sea-level rise, as reviewed in Woodroffe and Webster (2014). Many coral reefs are also directly subject to human-induced negative impacts such as increased sediment runoff, chemical pollution, nutrient-fueled harmful algal blooms, and damage from fishing activities including dynamite fishing (L. Burke et al., 2011; B. S. Halpern et al., 2015; Hodgson, 1999). Nutrient pollution (DeCarlo et al., 2020; Donovan et al., 2020), competition with macroalgae (Anton et al., 2020), and marine de-oxygenation also pose threats to reef systems (Bindoff et al., 2019).

Research results demonstrate strong agreement that severe coral reef degradation will likely continue throughout the current century even under optimistic climate mitigation scenarios, with coral abundance declining to 10%–30% of today's levels even with warming limited to 1.5°C (Hoegh-Guldberg et al., 2019). A recent analysis suggests that even warming of 1.5°C in CMIP6 models may shrink the extent of current refugia insulated from thermal stress to just 0.2% of current coral reef areas (Dixon et al., 2022). Warming of 2–2.5°C, well within

Table 10
Section Summary Box Synthesizing the Forcing Mechanism, Response Behavior, Reversibility, and Classification of Tropical, Shallow Coral Reef Die-Off

	Classification	Mechanism	Irreversibility
Tropical, shallow coral reef die-off	Tipping element. Local and regional tipping points for severe, recurrent coral bleaching well beyond ecosystem capacity to adapt and recover to present-day state (e.g., Dixon et al., 2022; Eakin et al., 2019; Frieler et al., 2013; Hoegh-Guldberg et al., 2018; Schleussner et al., 2016)	Increased ocean temperatures and more frequent marine heatwaves cause coral bleaching and elevated mortality, in conjunction with other stressors like ocean acidification, sea-level rise, marine pollution, and other climate and anthropogenic impacts	Irreversible biodiversity loss

projections for the 21st century under current emissions rates, would certainly cross tipping points, eliminating >99% of reef-building tropical corals and irreversibly transforming coral reef ecosystems (Frieler et al., 2013; Hoegh-Guldberg, 2014a, 2014b; Hoegh-Guldberg et al., 2018; Hughes et al., 2017; Schleussner et al., 2016).

Currently, a future in which tropical corals undergo significant ecosystem transitions represents the most likely outcome in the absence of extremely aggressive emissions mitigation efforts that limit global warming to 1.5°C or less. Although tropical corals may persist in some form, with limited localities or regions potentially serving as refugia from climate forcing (Dixon et al., 2022; Guest et al., 2018; Mies et al., 2020; Wyatt et al., 2020), chances are high that future coral ecosystems may appear completely unrecognizable compared to their state today (Table 10). Given the considerable sensitivity of reef habitats to even modest temperature increases under strong climate mitigation scenarios, combined with the impact of multiple stressors like land-based pollution and ocean acidification, avoiding a future in which tropical coral reefs degrade is becoming less possible.

3.2. Loss of Amazon Rainforest and Conversion of Significant Rainforest Area to Savanna-Like Vegetation

3.2.1. Background

The Amazon region of South America contains the world's largest expanses of old-growth tropical rainforest. This large ecosystem possesses global importance, alone producing an estimated 15% of total terrestrial photo-synthesis worldwide (Field et al., 1998). The rainforest region possesses rich biodiversity and also represents a major terrestrial biological carbon sink of some 0.4–0.6 Gt C per year (Malhi et al., 2006; Y. Pan et al., 2011), a flux of similar magnitude to the ~0.5–0.6 Gt C per year sequestered by all northern boreal forests globally (Y. Pan et al., 2011; Schaphoff et al., 2013). The Amazon is also responsible for 8% of global methane emissions, of which 83% is attributable mainly to wetlands and 17% are derived from biomass burning (Basso et al., 2021). The Amazon rainforest additionally contains a substantial amount of stored carbon in biomass and soil organic matter, tentatively estimated to range between 150 and 200 Gt C (Cerri et al., 2007; Gibbs et al., 2007; Malhi et al., 2006; S. S. Saatchi et al., 2011). Between all of these factors, the Amazon rainforest represents a critical component of the global carbon cycle.

As with many of the world's major rainforests, a significant fraction of precipitation over the Amazon rainforest is recycled water originating from the rainforest vegetation itself. While on average recycled water accounts for some 25%–35% of total precipitation in the Amazon region (Da Rocha et al., 2009; Eltahir & Bras, 1994; Salati et al., 1979; Zeng et al., 1996), the contribution of recycled water to total rainfall increases during the dry season. In the dry season, recycling is the majority source of regional water vapor, and also plays a role in initiating the onset of the wet season (W. Li & Fu, 2004; Wright et al., 2017). Between 70% and 76% of the Amazonian forest's photosynthesis seasonality may be explained by seasonal variations of solar radiation, while between 13% and 29% is dependent upon precipitation in parts of the basin where rainfall is lower than 2,000 mm yr^{-1}, with remaining areas influenced by both factors (Bertani et al., 2017; F. H. Wagner et al., 2016, 2017). Consequently, dry season precipitation and length for the Amazon region are directly linked to the total area and health of the rainforest system itself.

In addition to pressure from climatic stress factors, these forests face a more imminent threat. It is estimated that the Amazon forest has lost close to 20% of its pre-1970 areal extent, and since 1985 human impacts on the Amazon have increased by 174%, affecting 131.6 ± 17.8 Mha in 2018 (Zalles et al., 2021). One estimate calculates a net carbon loss from aboveground biomass in the Amazon of 5 Gt C between 1996 and 2017 as a

result of deforestation and disturbance (Bullock & Woodcock, 2020). At its peak around 2005, deforestation rates approached 30,000 sq km of clearcut or burned forest per year. This fell to an average of 6,000 sq km lost per year between 2011 and 2015 and has remained low relative to early 2000s rates. However, since 2012, the Amazon rainforest is experiencing a new increase in the rate of deforestation, with a peak in 2020 (Silva Junior et al., 2021). Satellite observations suggest that large areas of the Amazon are also suffering degradation due to smaller-scale disturbances that could potentially drive high carbon loss such as fire, drought, selective logging, and firewood collection (Bullock et al., 2020).

Some research efforts have focused on the risk that vegetation losses could ultimately reduce recycled precipitation inputs across large portions of the Amazon basin to the point where large rainforest trees become subject to increased mortality due to the dry season lengthening (Boers et al., 2017; Nobre & Borma, 2009). As rising numbers of trees die due to water stress (Phillips et al., 2009), further reducing the strength of the regional water cycle, dieback of rainforest vegetation becomes a self-sustaining positive feedback, ultimately causing significant sections of the Amazon rainforest to collapse and potentially shift toward a savanna-like type of ecosystem (Lyra et al., 2016; Nobre & Borma, 2009). At the same time, increased forest degradation by wildfires, selective logging and fragmentation represent immediate rainforest threats (Aragão et al., 2018; Brando et al., 2019; Silva et al., 2020; Silva Junior et al., 2020), leading to a loss of many ecosystem services, including biodiversity and carbon storage (Castellanos et al., 2022).

On a medium time-scale, these rainforests could shift toward seasonal forest as opposed to savanna grasslands (Malhi et al., 2009), emphasizing uncertainties in the ability of models to predict seasonal precipitation (Good et al., 2013), and highlighting the potential for CO_2 fertilization to compensate for biomass losses (Cox et al., 2013; Huntingford et al., 2013). Such factors could mean that changes for the Amazon forest will be driven by local human and climate-forced conditions, rather than one climatic threshold that would homogeneously affect the entire biome.

Large-scale Amazon ecosystem shifts are likely in the absence of climate mitigation, would severely impact local populations by radically altering regional ecology and climate (Castellanos et al., 2022), and could influence climate patterns around the world. Such changes have been hypothesized to potentially occur within a relatively short time frame of around 50 years (K. H. Cook & Vizy, 2008; Fonseca et al., 2019; Lyra et al., 2016), significantly reducing the strength of the Amazon system as a terrestrial natural carbon sink and also releasing considerable quantities of stored carbon to the atmosphere via decomposition, wildfire, and land-use changes. In fact, it has been demonstrated that the Amazon actually turned into a CO_2 source during some years, notably during the extreme droughts from 2010 to 2018 (Gatti et al., 2021).

3.2.2. Substantial Evidence Indicates That Significant Regions of the Amazon Are at Risk of Dieback Caused by Fires and Drought

Both observations as well as modeling studies have proposed a critical threshold for Amazon forest dieback, although ongoing debate continues to discuss this hypothesis and contest whether the region will respond to deforestation and climate change as a biome-wide tipping element. For example, there are uncertainties regarding the extent to which forest photosynthesis, respiration, carbon stocks, and tree mortality are sensitive to temperature, precipitation, CO_2 fertilization and their interactions with forest heterogeneity, soil nutrient availability, and physical structure (Fleischer et al., 2019; Green et al., 2020; Huntingford et al., 2008; Rammig et al., 2015). These factors complicate the effort to precisely determine the boundaries of regional critical thresholds. Nevertheless, the general threat of regional ecosystem shifts driven by wildfires, drought, and deforestation is well agreed upon within the research community.

Water represents a key variable for assessing the Amazon's future. The Amazon rainforest typically receives annual precipitation of approximately 2,200 mm; the western reaches of the region receive the highest amount of rainfall (3,000 mm) thanks to the topographic influence of the Andes mountains (Salati & Vose, 1984), and these wettest portions of the rainforest are likely to survive even under drier conditions triggered by dieback. The lower limit of precipitation necessary to maintain a closed-canopy tropical rainforest sits at around 1,600 mm/yr (Hirota et al., 2011). The dry season, defined as when the rainfall is lower than evapotranspiration, varies from zero to 6 months in western to southern Amazonia, respectively (Berenguer et al., 2021). During the dry season, the Amazon region experiences a water deficit that is partially replenished by recharge during the wet season. Consequently, the twin factors of dry season severity and overall rainfall play central roles in maintaining existing rainforest cover (Malhi et al., 2009).

Changes in the seasonality of rainfall have already been observed. It has been demonstrated that the dry season length has increased over southern (R. Fu et al., 2013) and western (Espinoza et al., 2019) Amazonia, with an observed delay of the dry season's end and enhancement of the contrast between the dry and wet season (Anderson et al., 2018; Gatti et al., 2021). Moreover, the altered atmospheric moisture content of air passing over deforested areas results in less rain production relative to air passing over dense forests, leading to further projected rainfall reductions of 12% and 21% in wet season and dry season precipitation, respectively, across the Amazon by 2050 (Spracklen et al., 2012). For every percentage point increase in deforestation, the onset of the rainy season becomes delayed by 0.12–0.17 days (Leite-Filho et al., 2019, 2021) and 10% of additional forest loss induces a net reduction in annual rainfall of -49.2 ± 11.3 mm (Leite-Filho et al., 2021). Therefore, the rainfall cycle is already changing.

The southeastern Amazon basin currently experiences reduced rainfall relative to the rest of the basin, around 1,700 mm/yr—an effect that is attributed to higher intensity of land use (Salati & Vose, 1984). The frequency of drought events in the southern Amazon has also increased according to a study examining dry events from 1970 to 1999 (W. Li et al., 2008). Significant evidence suggests that the dry season has lengthened, particularly over the southern and southeastern Amazon (Dubreuil et al., 2012; R. Fu et al., 2013; Marengo et al., 2011). Observations have shown an increasing number of months with a cumulative water deficit and a rainier wet season in the southern region (Anderson et al., 2018), and an increase in temperature of 1.6–2.5°C from the west to south parts of the Amazon between the months of August and October over the last 40 years (Gatti et al., 2021). Moreover, extreme droughts have driven increased tree mortality (Anderson et al., 2010; Phillips et al., 2009, 2010), and exert long-lasting and cumulative effects on forest photosynthetic capacity (Anderson et al., 2018; S. Saatchi et al., 2013). CMIP6 models demonstrate general agreement that regional rainfall will continue to decline over the 21st century under unmitigated climate scenarios (Parsons, 2020). Substantial uncertainty characterizes modeled future precipitation changes for the region (Good et al., 2013; W. Li et al., 2006; Parsons, 2020) and models' ability to represent subsurface hydrological processes remains limited (Brodribb et al., 2020; National Research Council, 2013).

At the same time, multiple factors exert important influences over Amazon ecosystem health (Figure 12). Increasing regional temperatures due to both local and global drivers (P. D. Jones, 1994; Victoria et al., 1998) elevate potential evaporation and reduce humidity, increasing quantities of dry fuel and heightening fire risk (Burton et al., 2021; Cochrane & Barber, 2009; Cochrane & Schulze, 1999; Pueyo et al., 2010). The seasonality and magnitude of rainfall may change due to shifts in the El-Nino Southern Oscillation (Aragão et al., 2018), although predictions remain highly uncertain. Some research has suggested that elevated CO_2 concentrations may reduce the rate of stomatal leaf opening in trees, lowering evapotranspiration and thereby further weakening recycled precipitation (Lammertsma et al., 2011; A. P. Walker et al., 2014). Recent advances in soil-plant hydraulic modeling have also highlighted higher general potential vulnerability of forest ecosystems to drought than previously suggested by traditional ecological niche-based models (Brodribb et al., 2019, 2020; Martin-StPaul et al., 2017). While knowledge gaps remain regarding plant physiological modeling and the ability of trees to adapt or acclimate to long-term increases in temperature and water stress, such newer approaches are producing more rapid increases in tree mortality in response to climate-induced drought (Brodribb et al., 2020).

The influence of these diverse factors complicates efforts to more precisely define the critical boundaries to Amazon rainforest stability. A temperature increase of 3–4°C (Nobre et al., 2016), deforestation of >40% (Nobre et al., 2016), or precipitation decrease of 30%–40% (Lenton et al., 2008; Salazar & Nobre, 2010) each have been proposed as thresholds independently capable of initiating Amazon dieback according to models, but all three factors are currently occurring simultaneously with mutually reinforcing effects (Boers et al., 2017; Staal, Flores, et al., 2020). Based on rainfall levels corresponding to current rainforest extent, modeling of projected hydrological changes under high-emissions scenarios suggest the potential for committed Amazon tipping behavior by end-of-century driven by rainfall shifts alone (Staal, Fetzer, et al., 2020). Lovejoy and Nobre have proposed a deforestation extent of 20%–25% as the tipping point of savannization, suggesting that the current Amazon system already stands perilously close to a critical threshold (Lovejoy & Nobre, 2018), beyond which a strong self-sustaining water stress feedback will act to convert 50%–70% (K. H. Cook & Vizy, 2008; Lyra et al., 2016) of the region to a savanna-type ecosystem. These thresholds have been defined based on an intact forest perspective, but with the increased extent of human-modified forests negatively impacting forest function and reducing carbon stocks through fires, logging degradation, and edge effects from fragmentation (changes to flora, fauna, and microclimate from an increase in exposed forest edge) lower thresholds could even be considered. Overall, the
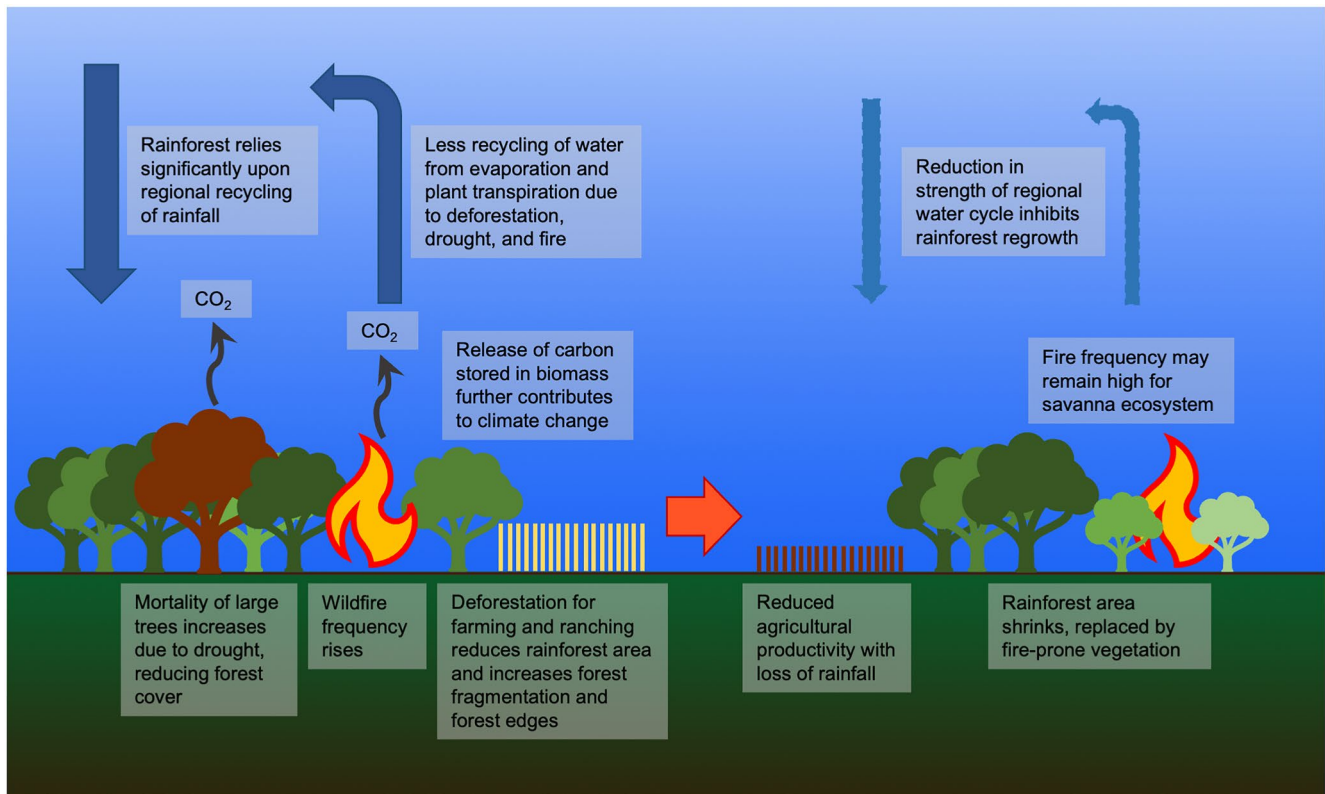
Figure 12. Schematic diagram of causes, feedbacks, and impacts associated with Amazon rainforest mortality.

IPCC AR6 WG1 report assigned low confidence to the crossing of a regional critical threshold before 2100, but emphasized that continued deforestation raises the probability of transgressing a threshold this century (Canadell et al., 2021).

Increases in wildfires as a result of drying play an immediate and serious role in driving forest loss (Brando et al., 2019). Field studies have indicated that while prolonged drought does eventually raise mortality rates for rainforest trees, this only occurred after the third consecutive year of a particularly intense simulated drought (Nepstad et al., 2007). In contrast, a forest fire during a drought period can kill half the adult trees in the affected area within a much shorter period (Balch et al., 2015; Brando et al., 2014; Nepstad et al., 1999). Recovery of fire-affected forest can require many decades, resulting in strong net CO_2 emissions from long-term reductions in carbon storage (Silva et al., 2020). Forest fire gross emissions alone during drought years (989 ± 504 Tg CO_2 year^{-1}) are more than half as great as carbon emissions from old-growth forest deforestation (Aragão et al., 2018). Tree mortality and reduced canopy cover caused by fire can in turn permit invasive, more fire-prone grasses to invade the forest floor, increasing the region's susceptibility to fire and driving conversion to grassland that primarily results from dryness and fire, not drought-induced water stress (Balch et al., 2015). A recent remote sensing study examining changes in aboveground biomass across Amazonia over the last decade supports the hypothesis that forest degradation may already drive more biomass loss than deforestation (Qin et al., 2021). A newly published aerial survey of carbon emissions over Amazonia concludes that southeastern Amazonia has transitioned to a net source of atmospheric carbon due to the effects of deforestation, fire, and shifts in regional climate (Gatti et al., 2021).

An increase by more than 200% in fire-induced tree mortality has been observed during a severe drought event, when high temperatures and fuel loads were higher than the long-term average, leading to a decline in canopy cover from 23% to 31% and in aboveground biomass from 12% to 30% and an increase in grasses in the forest edges (Brando et al., 2014). During 2007, a year with positive temperature anomalies, more than 11,000 km^2 of forests burned in the Amazon; during the extreme 2010 drought, over 5,000 km^2 burned and during the El Niño in 2015/16, over 9,000 km^2 of forests burned (Silva Junior et al., 2019). Estimates focused on southern Amazonian

forests suggest that 12% and 5% of forests in the Upper Xingu Region burned during 2007 and 2010 respectively (Brando et al., 2014). This extent of fire-affected forests, coupled with the increase in fragmentation (Silva Junior et al., 2021) is turning these forests into a different ecosystem state (Berenguer et al., 2014, 2021), with a long-term negative impact on its functioning (Silva et al., 2020).

3.2.3. Loss of Amazon Rainforest Could Occur Over Decades to a Century and Cause Important Climate, Human, and Ecosystem Impacts

According to the rainfall-driven dieback theory, after crossing a critical threshold, affected portions of the Amazon would undergo savannization over a timeframe of between several decades to a century (Lenton et al., 2008; Lovejoy & Nobre, 2018; Nepstad et al., 2008; Nobre & Borma, 2009; Nobre et al., 1991). Collapse begins with die-off of the largest trees as soil moisture becomes increasingly depleted (Ivanov et al., 2012; Nepstad et al., 2008), progressively thinning the forest canopy. This transition would likely be accompanied by intensification of wildfires as dead vegetation and drier conditions contribute toward higher fire risk (Brando et al., 2014; Cochrane & Barber, 2009; Cochrane & Schulze, 1999). A modeling study projects significant future increases in land area with a fire relative probability of 0.3 or greater under RCP4.5 emissions scenarios (+21.3% increase in area with FRP > 0.3), with substantially greater fire risk (+113.5% increase in area with FRP > 0.3) for a high-deforestation RCP8.5 scenario (Fonseca et al., 2019). This drought-fire feedback might in fact independently drive ecosystem shifts, dominating over impacts from water stress and resulting in a pattern of forest loss driven by more local factors as opposed to a biome-wide threshold (Balch et al., 2015; Brando et al., 2014, 2019). Once savannization or conversion to a more seasonal forest has occurred, significant hysteresis may inhibit the return of rainforest vegetation even over very long timescales, thanks to potentially more frequent fires and drier climate acting as conditions upon the vegetation's ability to regenerate dense tropical forest and large tree species. Paleoclimate evidence confirms that regrowth of rainforest cover often lagged significantly behind the return of wet conditions to South America during past periods of the Holocene (Ledru et al., 1998).

Degradation and areal reduction of the Amazon rainforest might even still occur under strong climate mitigation scenarios, with significant biomass losses possible at 1.5–2°C of warming (Hoegh-Guldberg et al., 2018). Deforestation can also drive fragmentation of forest landscapes, leading to forest degradation and significant carbon losses through edge effects (Silva Junior et al., 2020). For example, it has been estimated that edge effects created by forest fragmentation can contribute 63 ± 8 Tg C year^{-1} to emissions, corresponding to one-third of losses from deforestation for the 2001 to 2015 period (Silva Junior et al., 2020). However, forest management policy could act as a strong lever upon the Amazon's ecosystem health, with a halt to new deforestation potentially reducing burned area by 2050 by 30% and accompanying greenhouse gas emissions by 56% (Brando et al., 2019). Fire suppression also represents a potentially powerful tool to reduce rainforest loss by preventing positive feedbacks between fire and savannization. As the Amazon rainforest is naturally warm, forest litter decomposes rapidly and does not accumulate as it does in some temperate forests, meaning that aggressive fire suppression carries no risk of intensifying future fires.

Loss of large portions of the Amazon rainforest would carry significant implications for the strength of the Amazon carbon sink as well as the fate of the organic carbon within Amazon vegetative and soil biomass. Rainforest degradation could likely shift the Amazon region from a carbon sink of up to 0.6 Pg/yr (Malhi et al., 2006) to a potentially strong carbon source (Nobre & Borma, 2009), which has already been observed during some extreme dry or hot years (Gatti et al., 2021). Modeling of an Amazon rainforest dieback scenario under moderate emissions (713 ppm in 2100) produced an additional 0.3°C of warming globally as a result of rainforest loss (R. Betts et al., 2008).

Precise estimates of the carbon impact of Amazon dieback are subject to variability due to uncertainty regarding the potential extent of forest loss, the current size of the Amazon forest carbon pool, and potential timescales of change. A recent modeling analysis using CMIP6 rainfall projections under a high-end RCP8.5 emissions scenario found a large potential reduction in stable Amazon forest area of up to 3.27 million km^2 due to hydrological changes (Staal, Fetzer, et al., 2020). Under a RCP8.5 emissions pathway with continued deforestation, carbon dioxide emissions from intensifying fires were estimated to sum to 4.6 Gt by 2050 (Brando et al., 2019). However, carbon release as a result of forest fire can eventually be partially offset by recovery of vegetation within the burned areas (Silva et al., 2020). Carbon emissions from losses in forest area may also be potentially compensated for if the positive response of rainforest vegetation to increased carbon dioxide levels is large (strong CO_2 fertilization). As the effect of CO_2 fertilization upon plant growth remains highly uncertain, this complicates

Table 11
Section Summary Box Synthesizing the Forcing Mechanism, Response Behavior, Reversibility, and Classification of Amazon Rainforest Dieback

	Classification	Mechanism	Irreversibility
Amazon rainforest dieback	Tipping element. Large-scale changes in Amazon rainforest extent and ecology, with potentially abrupt local/regional ecosystem shifts (Balch et al., 2015; Boers et al., 2017; Brando et al., 2014, 2019; Nobre & Borma, 2009; Phillips et al., 2009; Silva Junior et al., 2020; Staal, Flores, et al., 2020)	Regional climate shifts increase drought, intensifying tree mortality and wildfires. Shrinking rainforest extent in conjunction with deforestation in turn reduces recycled precipitation	Conversion of rainforest area to more seasonal forest or savanna-like ecosystem may be irreversible on timescales of a century or more

efforts to estimate the overall carbon impact of the world's tropical forests as they respond to climate change (Cox et al., 2013; Huntingford et al., 2013). However, recent observational evidence strongly suggests that the CO_2 fertilization effect is nearing saturation in African tropical forests as well as the Amazon on faster-than-predicted timescales (Hubau et al., 2020).

Amazon rainforest loss possesses acute regional ramifications. Degradation of the rainforest represents a serious threat to the livelihoods and lifestyles of Indigenous Amazonian peoples (Castellanos et al., 2022). Total rainfall throughout the Amazon basin may generally fall following dieback and savannization, placing regional agriculture at risk (Arvor et al., 2014; Leite-Filho et al., 2021; Oliveira et al., 2013). A study has found that for 40% deforestation, hydroelectric power generation from major dams on the Xingu River is substantially reduced thanks to falling river runoff (Stickler et al., 2013). That said, the complexity of rainfall dynamics means that impacts depend strongly on the spatial pattern of forest loss (Lawrence & Vandecar, 2015). Increased wildfire frequency and severity will additionally put regional communities at risk and create air pollution crises. Finally, dieback of the Amazon rainforest will represent a major threat to the biodiversity of this region (Esquivel-Muelbert et al., 2017; Gomes et al., 2019).

The Amazon forest dieback scenario stands among the more imminent, likely, and fast-acting of the tipping elements discussed in this review. Forest management policy will prove key to determining the future of the Amazon, as evidenced by temporary and marginal reductions in the rate of deforestation relative to the high pace of loss seen in the early 2000s (Daniel et al., 2014). Under present pressures, however, the Amazon rainforest is facing serious threats this century, with significant regional and global consequences accompanying its degradation (Table 11).

3.3. Loss of Summer Arctic Sea Ice

3.3.1. Background

The shrinking of Arctic sea ice area over the late 20th and early 21st centuries has been clearly documented by observations of decreasing sea ice extent in all months and all regions of the Arctic (Figure 13) (Notz & Stroeve, 2018), with strong reductions in area during summer within both the Pacific and Eurasian sectors (Årthun et al., 2021; Fetterer et al., 2017; Onarheim et al., 2018; Stroeve, Kattsov, et al., 2012; Stroeve, Serreze, et al., 2012). While summer ice loss has been dramatic, departures from average conditions have been largest in the shoulder seasons (Stroeve & Notz, 2018), with October 2020 showing more than 3 million km^2 less sea ice than the 1981–2010 average, or a departure of more than 3.6 standard deviations. From 1997 to 2007, perennial or multi-year Arctic sea ice in March has shrunk by an area of 1.5 million km^2 (Nghiem et al., 2007). Since 2012 however, summer ice loss has stabilized somewhat, with a mean September extent of 4.60 + 0.52 million km^2. Nevertheless, reductions in sea ice extent over the observational record has outpaced older IPCC model projections (Stroeve et al., 2007). While the spatial extent of marginal sea ice—areas of the Arctic Ocean with partial ice cover—has remained relatively constant over the past 40 years, the width of the marginal ice zone and its proportion as a fraction of total sea ice are both increasing (Rolph et al., 2020).

The characteristics of Arctic sea ice have also shifted, with multi-year sea ice at least five years old falling from 30% of Arctic ice to just 2% between 1984 and 2019 while first-year sea ice has increased from 40% to 60%–70% of Arctic sea ice area (Stroeve & Notz, 2018). At the same time, mean winter multi-year ice thickness has declined
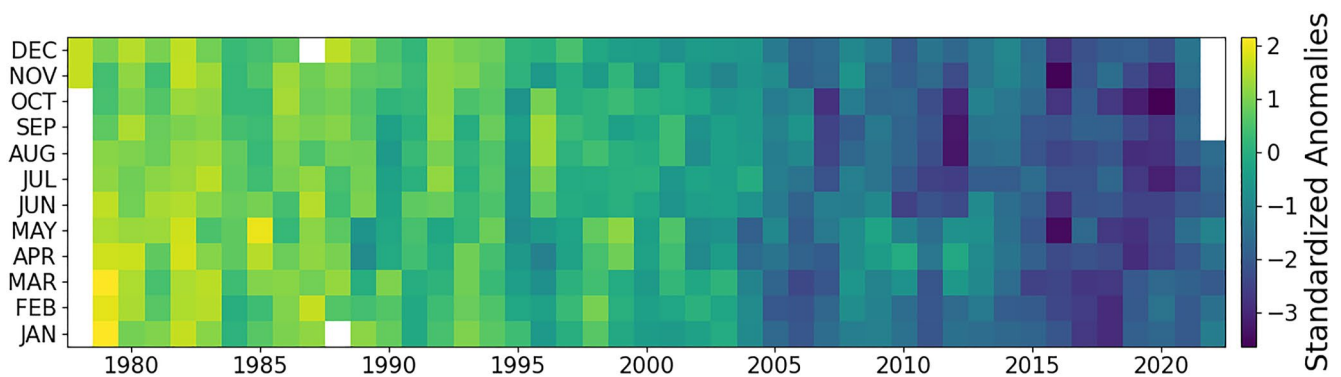
Figure 13. Hovmöller diagram showing standardized Arctic sea ice anomalies as observed over time, displayed as standard deviations relative to the 1981–2010 mean extent, as a function of year (*x*-axis) and month (*y*-axis).

from 3.6 to 1.9 m over a 30-year period from ∼1980 to 2010 (Kwok & Rothrock, 2009; Wadhams, 2012). As the Arctic ice cover thins, it becomes more vulnerable to anomalous atmospheric and/or oceanic forcing that can lead to rapid ice loss events, and a fast transition toward a seasonally ice free Arctic Ocean for example, (M. M. Holland et al., 2006; Vavrus et al., 2012).

The decline in Arctic sea ice is statistically attributable to a strong anthropogenic forcing from greenhouse gases (Notz & Marotzke, 2012), and also reflects profound changes in the timing of melt onset and autumn freeze-up (Notz & Stroeve, 2016, 2018). In addition to regional warming, several positive feedbacks are responsible for the rapid pace of shrinking sea ice extent. The well-known ice-albedo feedback, in which the melt-driven substitution of highly reflective sea ice for highly absorptive dark open ocean waters results in increased surface inputs of solar energy, contributes to further ice loss via ocean and lower atmospheric warming. Sea ice loss is marked by an increasing transition from multi-year to seasonal sea ice, which is thinner and therefore more vulnerable to melt (Haine & Martin, 2017). Reduced cooling from lowered summertime cloud cover may also be exerting a potential effect (Kay et al., 2008).

Other feedback processes such as earlier melt onset have enhanced the ice-albedo feedback (Stroeve, Kattsov, et al., 2012; Stroeve, Serreze, et al., 2012), increasing solar heat inputs across 85% of the Arctic region between 1979 and 2007 (Perovich et al., 2007) and driving a fast-paced increase in regional ocean temperatures of around 0.5 C per decade (Timmermans et al., 2017) that further melts summer ice cover. With larger areas of open water at the end of summer and increased ocean mixed-layer temperatures, autumn freeze-up is delayed as it takes time for the ocean to release the heat gained over summer back to the atmosphere. Thus, freeze-up trends largely drive the expanding open water period (e.g., Stroeve & Notz, 2018; Stroeve et al., 2014). Together, these factors contribute to "Arctic amplification" (M. M. Holland & Bitz, 2003) in which regional temperatures are increasing at a faster rate than elsewhere in the Northern Hemisphere (Serreze et al., 2009).

Some negative or stabilizing feedbacks do exist, moderating the pace of sea ice loss and may in part explain the last decade with no considerable summer ice loss compared to the prior decade. Thinner first-year sea ice grows more rapidly during periods of freezing, while ice-free areas lose heat to the atmosphere faster during winter, allowing thin ice cover to regrow quickly over large areas (Eisenman, 2012; Notz, 2009; Sturm & Massom, 2016; T. J. Wagner & Eisenman, 2015). While the later onset of freezing is a contributing factor to reduced sea ice extent, this shift in timing also limits snow accumulation that would otherwise insulate the ice and inhibit growth (Sturm & Massom, 2016). Indeed assessments of snow accumulation over sea ice suggest the snow is thinner than it used to be for example, (Stroeve et al., 2020; M. A. Webster et al., 2014). These effects mean that years with very low summer ice coverage could enhance recovery of ice area the following winter, leading to a rebound in ice extent (Bitz & Roe, 2004). Overall, however, such negative feedbacks are only marginally mitigating the rapid loss of Arctic sea ice and with continued winter warming and a longer ice-free season, eventually the ice will be too thin to survive the summer melt.

3.3.2. Rapid Decline of Arctic Sea Ice Extent Risks Episodic Ice-Free Summers Before Mid-Century

The literature points toward a linear, predictable response of summer sea ice extent in response to greenhouse gas emissions, despite large interannual variability in weather patterns, rather than an abrupt transition to seasonally

ice-free conditions (monthly average sea ice area of less than 1 million km^2) consistent with tipping point behavior (Eisenman & Wettlaufer, 2009; Notz & Stroeve, 2016; Stroeve & Notz, 2018; Tietsche et al., 2011; Winton, 2011). The linear relationship between sea ice area and cumulative greenhouse gases in the atmosphere reveals the Arctic is already in the process of transitioning toward ice-free summer conditions, with the first ice-free summer potentially occurring before mid-century (Notz & Stroeve, 2018; SIMIP Community, 2020). The complete loss of summer Arctic sea ice would represent an important shift for regional climate and ecology, triggering significant consequences for regional warming and for Arctic biodiversity (Constable et al., 2022; O'Neill et al., 2022). For high levels of warming, a possibility also emerges of a more rapid transition toward an ice-free Arctic in winter, once ice-free summer conditions become more common (Bathiany et al., 2016; Eisenman & Wettlaufer, 2009).

Unless greenhouse gas emissions are reduced, it is likely the Arctic will lose its summer ice cover within a few decades. While CMIP5 model projections predicted a high likelihood of ice-free summers in the second half of the 21st century without strong climate mitigation (Massonnet et al., 2012; Stroeve, Kattsov, et al., 2012), CMIP6 models suggest the first ice-free Septembers will happen before 2050 (SIMIP Community, 2020). Some uncertainty does exist regarding the exact timing when ice-free summers might be expected to first manifest, based partly on the large range of internal variability, with the first occurrence of sea-ice coverage falling to <1 million km^2 unlikely before 2040 under RCP2.6, but likely before 2040 under RCP8.5 (J.-Y. Lee et al., 2021; Meredith et al., 2019). Nevertheless, the strong relationship between ice loss and greenhouse forcing coupled with current emissions rates indicates a reasonable likelihood for the first ice-free summer to occur before mid-century (Stroeve & Notz, 2018). Modeling studies suggest that nothing short of extremely aggressive climate mitigation is likely to reduce the likelihood of future summer sea ice loss; only for warming of no more than 1.5°C is sea ice generally still present in summer by end-of-century (Jahn, 2018; Notz & Stroeve, 2018). For the majority of new CMIP6 models, the Arctic Ocean experiences its first ice-free September before 2050 even under 1.5°C pathways (SIMIP Community, 2020). Under 2.0°C of global warming we could be looking at around 3 months per year of ice-free conditions (Notz & Stroeve, 2018). However, CMIP6 models continue to exhibit a very wide range of spread and performance, reflecting internal variability.

While loss of summer Arctic sea ice represents a high-likelihood outcome under current rates of warming, a totally ice-free Arctic year-round remains unlikely outside of worst-case emissions scenarios (RCP8.5) (Bathiany et al., 2016; Winton, 2006). One earlier modeling analysis using IPCC AR4 models concluded that ice-free winter conditions required around 13°C mean annual warming at the north pole (Winton, 2006), and were unlikely to occur this century. The IPCC AR6 similarly finds it "very likely" that winter sea-ice persists in all scenarios throughout the 21st century in many of the CMIP6 models (Fox-Kemper et al., 2021). Loss of winter sea ice may however proceed more abruptly than the long-term decline in summer sea ice extent to date in a threshold-dependent manner, potentially occurring just a few years after the ocean becomes too warm to form ice in winter (Bathiany et al., 2016). The homogeneous thin state of winter sea ice under conditions of frequent ice-free summers further contributes to its rapid loss. At the same time, loss of winter sea ice is thought to be reversible based on models, merely requiring that winter sea temperatures fall back below freezing thresholds (Armour et al., 2011; Bathiany et al., 2016; C. Li et al., 2013; Ridley et al., 2012). Yet the loss of Arctic Ocean stratification, which is required to prevent winter sea ice formation, may impart hysteresis to subsequent winter sea ice reformation, a possibility that climate modeling studies have not yet investigated in sufficient detail. Indeed, global ice-ocean models and state-of-the-art coupled climate models struggle to accurately simulate an upper-ocean stratification that is as stable as observed (G. Holloway et al., 2007; Ilıcak et al., 2016; Rosenblum et al., 2021).

Areas of uncertainty do remain when attempting to model future Arctic sea ice area. Cloud feedbacks that are important for determining summer sea ice dynamics still remain challenging even for state-of-art models (Tietsche et al., 2011). Poor representation of the varying distribution of sea ice thicknesses over the Arctic region is another weakness of current models (M. M. Holland et al., 2011; Stroeve et al., 2014), likely due to varying ability to represent atmospheric circulation's influence on ice thickness (Bitz et al., 2002; Kwok & Rothrock, 2009; Stroeve et al., 2014). The influence of seasonal atmospheric processes upon sea ice dynamics remains incompletely understood and an active area of research (Topál et al., 2020). Nevertheless, such potential sources of error do not meaningfully affect the conclusion that ice-free summers across the Arctic Ocean will likely begin to occur starting before mid-century.

3.3.3. Loss of Summer Sea Ice Accelerates Regional Warming With Global Implications

With much of the region under permanent or extended daylight hours during summer months, ice-free conditions lead to a high potential for accelerated regional warming via the aforementioned ice-albedo feedback. Reductions in Arctic sea ice extent are implicated in enhanced Arctic warming that cannot be alternatively explained by cloud cover changes, internal climate variability, or variability in atmospheric and oceanic circulation (Screen & Simmonds, 2010; Screen et al., 2014; Serreze et al., 2009). Modeling analysis also indicates a strong sensitivity of Arctic temperatures to sea ice loss (Screen et al., 2014). This effect has driven rates of regional warming at two to four times the global average rate, and is expected to continue to contribute to Arctic amplification (Meredith et al., 2019; Rantanen et al., 2022; Screen & Simmonds, 2010). The scientific community is continuing to investigate the potential impact of Arctic sea ice decline upon weather and climate patterns in the Northern Hemisphere (Barnes & Screen, 2015; M. Kretschmer et al., 2020).

This ice-albedo feedback additionally influences global climate at large. A modeling analysis examining a future Arctic with seasonally absent sea ice in summer found that an ice-free summer Arctic accelerated the rate of temperature increase by ∼8%, increasing radiative forcing by 0.3 W/m^2, a warming contribution equal to that of atmospheric halocarbons (Hudson, 2011). A more recent analysis obtained a figure of 0.49 W/m^2 for a somewhat higher summer ice loss scenario in which summer sea ice remains low for a 5-month period (Wunderling et al., 2020).

The regional warming impact of significant reductions in Arctic sea ice extent also presents an indirect threat to global sea-level rise by promoting additional melt from the GIS, an interaction identified as important over the geologic past in paleoclimate models (Koenig et al., 2014).

Finally, the loss of summer Arctic sea ice carries significant ecological implications. Wildlife dependent on sea ice for shelter or survival may be severely impacted, and the transition to ice-free summer conditions may also cause substantial shifts to phytoplankton community structure, driving transitions in regional marine ecology (Meredith et al., 2019). Sea ice and its overlying snow cover also play an important role in how much light reaches the upper ocean, in turn influencing the amount of under-ice algae and phytoplankton blooms (e.g., Arrigo et al., 2012; Fernández-Méndez et al., 2015; Ulfsbo et al., 2014). The resulting impacts to wildlife and fishing will pose economic, social, and cultural threats to human communities across the Arctic (Constable et al., 2022; O'Neill et al., 2022).

A year-round ice-free Arctic remains a scenario not currently believed to be plausible until 2100 even under worst-case warming scenarios (Bathiany et al., 2016; Lenton, 2012; Winton, 2006). Furthermore, loss of Arctic sea ice can be reversed on shorter timescales than most of the other climate mechanisms discussed in this review, as sea ice extent can recover within decades if initial warming is reversed (Notz, 2009; Ridley et al., 2012). At present however, the Arctic sea ice system confronts an accelerated rate of warming, a rapid pace of sea ice decline, and an increasing likelihood of ice-free summer conditions occurring within a couple decades (Table 12).

4. Tipping Element Cascade Leading to Irreversible "Hothouse Earth" Warming

4.1. Background

In 2018, an article by Steffen et al. (2018) proposed a "Hothouse Earth" scenario, in which modern anthropogenic warming could trigger strong positive climate feedbacks leading to significant temperature increases well beyond those expected from human greenhouse gas forcing alone, potentially altering the long-term climate trajectory of the Earth itself, disrupting future glaciation and placing the biosphere in a newly created warmer equilibrium that could persist for hundreds of thousands of years.

Historically, the Earth has transitioned between numerous climate states, from the very warm Paleocene-Eocene Thermal Maximum 56 million years ago (McInerney & Wing, 2011) to the glacial and interglacial cycles of the Quaternary Period (2.6 million years ago to present). A "Hothouse Earth" pathway is suggested by Steffen et al. (2018) to reach, then significantly surpass, warming observed during the Mid-Miocene (15.5–17 million years ago, up to 4°C warmer than present).

Within the Quaternary period, which encompasses the entirety of recorded human history, cycles between glacial and interglacial periods have occurred with a periodicity of 100,000 years, primarily driven by slow changes in the Earth's orbit on timescales of approximately 100,000, 40,000, and 20,000 years (PAGES, 2016). Anthropogenic

Table 12
Section Summary Box Synthesizing the Forcing Mechanism, Response Behavior, Reversibility, and Classification of Arctic Sea Ice Decline

	Classification	Mechanism	Irreversibility
Loss of Arctic sea ice	Non-tipping element		
	Summer Arctic sea ice decline is not threshold-dependent (Eisenman & Wettlaufer, 2009; Notz & Stroeve, 2016; SIMIP Community, 2020; Stroeve & Notz, 2018; Tietsche et al., 2011)	Regional atmospheric and oceanic warming increases seasonal ice loss and reduces winter ice growth, in turn strengthening regional warming via ice-albedo feedback	Reversible
	Loss of winter Arctic sea ice may be threshold-dependent tipping element (Armour et al., 2011; Bathiany et al., 2016; Eisenman & Wettlaufer, 2009; Ridley et al., 2012; Winton, 2006)	Ocean warming in high-end, worst-case scenarios eventually could prevent ice formation in winter	Uncertain potential for Arctic Ocean stratification changes following the loss of winter Arctic sea ice to impart hysteresis to sea ice reformation

climate change, however, is driving changes in the Earth system at a rapid pace that the planet has rarely experienced apart from cataclysmic events such as asteroid impacts (Zeebe et al., 2016).

Current human greenhouse gas emissions and associated warming will likely influence the timing of the next ice age (Archer & Ganopolski, 2005; Berger & Loutre, 2002; Ganopolski et al., 2016; Lord et al., 2017; Talento & Ganopolski, 2021). Under today's orbital configuration, cumulative emissions of over 1,000 Gt C or CO_2 concentrations higher than 300 ppm are potentially sufficient to delay glaciation; these conditions would include all RCPs with emissions exceeding an RCP2.6 scenario (Ganopolski et al., 2016; Masson-Delmotte et al., 2013). Given the high importance of atmospheric greenhouse gas levels alongside orbital forcing for driving glacial-interglacial shifts, the long-term effects of anthropogenic climate change could conceivably influence the timing and development of the next glacial onset.

Paleoclimate evidence suggests that past climate states of the Earth may provide useful parallels with a warmer future world impacted by anthropogenic climate change, such as the Early Eocene (50 million years ago) and the Mid-Pliocene (3.3–3 million years ago) (K. D. Burke et al., 2018). Such periods were marked by notably higher mean surface temperatures (Early Eocene: $13 \pm 2.6°C$ warmer than present day; Mid-Pliocene 1.8–3.6°C warmer than present day), reduced (Mid-Pliocene) or absent (Early Eocene) ice-sheets, elevated sea-levels, and higher CO_2 concentrations (Early Eocene: 1,400 ppm; Mid-Pliocene: 400 ppm). Such paleoclimate analogs for a warmer earth such as the Eocene may also have been characterized by a greatly reduced extent of subtropical clouds (Schneider et al., 2019). The Mid-Miocene (15.5–17 million years ago, 2–4°C warmer, 300–500 ppm CO_2) (Greenop et al., 2014; Kominz et al., 2008) also holds some potential parallels with a warmer Earth. The range of conditions denoted by these past eras support the idea that a similar hotter future climate could remain stable over geologic time. Paleoevidence broadly indicates that large-scale, potentially interacting shifts in sea level, hydroclimate, the carbon cycle, and ocean circulation may have occurred in past periods of warming, influencing global climate on timescales of centuries to decades (G. J. Bowen et al., 2015; Brovkin et al., 2021; Dakos et al., 2008; Z. A. Thomas et al., 2020).

In describing the path toward a "Hothouse Earth" equilibrium, Steffen et al. (2018) suggest failure to meet a 2°C warming goal may trigger one or more tipping elements with lower critical thresholds. Additional warming brought on by these tipping elements could tip other tipping elements in a self-reinforcing cascade over centuries to millennia, potentially pushing the climate system several degrees hotter in response to even modest warming. A newer Nature Comment presented an updated risk assessment of a tipping element cascade with the argument that warming of 1–2°C globally already represents an unacceptably high risk of triggering major tipping elements (Lenton et al., 2019). One paper constructed causal networks based on a literature search that identified key parameters influencing different Earth system components, demonstrating a theoretical potential for cascading regime shifts due to shared drivers, one-way, and two-way interactions between systems (Rocha et al., 2018). A recent study using a conceptual network modeling approach similarly stressed the potential for tipping elements to interact, which could shift true critical thresholds within their potential ranges (Wunderling et al., 2021). At the same time, the IPCC AR6 WG1 report identified "no evidence" of global-scale non-linear climate system response for the next century in projections and expressed "low confidence" as to whether such behavior could

occur (D. Chen et al., 2021; Forster et al., 2021). The growing body of work on this subject nevertheless emphasizes uncertainties surrounding the collective impacts of tipping elements and their interactions (Armstrong McKay et al., 2022), highlighting the particular need for more quantitative and scenario-based modeling to assess the risks of significant additional climate change.

4.2. Near-Term Potential for Tipping Element Interactions (Before 2300)

Evaluation of the Hothouse Earth hypothesis involves considerable complexity, as rather than representing its own independent mechanism, the Hothouse Earth pathway effectively consists of numerous individual tipping elements (Table 13) and potential interconnections between them. Discussion of the Hothouse Earth hypothesis thus involves three questions: (a) what critical thresholds are tipping elements triggered at, (b) can the response from tipping elements with lower thresholds cause tipping of other tipping elements, and (c) what is the cumulative effect of all activated tipping elements and resulting climate feedbacks?

Identifying which tipping elements may cross critical thresholds first is relatively straightforward compared to the second and third questions. Earth system elements that this review indicates are at higher risk of crossing critical thresholds or undergoing substantial changes in response to warming this century under moderate (RCP4.5) emissions scenarios include loss of Arctic summer sea ice, loss of portions of the GIS, loss of portions of the West Antarctic Ice-sheet, Amazon rainforest dieback, boreal forest ecosystem shifts, some permafrost carbon release, and coral reef loss (Figure 14). In contrast, methane release from marine methane hydrates and stratocumulus cloud deck evaporation will likely require longer timescales and higher emissions forcing in order to occur at large scales, while disruptions of tropical monsoons may be contingent on large shifts in other Earth system components and are unlikely to occur as a direct response to changes in aerosol forcing or land cover (see Section 2.6). Critical thresholds for weakening of the AMOC remain unclear and a transition of this system to a different state may not occur this century (see Section 2.1). While the GIS and WAIS may transgress critical thresholds this century (see Section 2.3), timescales of ice loss may require many centuries to millennia to run to completion (Bakker et al., 2016; Clark et al., 2016; Golledge et al., 2015; Huybrechts & De Wolde, 1999).

The investigation of interactions between tipping elements and the potential for cascading behavior requires evaluation of several considerations related to how changes within one Earth system component could destabilize another. Relative timescales of system response are one key factor. Systems that evolve on longer timescales can be thought of as determining the background state for systems that respond on faster timescales (Dekker et al., 2018). Modeling of coupled systems of tipping elements shows that interactions can shift critical thresholds toward lower values, with some systems acting as "initiators" responsible for triggering a cascade (Klose et al., 2020; Wunderling et al., 2021). The magnitude of forcing could also strongly influence cascading behavior. Under a level of forcing that surpasses individual critical thresholds for many tipping elements, for instance, interactions may not cause any additional state shifts if all coupled tipping elements have already been forced into critical transitions (Wunderling et al., 2021). Similarly, an interaction between an extremely slow-changing system and a fast-changing system may be effectively inconsequential if the latter system will have already transitioned to a new state before the former system begins to impart a significant influence.

The directionality of interactions between Earth system components and the resulting networks they create may also determine the structure of a tipping chain, and are additionally subject to alignments in not just temporal but also spatial scales (Rocha et al., 2018). Heterogeneity within systems themselves, such as differences in landscapes, species composition, or microclimates, may result in different tipping behaviors, such as more gradual rather than abrupt changes to a network given the response of specific nodes to different drivers or critical thresholds (Scheffer, Carpenter, et al., 2012). Conceptual work has also explored mathematical frameworks for different cascading interactions, including back-tipping of a system back to its "normal" state (Klose et al., 2020) and interactions with systems that may transition between stable and oscillatory regimes (Dekker et al., 2018).

So far, research on cascading behavior has primarily leveraged conceptual modeling rather than process and scenario-based approaches, limiting the applicability of these results for investigating the third question of what the cumulative impacts of transitions by multiple tipping elements might be. Evaluation of potential impacts, for now, must rely upon the subject-specific literature.

Of the tipping elements likely to be triggered this century under current trends, Amazon rainforest dieback could contribute significantly toward climate change on a relatively fast time frame. This stems from the considerable range in estimates of the size of the Amazon forest carbon pool (150–200 Gt C), the strength of the current

Table 13
Summary of Scientific Understanding, Key Thresholds, and Impacts Associated With the Candidate Tipping Elements Covered in This Review

Candidate tipping element	Level of scientific understanding	Predictability by models	Key critical thresholds, global mean warming or otherwise	Climate impact	Timescale of impacts
AMOC weakening/ collapse	Moderate	Good agreement, significant model limitations	Uncertain	Weakening causes regional cooling, wind, precipitation, sea-level changes. Collapse would greatly magnify these impacts	Weakening occurs over centuries. Collapse would be abrupt or fast
Methane hydrate destabilization	Moderate	Low	Uncertain, long-term impacts higher but still small beyond ~3°C	Gradual long-term release of carbon to the Earth system	Centuries to multiple millennia
Greenland and Antarctic ice-sheet loss	Moderate	Moderate	Uncertain Greenland: 1.5–5°C West Antarctica: 1.5–3°C East Antarctica: Very uncertain	Multi-meter sea-level rise over centuries to millennia, irreversible ice-sheet loss	Centuries to millennia
Permafrost carbon release	Moderate	Moderate to low	Highly heterogenous, no firm continental-scale threshold behavior	Added emissions of carbon dioxide and methane	Years to decades, continuing for centuries
Boreal forest ecosystem shifts	Low	Low	Uncertain	Increase in wildfires, significant changes in soil and biomass carbon storage, regional albedo changes, major ecosystem shifts	Decades to a century
Stratocumulus cloud deck evaporation	Very low	Very low	~1,200 ppm CO2-eq	Uncertain. Cloud deck breakup may trigger added global warming	Uncertain. Abrupt to decades
Loss of shallow tropical coral reefs	Very high	High	Increasingly severe impacts beyond 1.5°C	Degradation of nearly all shallow tropical coral reefs worldwide, major socio-economic impacts	Decades
Amazon rainforest dieback	Moderate	Moderate	40% deforestation, ~3–4°C, 40% precipitation decrease, or some combination	Die-off of significant fractions of Amazon rainforest, intensification of wildfires, large ecosystem shifts, significant carbon emissions	Decades to a century
Disruption of tropical seasonal monsoons	Low	Moderate to low, but majority of models predict increase in monsoon rainfall	Thought to be non-tipping element	Gradual increase in mean seasonal precipitation across the monsoon domain	Decades
Loss of summer Arctic sea ice	High	Moderate to high	Summer ice loss scales linearly with temperature. Consistently ice-free summers likely for warming of ~2°C	Increased occurrence of ice-free summer Arctic, global warming feedback	Decades
Tipping element cascade	Low	Low	Uncertain	Significant additional global warming due to interacting tipping elements	Centuries to millennia

Amazon carbon sink (0.4–0.6 Gt C/yr), and the potential magnitude and timescales of conversion of rainforest to a different ecosystem (50%–70%, 50–100 years) (see Section 3.2).

In the northern high latitudes, shifts in boreal forest ecosystems (Section 2.5) also represent a potentially imminent and impactful tipping element. However, the sign, speed, and magnitude of boreal ecosystem changes and
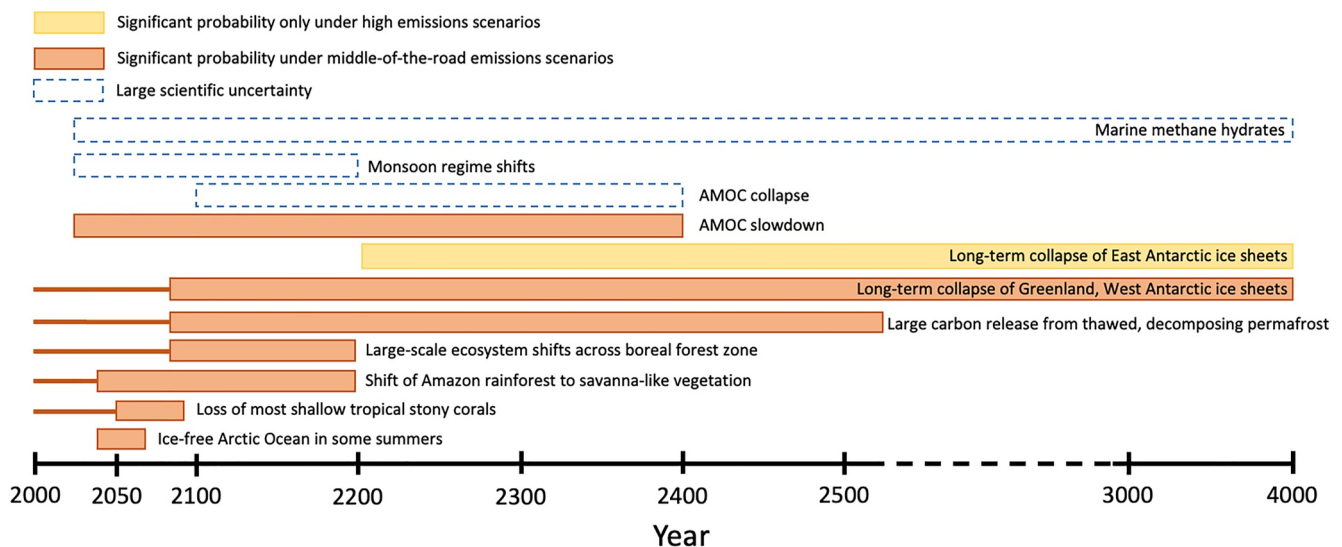
Figure 14. Illustration of the approximate time frames over which the reviewed Earth system components, including tipping elements, might be expected to respond to climate forcings. Horizontal lines to the left of some bars indicate that while the majority of large-scale system response may be projected to occur at some point in the future for certain Earth system elements, some shifts are already underway and are expected to continue.

their implications for carbon fluxes and land surface albedo remain highly uncertain. That said, current research cannot eliminate the possibility for a sizable net warming contribution to global climate. Gradual permafrost thaw (Section 2.4) could contribute significant additional carbon emissions over the near-term (92 Gt C by 2100 under RCP8.5) (Meredith et al., 2019). Abrupt permafrost thaw processes acting over faster timescales could emit up to ~18 Gt C by 2100 including considerable methane (Turetsky et al., 2019, 2020). Over this century, emissions from abrupt thaw could contribute approximately 6,771 Mt CH_4 (Mt C) and 10.95 Gt CO_2 (Gt C) under the worst-case RCP8.5 scenario (Turetsky et al., 2020). For Arctic sea ice (Section 3.3), a modeling scenario where sea ice extent is greatly reduced with a 1-month ice-free period every summer yields a change in radiative forcing of 0.3 W/m^2—climatically significant on a level similar to that of current anthropogenic forcing from atmospheric halocarbons (Hudson, 2011).

The remaining other imminent impacts—coral reef die-off (Section 3.1) and loss of mountain glaciers—will likely yield minimal to negligible additional warming or greenhouse forcing. From a climate perspective, it stands to reason that only tipping elements that drive significant changes to the Earth's energy balance or major Earth system dynamics—through greenhouse gas emissions, circulation shifts, or albedo changes—increase the risk of a tipping point cascade. Neither coral reef collapse nor mountain glacier melt are anticipated to meaningfully alter greenhouse gas fluxes, circulation systems, or planetary-scale albedo. Meanwhile, the likelihood of monsoon regime shifts remains a subject of active debate (Section 2.6).

To estimate the potential cumulative impact of these near-term tipping elements and Arctic sea ice loss on future climate projections through 2300, we leveraged the FaIR simple climate model (Millar et al., 2017; C. Smith et al., 2017) v1.6.3, adding further CO_2 emissions, CH_4 emissions, and radiative forcing changes produced from the response of tipping elements and Arctic sea ice to climate change under the SSP2-4.5 and SSP5-8.5 scenarios, as detailed in (Table 14). This prescribed approach to additional climate forcing does not and cannot simulate dynamic tipping behavior and interactions between tipping elements, but rather serves to illustrate the collective climate forcing from several tipping elements and climate feedbacks. For our "base" scenarios, we generated anthropogenic emissions inputs for FaIR using the MESSAGE-GLOBIOM SSP2-4.5 and REMIND-MAGPIE SSP5-8.5 annual mean emissions specified in the RCMIP protocol (https://www.rcmip.org/). Volcanic and solar forcings were taken from the same RCMIP scenarios. Emissions rates and forcings were linearly interpolated for individual years. We utilized a natural emissions time series updated for the CMIP6 by Chris Smith following the methodology of C. J. Smith et al. (2018).

For both the SSP2-4.5 and SSP8.5 pathways, we considered a "high," "middle," and "low" scenario, varying ECS and TCR accordingly and considering high, middle-ground, and low carbon fluxes and radiative forcing changes from tipping elements through 2300. For ECS, we chose low/median/high values of 2.3°K/3.1°K/4.7°K based on

Table 14

Additional CO_2 Emissions, CH_4 Emissions, and Radiative Forcing Incorporated Into SSP2-4.5 and SSP5-8.5 Emissions Pathways to Simulate Added Climate Impact of Tipping Elements and Arctic Sea Ice Loss Based on Available Estimates From Literature

	SSP2-4.5		SSP5-8.5		
	CO_2 emissions/yr, Gt C	CH_4 emissions/yr, Mt CH_4	CO_2 emissions/yr, Gt C	CH_4 emissions/yr, Mt CH_4	Reference(s) as basis for assumption
Gradual permafrost thaw	No net C fluxes (permafrost emissions compensated by vegetation uptake)	No net C fluxes (permafrost emissions compensated by vegetation uptake)	2010–2100: 0.55 (0.55–0.55) 2100–2200: 1.97 (0.50–3.41) 2200–2300: 0.98 (0.99–1.92)	2010–2100: 5.19 (2.22–8.89) 2100–2200: 37.33 (4.67–116.67) 2200–2300: 30.67 (14.67–104.00)	McGuire et al. (2018) and Schneider von Deimling et al. (2012)
Abrupt permafrost thaw	2000–2100: 0.032 (±26%) 2100–2300: 0.083 (±36%)	2000–2100: 41.87 (±26%) 2100–2300: 52.40 (±36%)	2000–2100: 0.01 to 0.18 (±26%) 2100–2300: 0.21 to 0.34 (±32%) Time-varying flux derived from Table S6 of Turetsky et al. (2020)	2000–2100: 51.47 to 65.92 (±26%) 2100–2300: 70.78 to 79.09 (±32%) Time-varying flux derived from Table S6 of Turetsky et al. (2020)	Turetsky et al. (2020)
Methane hydrate destabilization	None, assume all C fluxes occur as methane	2000–2100: 2.37 (0–4.73) 2100–2200: 1.41 (0–2.82) 2200–2300: 1.23 (0–2.45)	None, assume all C fluxes occur as methane	2000–2100: 5.91 (2.37–9.46) 2100–2200: 3.52 (1.41–5.64) 2200–2300: 3.06 (1.23–4.9)	K. Kretschmer et al. (2015)
Amazon forest dieback	2040–2100: 0.66 (±15%) 2100–2150: 0.30 (±15%)	None assumed	2040–2140: 0.70 (±15%) 2140–2200: 0.25 (±15%)	None assumed	Own assumptions, informed by Aragão et al. (2018), Fonseca et al. (2019), Silva et al. (2020), and Silva Junior et al. (2019, 2020)
	SSP2-4.5		SSP5-8.5		Reference(s) as basis for assumption
Arctic sea ice loss	Added radiative forcing climbs linearly from zero to 0.3 W/m² (±15%) by 2050, then to 0.5 W/m² (±15%) by 2100, remaining constant thereafter		Added radiative forcing climbs linearly from zero to 0.3 W/m² (±15%) by 2030, then to 0.6 W/m² (±15%) by 2100, then to 0.7 W/m² (±15%) by 2120, remaining constant thereafter		Hudson (2011), Pistone et al. (2019), and Wunderling et al. (2020)

Note. Values and percentages in parentheses indicate those selected under "high" and "low" scenarios.

Sherwood et al. (2020). For TCR, we selected a median value of 1.8°K based on Sherwood et al. (2020) and low and high values of 1°K and 2.5°K based on the IPCC AR5 likely range for TCR.

Permafrost CO_2 and methane emission rates are derived from estimates of cumulative carbon release through 2300 for gradual permafrost thaw processes (McGuire et al., 2018), and for abrupt thaw processes (Turetsky et al., 2020) under RCP4.5 and RCP8.5, linearly interpolating C fluxes in each year. Methane hydrate emissions utilize estimates for cumulative release by 2100, 2200, and 2300 from K. Kretschmer et al. (2015), aggressively assuming complete liberation of marine methane to the atmosphere. For emissions from gradual thaw, we assume 0.7% (0.3%–1.2%)/1.4% (0.7%–2.5%)/2.3% (1.1%–3.9%) of carbon is released as CH_4 from 2010 to 2100/2100–2200/2200–2300, based on Schneider von Deimling et al. (2012). We used described results for the SiBCASA, CLM4.5, and UVic RCP8.5 model runs in McGuire et al. (2018) as the middle, low, and high cases respectively for carbon release from gradual thaw under SSP5-8.5 warming. For SSP2-4.5, we assume that carbon fluxes from permafrost degradation are balanced by vegetation effects (McGuire et al., 2018). Low and high scenarios for CO_2 and CH_4 fluxes from abrupt thaw processes correspond to the one standard deviation ranges for RCP4.5 and RCP8.5 model results for 2100 and 2300 (Turetsky et al., 2020).

We base radiative forcing changes from reduced Arctic sea ice on work by Hudson (2011), Pistone et al. (2019), and Wunderling et al. (2020), applying additional radiative inputs reaching 0.3 W/m² by 2050 and 0.5 W/m² by 2100 for SSP2-4.5 and reaching 0.3 W/m² by 2030, 0.6 W/m² by 2100, and 0.7 W/m² by 2120 for SSP5-8.5, subtracting/adding 15% for low/high scenarios, respectively. This corresponds to an Arctic seasonally ice-free for a couple summer months after 2100 in SSP2-4.5, and an ice-free Arctic throughout the sunlit portion of the year after 2120 in SSP5-8.5. We note that while Earth system models already incorporate sea ice albedo feedbacks, climatological biases in the Arctic may produce lower sea ice loss and correspondingly weaker albedo feedbacks in many models (Shen et al., 2021).

To account for potential Amazon rainforest ecosystem shifts, we assumed a current ecosystem carbon stock of 200 Gt C (Cerri et al., 2007; Gibbs et al., 2007; Malhi et al., 2006; S. S. Saatchi et al., 2011), and assume conversion to savanna or grassland-like vegetation would lead to carbon storage per unit area half that of intact tropical rainforest. We further assume that forest areas degraded through edge effects and wildfire exhibit a long-term carbon storage capacity of 25% less than intact forest (Aragão et al., 2018; Silva Junior et al., 2020). Under SSP5-8.5, we assume 60% of Amazonia undergoes conversion from tropical forest to savanna/grassland between 2040 and 2140, with another 20% suffering from degradation due to fire and edge effects. Subsequently, the previously degraded 20% transitions to savanna/grassland between 2140 and 2200, with another 10% of previously intact forest suffering fire/edge degradation over this period. For SSP-4.5, we assume 30% of the region's tropical forest is converted to savanna/grassland between 2040 and 2100, another 20% suffering degradation. The previously degraded 20% transitions to savanna/grassland between 2100 and 2150, with another 10% of previously intact forest suffering degradation during this time.

We omit potential carbon fluxes or radiative forcing impacts from other candidate tipping elements (boreal forests, stratocumulus cloud decks, tropical monsoons, AMOC, and Greenland/Antarctic ice sheets) given higher uncertainty surrounding their potential impacts upon carbon cycling and planetary radiative balance under different warming scenarios. One or more of these tipping elements could add net contributions to warming, however current levels of scientific knowledge and confidence are insufficient to formulate assumptions that aren't largely arbitrary. As stratocumulus cloud deck evaporation remains a novel and uncertain hypothesis, we also omit this mechanism. We assume die-off of tropical coral reefs produces no global climate feedbacks.

Based on the synthesis of the above studies with this model, by 2100 the additional warming from these tipping elements is ~0.13°C (low: 0.06°C, high: 0.23°C) under SSP2-4.5 and ~0.21°C (low: 0.10°C, high: 0.36°C) under SSP5-8.5 relative to the original scenarios. By 2300 we find the selected tipping elements may produce additional warming of ~0.24°C (low: 0.11°C, high: 0.49°C) under SSP2-4.5 and ~0.52°C (low: 0.24°C, high: 1.09°C) under SSP5-8.5 relative to the original scenarios (Figure 15). The sum effect of these near-term tipping elements is significant in our model but secondary to the larger emissions trajectory. It thus seems unlikely that this additional warming is sufficient to self-perpetuate global-scale climate change independent of the human emissions pathway. Overall, our analysis suggests that anthropogenic emissions and climate sensitivity will determine the magnitude of warming over the next few centuries, with tipping elements and other carbon cycle feedbacks adding further uncertainty. Tipping elements carry substantial implications for carbon budgets and will accelerate rates of warming, but the potential for these mechanisms to drive a transition to a hothouse climate state within centuries remains unclear. More rigorous future modeling work should leverage a range of models and further explore possible scenarios, particularly in conjunction with general carbon cycle feedbacks.

4.3. Longer-Term Tipping Elements and Dynamics

Over long time frames of multiple centuries to millennia and beyond, assessment of the sensitivity of tipping elements to temporary overshoots of critical thresholds and evaluation of whether transitions are irreversible versus reversible become highly relevant to discussions of long-term tipping behavior and cascade behavior. Tipping elements discussed in this review that may act over longer timescales include collapse of ice sheets, weakening of the AMOC, long-term permafrost carbon release, and methane release from marine methane hydrates.

The cumulative effects of permafrost thaw and methane hydrate destabilization manifest over centuries and millennia, respectively (Archer et al., 2009; McGuire et al., 2018; Schuur et al., 2015; Turetsky et al., 2020). More recent research indicates that methane hydrate deposits will play a minimal role in global climate over coming centuries and millennia, as reviewed by Ruppel and Kessler (2017). Complete loss of land-based ice-sheets in Greenland is anticipated to require multiple millennia (Pattyn et al., 2018), while loss of the Western Antarctic
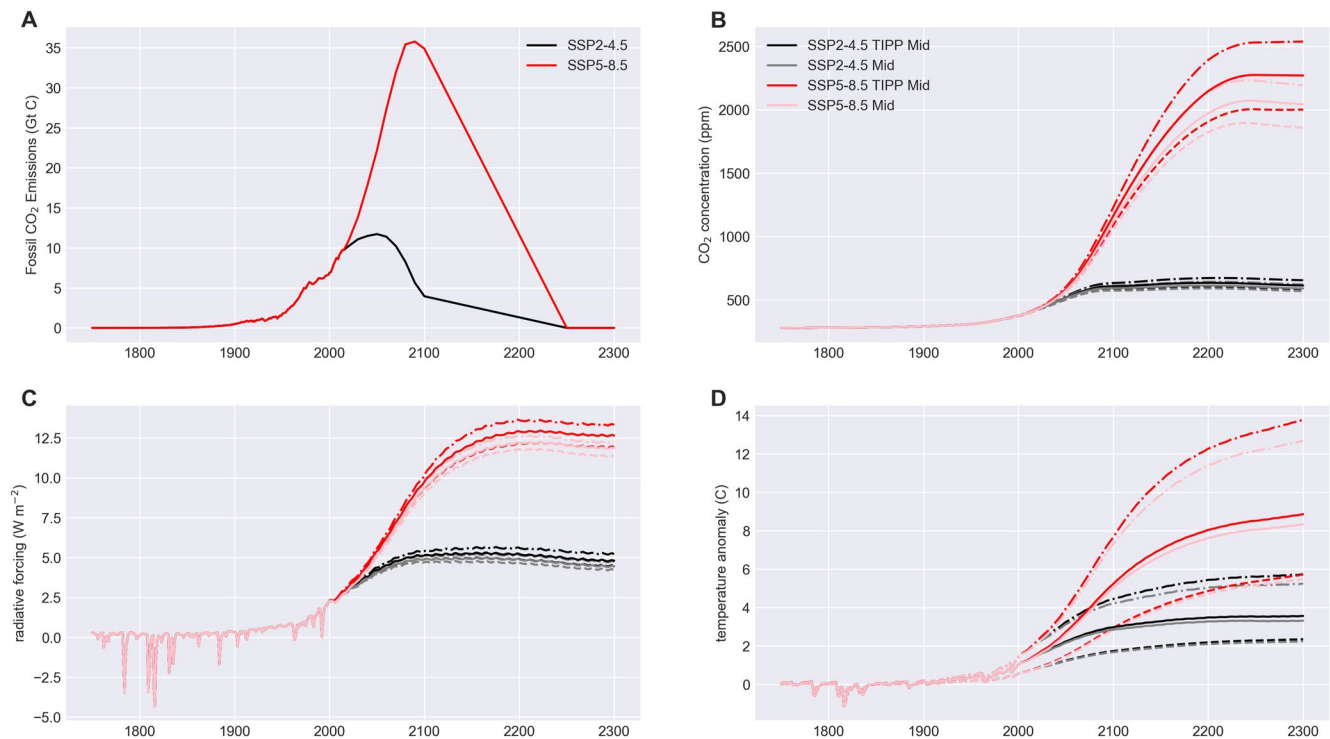
Figure 15. (a) Fossil fuel CO_2 emissions, (b) atmospheric CO_2 concentrations, (c) total radiative forcing, and (d) global mean surface temperature anomaly relative to pre-industrial (1861–1880 mean) temperatures, plotted from 1750 to 2300 for a baseline SSP2-4.5 (light gray) and SSP5-8.5 emissions scenario (light red) as well as for modified SSP2-4.5 TIPP (black) and SSP5-8.5 TIPP (red) scenarios incorporating additional CO_2 emissions, CH_4 emissions, and radiative forcing as a result of tipping elements (see Table 4). "Middle" scenarios are plotted using solid lines, while "high" and "low" scenarios are denoted with dot-dashed and dashed lines, respectively.

Ice-sheet similarly takes place over a time scale of centuries at minimum even under extreme scenarios (DeConto et al., 2021; Edwards et al., 2021; Golledge et al., 2015, 2019).

The likelihood of an AMOC shutdown (Section 2.1) within the 21st century is currently assessed as very low but uncertain (Collins et al., 2019; Fox-Kemper et al., 2021). A century or more may be required before a transition occurs (see Section 2.1.2), and projections remain inconclusive as to how much the AMOC may weaken in response to climate change. However, current climate models utilize a relatively simple representation of the AMOC and may exhibit excessive AMOC stability (W. Liu et al., 2017), while new oceanographic measurements continue to highlight limitations in our understanding of this system (Lozier et al., 2019) that impact confidence in model results. Apart from such uncertainties, it also remains unclear whether and to what degree broader climate impacts from a weakening AMOC could produce additional net global warming or carbon cycle feedbacks (Armstrong McKay et al., 2022; Parsons et al., 2014; Steffen et al., 2018; Wunderling et al., 2021).

Lenton et al. (2019) invoke the possibility of stratocumulus cloud deck evaporation (Section 2.7) acting as a potentially important tipping element. The level of greenhouse gas forcing required to cause marine stratocumulus cloud formations to break down may lie at around 1,200 ppm CO_2 (Schneider et al., 2019), a concentration not attained until toward the end of this century in aggressive, worst-case emissions pathways (Hausfather & Peters, 2020). This threshold and the cloud deck evaporation mechanism itself remain uncertain, warranting considerable additional research.

The classification of these and other tipping elements as irreversible or reversible depends heavily upon the timescale of interest and the degree to which applied climate forcings are reversed. Many studies model one or multiple systems' response to reversed forcing over sufficiently long timescales to assess equilibrium stable states (e.g., Garbe et al., 2020; Gregory et al., 2020; Ritchie et al., 2021; Wunderling et al., 2021). Indeed, one definition of an irreversible change given in both the (IPCC, 2021) and (Brovkin et al., 2021) refers simply to changes that require substantially more time to revert back to their original state than was required for the shift to the altered state. However, a change that requires more than a couple hundred years to reverse from a prior transition to a new state is arguably effectively irreversible from the perspective of human societies even if a shift is reversible over very

Table 15
List of Tipping Elements Discussed in This Review, Classified as Either Tipping Elements or Non-Tipping Elements Based on the Terminology of Kopp et al. (2016)

Candidate tipping element	Classification	Timescale of system response	Irreversibility
AMOC weakening/collapse	Tipping element	Slow (century or longer)	Potentially irreversible
Methane hydrate destabilization	Non-tipping element	Slow (centuries to millennia)	Irreversible
Greenland and Antarctic ice-sheet loss	Tipping element	Slow (centuries to millennia)	Irreversible
Permafrost carbon release	Tipping element	Slow (centuries)	Irreversible
Boreal forest ecosystem shifts	Tipping element	Potentially fast	Uncertain
Stratocumulus cloud deck evaporation	Tipping element	Potentially abrupt or fast	Irreversible.
Loss of shallow tropical coral reefs	Tipping element	Abrupt to fast	Irreversible
Amazon rainforest dieback	Tipping element	Fast	Irreversible
Abrupt transitions in S. Asian, African monsoon regime	Non-tipping element	Not applicable	Reversible
Loss of Arctic sea ice	Summer sea ice: Non-tipping element	Abrupt to fast	Reversible
	Winter sea ice: Tipping element		

Note. The timescale of system-wide response to any tipping behavior is further classified as abrupt (taking place within a couple decades with no time lag), fast (several decades), or slow (longer than a century). Finally, impacts are classified as reversible (reversion to original system state within a century possible upon applying opposite forcing), or irreversible (reversion to original system state requires centuries or longer, and/or different opposite forcing of a significantly larger magnitude than the original change in forcing applied to achieve the altered system state).

long timescales that allow a return to the original equilibrium. As such, we identify the tipping elements covered in this review as irreversible or reversible (Table 15) based on whether changes can revert within a century following a return to a pre-industrial climate.

If human societies only succeed in significantly reducing greenhouse gas concentrations after having passed certain temperature thresholds, the ability of a tipping element to recover from a temporary transgression or "overshoot" of its critical threshold may determine its evolution over multi-century timescales and longer. Ritchie et al. (2021) used simple models to demonstrate how sufficiently brief and limited overshoots of critical thresholds for "slow-onset" tipping elements could avoid triggering a transition into an alternative long-term state. Dynamical long-term modeling of a reduced GIS under different scenarios also demonstrates some capacity for re-growth of ice under a return to pre-industrial climate, implying overshoot recovery potential if the period of temperature threshold exceedance was brief relative to timescales of ice loss (Gregory et al., 2020).

For tipping elements with long timescales of action, their overall climate impacts in the distant future may be somewhat mitigated by drawdown of atmospheric greenhouse gases via natural carbon sinks. Multi-millennial modeling of several high-forcing scenarios indicates that CO_2 levels ultimately decline by hundreds of parts per million over the course of one to two millennia, driven by natural sinks (Clark et al., 2016). An extended time horizon also leaves a significant opportunity for human society to conduct further greenhouse gas removal from the atmosphere through carbon removal methods over future centuries. Many of the future emission scenarios that limit warming to 2°C or below by 2100 already include large-scale use of negative emissions technologies, and the use of these could logically be extended and expanded in following centuries (Riahi et al., 2017).

Overall, many of the long-term tipping elements discussed above exert climate impacts gradually over lengthy timeframes, while other factors such as an AMOC collapse, stratocumulus cloud deck evaporation, or destabilization of marine methane hydrate deposits may represent high-risk but uncertain or low-probability outcomes. The hypothesis that multiple tipping elements can cascade resulting in several degrees of additional warming remains in need of additional substantiation through quantitative, scenario-based modeling. The current literature suggests that additional global-scale climate impacts from tipping elements are significant, but secondary in relative terms to the future trajectory of anthropogenic emissions and to uncertainties in climate sensitivity. Nevertheless, the risks of a tipping element cascade and long-term alteration of the Earth's climate trajectory are sufficiently large that any future updates in our understanding of individual tipping elements will motivate reassessment of the dangers of significant additional climate change.
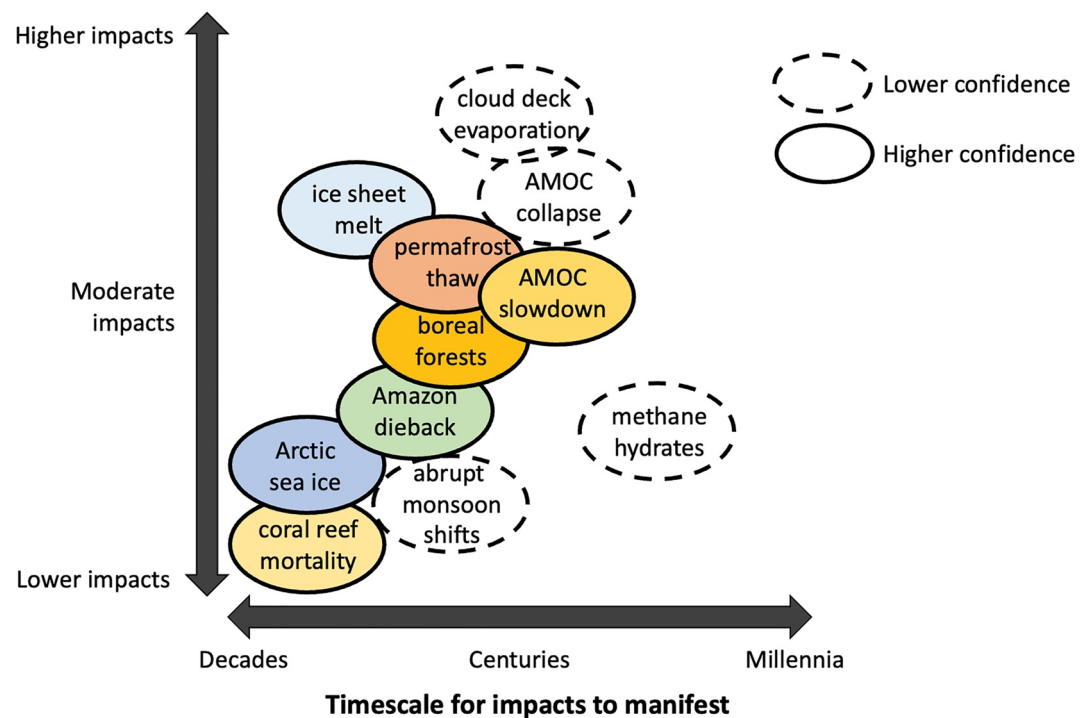
Figure 16. Qualitative two-dimensional organization of individual candidate tipping elements covered in this report. Candidate tipping elements are organized vertically according to expected negative global-scale climate impacts upon human societies (see Section 4), considering added warming potential, sea-level rise, ecosystem shifts, and atmospheric and oceanic circulation changes (y-axis) and horizontally based on the timeframe over which those impacts are expected to manifest under a middle-of-the-road to high-end emissions scenario. Candidate tipping elements are qualitatively categorized as lower confidence (dashed outline) or higher confidence (solid outline). Colors are arbitrarily assigned for visual presentation.

5. Conclusion

Considering the candidate tipping elements reviewed here as an ensemble (Table 15), some useful commonalities emerge that highlight shared characteristics between some of these systems as well as important priorities for guiding future research. The time frame over which tipping elements act is one important factor for assessing risks and impacts. Some tipping elements will respond strongly to climate forcing on shorter timescales within this century, while other tipping elements may or may not cross tipping thresholds this century and are believed to undergo shifts over much longer timescales of a couple centuries to millennia. Next, a major consideration for some tipping elements is the degree to which future reductions of anthropogenic emissions consistent with middle-of-the-road or low end-of-century warming pathways may considerably mitigate the degree of future change these systems undergo. Finally, a number of similarities in current knowledge gaps highlight potentially productive directions for new research that could reduce remaining uncertainties regarding critical thresholds, impacts, and possible interactions between tipping elements.

Relatively few of the candidate tipping elements covered in this review are thought to demonstrate a potential for "abrupt" substantial change occurring within a couple of decades this century (Figure 16). Large scale die-off of shallow tropical coral reefs could take place on an abrupt timescale in the coming decades (Dixon et al., 2022; Frieler et al., 2013; Hoegh-Guldberg et al., 2019). While Arctic sea ice is a non-tipping element (Notz & Stroeve, 2016), the transition toward seasonally ice-free conditions in summer may occur within the next few decades. Some tipping elements such as stratocumulus cloud deck evaporation or loss of winter Arctic sea ice are at a low risk of crossing critical thresholds this century except under worst-case emissions pathways, but could potentially tip into an altered state on abrupt timescales (Bathiany et al., 2016; Schneider et al., 2019).

A couple candidate tipping elements are possibly at risk of shifting into new states on fast timescales of decades to a century under continued climate change. The Amazon rainforest is under considerable stress due to an intensification of the fire regime (Aragão et al., 2018), changes to regional hydroclimate (Anderson et al., 2018), and

ongoing deforestation, fragmentation, and degradation (Silva Junior et al., 2020) and may undergo major ecosystem shifts in as little as several decades (Fonseca et al., 2019; Lyra et al., 2016). The composition and extent of northern boreal forest ecosystems are expected to continue to shift over many decades to a couple centuries in response to climate change for example, (Gauthier et al., 2015; Shuman et al., 2015), although complex, competing feedbacks and ecological interactions complicate efforts to assess overall climate impacts.

Several candidate tipping elements—permafrost thaw, methane hydrate destabilization, weakening of the AMOC, and ice-sheet collapse—cumulatively act on longer timescales of centuries to millennia, as opposed to undergoing abrupt change in a matter of years to decades. While the bulk of permafrost carbon release will take place over centuries, climatically significant quantities of carbon could be liberated from permafrost in the near term (McGuire et al., 2018; Turetsky et al., 2020). Climate forcing could force the West Antarctic and GIS into committed long-term losses this century, although collapse of these ice-sheets may require many centuries to millennia (DeConto et al., 2021; Edwards et al., 2021; Gregory et al., 2020). While most models project weakening of the AMOC over the 21st century as opposed to collapse even under high emissions scenarios, the stability of the AMOC over the next couple centuries in response to potential future global warming remains uncertain and a subject of active research (Boers, 2021; W. Liu et al., 2017), and transitions in the AMOC may have contributed strongly to past shifts in global climate on timescales of a few centuries or even decades (Brovkin et al., 2021; Ganopolski & Rahmstorf, 2001). Meanwhile, potential atmospheric carbon release from marine methane hydrate deposits may be minimal even over long timescales (K. Kretschmer et al., 2015; Mestdagh et al., 2017; Ruppel & Kessler, 2017).

Our review does not cover the full range of Earth system components that have been proposed to be candidate tipping elements over the last few decades. A number of other systems have been described as potential tipping elements, such as disruptions to the El Niño Southern Oscillation, loss of Antarctic sea ice, changes to snow cover in the Northern Hemisphere, and future shifts in ocean temperatures and oxygen levels, but are not expected to exhibit tipping behavior in response to warming (Ranasinghe et al., 2021). The potential for tipping behavior in the El Niño Southern Oscillation is controversial and contested, and other authors have excluded this system from consideration as a tipping element based on such considerations (Armstrong McKay et al., 2022; Wunderling et al., 2021). This and other candidate tipping elements are less widely discussed, with weaker evidence regarding the risk of tipping behavior and more of the published research suggesting that these systems are non-tipping elements (Ranasinghe et al., 2021). While we have reviewed the current literature on several other systems currently assessed to be non-tipping elements such as summer Arctic sea ice and tropical seasonal monsoons, these systems have been much more commonly invoked as candidate tipping elements in the earth science literature.

Most of the candidate tipping elements detailed in this review are not yet committed to fixed, substantial changes in response to warming. Ambitious efforts to reduce global greenhouse gas emissions could significantly reduce the long-term impacts associated with the responses of these systems to climate change. Under middle-of-the-road pathways, our synthesis of existing research suggests reduced AMOC weakening and reduced risks of AMOC collapse (Bakker et al., 2016; J.-Y. Lee et al., 2021), reduced sea-level contributions from the Greenland and Antarctic ice-sheets (DeConto et al., 2021; Edwards et al., 2021), a smaller magnitude of permafrost carbon release (McGuire et al., 2018; Schneider Von Deimling et al., 2015; Turetsky et al., 2020), smaller shifts in boreal forest ecosystems (Foster et al., 2019; Shuman et al., 2015; Wu et al., 2017), and lower impacts on tropical forests in Amazonia from fire and climate shifts (Fonseca et al., 2019; Lyra et al., 2016) relative to high-end emissions pathways. A middle-of-the-road emissions scenario may completely avert the destabilization of marine methane hydrates or stratocumulus cloud decks. "Slow-onset" tipping points may also exhibit some resiliency due to the longer timescales over which they respond to climate forcing, potentially allowing for recovery to the original system state if overshoots of critical thresholds are smaller and/or limited in duration (Ritchie et al., 2021).

At the same time, the sensitivity of many tipping elements to climate forcing remains unknown, with an increasing risk of transgressing critical thresholds for progressively higher warming in the range of 1.5°C–3°C given the lower end of uncertainty ranges (Armstrong McKay et al., 2022). Furthermore, a number of Earth system components are likely to undergo significant changes even assuming more ambitious world efforts to limit global warming to 1.5°C. Loss of Arctic summer sea ice and coral die-off in shallow tropical coral reef ecosystems will continue even under lower warming scenarios, with intermittently ice-free Arctic conditions in September (Notz & Stroeve, 2018; SIMIP Community, 2020) and major global declines in coral abundance (Hoegh-Guldberg

et al., 2019) likely to occur within the next several decades. Permafrost thaw and carbon release from tropical rainforests are already occurring under the present-day climate (Biskaborn et al., 2019; Gatti et al., 2021) and will continue to intensify over the 21st century under continued warming. While tropical seasonal monsoons are not thought to be at risk of tipping behavior, changes in monsoon intensity and seasonality will continue under moderate warming scenarios (SSP2-4.5) (B. Wang, Jin, & Liu, 2020).

For some tipping elements, future consequences depend not only on reduction of emissions but also upon limiting the impact of human activities on land and ocean ecosystems. Tropical coral reefs face a variety of stressors apart from rising temperatures, sea-level rise, and ocean acidification, including marine pollution, sediment runoff, and direct damage from fishing and harvesting. Limiting deforestation will help promote the long-term health of the Amazon tropical forest, while forest management policies across countries in the northern high latitudes will also affect the future response of boreal forests to a warming climate. Reducing ecosystem impacts alongside efforts to cut greenhouse gas emissions, potentially in combination with deployment of negative emissions technologies at scale, could help reduce the long-term changes that tipping elements might undergo.

Simultaneously, this review points toward considerable remaining knowledge gaps associated with estimating the probability and impacts of many tipping elements. In addition to the more subject-specific areas of uncertainty covered in the preceding sections, some common priorities for future work are apparent. A continued need exists in particular for quantitative, process and scenario-based modeling of interactions between tipping elements and carbon cycle feedbacks and their implications for global climate. Regarding specific Earth system components, further attention toward modeling long-term outcomes under lower to middle-of-the-road warming scenarios (e.g., SSP1-1.9, SSP2-2.6, SSP2-4.5) will help constrain potential critical thresholds more precisely. For conceptual and theoretical work on tipping elements, greater efforts to represent heterogeneity in systems and consider multiple drivers could provide additional useful insights relative to the traditional approach of considering single systems that respond to the transgression of a clear critical threshold by a single controlling variable. More fundamentally, efforts to refine formal definitions and categorizations of tipping elements in consideration of factors like spatial heterogeneity, multi-stability, or different types of tipping behavior will help clarify future scientific discussion. Finally, additional study of paleoclimate records carries the potential to provide direct insights into the behavior of tipping elements and interactions between such systems in the Earth's past (Brovkin et al., 2021; Z. A. Thomas et al., 2020).

Overall, tipping elements will play a climatically significant role over the course of the 21st century, but the possibility of a "tipping point cascade" driving a couple or more degrees of additional warming over the next couple centuries remains unlikely. Nevertheless, tipping elements presently remain one of the larger unknowns involved in predicting future warming and climate impacts. Continuing to better constrain the range of uncertainty surrounding the likelihood and projected impacts of tipping elements will benefit not only the earth science community but also policymakers and planners seeking to assess risks and craft effective climate policies moving forwards. As scientific understanding of tipping elements improves further, the potential for abrupt climate change and for tipping element interactions will require ongoing re-assessment.

Conflict of Interest

The authors declare no conflicts of interest relevant to this study.

Data Availability Statement

Python code and data files needed to replicate our simple FaIR modeling exercise are available at Zenodo using the following DOI: https://doi.org/10.5281/zenodo.7038980.

References

Abbott, B. W., & Jones, J. B. (2015). Permafrost collapse alters soil carbon stocks, respiration, CH₄, and N₂O in upland tundra. *Global Change Biology*, *21*(12), 4570–4587. https://doi.org/10.1111/gcb.13069

Abbott, B. W., Jones, J. B., Godsey, S. E., Larouche, J. R., & Bowden, W. B. (2015). Patterns and persistence of hydrologic carbon and nutrient export from collapsing upland permafrost. *Biogeosciences*, *12*(12), 3725–3740. https://doi.org/10.5194/bg-12-3725-2015

Adkins, J., de Menocal, P., & Eshel, G. (2006). The "African humid period" and the record of marine upwelling from excess ²³⁰Th in Ocean Drilling Program Hole 658C. *Paleoceanography*, *21*(4), PA4203. https://doi.org/10.1029/2005PA001200

Aeberhardt, M., Blatter, M., & Stocker, T. F. (2000). Variability on the century time scale and regime changes in a stochastically forced zonally averaged ocean-atmosphere model. *Geophysical Research Letters*, *27*(9), 1303–1306. https://doi.org/10.1029/1999GL011103

Albano, L. J., Turetsky, M. R., Mack, M. C., & Kane, E. S. (2021). Deep roots of *Carex aquatilis* have greater ammonium uptake capacity than shallow roots in peatlands following permafrost thaw. *Plant and Soil*, *465*(1–2), 261–272. https://doi.org/10.1007/s11104-021-04978-x

Alexander, H. D., & Mack, M. C. (2016). A canopy shift in interior Alaskan boreal forests: Consequences for above- and belowground carbon and nitrogen pools during post-fire succession. *Ecosystems*, *19*(1), 98–114. https://doi.org/10.1007/s10021-015-9920-7

Alkhayuon, H., Ashwin, P., Jackson, L. C., Quinn, C., & Wood, R. A. (2019). Basin bifurcations, oscillatory instability and rate-induced thresholds for Atlantic meridional overturning circulation in a global oceanic box model. *Proceedings of the Royal Society A: Mathematical, Physical & Engineering Sciences*, *475*(2225), 20190051. https://doi.org/10.1098/rspa.2019.0051

Allen, C. D., Macalady, A. K., Chenchouni, H., Bachelet, D., McDowell, N., Vennetier, M., et al. (2010). A global overview of drought and heat-induced tree mortality reveals emerging climate change risks for forests. *Forest Ecology and Management*, *259*(4), 660–684. https://doi.org/10.1016/j.foreco.2009.09.001

Alley, R. B., Anandakrishnan, S., & Jung, P. (2001). Stochastic resonance in the North Atlantic. *Paleoceanography*, *16*(2), 190–198. https://doi.org/10.1029/2000pa000518

Anderson, L. O., Malhi, Y., Aragão, L. E. O. C., Ladle, R., Arai, E., Barbier, N., & Phillips, O. (2010). Remote sensing detection of droughts in Amazonian forest canopies. *New Phytologist*, *187*(3), 733–750. https://doi.org/10.1111/j.1469-8137.2010.03355.x

Anderson, L. O., Ribeiro Neto, G., Cunha, A. P., Fonseca, M. G., Mendes de Moura, Y., Dalagnol, R., et al. (2018). Vulnerability of Amazonian forests to repeated droughts. *Philosophical Transactions of the Royal Society B: Biological Sciences*, *373*(1760), 20170411. https://doi.org/10.1098/rstb.2017.0411

Andresen, C. G., Lawrence, D. M., Wilson, C. J., McGuire, A. D., Koven, C., Schaefer, K., et al. (2020). Soil moisture and hydrology projections of the permafrost region—A model intercomparison. *The Cryosphere*, *14*(2), 445–459. https://doi.org/10.5194/tc-14-445-2020

Anton, A., Randle, J. L., Garcia, F. C., Rossbach, S., Ellis, J. I., Weinzierl, M., & Duarte, C. M. (2020). Differential thermal tolerance between algae and corals may trigger the proliferation of algae in coral reefs. *Global Change Biology*, *26*(8), 4316–4327. https://doi.org/10.1111/gcb.15141

Aragão, L. E. O. C., Anderson, L. O., Fonseca, M. G., Rosan, T. M., Vedovato, L. B., Wagner, F. H., et al. (2018). 21st Century drought-related fires counteract the decline of Amazon deforestation carbon emissions. *Nature Communications*, *9*(1), 536. https://doi.org/10.1038/s41467-017-02771-y

Archer, D. (2007). Methane hydrate stability and anthropogenic climate change. In *European Geosciences Union* (Vol. 4). Retrieved from https://hal.archives-ouvertes.fr/hal-00297882

Archer, D. (2015). A model of the methane cycle, permafrost, and hydrology of the Siberian continental margin. *Biogeosciences*, *12*(10), 2953–2974. https://doi.org/10.5194/bg-12-2953-2015

Archer, D., Buffett, B., & Brovkin, V. (2009). Ocean methane hydrates as a slow tipping point in the global carbon cycle. *Proceedings of the National Academy of Sciences of the United States of America*, *106*(49), 20596–20601. https://doi.org/10.1073/pnas.0800885105

Archer, D., & Ganopolski, A. (2005). A movable trigger: Fossil fuel CO_2 and the onset of the next glaciation. *Geochemistry, Geophysics, Geosystems*, *6*(5), Q05003. https://doi.org/10.1029/2004GC000891

Armour, K. C., Eisenman, I., Blanchard-Wrigglesworth, E., McCusker, K. E., & Bitz, C. M. (2011). The reversibility of sea ice loss in a state-of-the-art climate model. *Geophysical Research Letters*, *38*(16), L16705. https://doi.org/10.1029/2011GL048739

Armstrong McKay, D. I., Staal, A., Abrams, J. F., Winkelmann, R., Sakschewski, B., Loriani, S., et al. (2022). Exceeding 1.5°C global warming could trigger multiple climate tipping points. *Science*, *377*(6611), eabn7950. https://doi.org/10.1126/science.abn7950

Arrigo, K. R., Perovich, D. K., Pickart, R. S., Brown, Z. W., Van Dijken, G. L., Lowry, K. E., et al. (2012). Massive phytoplankton blooms under Arctic sea ice. *Science*, *336*(6087), 1408. https://doi.org/10.1126/science.1215065

Årthun, M., Onarheim, I. H., Dörr, J., & Eldevik, T. (2021). The seasonal and regional transition to an ice-free Arctic. *Geophysical Research Letters*, *48*(1), e2020GL090825. https://doi.org/10.1029/2020GL090825

Arvor, D., Dubreuil, V., Ronchail, J., Simões, M., & Funatsu, B. M. (2014). Spatial patterns of rainfall regimes related to levels of double cropping agriculture systems in Mato Grosso (Brazil). *International Journal of Climatology*, *34*(8), 2622–2633. https://doi.org/10.1002/joc.3863

Ashwin, P., Wieczorek, S., Vitolo, R., & Cox, P. (2012). Tipping points in open systems: Bifurcation, noise-induced and rate-dependent examples in the climate system. *Philosophical Transactions of the Royal Society A: Mathematical, Physical & Engineering Sciences*, *370*(1962), 1166–1184. https://doi.org/10.1098/rsta.2011.0306

Austermann, J., Hoggard, M. J., Latychev, K., Richards, F. D., & Mitrovica, J. X. (2021). The effect of lateral variations in Earth structure on Last Interglacial sea level. *Geophysical Journal International*, *227*(3), 1938–1960. https://doi.org/10.1093/gji/ggab289

Baker, A. C., Glynn, P. W., & Riegl, B. (2008). Climate change and coral reef bleaching: An ecological assessment of long-term impacts, recovery trends and future outlook. *Estuarine, Coastal and Shelf Science*, *80*(4), 435–471. https://doi.org/10.1016/j.ecss.2008.09.003

Bakker, P., Schmittner, A., Lenaerts, J. T. M., Abe-Ouchi, A., Bi, D., van den Broeke, M. R., et al. (2016). Fate of the Atlantic Meridional Overturning Circulation: Strong decline under continued warming and Greenland melting. *Geophysical Research Letters*, *43*(23), 12252–12260. https://doi.org/10.1002/2016GL070457

Balch, J. K., Brando, P. M., Nepstad, D. C., Coe, M. T., Silvério, D., Massad, T. J., et al. (2015). The susceptibility of southeastern Amazon forests to fire: Insights from a large-scale burn experiment. *BioScience*, *65*(9), 893–905. https://doi.org/10.1093/biosci/biv106

Balshi, M. S., McGuire, A. D., Duffy, P., Flannigan, M., Walsh, J., & Melillo, J. (2009). Assessing the response of area burned to changing climate in western boreal North America using a Multivariate Adaptive Regression Splines (MARS) approach. *Global Change Biology*, *15*(3), 578–600. https://doi.org/10.1111/j.1365-2486.2008.01679.x

Baltzer, J. L., Day, N. J., Walker, X. J., Greene, D., Mack, M. C., Alexander, H. D., et al. (2021). Increasing fire and the decline of fire adapted black spruce in the boreal forest. *Proceedings of the National Academy of Sciences*, *118*(45), e2024872118. https://doi.org/10.1073/pnas.2024872118

Baltzer, J. L., Veness, T., Chasmer, L. E., Sniderhan, A. E., & Quinton, W. L. (2014). Forests on thawing permafrost: Fragmentation, edge effects, and net forest loss. *Global Change Biology*, *20*(3), 824–834. https://doi.org/10.1111/gcb.12349

Bamber, J. L., Westaway, R. M., Marzeion, B., & Wouters, B. (2018a). The land ice contribution to sea level during the satellite era. *Environmental Research Letters*, *13*(6), 63008. https://doi.org/10.1088/1748-9326/aac2f0

Bamber, J. L., Westaway, R. M., Marzeion, B., & Wouters, B. (2018b). A new synthesis of annual land ice mass trends 1992 to 2016. Supplement to: Bamber, JL et al. (2018): The land ice contribution to sea level during the satellite era. *Environmental Research Letters*, *13*(6), 063008. https://doi.org/10.1088/1748-9326/Aac2f0

Barletta, V. R., Bevis, M., Smith, B. E., Wilson, T., Brown, A., Bordoni, A., et al. (2018). Observed rapid bedrock uplift in Amundsen Sea Embayment promotes ice-sheet stability. *Science*, *360*(6395), 1335–1339. https://doi.org/10.1126/science.aao1447

Barnes, E. A., & Screen, J. A. (2015). The impact of Arctic warming on the midlatitude jet-stream: Can it? Has it? Will it? *WIREs Climate Change*, *6*(3), 277–286. https://doi.org/10.1002/wcc.337

Bassis, J. N., Berg, B., Crawford, A. J., & Benn, D. I. (2021). Transition to marine ice cliff instability controlled by ice thickness gradients and velocity. *Science*, *372*(6548), 1342–1344. https://doi.org/10.1126/science.abf6271

Bassis, J. N., & Jacobs, S. (2013). Diverse calving patterns linked to glacier geometry. *Nature Geoscienc*e, 6(10), 833–836. https://doi.org/10.1038/ngeo1887

Bassis, J. N., & Walker, C. C. (2012). Upper and lower limits on the stability of calving glaciers from the yield strength envelope of ice. *Proceedings of the Royal Society A: Mathematical, Physical & Engineering Sciences*, *468*(2140), 913–931. https://doi.org/10.1098/rspa.2011.0422

Basso, L. S., Marani, L., Gatti, L. V., Miller, J. B., Gloor, M., Melack, J., et al. (2021). Amazon methane budget derived from multi-year airborne observations highlights regional variations in emissions. *Communications Earth & Environment*, *2*(1), 246. https://doi.org/10.1038/s43247-021-00314-4

Bathiany, S., Notz, D., Mauritsen, T., Raedel, G., & Brovkin, V. (2016). On the potential for abrupt Arctic winter sea ice loss. *Journal of Climate*, *29*(7), 2703–2719. https://doi.org/10.1175/JCLI-D-15-0466.1

Bathiany, S., Scheffer, M., Van Nes, E. H., Williamson, M. S., & Lenton, T. M. (2018). Abrupt climate change in an oscillating world. *Scientific Reports*, *8*(1), 5040. https://doi.org/10.1038/s41598-018-23377-4

Beaufort, L., Probert, I., de Garidel-Thoron, T., Bendif, E. M., Ruiz-Pino, D., Metzl, N., et al. (2011). Sensitivity of coccolithophores to carbonate chemistry and ocean acidification. *Nature*, *476*(7358), 80–83. https://doi.org/10.1038/nature10295

Beck, P. S. A., Goetz, S. J., Mack, M. C., Alexander, H. D., Jin, Y., Randerson, J. T., & Loranty, M. M. (2011). The impacts and implications of an intensifying fire regime on Alaskan boreal forest composition and albedo. *Global Change Biology*, *17*(9), 2853–2866. https://doi.org/10.1111/j.1365-2486.2011.02412.x

Beck, P. S. A., Juday, G. P., Alix, C., Barber, V. A., Winslow, S. E., Sousa, E. E., et al. (2011). Changes in forest productivity across Alaska consistent with biome shift. *Ecology Letters*, *14*(4), 373–379. https://doi.org/10.1111/j.1461-0248.2011.01598.x

Bell, R. E. (2008). The role of subglacial water in ice-sheet mass balance. *Nature Geoscience*, *1*(5), 297–304. https://doi.org/10.1038/ngeo186

Bender, F. A. M., Ramanathan, V., & Tselioudis, G. (2012). Changes in extratropical storm track cloudiness 1983–2008: Observational support for a poleward shift. *Climate Dynamics*, *38*(9–10), 2037–2053. https://doi.org/10.1007/s00382-011-1065-6

Berchet, A., Bousquet, P., Pison, I., Locatelli, R., Chevallier, F., Paris, J.-D., et al. (2016). Atmospheric constraints on the methane emissions from the East Siberian Shelf. *Atmospheric Chemistry and Physics*, *16*(6), 4147–4157. https://doi.org/10.5194/acp-16-4147-2016

Berenguer, E., Carvalho, N., Anderson, L. O., Aragão, L. E. O. C., França, F., & Barlow, J. (2021). Improving the spatial-temporal analysis of Amazonian fires. *Global Change Biology*, *27*(3), 469–471. https://doi.org/10.1111/gcb.15425

Berenguer, E., Ferreira, J., Gardner, T. A., Aragão, L. E. O. C., De Camargo, P. B., Cerri, C. E., et al. (2014). A large-scale field assessment of carbon stocks in human-modified tropical forests. *Global Change Biology*, *20*(12), 3713–3726. https://doi.org/10.1111/gcb.12627

Berger, A., & Loutre, M. F. (2002). An exceptionally long interglacial ahead? *Science*, *297*(5585), 1287–1288. https://doi.org/10.1126/science.1076120

Bertani, G., Wagner, F. H., Anderson, L. O., & Aragão, L. E. O. C. (2017). Chlorophyll fluorescence data reveals climate-related photosynthesis seasonality in Amazonian forests. *Remote Sensing*, *9*(12), 1275. https://doi.org/10.3390/rs9121275

Betts, R., Sanderson, M., & Woodward, S. (2008). Effects of large-scale Amazon forest degradation on climate and air quality through fluxes of carbon dioxide, water, energy, mineral dust and isoprene. *Philosophical Transactions of the Royal Society B: Biological Sciences*, *363*(1498), 1873–1880. https://doi.org/10.1098/rstb.2007.0027

Betts, R. A. (2000). Offset of the potential carbon sink from boreal forestation by decreases in surface albedo. *Nature*, *408*(6809), 187–190. https://doi.org/10.1038/35041545

Bevis, M., Harig, C., Khan, S. A., Brown, A., Simons, F. J., Willis, M., et al. (2019). Accelerating changes in ice mass within Greenland, and the ice sheet's sensitivity to atmospheric forcing. *Proceedings of the National Academy of Sciences of the United States of America*, *116*(6), 1934–1939. https://doi.org/10.1073/pnas.1806562116

Bi, J., Xu, L., Samanta, A., Zhu, Z., & Myneni, R. (2013). Divergent arctic-boreal vegetation changes between North America and Eurasia over the past 30 years. *Remote Sensing*, *5*, 2093–2112. https://doi.org/10.3390/rs5052093

Biastoch, A., Böning, C. W., Getzlaff, J., Molines, J.-M., & Madec, G. (2008). Causes of interannual–decadal variability in the meridional overturning circulation of the midlatitude North Atlantic Ocean. *Journal of Climate*, *21*(24), 6599–6615. https://doi.org/10.1175/2008JCLI2404.1

Biastoch, A., Treude, T., Rüpke, L. H., Riebesell, U., Roth, C., Burwicz, E. B., et al. (2011). Rising Arctic Ocean temperatures cause gas hydrate destabilization and ocean acidification. *Geophysical Research Letters*, *38*(8), L08602. https://doi.org/10.1029/2011GL047222

Biasutti, M. (2016). What brings rain to the Sahel? *Nature Climate Change*, *6*(10), 897–898. https://doi.org/10.1038/nclimate3080

Biasutti, M. (2019). Rainfall trends in the African Sahel: Characteristics, processes, and causes. *WIREs Climate Change*, *10*(4), e591. https://doi.org/10.1002/wcc.591

Biasutti, M., & Giannini, A. (2006). Robust Sahel drying in response to late 20th century forcings. *Geophysical Research Letters*, *33*(11), L11706. https://doi.org/10.1029/2006GL026067

Biasutti, M., Voigt, A., Boos, W. R., Braconnot, P., Hargreaves, J. C., Harrison, S. P., et al. (2018). Global energetics and local physics as drivers of past, present and future monsoons. *Nature Geoscience*, *11*(6), 392–400. https://doi.org/10.1038/s41561-018-0137-1

Bigelow, N. H., Brubaker, L. B., Edwards, M. E., Harrison, S. P., Prentice, I. C., Anderson, P. M., et al. (2003). Climate change and Arctic ecosystems: 1. Vegetation changes north of 55°N between the last glacial maximum, mid-Holocene, and present. *Journal of Geophysical Research*, *108*(D19), 8170. https://doi.org/10.1029/2002JD002558

Bindoff, N. L., Cheung, W. W. L., Kairo, J. G., Arístegui, J., Guinder, V. A., Hallberg, R., et al. (2019). Changing ocean, marine ecosystems, and dependent communities. In *IPCC Special Report on the Ocean and Cryosphere in a Changing Climate*. Retrieved from https://www.ipcc.ch/report/srocc/

Bingham, R. J., Hughes, C. W., Roussenov, V., & Williams, R. G. (2007). Meridional coherence of the North Atlantic meridional overturning circulation. *Geophysical Research Letters*, *34*(23), L23606. https://doi.org/10.1029/2007GL031731

Birkeland, C. (2019). Chapter 2—Global status of coral reefs. In *Combination, disturbances and stressors become ratchets*. In *World Seas: An Environmental Evaluation (Second Edition) Volume III: Ecological Issues and Environmental Impacts*. https://doi.org/10.1016/B978-0-12-805052-1.00002-4

Biskaborn, B. K., Smith, S. L., Noetzli, J., Matthes, H., Vieira, G., Streletskiy, D. A., et al. (2019). Permafrost is warming at a global scale. *Nature Communications*, *10*(1), 264. https://doi.org/10.1038/s41467-018-08240-4

Bitz, C. M., Fyfe, J. C., & Flato, G. M. (2002). Sea ice response to wind forcing from AMIP models. *Journal of Climate*, 15(5), 522–536. https://doi.org/10.1175/1520-0442(2002)015<0522:SIRTWF>2.0.CO;2

Bitz, C. M., & Roe, G. H. (2004). A mechanism for the high rate of sea ice thinning in the Arctic Ocean. *Journal of Climate*, *17*(18), 3623–3632. https://doi.org/10.1175/1520-0442(2004)017<3623:AMFTHR>2.0.CO;2

Bjorkman, A. D., Myers-Smith, I. H., Elmendorf, S. C., Normand, S., Rüger, N., Beck, P. S. A., et al. (2018). Plant functional trait change across a warming tundra biome. *Nature*, *562*(7725), 57–62. https://doi.org/10.1038/s41586-018-0563-7

Blossey, P. N., Bretherton, C. S., Zhang, M., Cheng, A., Endo, S., Heus, T., et al. (2013). Marine low cloud sensitivity to an idealized climate change: The CGILS LES intercomparison. *Journal of Advances in Modeling Earth Systems*, *5*(2), 234–258. https://doi.org/10.1002/jame.20025

Bock, M., Schmitt, J., Beck, J., Seth, B., Chappellaz, J., & Fischer, H. (2017). Glacial/interglacial wetland, biomass burning, and geologic methane emissions constrained by dual stable isotopic CH$_4$ ice core records. *Proceedings of the National Academy of Sciences*, *114*(29), E5778–E5786. https://doi.org/10.1073/pnas.1613883114

Boening, C., Lebsock, M., Landerer, F., & Stephens, G. (2012). Snowfall-driven mass change on the East Antarctic ice sheet. *Geophysical Research Letters*, *39*(21), L21501. https://doi.org/10.1029/2012GL053316

Boers, N. (2021). Observation-based early-warning signals for a collapse of the Atlantic Meridional Overturning Circulation. *Nature Climate Change*, *11*(8), 680–688. https://doi.org/10.1038/s41558-021-01097-4

Boers, N., Marwan, N., Barbosa, H. M. J., & Kurths, J. (2017). A deforestation-induced tipping point for the South American monsoon system. *Scientific Reports*, *7*(1), 41489. https://doi.org/10.1038/srep41489

Boers, N., & Rypdal, M. (2021). Critical slowing down suggests that the western Greenland Ice Sheet is close to a tipping point. *Proceedings of the National Academy of Sciences*, *118*(21), e2024192118. https://doi.org/10.1073/pnas.2024192118

Bollasina, M. A., Ming, Y., & Ramaswamy, V. (2011). Anthropogenic aerosols and the weakening of the South Asian summer monsoon. *Science*, *334*(6055), 502–505. https://doi.org/10.1126/science.1204994

Bonan, G. B., Pollard, D., & Thompson, S. L. (1992). Effects of boreal forest vegetation on global climate. *Nature*, *359*(6397), 716–718. https://doi.org/10.1038/359716a0

Böning, C. W., Behrens, E., Biastoch, A., Getzlaff, K., & Bamber, J. L. (2016). Emerging impact of Greenland meltwater on deepwater formation in the North Atlantic Ocean. *Nature Geoscience*, *9*(7), 523–527. https://doi.org/10.1038/ngeo2740

Bonnaventure, P. P., Smith, S. L., Lamoureux, S. F., Way, R. G., Ednie, M., Bouchard, F., et al. (2018). Permafrost. In *From science to policy in the Eastern Canadian Arctic: An Integrated Regional Impact Study (IRIS) of climate change and modernization* (pp. 119–139). ArcticNet.

Boos, W. R., & Emanuel, K. A. (2009). Annual intensification of the Somali jet in a quasi-equilibrium framework: Observational composites. *Quarterly Journal of the Royal Meteorological Society*, *135*(639), 319–335. https://doi.org/10.1002/qj.388

Boos, W. R., & Korty, R. L. (2016). Regional energy budget control of the intertropical convergence zone and application to mid-Holocene rainfall. *Nature Geoscience*, *9*(12), 892–897. https://doi.org/10.1038/ngeo2833

Boos, W. R., & Storelvmo, T. (2016a). Linear scaling for monsoons based on well-verified balance between adiabatic cooling and latent heat release. *Proceedings of the National Academy of Sciences of the United States of America*, *113*(17), E2350–E2351. https://doi.org/10.1073/pnas.1603626113

Boos, W. R., & Storelvmo, T. (2016b). Near-linear response of mean monsoon strength to a broad range of radiative forcings. *Proceedings of the National Academy of Sciences of the United States of America*, *113*(6), 1510–1515. https://doi.org/10.1073/pnas.1517143113

Bopp, L., Resplandy, L., Orr, J. C., Doney, S. C., Dunne, J. P., Gehlen, M., et al. (2013). Multiple stressors of ocean ecosystems in the 21st century: Projections with CMIP5 models. *Biogeosciences*, *10*(10), 6225–6245. https://doi.org/10.5194/bg-10-6225-2013

Born, A., Stocker, T. F., & Sandø, A. B. (2016). Transport of salt and freshwater in the Atlantic Subpolar Gyre. *Ocean Dynamics*, *66*(9), 1051–1064. https://doi.org/10.1007/s10236-016-0970-y

Born, A., Stocker, T. F., Raible, C. C., & Levermann, A. (2013). Is the Atlantic subpolar gyre bistable in comprehensive coupled climate models? *Climate Dynamics*, *40*(11), 2993–3007. https://doi.org/10.1007/s00382-012-1525-7

Boswell, R., & Collett, T. S. (2011). Current perspectives on gas hydrate resources. *Energy & Environmental Science*, 4, 1206–1215. https://doi.org/10.1039/c0ee00203h

Boucher, O., Halloran, P. R., Burke, E. J., Doutriaux-Boucher, M., Jones, C. D., Lowe, J., et al. (2012). Reversibility in an Earth System model in response to CO$_2$ concentration changes. *Environmental Research Letters*, *7*(2), 24013. https://doi.org/10.1088/1748-9326/7/2/024013

Boudreau, B. P., Luo, Y., Meysman, F. J. R., Middelburg, J. J., & Dickens, G. R. (2015). Gas hydrate dissociation prolongs acidification of the Anthropocene oceans. *Geophysical Research Letters*, *42*(21), 9337–9344A. https://doi.org/10.1002/2015GL065779

Bove, C. B., Ries, J. B., Davies, S. W., Westfield, I. T., Umbanhowar, J., & Castillo, K. D. (2019). Common Caribbean corals exhibit highly variable responses to future acidification and warming. *Proceedings of the Royal Society B: Biological Sciences*, *286*(1900), 20182840. https://doi.org/10.1098/rspb.2018.2840

Bowen, G. J., Maibauer, B. J., Kraus, M. J., Röhl, U., Westerhold, T., Steimke, A., et al. (2015). Two massive, rapid releases of carbon during the onset of the Palaeocene–Eocene thermal maximum. *Nature Geoscience*, *8*(1), 44–47. https://doi.org/10.1038/ngeo2316

Bowen, J. C., Ward, C. P., Kling, G. W., & Cory, R. M. (2020). Arctic amplification of global warming strengthened by sunlight oxidation of permafrost carbon to CO$_2$. *Geophysical Research Letters*, *47*(12), e2020GL087085. https://doi.org/10.1029/2020GL087085

Box, J. E., & Colgan, W. (2013). Greenland ice sheet mass balance reconstruction. Part III: Marine ice loss and total mass balance (1840–2010). *Journal of Climate*, *26*(18), 6990–7002. https://doi.org/10.1175/JCLI-D-12-00546.1

Box, J. E., Hubbard, A., Bahr, D. B., Colgan, W. T., Fettweis, X., Mankoff, K. D., et al. (2022). Greenland ice sheet climate disequilibrium and committed sea-level rise. *Nature Climate Change*, *12*(9), 808–813. https://doi.org/10.1038/s41558-022-01441-2

Boyd, M. A., Berner, L. T., Foster, A. C., Goetz, S. J., Rogers, B. M., Walker, X. J., & Mack, M. C. (2021). Historic declines in growth portend trembling aspen death during a contemporary leaf miner outbreak in Alaska. *Ecosphere*, *12*(6), e03569. https://doi.org/10.1002/ecs2.3569

Bozbiyik, A., Steinacher, M., Joos, F., Stocker, T. F., & Menviel, L. (2011). Fingerprints of changes in the terrestrial carbon cycle in response to large reorganizations in ocean circulation. *Climate of the Past*, *7*(1), 319–338. https://doi.org/10.5194/cp-7-319-2011

Bradshaw, C. J. A., & Warkentin, I. G. (2015). Global estimates of boreal forest carbon stocks and flux. *Global and Planetary Change*, *128*, 24–30. https://doi.org/10.1016/j.gloplacha.2015.02.004

Brando, P. M., Balch, J. K., Nepstad, D. C., Morton, D. C., Putz, F. E., Coe, M. T., et al. (2014). Abrupt increases in Amazonian tree mortality due to drought-fire interactions. *Proceedings of the National Academy of Sciences of the United States of America*, *111*(17), 6347–6352. https://doi.org/10.1073/pnas.1305499111

Brando, P. M., Soares-Filho, B., Rodrigues, L., Assunção, A., Morton, D., Tuchschneider, D., et al. (2019). The gathering firestorm in southern Amazonia. *Science Advances*, *6*(2), eaay1632. https://doi.org/10.1126/sciadv.aay1632

Bretherton, C. S. (2015). Insights into low-latitude cloud feedbacks from high-resolution models. *Philosophical Transactions of the Royal Society A: Mathematical, Physical & Engineering Sciences*, *373*(2054), 20140415. https://doi.org/10.1098/rsta.2014.0415

Bretherton, C. S., & Wyant, M. C. (1997). Moisture transport, lower-tropospheric stability, and decoupling of cloud-topped boundary layers. *Journal of the Atmospheric Sciences*, *54*(1), 148–167. https://doi.org/10.1175/1520-0469(1997)054<0148:MTLTSA>2.0.CO;2

Brodribb, T. J., Cochard, H., & Dominguez, C. R. (2019). Themed issue article: Climate change impact on urban and natural measuring the pulse of trees; using the vascular system to predict tree mortality in the 21st century. *Conservation Physiology*, *7*, 1–7.

Brodribb, T. J., Powers, J., Cochard, H., & Choat, B. (2020). Hanging by a thread? Forests and drought. *Science*, *368*(6488), 261–266. https://doi.org/10.1126/science.aat7631

Broecker, W. S. (1991). The great ocean conveyor. *Oceanography*, 4(2), 79–89. https://doi.org/10.1016/s0262-4079(08)61198-7

Broecker, W. S., Peteet, D. M., & Rind, D. (1985). Does the ocean–atmosphere system have more than one stable mode of operation? *Nature*, *315*(6014), 21–26. https://doi.org/10.1038/315021a0

Brovkin, V., Brook, E., Williams, J. W., Bathiany, S., Lenton, T. M., Barton, M., et al. (2021). Past abrupt changes, tipping points and cascading impacts in the Earth system. *Nature Geoscience*, *14*(8), 550–558. https://doi.org/10.1038/s41561-021-00790-5

Brown, B. E., Dunne, R. P., Goodson, M. S., & Douglas, A. E. (2002). Experience shapes the susceptibility of a reef coral to bleaching. *Coral Reefs*, *21*(2), 119–126. https://doi.org/10.1007/s00338-002-0215-z

Bruno, J. F., & Selig, E. R. (2007). Regional decline of coral cover in the Indo-Pacific: Timing, extent, and subregional comparisons. *PLoS One*, *2*(8), e711. https://doi.org/10.1371/journal.pone.0000711

Bryden, H. L., Johns, W. E., King, B. A., McCarthy, G., McDonagh, E. L., Moat, B. I., & Smeed, D. A. (2020). Reduction in ocean heat transport at 26°N since 2008 cools the eastern subpolar gyre of the North Atlantic Ocean. *Journal of Climate*, *33*(5), 1677–1689. https://doi.org/10.1175/JCLI-D-19-0323.1

Bryden, H. L., Longworth, H. R., & Cunningham, S. A. (2005). Slowing of the Atlantic meridional overturning circulation at 25°N. *Nature*, *438*(7068), 655–657. https://doi.org/10.1038/nature04385

Buckley, M. W., Ferreira, D., Campin, J. M., Marshall, J., & Tulloch, R. (2012). On the relationship between decadal buoyancy anomalies and variability of the Atlantic meridional overturning circulation. *Journal of Climate*, *25*(23), 8009–8030. https://doi.org/10.1175/JCLI-D-11-00505.1

Buckley, M. W., & Marshall, J. (2016). Observations, inferences, and mechanisms of the atlantic meridional overturning circulation: A review. *Reviews of Geophysics*, *54*(1), 5–63. https://doi.org/10.1002/2015RG000493

Bullock, E. L., & Woodcock, C. E. (2020). Carbon loss and removal due to forest disturbance and regeneration in the Amazon. *Science of the Total Environment*, *764*, 142839. https://doi.org/10.1016/j.scitotenv.2020.142839

Bullock, E. L., Woodcock, C. E., Souza, C., Jr., & Olofsson, P. (2020). Satellite-based estimates reveal widespread forest degradation in the Amazon. *Global Change Biology*, *26*(5), 2956–2969. https://doi.org/10.1111/gcb.15029

Bulthuis, K., Arnst, M., Sun, S., & Pattyn, F. (2019). Uncertainty quantification of the multi-centennial response of the Antarctic ice sheet to climate change. *The Cryosphere*, *13*(4), 1349–1380. https://doi.org/10.5194/tc-13-1349-2019

Burke, E. J., Zhang, Y., & Krinner, G. (2020). Evaluating permafrost physics in the Coupled Model Intercomparison Project 6 (CMIP6) models and their sensitivity to climate change. *The Cryosphere*, *14*(9), 3155–3174. https://doi.org/10.5194/tc-14-3155-2020

Burke, K. D., Williams, J. W., Chandler, M. A., Haywood, A. M., Lunt, D. J., & Otto-Bliesner, B. L. (2018). Pliocene and Eocene provide best analogs for near-future climates. *Proceedings of the National Academy of Sciences*, *115*(52), 13288–13293. https://doi.org/10.1073/pnas.1809600115

Burke, L., Reytar, K., Spalding, M., & Perry, A. (2011). Reefs at risk revisited. In *Reefs at risk revisited*. Retrieved from http://www.pubmedcentral.nih.gov/articlerender.fcgi?artid=3150666&tool=pmcentrez&rendertype=abstract

Burrell, A., Kukavskaya, E., Baxter, R., Sun, Q., & Barrett, K. (2021). Post-fire recruitment failure as a driver of forest to non-forest ecosystem shifts in boreal regions.In In J. G. Canadell & R. B. Jackson (Eds.), *Ecosystem collapse and climate change*. https://doi.org/10.1007/978-3-030-71330-0_4

Burton, C., Kelley, D. I., Jones, C. D., Betts, R. A., Cardoso, M., & Anderson, L. (2021). South American fires and their impacts on ecosystems increase with continued emissions. *Climate Resilience and Sustainability*, *1*(1), e8. https://doi.org/10.1002/cli2.8

Caballero, R., & Huber, M. (2013). State-dependent climate sensitivity in past warm climates and its implications for future climate projections. *Proceedings of the National Academy of Sciences*, *110*(35), 14162–14167. https://doi.org/10.1073/pnas.1303365110

Caesar, L., McCarthy, G. D., Thornalley, D. J. R., Cahill, N., & Rahmstorf, S. (2021). Current Atlantic Meridional Overturning Circulation weakest in last millennium. *Nature Geoscience*, *14*(3), 118–120. https://doi.org/10.1038/s41561-021-00699-z

Caesar, L., Rahmstorf, S., Robinson, A., Feulner, G., & Saba, V. (2018). Observed fingerprint of a weakening Atlantic Ocean overturning circulation. *Nature*, *556*(7700), 191–196. https://doi.org/10.1038/s41586-018-0006-5

Cai, Y., Lenton, T. M., & Lontzek, T. S. (2016). Risk of multiple interacting tipping points should encourage rapid CO_2 emission reduction. *Nature Climate Change*, *6*(5), 520–525. https://doi.org/10.1038/nclimate2964

Canadell, J. G., Monteiro, P. M. S., Costa, M. H., Da Cunha, L. C., Cox, P. M., Alexey, V., et al. (2021). Chapter 5: Global carbon and other biogeochemical cycles and feedbacks. In *Climate Change 2021: The Physical Science Basis. Contribution of Working Group I to the Sixth Assessment Report of the Intergovernmental Panel on Climate Change*. Cambridge University Press.

Carpino, O. A., Berg, A. A., Quinton, W. L., & Adams, J. R. (2018). Climate change and permafrost thaw-induced boreal forest loss in northwestern Canada. *Environmental Research Letters*, *13*(8), 084018. https://doi.org/10.1088/1748-9326/aad74e

Carroll, D., Sutherland, D. A., Hudson, B., Moon, T., Catania, G. A., Shroyer, E. L., et al. (2016). The impact of glacier geometry on meltwater plume structure and submarine melt in Greenland fjords. *Geophysical Research Letters*, *43*(18), 9739–9748. https://doi.org/10.1002/2016GL070170

Castellanos, E., Lemos, M. F., Astigarraga, L., Chacón, N., Cuvi, N., Huggel, C., et al. (2022). Chapter 12: Central and South America. In *Climate Change 2022: Impacts, Adaptation, and Vulnerability. Contribution of Working Group II to the Sixth Assessment Report of the Intergovernmental Panel on Climate Change*. Retrieved from https://www.ipcc.ch/report/ar6/wg2/

Cerri, C. E. P., Easter, M., Paustian, K., Killian, K., Coleman, K., Bernoux, M., et al. (2007). Predicted soil organic carbon stocks and changes in the Brazilian Amazon between 2000 and 2030. *Agriculture, Ecosystems & Environment*, *122*(1), 58–72. https://doi.org/10.1016/j.agee.2007.01.008

Chadburn, S. E., Burke, E. J., Cox, P. M., Friedlingstein, P., Hugelius, G., & Westermann, S. (2017). An observation-based constraint on permafrost loss as a function of global warming. *Nature Climate Change*, *7*(5), 340–344. https://doi.org/10.1038/nclimate3262

Chan, E. W., Shiller, A. M., Joung, D. J., Arrington, E. C., Valentine, D. L., Redmond, M. C., et al. (2019). Investigations of aerobic methane oxidation in two marine seep environments: Part 1—Chemical kinetics. *Journal of Geophysical Research: Oceans*, *124*(12), 8852–8868. https://doi.org/10.1029/2019JC015594

Chapin, F. S., Sturm, M., Serreze, M. C., McFadden, J. P., Key, J. R., Lloyd, A. H., et al. (2005). Role of land-surface changes in Arctic summer warming. *Science*, *310*(5748), 657–660. https://doi.org/10.1126/science.1117368

Charney, J. G. (1975). Dynamics of deserts and drought in the Sahel. *Quarterly Journal of the Royal Meteorological Society*, *101*(428), 193–202. https://doi.org/10.1002/qj.49710142802

Charney, J. G., & Eliassen, A. (1964). On the growth of the hurricane depression. *Journal of the Atmospheric Sciences*, 21(1), 68–75. https://doi.org/10.1175/1520-0469(1964)021<0068:OTGOTH>2.0.CO;2

Chen, D., Rojas, M., Samset, B. H., Cobb, K., Diongue Niang, A., Edwards, P., et al. (2021). Chapter 1: Framing, context, and methods. In *Climate Change 2021: The Physical Science Basis. Contribution of Working Group I to the Sixth Assessment Report of the Intergovernmental Panel on Climate Change*. Cambridge University Press.

Chen, X., & Tung, K.-K. (2018). Global surface warming enhanced by weak Atlantic overturning circulation. *Nature*, *559*(7714), 387–391. https://doi.org/10.1038/s41586-018-0320-y

Chen, Y., Lara, M. J., Jones, B. M., Frost, G. V., & Hu, F. S. (2021). Thermokarst acceleration in Arctic tundra driven by climate change and fire disturbance. *One Earth*, *4*(12), 1718–1729. https://doi.org/10.1016/j.oneear.2021.11.011

Chen, Z., Zhou, T., Zhang, L., Chen, X., Zhang, W., & Jiang, J. (2020). Global land monsoon precipitation changes in CMIP6 projections. *Geophysical Research Letters*, *47*(14), e2019GL086902. https://doi.org/10.1029/2019GL086902

Cheng, H., Edwards, R. L., Sinha, A., Spötl, C., Yi, L., Chen, S., et al. (2016). The Asian monsoon over the past 640,000 years and ice age terminations. *Nature*, *534*(7609), 640–646. https://doi.org/10.1038/nature18591

Chiang, J. C. H., & Bitz, C. M. (2005). Influence of high latitude ice cover on the marine Intertropical Convergence Zone. *Climate Dynamics*, *25*(5), 477–496. https://doi.org/10.1007/s00382-005-0040-5

Choi, Y., Morlighem, M., Rignot, E., & Wood, M. (2021). Ice dynamics will remain a primary driver of Greenland ice sheet mass loss over the next century. *Communications Earth & Environment*, *2*(1), 26. https://doi.org/10.1038/s43247-021-00092-z

Christensen, J. H., Kanikicharla, K. K., Aldrian, E., An, S. I., Cavalcanti, I. F. A., de Castro, M., et al. (2013). Climate phenomena and their relevance for future regional climate change. In *Climate Change 2013: The Physical Science Basis. Working Group I Contribution to the Fifth Assessment Report of the Intergovernmental Panel on Climate Change*. https://doi.org/10.1017/CBO9781107415324.028

Circone, S., Kirby, S. H., & Stern, L. A. (2005). Thermal regulation of methane hydrate dissociation: Implications for gas production models. *Energy & Fuels*, *19*(6), 2357–2363. https://doi.org/10.1021/ef0500437

Clark, P. U., Marshall, S., Clarke, G. K. C., Hostetler, S. W., Licciardi, J. M., & Teller, J. T. (2001). Freshwater forcing of abrupt climate change during the last glaciation. *Science*, *293*(5528), 283–287. https://doi.org/10.1126/science.1062517

Clark, P. U., Pisias, N., Stocker, T., & Weaver, A. (2002). The role of the thermohaline circulation in abrupt climate change. *Nature*, *415*(6874), 863–869. https://doi.org/10.1038/415863a

Clark, P. U., Shakun, J. D., Marcott, S. A., Mix, A. C., Eby, M., Kulp, S., et al. (2016). Consequences of twenty-first-century policy for multi-millennial climate and sea-level change. *Nature Climate Change*, *6*(4), 360–369. https://doi.org/10.1038/nclimate2923

Claussen, M., Brovkin, V., Ganopolski, A., Kubatzki, C., & Petoukhov, V. (2003). Climate change in northern Africa: The past is not the future. *Climatic Change*, *57*(1), 99–118. https://doi.org/10.1023/A:1022115604225

Claypool, G. E., & Kvenvolden, K. A. (1983). Methane and other hydrocarbon gases in marine sediment. *Annual Review of Earth and Planetary Sciences*, *11*(1), 299–327. https://doi.org/10.1146/annurev.ea.11.050183.001503

Clerc, F., Minchew, B. M., & Behn, M. D. (2019). Marine ice cliff instability mitigated by slow removal of ice shelves. *Geophysical Research Letters*, *46*(21), 12108–12116. https://doi.org/10.1029/2019GL084183

Cochrane, M. A., & Barber, C. P. (2009). Climate change, human land use and future fires in the Amazon. *Global Change Biology*, *15*(3), 601–612. https://doi.org/10.1111/j.1365-2486.2008.01786.x

Cochrane, M. A., & Schulze, M. D. (1999). Fire as a recurrent event in tropical forests of the eastern Amazon: Effects on forest structure, biomass, and species composition. *Biotropica*, *31*(1), 2–16. https://doi.org/10.2307/2663955

COHMAP Members. (1988). Climatic changes of the last 18,000 years: Observations and model simulations. *Science*, *241*(4869), 1043–1052. https://doi.org/10.1126/science.241.4869.1043

Coles, S. L., & Brown, B. E. (2003). Coral bleaching—Capacity for acclimatization and adaptation. *Advances in Marine Biology*, *46*, 183–223. https://doi.org/10.1016/S0065-2881(03)46004-5

Collins, M., Sutherland, M., Bouwer, L., Cheong, S.-M., Frölicher, T. L., Jacot Des Combes, H., et al. (2019). Extremes, abrupt changes and managing risks. In *IPCC Special Report on the Ocean and Cryosphere in a Changing Climate*. Retrieved from https://report.ipcc.ch/srocc/pdf/SROCC_FinalDraft_Chapter6.pdf

Constable, A. J., Harper, S., Dawson, J., Holsman, K., Mustonen, T., Piepenburg, D., & Rost, B. (2022). Cross-chapter paper 6: Polar regions. In *Climate Change 2022: Impacts, Adaptation, and Vulnerability. Contribution of Working Group II to the Sixth Assessment Report of the Intergovernmental Panel on Climate Change*. Cambridge University Press.

Cook, C. P., Van De Flierdt, T., Williams, T., Hemming, S. R., Iwai, M., Kobayashi, M., et al. (2013). Dynamic behaviour of the East Antarctic ice sheet during Pliocene warmth. *Nature Geoscience*, *6*(9), 765–769. https://doi.org/10.1038/ngeo1889

Cook, K. H., & Vizy, E. K. (2008). Effects of twenty-first-century climate change on the Amazon rain forest. *Journal of Climate*, *21*(3), 542–560. https://doi.org/10.1175/2007JCLI1838.1

Cornford, S. L., Martin, D. F., Payne, A. J., Ng, E. G., Le Brocq, A. M., Gladstone, R. M., et al. (2015). Century-scale simulations of the response of the West Antarctic Ice Sheet to a warming climate. *The Cryosphere*, *9*(4), 1579–1600. https://doi.org/10.5194/tc-9-1579-2015

Coulon, V., Bulthuis, K., Whitehouse, P. L., Sun, S., Haubner, K., Zipf, L., & Pattyn, F. (2021). Contrasting response of West and East Antarctic ice sheets to glacial isostatic adjustment. *Journal of Geophysical Research: Earth Surface*, *126*(7), e2020JF006003. https://doi.org/10.1029/2020JF006003

Cox, P. M., Pearson, D., Booth, B. B., Friedlingstein, P., Huntingford, C., Jones, C. D., & Luke, C. M. (2013). Sensitivity of tropical carbon to climate change constrained by carbon dioxide variability. *Nature*, *494*(7437), 341–344. https://doi.org/10.1038/nature11882

Crawford, A. J., Benn, D. I., Todd, J., Åström, J. A., Bassis, J. N., & Zwinger, T. (2021). Marine ice-cliff instability modeling shows mixed-mode ice-cliff failure and yields calving rate parameterization. *Nature Communications*, *12*(1), 2701. https://doi.org/10.1038/s41467-021-23070-7

Cunningham, S. A., Kanzow, T., Rayner, D., Baringer, M. O., Johns, W. E., Marotzke, J., et al. (2007). Temporal variability of the Atlantic meridional overturning circulation at 26.5°N. *Science*, *317*(5840), 935–938. https://doi.org/10.1126/science.1141304

Dakos, V., Scheffer, M., van Nes, E. H., Brovkin, V., Petoukhov, V., & Held, H. (2008). Slowing down as an early warning signal for abrupt climate change. *Proceedings of the National Academy of Sciences*, *105*(38), 14308–14312. https://doi.org/10.1073/pnas.0802430105

Daniel, N., David, M., Claudia, S., Ane, A., Andrea, A., Briana, S., et al. (2014). Slowing Amazon deforestation through public policy and interventions in beef and soy supply chains. *Science*, *344*(6188), 1118–1123. https://doi.org/10.1126/science.1248525

Dansgaard, W., Johnsen, S. J., Clausen, H. B., Dahl-Jensen, D., Gundestrup, N. S., Hammer, C. U., et al. (1993). Evidence for general instability of past climate from a 250-kyr ice-core record. *Nature*, *364*(6434), 218–220. https://doi.org/10.1038/364218a0

Da Rocha, H. R., Manzi, A. O., Cabral, O. M., Miller, S. D., Goulden, M. L., Saleska, S. R., et al. (2009). Patterns of water and heat flux across a biome gradient from tropical forest to savanna in Brazil. *Journal of Geophysical Research*, *114*(1), G00B12. https://doi.org/10.1029/2007JG000640

de la Giroday, H.-M. C., Carroll, A. L., & Aukema, B. H. (2012). Breach of the northern Rocky Mountain geoclimatic barrier: Initiation of range expansion by the mountain pine beetle. *Journal of Biogeography*, *39*(6), 1112–1123. https://doi.org/10.1111/j.1365-2699.2011.02673.x

Dean, J. F., Middelburg, J. J., Röckmann, T., Aerts, R., Blauw, L. G., Egger, M., et al. (2018). Methane feedbacks to the global climate system in a warmer world. *Reviews of Geophysics*, *56*(1), 207–250. https://doi.org/10.1002/2017RG000559

De'Ath, G., Fabricius, K. E., Sweatman, H., & Puotinen, M. (2012). The 27-year decline of coral cover on the Great Barrier Reef and its causes. *Proceedings of the National Academy of Sciences of the United States of America*, *109*(44), 17995–17999. https://doi.org/10.1073/pnas.1208909109

DeCarlo, T. M., Cohen, A. L., Barkley, H. C., Cobban, Q., Young, C., Shamberger, K. E., et al. (2015). Coral macrobioerosion is accelerated by ocean acidification and nutrients. *Geology*, *43*(1), 7–10. https://doi.org/10.1130/G36147.1

DeCarlo, T. M., Gajdzik, L., Ellis, J., Coker, D. J., Roberts, M. B., Hammerman, N. M., et al. (2020). Nutrient-supplying ocean currents modulate coral bleaching susceptibility. *Science Advances*, *6*(34), eabc5493. https://doi.org/10.1126/sciadv.abc5493

DeConto, R. M., & Pollard, D. (2016). Contribution of Antarctica to past and future sea-level rise. *Nature*, *531*(7596), 591–597. https://doi.org/10.1038/nature17145

DeConto, R. M., Pollard, D., Alley, R. B., Velicogna, I., Gasson, E., Gomez, N., et al. (2021). The Paris Climate Agreement and future sea-level rise from Antarctica. *Nature*, *593*(7857), 83–89. https://doi.org/10.1038/s41586-021-03427-0

Defrance, D., Ramstein, G., Charbit, S., Vrac, M., Famien, A. M., Sultan, B., et al. (2017). Consequences of rapid ice sheet melting on the Sahelian population vulnerability. *Proceedings of the National Academy of Sciences of the United States of America*, *114*(25), 6533–6538. https://doi.org/10.1073/pnas.1619358114

De Groot, W. J., Flannigan, M. D., & Cantin, A. S. (2013). Climate change impacts on future boreal fire regimes. *Forest Ecology and Management*, *294*, 35–44. https://doi.org/10.1016/j.foreco.2012.09.027

Dekker, M. M., von der Heydt, A. S., & Dijkstra, H. A. (2018). Cascading transitions in the climate system. *Earth System Dynamics*, *9*(4), 1243–1260. https://doi.org/10.5194/esd-9-1243-2018

Delworth, T. L., & Zeng, F. (2016). The impact of the North Atlantic Oscillation on climate through its influence on the Atlantic meridional overturning circulation. *Journal of Climate*, *29*(3), 941–962. https://doi.org/10.1175/JCLI-D-15-0396.1

de Menocal, P., Ortiz, J., Guilderson, T., Adkins, J., Sarnthein, M., Baker, L., & Yarusinsky, M. (2000). Abrupt onset and termination of the African Humid Period:: Rapid climate responses to gradual insolation forcing. *Quaternary Science Reviews*, *19*(1), 347–361. https://doi.org/10.1016/S0277-3791(99)00081-5

de Moel, H., Ganssen, G. M., Peeters, F. J. C., Jung, S. J. A., Kroon, D., Brummer, G. J. A., & Zeebe, R. E. (2009). Planktic foraminiferal shell thinning in the Arabian Sea due to anthropogenic ocean acidification? *Biogeosciences*, *6*(9), 1917–1925. https://doi.org/10.5194/bg-6-1917-2009

Deplazes, G., Lückge, A., Peterson, L. C., Timmermann, A., Hamann, Y., Hughen, K. A., et al. (2013). Links between tropical rainfall and North Atlantic climate during the last glacial period. *Nature Geoscience*, *6*(3), 213–217. https://doi.org/10.1038/ngeo1712

Descombes, P., Wisz, M. S., Leprieur, F., Parravicini, V., Heine, C., Olsen, S. M., et al. (2015). Forecasted coral reef decline in marine biodiversity hotspots under climate change. *Global Change Biology*, *21*(7), 2479–2487. https://doi.org/10.1111/gcb.12868

de Vrese, P., & Brovkin, V. (2021). Timescales of the permafrost carbon cycle and legacy effects of temperature overshoot scenarios. *Nature Communications*, *12*(1), 2688. https://doi.org/10.1038/s41467-021-23010-5

de Vries, P., & Weber, S. L. (2005). The Atlantic freshwater budget as a diagnostic for the existence of a stable shut down of the meridional overturning circulation. *Geophysical Research Letters*, *32*(9), L09606. https://doi.org/10.1029/2004GL021450

Dickens, G. R. (2011). Down the Rabbit Hole: Toward appropriate discussion of methane release from gas hydrate systems during the Paleocene-Eocene thermal maximum and other past hyperthermal events. *Climate of the Past*, *7*(3), 831–846. https://doi.org/10.5194/cp-7-831-2011

Dickens, W. A., Kuhn, G., Leng, M. J., Graham, A. G. C., Dowdeswell, J. A., Meredith, M. P., et al. (2019). Enhanced glacial discharge from the eastern Antarctic Peninsula since the 1700s associated with a positive Southern Annular Mode. *Scientific Reports*, *9*(1), 14606. https://doi.org/10.1038/s41598-019-50897-4

Dieleman, C. M., Rogers, B. M., Potter, S., Veraverbeke, S., Johnstone, J. F., Laflamme, J., et al. (2020). Wildfire combustion and carbon stocks in the southern Canadian boreal forest: Implications for a warming world. *Global Change Biology*, *26*(11), 6062–6079. https://doi.org/10.1111/gcb.15158

Dixit, V., Sherwood, S., Geoffroy, O., & Mantsis, D. (2018). The role of nonlinear drying above the boundary layer in the mid-Holocene African monsoon. *Journal of Climate*, *31*(1), 233–249. https://doi.org/10.1175/JCLI-D-17-0234.1

Dixon, A. M., Forster, P. M., Heron, S. F., Stoner, A. M. K., & Beger, M. (2022). Future loss of local-scale thermal refugia in coral reef ecosystems. *PLOS Climate*, *1*(2), e0000004. https://doi.org/10.1371/journal.pclm.0000004

Dolman, A. J., Shvidenko, A., Schepaschenko, D., Ciais, P., Tchebakova, N., Chen, T., et al. (2012). An estimate of the terrestrial carbon budget of Russia using inventory-based, eddy covariance and inversion methods. *Biogeosciences*, *9*(12), 5323–5340. https://doi.org/10.5194/bg-9-5323-2012

Donner, S. D., Skirving, W. J., Little, C. M., Oppenheimer, M., & Hoegh-Guldberg, O. (2005). Global assessment of coral bleaching and required rates of adaptation under climate change. *Global Change Biology*, *11*(12), 2251–2265. https://doi.org/10.1111/j.1365-2486.2005.01073.x

Donovan, M. K., Adam, T. C., Shantz, A. A., Speare, K. E., Munsterman, K. S., Rice, M. M., et al. (2020). Nitrogen pollution interacts with heat stress to increase coral bleaching across the seascape. *Proceedings of the National Academy of Sciences*, *117*(10), 5351–5357. https://doi.org/10.1073/pnas.1915395117

Douglas, T. A., Turetsky, M. R., & Koven, C. D. (2020). Increased rainfall stimulates permafrost thaw across a variety of Interior Alaskan boreal ecosystems. *Npj Climate and Atmospheric Science*, *3*(1), 28. https://doi.org/10.1038/s41612-020-0130-4

Douville, H., Raghavan, K., Renwick, J., Allan, R., Arias, P., Barlow, M., et al. (2021). Chapter 8: Water cycle changes. In *Climate Change 2021: The Physical Science Basis. Contribution of Working Group I to the Sixth Assessment Report of the Intergovernmental Panel on Climate Change*. https://doi.org/10.1017/9781009157896.010

Drijfhout, S., Bathiany, S., Beaulieu, C., Brovkin, V., Claussen, M., Huntingford, C., et al. (2015). Catalogue of abrupt shifts in intergovernmental panel on climate change climate models. *Proceedings of the National Academy of Sciences*, *112*(43), E5777–E5786. https://doi.org/10.1073/pnas.1511451112

Dubreuil, V., Debortoli, N., Funatsu, B., Nédélec, V., & Durieux, L. (2012). Impact of land-cover change in the Southern Amazonia climate: A case study for the region of Alta Floresta, Mato Grosso, Brazil. *Environmental Monitoring and Assessment*, *184*(2), 877–891. https://doi.org/10.1007/s10661-011-2006-x

Durack, P. J., Wijffels, S. E., & Matear, R. J. (2012). Ocean salinities reveal strong global water cycle intensification during 1950 to 2000. *Science*, *336*(6080), 455–458. https://doi.org/10.1126/science.1212222

Dusenge, M. E., Madhavji, S., & Way, D. A. (2020). Contrasting acclimation responses to elevated CO_2 and warming between an evergreen and a deciduous boreal conifer. *Global Change Biology*, *26*(6), 3639–3657. https://doi.org/10.1111/gcb.15084

Dutton, A., Carlson, A. E., Long, A. J., Milne, G. A., Clark, P. U., DeConto, R., et al. (2015). Sea-level rise due to polar ice-sheet mass loss during past warm periods. *Science*, *349*(6244), aaa4019. https://doi.org/10.1126/science.aaa4019

Dyer, B., Austermann, J., D'Andrea, W. J., Creel, R. C., Sandstrom, M. R., Cashman, M., et al. (2021). Sea-level trends across the Bahamas constrain peak last interglacial ice melt. *Proceedings of the National Academy of Sciences*, *118*(33), e2026839118. https://doi.org/10.1073/pnas.2026839118

Dyonisius, M. N., Petrenko, V. V., Smith, A. M., Hua, Q., Yang, B., Schmitt, J., et al. (2020). Old carbon reservoirs were not important in the deglacial methane budget. *Science*, *367*(6480), 907–910. https://doi.org/10.1126/science.aax0504

Eakin, C. M., Sweatman, H. P. A., & Brainard, R. E. (2019). The 2014–2017 global-scale coral bleaching event: Insights and impacts. *Coral Reefs*, *38*(4), 539–545. https://doi.org/10.1007/s00338-019-01844-2

Eastman, R., Warren, S. G., & Hahn, C. J. (2011). Variations in cloud cover and cloud types over the ocean from surface observations, 1954–2008. *Journal of Climate*, *24*(22), 5914–5934. https://doi.org/10.1175/2011JCLI3972.1

Edwards, T. L., Brandon, M. A., Durand, G., Edwards, N. R., Golledge, N. R., Holden, P. B., et al. (2019). Revisiting Antarctic ice loss due to marine ice-cliff instability. *Nature*, *566*(7742), 58–64. https://doi.org/10.1038/s41586-019-0901-4

Edwards, T. L., Nowicki, S., Marzeion, B., Hock, R., Goelzer, H., Seroussi, H., et al. (2021). Projected land ice contributions to twenty-first-century sea level rise. *Nature*, *593*(7857), 74–82. https://doi.org/10.1038/s41586-021-03302-y

Ehlert, D., & Zickfeld, K. (2018). Irreversible ocean thermal expansion under carbon dioxide removal. *Earth System Dynamics*, *9*(1), 197–210. https://doi.org/10.5194/esd-9-197-2018

Eisenman, I. (2012). Factors controlling the bifurcation structure of sea ice retreat. *Journal of Geophysical Research*, *117*(1), 1–18. https://doi.org/10.1029/2011JD016164

Eisenman, I., & Wettlaufer, J. S. (2009). Nonlinear threshold behavior during the loss of Arctic sea ice. *Proceedings of the National Academy of Sciences of the United States of America*, *106*(1), 28–32. https://doi.org/10.1073/pnas.0806887106

Elliott, S., Maltrud, M., Reagan, M., Moridis, G., & Cameron-Smith, P. (2011). Marine methane cycle simulations for the period of early global warming. *Journal of Geophysical Research*, *116*(1), 1–13. https://doi.org/10.1029/2010JG001300

Eltahir, E. A. B., & Bras, R. L. (1994). Precipitation recycling in the Amazon basin. *Quarterly Journal of the Royal Meteorological Society*, *120*(518), 861–880. https://doi.org/10.1002/qj.49712051806

Emanuel, K. A., David Neelin, J., & Bretherton, C. S. (1994). On large-scale circulations in convecting atmospheres. *Quarterly Journal of the Royal Meteorological Society*, *120*(519), 1111–1143. https://doi.org/10.1002/qj.49712051902

Enderlin, E. M., Howat, I. M., Jeong, S., Noh, M.-J., van Angelen, J. H., & van den Broeke, M. R. (2014). An improved mass budget for the Greenland ice sheet. *Geophysical Research Letters*, *41*(3), 866–872. https://doi.org/10.1002/2013GL059010

Espinoza, J. C., Ronchail, J., Marengo, J. A., & Segura, H. (2019). Contrasting North–South changes in Amazon wet-day and dry-day frequency and related atmospheric features (1981–2017). *Climate Dynamics*, *52*(9), 5413–5430. https://doi.org/10.1007/s00382-018-4462-2

Esquivel-Muelbert, A., Galbraith, D., Dexter, K. G., Baker, T. R., Lewis, S. L., Meir, P., et al. (2017). Biogeographic distributions of neotropical trees reflect their directly measured drought tolerances. *Scientific Reports*, *7*(1), 1–11. https://doi.org/10.1038/s41598-017-08105-8

Estop-Aragonés, C., Olefeldt, D., Abbott, B. W., Chanton, J. P., Czimczik, C. I., Dean, J. F., et al. (2020). Assessing the potential for mobilization of old soil carbon after permafrost thaw: A synthesis of ^{14}C measurements from the northern permafrost region. *Global Biogeochemical Cycles*, *34*(9), e2020GB006672. https://doi.org/10.1029/2020GB006672

Euskirchen, E. S., McGuire, A. D., Kicklighter, D. W., Zhuang, Q., Clein, J. S., Dargaville, R. J., et al. (2006). Importance of recent shifts in soil thermal dynamics on growing season length, productivity, and carbon sequestration in terrestrial high-latitude ecosystems. *Global Change Biology*, *12*(4), 731–750. https://doi.org/10.1111/j.1365-2486.2006.01113.x

Eyring, V., Bony, S., Meehl, G. A., Senior, C. A., Stevens, B., Stouffer, R. J., & Taylor, K. E. (2016). Overview of the Coupled Model Intercomparison Project Phase 6 (CMIP6) experimental design and organization. *Geoscientific Model Development*, *9*(5), 1937–1958. https://doi.org/10.5194/gmd-9-1937-2016

Ezer, T., Atkinson, L. P., Corlett, W. B., & Blanco, J. L. (2013). Gulf Stream's induced sea level rise and variability along the U.S. mid-Atlantic coast. *Journal of Geophysical Research: Oceans*, *118*(2), 685–697. https://doi.org/10.1002/jgrc.20091

Fasullo, J., & Webster, P. J. (2003). A hydrological definition of Indian monsoon onset and withdrawal. *Journal of Climate*, *16*(19), 3200–3211. https://doi.org/10.1175/1520-0442(2003)016<3200a:AHDOIM>2.0.CO;2

Favier, L., Durand, G., Cornford, S. L., Gudmundsson, G. H., Gagliardini, O., Gillet-Chaulet, F., et al. (2014). Retreat of Pine Island Glacier controlled by marine ice-sheet instability. *Nature Climate Change*, *4*(2), 117–121. https://doi.org/10.1038/nclimate2094

Fernández-Méndez, M., Katlein, C., Rabe, B., Nicolaus, M., Peeken, I., Bakker, K., et al. (2015). Photosynthetic production in the central Arctic Ocean during the record sea-ice minimum in 2012. *Biogeosciences*, *12*(11), 3525–3549. https://doi.org/10.5194/bg-12-3525-2015

Ferrario, F., Beck, M. W., Storlazzi, C. D., Micheli, F., Shepard, C. C., & Airoldi, L. (2014). The effectiveness of coral reefs for coastal hazard risk reduction and adaptation. *Nature Communications*, *5*, 1–9. https://doi.org/10.1038/ncomms4794

Ferré, B., Jansson, P. G., Moser, M., Serov, P., Portnov, A., Graves, C. A., et al. (2020). Reduced methane seepage from Arctic sediments during cold bottom-water conditions. *Nature Geoscience*, *13*(2), 144–148. https://doi.org/10.1038/s41561-019-0515-3

Fetterer, F., Knowles, K., Meier, W. N., Savoie, M., & Windnagel, A. K. (2017). Sea ice index, version 3. https://doi.org/10.7265/N5K072F8

Field, C. B., Behrenfeld, M. J., Randerson, J. T., & Falkowski, P. (1998). Primary production of the biosphere: Integrating terrestrial and oceanic components. *Science*, *281*(5374), 237–240. https://doi.org/10.1126/science.281.5374.237

Findlater, J. (1969). A major low-level air current near the Indian Ocean during the northern summer. *Quarterly Journal of the Royal Meteorological Society*, *95*(404), 362–380. https://doi.org/10.1002/qj.49709540409

Fisher, R. A., Koven, C. D., Anderegg, W. R. L., Christoffersen, B. O., Dietze, M. C., Farrior, C. E., et al. (2018). Vegetation demographics in Earth system models: A review of progress and priorities. *Global Change Biology*, *24*(1), 35–54. https://doi.org/10.1111/gcb.13910

Flannigan, M., Stocks, B., Turetsky, M., & Wotton, M. (2009). Impacts of climate change on fire activity and fire management in the circumboreal forest. *Global Change Biology*, *15*(3), 549–560. https://doi.org/10.1111/j.1365-2486.2008.01660.x

Fleischer, K., Rammig, A., De Kauwe, M. G., Walker, A. P., Domingues, T. F., Fuchslueger, L., et al. (2019). Amazon forest response to CO_2 fertilization dependent on plant phosphorus acquisition. *Nature Geoscience*, *12*(9), 736–741. https://doi.org/10.1038/s41561-019-0404-9

Foley, J. A., Kutzbach, J. E., Coe, M. T., & Levis, S. (1994). Feedbacks between climate and boreal forests during the Holocene epoch. *Nature*, *371*(6492), 52–54. https://doi.org/10.1038/371052a0

Folland, C. K., Palmer, T. N., & Parker, D. E. (1986). Sahel rainfall and worldwide sea temperatures, 1901–85. *Nature*, *320*(6063), 602–607. https://doi.org/10.1038/320602a0

Fonseca, M. G., Alves, L. M., Aguiar, A. P. D., Arai, E., Anderson, L. O., Rosan, T. M., et al. (2019). Effects of climate and land-use change scenarios on fire probability during the 21st century in the Brazilian Amazon. *Global Change Biology*, 25(9), 2931–2946. https://doi.org/10.1111/gcb.14709

Fontaine, B., Gaetani, M., Ullmann, A., & Roucou, P. (2011). Time evolution of observed July–September sea surface temperature-Sahel climate teleconnection with removed quasi-global effect (1900–2008). *Journal of Geophysical Research*, 116(D4), D04105. https://doi.org/10.1029/2010JD014843

Fontela, M., García-Ibáñez, M. I., Hansell, D. A., Mercier, H., & Pérez, F. F. (2016). Dissolved organic carbon in the North Atlantic meridional overturning circulation. *Scientific Reports*, 6(1), 26931. https://doi.org/10.1038/srep26931

Forster, P., Storelvmo, T., Armour, K., Collins, W., Dufresne, J.-L., Frame, D., et al. (2021). Chapter 7: The Earth's energy budget, climate feedbacks, and climate sensitivity. In *Climate Change 2021: The Physical Science Basis. Contribution of Working Group I to the Sixth Assessment Report of the Intergovernmental Panel on Climate Change*. Cambridge University Press.

Foster, A. C., Armstrong, A. H., Shuman, J. K., Shugart, H. H., Rogers, B. M., Mack, M. C., et al. (2019). Importance of tree- and species-level interactions with wildfire, climate, and soils in interior Alaska: Implications for forest change under a warming climate. *Ecological Modelling*, 409, 108765. https://doi.org/10.1016/j.ecolmodel.2019.108765

Fox-Kemper, B., Hewitt, H. T., Xiao, C., Aðalgeirsdóttir, G., Drijfhout, S. S., Edwards, T. L., et al. (2021). Ocean, cryosphere and sea level change. In *Climate Change 2021: The Physical Science Basis. Contribution of Working Group I to the Sixth Assessment Report of the Intergovernmental Panel on Climate Change*.

Frajka-Williams, E. (2015). Estimating the Atlantic overturning at 26°N using satellite altimetry and cable measurements. *Geophysical Research Letters*, 42(9), 3458–3464. https://doi.org/10.1002/2015GL063220

Fraser, R. H., Kokelj, S. V., Lantz, T. C., McFarlane-Winchester, M., Olthof, I., & Lacelle, D. (2018). Climate sensitivity of high arctic permafrost terrain demonstrated by widespread ice-wedge thermokarst on Banks Island. *Remote Sensing*, 10(6), 954. https://doi.org/10.3390/rs10060954

Fretwell, P., Pritchard, H. D., Vaughan, D. G., Bamber, J. L., Barrand, N. E., Bell, R., et al. (2013). Bedmap2: Improved ice bed, surface and thickness datasets for Antarctica. *The Cryosphere*, 7(1), 375–393. https://doi.org/10.5194/tc-7-375-2013

Frieler, K., Meinshausen, M., Golly, A., Mengel, M., Lebek, K., Donner, S. D., & Hoegh-Guldberg, O. (2013). Limiting global warming to 2°C is unlikely to save most coral reefs. *Nature Climate Change*, 3(2), 165–170. https://doi.org/10.1038/nclimate1674

Fu, R., Yin, L., Li, W., Arias, P. A., Dickinson, R. E., Huang, L., et al. (2013). Increased dry-season length over southern Amazonia in recent decades and its implication for future climate projection. *Proceedings of the National Academy of Sciences of the United States of America*, 110(45), 18110–18115. https://doi.org/10.1073/pnas.1302584110

Fu, Y., Li, F., Karstensen, J., & Wang, C. (2020). A stable Atlantic Meridional Overturning Circulation in a changing North Atlantic ocean since the 1990s. *Science Advances*, 6(48). https://doi.org/10.1126/sciadv.abc7836

Ganopolski, A., & Rahmstorf, S. (2001). Rapid changes of glacial climate simulated in a coupled climate model. *Nature*, 409(6817), 153–158. https://doi.org/10.1038/35051500

Ganopolski, A., Winkelmann, R., & Schellnhuber, H. J. (2016). Critical insolation-CO_2 relation for diagnosing past and future glacial inception. *Nature*, 529(7585), 200–203. https://doi.org/10.1038/nature16494

Garbe, J., Albrecht, T., Levermann, A., Donges, J. F., & Winkelmann, R. (2020). The hysteresis of the Antarctic ice sheet. *Nature*, 585(7826), 538–544. https://doi.org/10.1038/s41586-020-2727-5

Garcia-Tigreros, F., & Kessler, J. D. (2018). Limited acute influence of aerobic methane oxidation on ocean carbon dioxide and pH in Hudson Canyon, northern U.S. Atlantic margin. *Journal of Geophysical Research: Biogeosciences*, 123(7), 2135–2144. https://doi.org/10.1029/2018JG004384

Garcia-Tigreros, F., Leonte, M., Ruppel, C. D., Ruiz-Angulo, A., Joung, D. J., Young, B., & Kessler, J. D. (2021). Estimating the impact of seep methane oxidation on ocean pH and dissolved inorganic radiocarbon along the U.S. mid-Atlantic Bight. *Journal of Geophysical Research: Biogeosciences*, 126(1), e2019JG005621. https://doi.org/10.1029/2019JG005621

Gardner, T. A., Côté, I. M., Gill, J. A., Grant, A., & Watkinson, A. R. (2003). Long-term region-wide declines in Caribbean corals. *Science*, 301(5635), 958–960. https://doi.org/10.1126/science.1086050

Gasse, F. (2000). Hydrological changes in the African tropics since the last glacial maximum. *Quaternary Science Reviews*, 19(1), 189–211. https://doi.org/10.1016/S0277-3791(99)00061-X

Gastineau, G., L'Hévéder, B., Codron, F., & Frankignoul, C. (2016). Mechanisms determining the winter atmospheric response to the Atlantic overturning circulation. *Journal of Climate*, 29(10), 3767–3785. https://doi.org/10.1175/JCLI-D-15-0326.1

Gatti, L. V., Basso, L. S., Miller, J. B., Gloor, M., Gatti Domingues, L., Cassol, H. L. G., et al. (2021). Amazonia as a carbon source linked to deforestation and climate change. *Nature*, 595(7867), 388–393. https://doi.org/10.1038/s41586-021-03629-6

Gauthier, S., Bernier, P., Kuuluvainen, T., Shvidenko, A. Z., & Schepaschenko, D. G. (2015). Boreal forest health and global change. *Science*, 349(6250), 819–822. https://doi.org/10.1126/science.aaa9092

Giannini, A., Saravanan, R., & Chang, P. (2003). Oceanic forcing of Sahel rainfall on interannual to interdecadal time scales. *Science*, 302(5647), 1027–1030. https://doi.org/10.1126/science.1089357

Gibbs, H. K., Brown, S., Niles, J. O., & Foley, J. A. (2007). Monitoring and estimating tropical forest carbon stocks: Making REDD a reality. *Environmental Research Letters*, 2(4), 045023. https://doi.org/10.1088/1748-9326/2/4/045023

Gibson, C. M., Brinkman, T., Cold, H., Brown, D., & Turetsky, M. (2021). Identifying increasing risks of hazards for northern land-users caused by permafrost thaw: Integrating scientific and community-based research approaches. *Environmental Research Letters*, 16(6), 64047. https://doi.org/10.1088/1748-9326/abfc79

Gibson, C. M., Chasmer, L. E., Thompson, D. K., Quinton, W. L., Flannigan, M. D., & Olefeldt, D. (2018). Wildfire as a major driver of recent permafrost thaw in boreal peatlands. *Nature Communications*, 9(1), 3041. https://doi.org/10.1038/s41467-018-05457-1

Global Sea Level Budget Group. (2018). Global sea-level budget 1993–present. *Earth System Science Data*, 10(3), 1551–1590. https://doi.org/10.5194/essd-10-1551-2018

Goddard, P. B., Yin, J., Griffies, S. M., & Zhang, S. (2015). An extreme event of sea-level rise along the Northeast coast of North America in 2009–2010. *Nature Communications*, 6(1), 6346. https://doi.org/10.1038/ncomms7346

Goelzer, H., Nowicki, S., Payne, A., Larour, E., Seroussi, H., Lipscomb, W. H., et al. (2020). The future sea-level contribution of the Greenland ice sheet: A multi-model ensemble study of ISMIP6. *The Cryosphere*, 14(9), 3071–3096. https://doi.org/10.5194/tc-14-3071-2020

Goetz, S. J., Mack, M. C., Gurney, K. R., Randerson, J. T., & Houghton, R. A. (2007). Ecosystem responses to recent climate change and fire disturbance at northern high latitudes: Observations and model results contrasting northern Eurasia and North America. *Environmental Research Letters*, 2(4), 045031. https://doi.org/10.1088/1748-9326/2/4/045031

Golledge, N. R., Keller, E. D., Gomez, N., Naughten, K. A., Bernales, J., Trusel, L. D., & Edwards, T. L. (2019). Global environmental consequences of twenty-first-century ice-sheet melt. *Nature*, 566(7742), 65–72. https://doi.org/10.1038/s41586-019-0889-9

Golledge, N. R., Kowalewski, D. E., Naish, T. R., Levy, R. H., Fogwill, C. J., & Gasson, E. G. W. (2015). The multi-millennial Antarctic commitment to future sea-level rise. *Nature*, *526*(7573), 421–425. https://doi.org/10.1038/nature15706

Gomes, V. H. F., Vieira, I. C. G., Salomão, R. P., & ter Steege, H. (2019). Amazonian tree species threatened by deforestation and climate change. *Nature Climate Change*, *9*(7), 547–553. https://doi.org/10.1038/s41558-019-0500-2

Good, P., Jones, C., Lowe, J., Betts, R., & Gedney, N. (2013). Comparing tropical forest projections from two generations of Hadley Centre Earth System models, HadGEM2-ES and HadCM3LC. *Journal of Climate*, *26*(2), 495–511. https://doi.org/10.1175/JCLI-D-11-00366.1

Goswami, B. N., & Xavier, P. K. (2005). ENSO control on the south Asian monsoon through the length of the rainy season. *Geophysical Research Letters*, *32*(18), L18717. https://doi.org/10.1029/2005GL023216

Green, J. K., Berry, J., Ciais, P., Zhang, Y., & Gentine, P. (2020). Amazon rainforest photosynthesis increases in response to atmospheric dryness. *Science Advances*, *6*(47), eabb7232. https://doi.org/10.1126/sciadv.abb7232

Greenop, R., Foster, G. L., Wilson, P. A., & Lear, C. H. (2014). Middle Miocene climate instability associated with high-amplitude CO_2 variability. *Paleoceanography*, *29*(9), 845–853. https://doi.org/10.1002/2014PA002653

Gregory, J. M., George, S. E., & Smith, R. S. (2020). Large and irreversible future decline of the Greenland ice sheet. *The Cryosphere*, *14*(12), 4299–4322. https://doi.org/10.5194/tc-14-4299-2020

Gregory, J. M., Huybrechts, P., & Raper, S. C. B. (2004). Threatened loss of the Greenland ice-sheet. *Nature*, *428*(6983), 616. https://doi.org/10.1038/428616a

Gruber, S. (2012). Derivation and analysis of a high-resolution estimate of global permafrost zonation. *The Cryosphere*, *6*(1), 221–233. https://doi.org/10.5194/tc-6-221-2012

Gudmundsson, G. H. (2013). Ice-shelf buttressing and the stability of marine ice sheets. *The Cryosphere*, 7(2), 647–655. https://doi.org/10.5194/tc-7-647-2013

Gudmundsson, G. H., Krug, J., Durand, G., Favier, L., & Gagliardini, O. (2012). The stability of grounding lines on retrograde slopes. *The Cryosphere*, *6*(6), 1497–1505. https://doi.org/10.5194/tc-6-1497-2012

Gudmundsson, G. H., Paolo, F. S., Adusumilli, S., & Fricker, H. A. (2019). Instantaneous Antarctic ice sheet mass loss driven by thinning ice shelves. *Geophysical Research Letters*, *46*(23), 13903–13909. https://doi.org/10.1029/2019GL085027

Guest, J. R., Edmunds, P. J., Gates, R. D., Kuffner, I. B., Andersson, A. J., Barnes, B. B., et al. (2018). A framework for identifying and characterising coral reef "oases" against a backdrop of degradation. *Journal of Applied Ecology*, *55*(6), 2865–2875. https://doi.org/10.1111/1365-2664.13179

Gupta, A., Lachance, J., Sloan, E. D., & Koh, C. A. (2008). Measurements of methane hydrate heat of dissociation using high pressure differential scanning calorimetry. *Chemical Engineering Science*, *63*(24), 5848–5853. https://doi.org/10.1016/j.ces.2008.09.002

Haarsma, R. J., Selten, F. M., & Drijfhout, S. S. (2015). Decelerating Atlantic meridional overturning circulation main cause of future west European summer atmospheric circulation changes. *Environmental Research Letters*, *10*(9), 094007. https://doi.org/10.1088/1748-9326/10/9/094007

Haine, T. W. N., & Martin, T. (2017). The Arctic-Subarctic sea ice system is entering a seasonal regime: Implications for future Arctic amplification. *Scientific Reports*, *7*(1), 1–9. https://doi.org/10.1038/s41598-017-04573-0

Halpern, B. S., Frazier, M., Potapenko, J., Casey, K. S., Koenig, K., Longo, C., et al. (2015). Spatial and temporal changes in cumulative human impacts on the world's ocean. *Nature Communications*, *6*, 1–7. https://doi.org/10.1038/ncomms8615

Halpern, D., & Woiceshyn, P. M. (1999). Onset of the Somali jet in the Arabian Sea during June 1997. *Journal of Geophysical Research*, *104*(C8), 18041–18046. https://doi.org/10.1029/1999JC900141

Halsey, L. A., Vitt, D. H., & Zoltai, S. C. (1995). Disequilibrium response of permafrost in boreal continental western Canada to climate change. *Climatic Change*, *30*(1), 57–73. https://doi.org/10.1007/BF01093225

Hamlington, B. D., Gardner, A. S., Ivins, E., Lenaerts, J. T. M., Reager, J. T., Trossman, D. S., et al. (2020). Understanding of contemporary regional sea-level change and the implications for the future. *Reviews of Geophysics*, *58*(3), e2019RG000672. https://doi.org/10.1029/2019rg000672

Hanes, C. C., Wang, X., Jain, P., Parisien, M. A., Little, J. M., & Flannigan, M. D. (2019). Fire-regime changes in Canada over the last half century. *Canadian Journal of Forest Research*, *49*(3), 256–269. https://doi.org/10.1139/cjfr-2018-0293

Hansen, W. D., Fitzsimmons, R., Olnes, J., & Williams, A. P. (2020). An alternate vegetation type proves resilient and persists for decades following forest conversion in the North American boreal biome. *Journal of Ecology*, *109*(1), 85–98. https://doi.org/10.1111/1365-2745.13446

Hausfather, Z., & Peters, G. P. (2020). Emissions—The "business as usual" story is misleading. *Nature*, *577*(7792), 618–620. https://doi.org/10.1038/d41586-020-00177-3

Heffernan, L., Estop-Aragonés, C., Knorr, K.-H., Talbot, J., & Olefeldt, D. (2020). Long-term impacts of permafrost thaw on carbon storage in peatlands: Deep losses offset by surficial accumulation. *Journal of Geophysical Research: Biogeosciences*, *125*(3), e2019JG005501. https://doi.org/10.1029/2019JG005501

Heinrich, H. (1988). Origin and consequences of cyclic ice rafting in the Northeast Atlantic Ocean during the past 130,000 years. *Quaternary Research*, *29*(2), 142–152. https://doi.org/10.1016/0033-5894(88)90057-9

Heinze, C., Meyer, S., Goris, N., Anderson, L., Steinfeldt, R., Chang, N., et al. (2015). The ocean carbon sink—Impacts, vulnerabilities and challenges. *Earth System Dynamics*, *6*(1), 327–358. https://doi.org/10.5194/esd-6-327-2015

Held, I. M., Delworth, T. L., Lu, J., Findell, K. L., & Knutson, T. R. (2005). Simulation of Sahel drought in the 20th and 21st centuries. *Proceedings of the National Academy of Sciences of the United States of America*, *102*(50), 17891–17896. https://doi.org/10.1073/pnas.0509057102

Held, I. M., & Soden, B. J. (2006). Robust responses of the hydrological cycle to global warming. *Journal of Climate*, *19*(21), 5686–5699. https://doi.org/10.1175/JCLI3990.1

Heron, S. F., Maynard, J. A., Van Hooidonk, R., & Eakin, C. M. (2016). Warming trends and bleaching stress of the world's coral reefs 1985–2012. *Scientific Reports*, *6*(1), 38402. https://doi.org/10.1038/srep38402

Heuzé, C. (2017). North Atlantic deep water formation and AMOC in CMIP5 models. *Ocean Science*, *13*(4), 609–622. https://doi.org/10.5194/os-13-609-2017

Hill, S. A. (2019). Theories for past and future monsoon rainfall changes. *Current Climate Change Reports*, 5(3), 160–171. https://doi.org/10.1007/s40641-019-00137-8

Hirota, M., Holmgren, M., Van Nes, E. H., & Scheffer, M. (2011). Global resilience of tropical forest and savanna to critical transitions. *Science*, *334*(6053), 232–235. https://doi.org/10.1126/science.1210657

Hirschi, J. J.-M., Barnier, B., Böning, C., Biastoch, A., Blaker, A. T., Coward, A., et al. (2020). The Atlantic meridional overturning circulation in high-resolution models. *Journal of Geophysical Research: Oceans*, *125*(4), e2019JC015522. https://doi.org/10.1029/2019JC015522

Hjort, J., Streletskiy, D., Doré, G., Wu, Q., Bjella, K., & Luoto, M. (2022). Impacts of permafrost degradation on infrastructure. *Nature Reviews Earth & Environment*, *3*(1), 24–38. https://doi.org/10.1038/s43017-021-00247-8

Hmiel, B., Petrenko, V. V., Dyonisius, M. N., Buizert, C., Smith, A. M., Place, P. F., et al. (2020). Preindustrial $^{14}CH_4$ indicates greater anthropogenic fossil CH_4 emissions. *Nature*, *578*(7795), 10–14. https://doi.org/10.1038/s41586-020-1991-8

Hodgson, G. (1999). A global assessment of human effects on coral reefs. *Marine Pollution Bulletin*, *38*(5), 345–355. https://doi.org/10.1016/S0025-326X(99)00002-8

Hoegh-Guldberg, O. (2014a). Coral reef sustainability through adaptation: Glimmer of hope or persistent mirage? *Current Opinion in Environmental Sustainability*, *7*, 127–133. https://doi.org/10.1016/j.cosust.2014.01.005

Hoegh-Guldberg, O. (2014b). Coral reefs in the Anthropocene: Persistence or the end of the line? *Geological Society Special Publication*, *395*(1), 167–183. https://doi.org/10.1144/SP395.17

Hoegh-Guldberg, O., Jacob, D., Taylor, M., Bindi, M., Brown, S., Camilloni, I., et al. (2018). Impacts of 1.5°C global warming on natural and human systems. In *Global warming of 1.5°C. An IPCC Special Report on the impacts of global warming of 1.5°C above pre-industrial levels and related global greenhouse gas emission pathways, in the context of strengthening the global response to the threat of climate change*.

Hoegh-Guldberg, O., Jacob, D., Taylor, M., Guillén Bolaños, T., Bindi, M., Brown, S., et al. (2019). The human imperative of stabilizing global climate change at 1.5°C. *Science*, *365*(6459). https://doi.org/10.1126/science.aaw6974

Hoegh-Guldberg, O., Mumby, P. J., Hooten, A. J., Steneck, R. S., Greenfield, P., Gomez, E., et al. (2007). Coral reefs under rapid climate change and ocean acidification. *Science*, *318*(5857), 1737–1742. https://doi.org/10.1126/science.1152509

Hoell, A., Funk, C., Barlow, M., & Shukla, S. (2016). Recent and Possible Future Variations in the North American Monsoon. In L. M. V. de Carvalho & C. Jones (Eds.), *The monsoons and climate change: Observations and modeling*. https://doi.org/10.1007/978-3-319-21650-8_7

Hogg, E. H., Brandt, J. P., Brandt, J. P., & Michaelian, M. (2008). Impacts of a regional drought on the productivity, dieback, and biomass of western Canadian aspen forests. *Canadian Journal of Forest Research*, *38*(6), 1373–1384. https://doi.org/10.1139/X08-001

Holland, M. M., Bailey, D. A., & Vavrus, S. (2011). Inherent sea ice predictability in the rapidly changing Arctic environment of the Community Climate System Model, version 3. *Climate Dynamics*, *36*(7), 1239–1253. https://doi.org/10.1007/s00382-010-0792-4

Holland, M. M., & Bitz, C. M. (2003). Polar amplification of climate change in coupled models. *Climate Dynamics*, *21*(3), 221–232. https://doi.org/10.1007/s00382-003-0332-6

Holland, M. M., Bitz, C. M., & Tremblay, B. (2006). Future abrupt reductions in the summer Arctic sea ice. *Geophysical Research Letters*, *33*(23), L23503. https://doi.org/10.1029/2006GL028024

Holland, P. R., Bracegirdle, T. J., Dutrieux, P., Jenkins, A., & Steig, E. J. (2019). West Antarctic ice loss influenced by internal climate variability and anthropogenic forcing. *Nature Geoscience*, *12*(9), 718–724. https://doi.org/10.1038/s41561-019-0420-9

Holloway, G., Dupont, F., Golubeva, E., Häkkinen, S., Hunke, E., Jin, M., et al. (2007). Water properties and circulation in Arctic Ocean models. *Journal of Geophysical Research*, *112*(C4), C04S03. https://doi.org/10.1029/2006JC003642

Holloway, J. E., & Lewkowicz, A. G. (2020). Half a century of discontinuous permafrost persistence and degradation in western Canada. *Permafrost and Periglacial Processes*, *31*(1), 85–96. https://doi.org/10.1002/ppp.2017

Holloway, J. E., Lewkowicz, A. G., Douglas, T. A., Li, X., Turetsky, M. R., Baltzer, J. L., & Jin, H. (2020). Impact of wildfire on permafrost landscapes: A review of recent advances and future prospects. *Permafrost and Periglacial Processes*, *31*(3), 371–382. https://doi.org/10.1002/ppp.2048

Hopcroft, P. O., & Valdes, P. J. (2021). Paleoclimate-conditioning reveals a North Africa land–atmosphere tipping point. *Proceedings of the National Academy of Sciences*, *118*(45), e2108783118. https://doi.org/10.1073/pnas.2108783118

Hornbach, M. J., Saffer, D. M., & Holbrook, W. S. (2004). Critically pressured free-gas reservoirs below gas-hydrate provinces. *Nature*, *427*(6970), 142–144. https://doi.org/10.1038/nature02172

Hubau, W., Lewis, S. L., Phillips, O. L., Affum-Baffoe, K., Beeckman, H., Cuní-Sanchez, A., et al. (2020). Asynchronous carbon sink saturation in African and Amazonian tropical forests. *Nature*, *579*(7797), 80–87. https://doi.org/10.1038/s41586-020-2035-0

Hudson, S. R. (2011). Estimating the global radiative impact of the sea ice-albedo feedback in the Arctic. *Journal of Geophysical Research*, *116*(16), D16102. https://doi.org/10.1029/2011JD015804

Hughes, T. P., Anderson, K. D., Connolly, S. R., Heron, S. F., Kerry, J. T., Lough, J. M., et al. (2018). Spatial and temporal patterns of mass bleaching of corals in the Anthropocene. *Science*, *359*(6371), 80–83. https://doi.org/10.1126/science.aan8048

Hughes, T. P., Kerry, J. T., Álvarez-Noriega, M., Álvarez-Romero, J. G., Anderson, K. D., Baird, A. H., et al. (2017). Global warming and recurrent mass bleaching of corals. *Nature*, *543*(7645), 373–377. https://doi.org/10.1038/nature21707

Hughes, T. P., Kerry, J. T., Baird, A. H., Connolly, S. R., Chase, T. J., Dietzel, A., et al. (2019). Global warming impairs stock–recruitment dynamics of corals. *Nature*, *568*(7752), 387–390. https://doi.org/10.1038/s41586-019-1081-y

Hughes, T. P., Kerry, J. T., Connolly, S. R., Baird, A. H., Eakin, C. M., Heron, S. F., et al. (2019). Ecological memory modifies the cumulative impact of recurrent climate extremes. *Nature Climate Change*, *9*(1), 40–43. https://doi.org/10.1038/s41558-018-0351-2

Huntingford, C., Fisher, R. A., Mercado, L., Booth, B. B. B., Sitch, S., Harris, P. P., et al. (2008). Towards quantifying uncertainty in predictions of Amazon 'dieback'. *Philosophical Transactions of the Royal Society B: Biological Sciences*, *363*(1498), 1857–1864. https://doi.org/10.1098/rstb.2007.0028

Huntingford, C., Zelazowski, P., Galbraith, D., Mercado, L. M., Sitch, S., Fisher, R., et al. (2013). Simulated resilience of tropical rainforests to CO_2-induced climate change. *Nature Geoscience*, *6*(4), 268–273. https://doi.org/10.1038/ngeo1741

Huntzinger, D. N., Schaefer, K., Schwalm, C., Fisher, J. B., Hayes, D., Stofferahn, E., et al. (2020). Evaluation of simulated soil carbon dynamics in Arctic-Boreal ecosystems. *Environmental Research Letters*, *15*(2), 25005. https://doi.org/10.1088/1748-9326/ab6784

Huybrechts, P., & De Wolde, J. (1999). The dynamic response of the Greenland and Antarctic ice sheets to multiple-century climatic warming. *Journal of Climate*, *12*(8), 2169–2188. https://doi.org/10.1175/1520-0442(1999)012<2169:tdrotg>2.0.co;2

Huybrechts, P., Letreguilly, A., & Reeh, N. (1991). The Greenland ice sheet and greenhouse warming. *Global and Planetary Change*, *3*(4), 399–412. https://doi.org/10.1016/0921-8181(91)90119-H

Ilıcak, M., Drange, H., Wang, Q., Gerdes, R., Aksenov, Y., Bailey, D., et al. (2016). An assessment of the Arctic Ocean in a suite of interannual CORE-II simulations. Part III: Hydrography and fluxes. *Ocean Modelling*, *100*, 141–161. https://doi.org/10.1016/j.ocemod.2016.02.004

IPCC. (2021). Climate change 2021. The physical science basis. Contribution of Working Group 1 to Sixth Assessment Report of the Intergovernmental Panel on Climate Change. Retrieved from https://www.ipcc.ch/report/ar6/wg1/

Ivanov, V. Y., Hutyra, L. R., Wofsy, S. C., Munger, J. W., Saleska, S. R., De Oliveira, R. C., & De Camargo, P. B. (2012). Root niche separation can explain avoidance of seasonal drought stress and vulnerability of overstory trees to extended drought in a mature Amazonian forest. *Water Resources Research*, *48*(12), 1–21. https://doi.org/10.1029/2012WR011972

Jackson, J. B. C., Donovan, M. K., Cramer, K. L., & Lam, W. (2014). *Status and trends of Caribbean coral reefs: 1970–2012*. *Global Coral Reef Monitoring Network*. IUCN.

Jackson, L. C., Dubois, C., Forget, G., Haines, K., Harrison, M., Iovino, D., et al. (2019). The mean state and variability of the North Atlantic circulation: A perspective from ocean reanalyses. *Journal of Geophysical Research: Oceans*, *124*(12), 9141–9170. https://doi.org/10.1029/2019JC015210

Jackson, L. C., Kahana, R., Graham, T., Ringer, M. A., Woollings, T., Mecking, J. V., & Wood, R. A. (2015). Global and European climate impacts of a slowdown of the AMOC in a high resolution GCM. *Climate Dynamics*, *45*(11–12), 3299–3316. https://doi.org/10.1007/s00382-015-2540-2

Jackson, L. C., Peterson, K. A., Roberts, C. D., & Wood, R. A. (2016). Recent slowing of Atlantic overturning circulation as a recovery from earlier strengthening. *Nature Geoscience*, *9*(7), 518–522. https://doi.org/10.1038/ngeo2715

Jackson, L. C., & Wood, R. A. (2018). Hysteresis and resilience of the AMOC in an eddy-permitting GCM. *Geophysical Research Letters*, *45*(16), 8547–8556. https://doi.org/10.1029/2018GL078104

Jahn, A. (2018). Reduced probability of ice-free summers for 1.5°C compared to 2°C warming. *Nature Climate Change*, 8(5), 409–413. https://doi.org/10.1038/s41558-018-0127-8

James, M., Lewkowicz, A. G., Smith, S. L., & Miceli, C. M. (2013). Multi-decadal degradation and persistence of permafrost in the Alaska Highway corridor, northwest Canada. *Environmental Research Letters*, *8*(4), 045013. https://doi.org/10.1088/1748-9326/8/4/045013

Jenkins, A., Dutrieux, P., Jacobs, S., Steig, E. J., Gudmundsson, G. H., Smith, J., & Heywood, K. J. (2016). Decadal ocean forcing and Antarctic ice sheet response: Lessons from the Amundsen Sea. *Oceanography*, *29*(4), 106–117. https://doi.org/10.5670/oceanog.2016.103

Jiang, L., Zhang, F., Guo, M. L., Guo, Y. J., Zhang, Y. Y., Zhou, G. W., et al. (2018). Increased temperature mitigates the effects of ocean acidification on the calcification of juvenile *Pocillopora damicornis*, but at a cost. *Coral Reefs*, *37*(1), 71–79. https://doi.org/10.1007/s00338-017-1634-1

Jin, C., Wang, B., & Liu, J. (2020). Future changes and controlling factors of the eight regional monsoons projected by CMIP6 models. *Journal of Climate*, *33*(21), 9307–9326. https://doi.org/10.1175/JCLI-D-20-0236.1

Jin, Q., & Wang, C. (2017). A revival of Indian summer monsoon rainfall since 2002. *Nature Climate Change*, *7*(8), 587–594. https://doi.org/10.1038/NCLIMATE3348

Jobbágy, E. G., & Jackson, R. B. (2000). The vertical distribution of soil organic carbon and its relation to climate and vegetation. *Ecological Applications*, *10*(2), 423–436. https://doi.org/10.1890/1051-0761(2000)010[0423:TVDOSO]2.0.CO;2

Johnson, H. P., Miller, U. K., Salmi, M. S., & Solomon, E. A. (2015). Analysis of bubble plume distributions to evaluate methane hydrate decomposition on the continental slope. *Geochemistry, Geophysics, Geosystems*, *16*(11), 3825–3839. https://doi.org/10.1002/2015GC005955

Johnstone, J. F., Hollingsworth, T. N., Chapin, F. S., & Mack, M. C. (2010). Changes in fire regime break the legacy lock on successional trajectories in Alaskan boreal forest. *Global Change Biology*, *16*(4), 1281–1295. https://doi.org/10.1111/j.1365-2486.2009.02051.x

Jokiel, P. L., & Coles, S. L. (1990). Response of Hawaiian and other Indo-Pacific reef corals to elevated temperature. *Coral Reefs*, *8*(4), 155–162. https://doi.org/10.1007/BF00265006

Jones, M. C., Harden, J., O'Donnell, J., Manies, K., Jorgenson, T., Treat, C., & Ewing, S. (2017). Rapid carbon loss and slow recovery following permafrost thaw in boreal peatlands. *Global Change Biology*, *23*(3), 1109–1127. https://doi.org/10.1111/gcb.13403

Jones, P. D. (1994). Hemispheric surface air temperature variations: A reanalysis and an update to 1993. *Journal of Climate*, *7*(11), 1794–1802. https://doi.org/10.1175/1520-0442(1994)007<1794:HSATVA>2.0.CO;2

Joos, F., Plattner, G.-K., Stocker, T. F., Marchal, O., & Schmittner, A. (1999). Global warming and marine carbon cycle feedbacks on future atmospheric CO_2. *Science*, *284*(5413), 464–467. https://doi.org/10.1126/science.284.5413.464

Jorgenson, M. T., Romanovsky, V., Harden, J., Shur, Y., Donnell, J. O., Schuur, E. A. G., et al. (2010). Resilience and vulnerability of permafrost to climate change. *Canadian Journal of Forest Research*, *40*(7), 1219–1236. https://doi.org/10.1139/x10-060

Joughin, I., Smith, B. E., & Medley, B. (2014). Marine ice sheet collapse potentially under way for the Thwaites Glacier Basin, West Antarctica. *Science*, *344*(6185), 735–738. https://doi.org/10.1126/science.1249055

Ju, J., & Masek, J. G. (2016). The vegetation greenness trend in Canada and US Alaska from 1984-2012 Landsat data. *Remote Sensing of Environment*, *176*, 1–16. https://doi.org/10.1016/j.rse.2016.01.001

Jury, C. P., & Toonen, R. J. (2019). Adaptive responses and local stressor mitigation drive coral resilience in warmer, more acidic oceans. *Proceedings of the Royal Society B: Biological Sciences*, *286*(1902), 20190614. https://doi.org/10.1098/rspb.2019.0614

Karspeck, A. R., Stammer, D., Köhl, A., Danabasoglu, G., Balmaseda, M., Smith, D. M., et al. (2017). Comparison of the Atlantic meridional overturning circulation between 1960 and 2007 in six ocean reanalysis products. *Climate Dynamics*, *49*(3), 957–982. https://doi.org/10.1007/s00382-015-2787-7

Kasischke, E. S. (2000). Boreal ecosystems in the global carbon cycle. In E. S. Kasischke & B. J. Stocks (Eds.), *Fire, climate change, and carbon cycling in the boreal forest* (pp. 19–30). https://doi.org/10.1007/978-0-387-21629-4_2

Kasischke, E. S., & Turetsky, M. R. (2006). Recent changes in the fire regime across the North American boreal region—Spatial and temporal patterns of burning across Canada and Alaska. *Geophysical Research Letters*, *33*(9), L09703. https://doi.org/10.1029/2006GL025677

Kay, J. E., L'Ecuyer, T., Gettelman, A., Stephens, G., & O'Dell, C. (2008). The contribution of cloud and radiation anomalies to the 2007 Arctic sea ice extent minimum. *Geophysical Research Letters*, *35*(8), 1–5. https://doi.org/10.1029/2008GL033451

Kersalé, M., Lamont, T., Speich, S., Terre, T., Laxenaire, R., Roberts, M. J., et al. (2018). Moored observations of mesoscale features in the Cape Basin: Characteristics and local impacts on water mass distributions. *Ocean Science*, *14*(5), 923–945. https://doi.org/10.5194/os-14-923-2018

Kessler, J. D., Reeburgh, W. S., Southon, J., & Varela, R. (2005). Fossil methane source dominates Cariaco Basin water column methane geochemistry. *Geophysical Research Letters*, *32*(12), L12609. https://doi.org/10.1029/2005GL022984

Kessler, J. D., Reeburgh, W. S., Valentine, D. L., Kinnaman, F. S., Peltzer, E. T., Brewer, P. G., et al. (2008). A survey of methane isotope abundance (^{14}C, ^{13}C, ^{2}H) from five nearshore marine basins that reveals unusual radiocarbon levels in subsurface waters. *Journal of Geophysical Research*, *113*(C12), C12021. https://doi.org/10.1029/2008JC004822

Kessler, J. D., Valentine, D. L., Redmond, M. C., Du, M., Chan, E. W., Mendes, S. D., et al. (2011). A persistent oxygen anomaly reveals the fate of spilled methane in the deep Gulf of Mexico. *Science*, *331*(6015), 312–315. https://doi.org/10.1126/science.1199697

Keuper, F., Wild, B., Kummu, M., Beer, C., Blume-Werry, G., Fontaine, S., et al. (2020). Carbon loss from northern circumpolar permafrost soils amplified by rhizosphere priming. *Nature Geoscience*, *13*(8), 560–565. https://doi.org/10.1038/s41561-020-0607-0

Kharuk, V. I., Im, S. T., & Soldatov, V. V. (2020). Siberian silkmoth outbreaks surpassed geoclimatic barrier in Siberian Mountains. *Journal of Mountain Science*, *17*(8), 1891–1900. https://doi.org/10.1007/s11629-020-5989-3

Kharuk, V. I., Ranson, K. J., & Dvinskaya, M. L. (2008). Wildfires dynamic in the larch dominance zone. *Geophysical Research Letters*, *35*(1), L01402. https://doi.org/10.1029/2007GL032291

Khazendar, A., Rignot, E., Schroeder, D. M., Seroussi, H., Schodlok, M. P., Scheuchl, B., et al. (2016). Rapid submarine ice melting in the grounding zones of ice shelves in West Antarctica. *Nature Communications*, *7*, 1–8. https://doi.org/10.1038/ncomms13243

Kilbourne, K. H., Wanamaker, A. D., Moffa-Sanchez, P., Reynolds, D. J., Amrhein, D. E., Butler, P. G., et al. (2022). Atlantic circulation change still uncertain. *Nature Geoscience*, *15*(3), 165–167. https://doi.org/10.1038/s41561-022-00896-4

Kirschke, S., Bousquet, P., Ciais, P., Saunois, M., Canadell, J. G., Dlugokencky, E. J., et al. (2013). Three decades of global methane sources and sinks. *Nature Geoscience*, *6*(10), 813–823. https://doi.org/10.1038/ngeo1955

Kjeldsen, K. K., Korsgaard, N. J., Bjørk, A. A., Khan, S. A., Box, J. E., Funder, S., et al. (2015). Spatial and temporal distribution of mass loss from the Greenland Ice Sheet since AD 1900. *Nature*, *528*(7582), 396–400. https://doi.org/10.1038/nature16183

Klein, S. G., Geraldi, N. R., Anton, A., Schmidt-Roach, S., Ziegler, M., Cziesielski, M. J., et al. (2022). Projecting coral responses to intensifying marine heatwaves under ocean acidification. *Global Change Biology*, *28*(5), 1753–1765. https://doi.org/10.1111/gcb.15818

Klockmann, M., Mikolajewicz, U., Kleppin, H., & Marotzke, J. (2020). Coupling of the subpolar gyre and the overturning circulation during abrupt glacial climate transitions. *Geophysical Research Letters*, *47*(21), e2020GL090361. https://doi.org/10.1029/2020GL090361

Klose, A. K., Karle, V., Winkelmann, R., & Donges, J. F. (2020). Emergence of cascading dynamics in interacting tipping elements of ecology and climate. *Royal Society Open Science*, *7*(6), 200599. https://doi.org/10.1098/rsos.200599

Kloster, S., Mahowald, N. M., Randerson, J. T., & Lawrence, P. J. (2012). The impacts of climate, land use, and demography on fires during the 21st century simulated by CLM-CN. *Biogeosciences*, *9*(1), 509–525. https://doi.org/10.5194/bg-9-509-2012

Koenig, S. J., DeConto, R. M., & Pollard, D. (2014). Impact of reduced Arctic sea ice on Greenland ice sheet variability in a warmer than present climate. *Geophysical Research Letters*, *41*(11), 3933–3942. https://doi.org/10.1002/2014GL059770

Kokelj, S. V., Tunnicliffe, J., Lacelle, D., Lantz, T. C., Chin, K. S., & Fraser, R. (2015). Increased precipitation drives mega slump development and destabilization of ice-rich permafrost terrain, northwestern Canada. *Global and Planetary Change*, *129*, 56–68. https://doi.org/10.1016/j.gloplacha.2015.02.008

Kominz, M. A., Browning, J. V., Miller, K. G., Sugarman, P. J., Mizintseva, S., & Scotese, C. R. (2008). Late Cretaceous to Miocene sea-level estimates from the New Jersey and Delaware coastal plain coreholes: An error analysis. *Basin Research*, *20*(2), 211–226. https://doi.org/10.1111/j.1365-2117.2008.00354.x

Kopp, R. E., Shwom, R. L., Wagner, G., & Yuan, J. (2016). Tipping elements and climate–economic shocks: Pathways toward integrated assessment. *Earth's Future*, *4*(8), 346–372. https://doi.org/10.1002/2016EF000362

Koven, C. D., Lawrence, D. M., & Riley, W. J. (2015). Permafrost carbon-climate feedback is sensitive to deep soil carbon decomposability but not deep soil nitrogen dynamics. *Proceedings of the National Academy of Sciences of the United States of America*, *112*(12), 3752–3757. https://doi.org/10.1073/pnas.1415123112

Koven, C. D., Riley, W. J., & Stern, A. (2013). Analysis of permafrost thermal dynamics and response to climate change in the CMIP5 Earth system models. *Journal of Climate*, *26*(6), 1877–1900. https://doi.org/10.1175/JCLI-D-12-00228.1

Koven, C. D., Schuur, E. A. G., Schädel, C., Bohn, T. J., Burke, E. J., Chen, G., et al. (2015). A simplified, data-constrained approach to estimate the permafrost carbon–climate feedback. *Philosophical Transactions of the Royal Society A: Mathematical, Physical and Engineering Sciences*, *373*(2054), 20140423. https://doi.org/10.1098/rsta.2014.0423

Kretschmer, K., Biastoch, A., Rüpke, L., & Burwicz, E. (2015). Modeling the fate of methane hydrates under global warming. *Global Biogeochemical Cycles*, *29*(5), 610–625. https://doi.org/10.1002/2014GB005011

Kretschmer, M., Zappa, G., & Shepherd, T. G. (2020). The role of Barents–Kara sea ice loss in projected polar vortex changes. *Weather and Climate Dynamics*, *1*(2), 715–730. https://doi.org/10.5194/wcd-1-715-2020

Kriegler, E., Hall, J. W., Held, H., Dawson, R., & Schellnhuber, H. J. (2009). Imprecise probability assessment of tipping points in the climate system. *Proceedings of the National Academy of Sciences of the United States of America*, *106*(13), 5041–5046. https://doi.org/10.1073/pnas.0809117106

Krishnamurti, T. N., Ardanuy, P., Ramanathan, Y., & Pasch, R. (1981). On the onset vortex of the summer monsoon. *Monthly Weather Review*, *109*(2), 344–363. https://doi.org/10.1175/1520-0493(1981)109<0344:OTOVOT>2.0.CO;2

Kroeker, K. J., Kordas, R. L., Crim, R. N., & Singh, G. G. (2010). Meta-analysis reveals negative yet variable effects of ocean acidification on marine organisms. *Ecology Letters*, *13*(11), 1419–1434. https://doi.org/10.1111/j.1461-0248.2010.01518.x

Kurz, W. A., Stinson, G., Rampley, G. J., Dymond, C. C., & Neilson, E. T. (2008). Risk of natural disturbances makes future contribution of Canada's forests to the global carbon cycle highly uncertain. *Proceedings of the National Academy of Sciences of the United States of America*, *105*(5), 1551–1555. https://doi.org/10.1073/pnas.0708133105

Kwok, R., & Rothrock, D. A. (2009). Decline in Arctic sea ice thickness from submarine and ICESat records: 1958-2008. *Geophysical Research Letters*, *36*(15), 1–5. https://doi.org/10.1029/2009GL039035

Lammertsma, E. I., De Boer, H. J., Dekker, S. C., Dilcher, D. L., Lotter, A. F., & Wagner-Cremer, F. (2011). Global CO_2 rise leads to reduced maximum stomatal conductance in Florida vegetation. *Proceedings of the National Academy of Sciences of the United States of America*, *108*(10), 4035–4040. https://doi.org/10.1073/pnas.1100371108

Lara, M. J., McGuire, A. D., Euskirchen, E. S., Genet, H., Yi, S., Rutter, R., et al. (2020). Local-scale Arctic tundra heterogeneity affects regional-scale carbon dynamics. *Nature Communications*, *11*(1), 4925. https://doi.org/10.1038/s41467-020-18768-z

Larour, E., Seroussi, H., Adhikari, S., Ivins, E., Caron, L., Morlighem, M., & Schlegel, N. (2019). Slowdown in Antarctic mass loss from solid Earth and sea-level feedbacks. *Science*, *364*(6444), eaav7908. https://doi.org/10.1126/science.aav7908

Latif, M., Sun, J., Visbeck, M., & Hadi Bordbar, M. (2022). Natural variability has dominated atlantic meridional overturning circulation since 1900. *Nature Climate Change*, *12*(5), 455–460. https://doi.org/10.1038/s41558-022-01342-4

Laufkötter, C., Zscheischler, J., & Frölicher, T. L. (2020). High-impact marine heatwaves attributable to human-induced global warming. *Science*, *369*(6511), 1621–1625. https://doi.org/10.1126/science.aba0690

Laurion, I., Massicotte, P., Mazoyer, F., Negandhi, K., & Mladenov, N. (2020). Weak mineralization despite strong processing of dissolved organic matter in Eastern Arctic tundra ponds. *Limnology and Oceanography*, *66*(S1), S47–S63. https://doi.org/10.1002/lno.11634

Lauvset, S. K., Gruber, N., Landschützer, P., Olsen, A., & Tjiputra, J. (2015). Trends and drivers in global surface ocean pH over the past 3 decades. *Biogeosciences*, *12*(5), 1285–1298. https://doi.org/10.5194/bg-12-1285-2015

Lawrence, D., & Vandecar, K. (2015). Effects of tropical deforestation on climate and agriculture. *Nature Climate Change*, 5(1), 27–36. https://doi.org/10.1038/nclimate2430

Lawrence, D. M., Slater, A. G., & Swenson, S. C. (2012). Simulation of present-day and future permafrost and seasonally frozen ground conditions in CCSM4. *Journal of Climate*, *25*(7), 2207–2225. https://doi.org/10.1175/JCLI-D-11-00334.1

Le Brocq, A. M., Payne, A. J., & Vieli, A. (2010). An improved Antarctic dataset for high resolution numerical ice sheet models (ALBMAP v1). *Earth System Science Data*, *2*(2), 247–260. https://doi.org/10.5194/essd-2-247-2010

Ledru, M. P., Salgado-Labouriau, M. L., & Lorscheitter, M. L. (1998). Vegetation dynamics in southern and central Brazil during the last 10,000 yr B.P. *Review of Palaeobotany and Palynology*, *99*(2), 131–142. https://doi.org/10.1016/S0034-6667(97)00049-3

Lee, H., Ekici, A., Tjiputra, J., Muri, H., Chadburn, S. E., Lawrence, D. M., & Schwinger, J. (2019). The response of permafrost and high-latitude ecosystems under large-scale stratospheric aerosol injection and its termination. *Earth's Future*, *7*(6), 605–614. https://doi.org/10.1029/2018EF001146

Lee, H., Swenson, S. C., Slater, A. G., & Lawrence, D. M. (2014). Effects of excess ground ice on projections of permafrost in a warming climate. *Environmental Research Letters*, *9*(12), 124006. https://doi.org/10.1088/1748-9326/9/12/124006

Lee, J.-E., Risi, C., Fung, I., Worden, J., Scheepmaker, R. A., Lintner, B., & Frankenberg, C. (2012). Asian monsoon hydrometeorology from TES and SCIAMACHY water vapor isotope measurements and LMDZ simulations: Implications for speleothem climate record interpretation. *Journal of Geophysical Research*, *117*(D15), D15112. https://doi.org/10.1029/2011JD017133

Lee, J.-Y., Marotzke, J., Bala, G., Cao, L., Corti, S., Dunne, J. P., et al. (2021). Chapter 4: Future global climate: Scenario-based projections and near-term information. In *Climate change 2021: The physical science basis. Contribution of Working Group I to the Sixth Assessment Report of the Intergovernmental Panel on Climate Change* (p. 195). Retrieved from https://www.ipcc.ch/report/ar6/wg1/#FullReport

Leite-Filho, A. T., de Sousa Pontes, V. Y., & Costa, M. H. (2019). Effects of deforestation on the onset of the rainy season and the duration of dry spells in southern Amazonia. *Journal of Geophysical Research: Atmospheres*, *124*(10), 5268–5281. https://doi.org/10.1029/2018JD029537

Leite-Filho, A. T., Soares-Filho, B. S., Davis, J. L., Abrahão, G. M., & Börner, J. (2021). Deforestation reduces rainfall and agricultural revenues in the Brazilian Amazon. *Nature Communications*, *12*(1), 2591. https://doi.org/10.1038/s41467-021-22840-7

Lenaerts, J. T. M., Van Angelen, J. H., Van Den Broeke, M. R., Gardner, A. S., Wouters, B., & Van Meijgaard, E. (2013). Irreversible mass loss of Canadian Arctic Archipelago glaciers. *Geophysical Research Letters*, *40*(5), 870–874. https://doi.org/10.1002/grl.50214

Lenton, T. M. (2011). Early warning of climate tipping points. *Nature Climate Change*, *1*(4), 201–209. https://doi.org/10.1038/nclimate1143

Lenton, T. M. (2012). Arctic climate tipping points. *Ambio*, *41*(1), 10–22. https://doi.org/10.1007/s13280-011-0221-x

Lenton, T. M., Held, H., Kriegler, E., Hall, J. W., Lucht, W., Rahmstorf, S., & Schellnhuber, H. J. (2008). Tipping elements in the Earth's climate system. *Proceedings of the National Academy of Sciences of the United States of America*, *105*(6), 1786–1793. https://doi.org/10.1073/pnas.0705414105

Lenton, T. M., Rockström, J., Gaffney, O., Rahmstorf, S., Richardson, K., Steffen, W., & Schellnhuber, H. J. (2019). Climate tipping points—Too risky to bet against. *Nature*, *575*(7784), 592–595. https://doi.org/10.1038/d41586-019-03595-0

Lenton, T. M., & Schellnhuber, H. J. (2007). Tipping the scales. *Nature Climate Change*, *1*(712), 97–98. https://doi.org/10.1038/climate.2007.65

Leonte, M., Ruppel, C. D., Ruiz-Angulo, A., & Kessler, J. D. (2020). Surface methane concentrations along the Mid-Atlantic Bight driven by aerobic subsurface production rather than seafloor gas seeps. *Journal of Geophysical Research: Oceans*, *125*(5), e2019JC015989. https://doi.org/10.1029/2019JC015989

Levermann, A., Griesel, A., Hofmann, M., Montoya, M., & Rahmstorf, S. (2005). Dynamic sea level changes following changes in the thermohaline circulation. *Climate Dynamics*, *24*(4), 347–354. https://doi.org/10.1007/s00382-004-0505-y

Levermann, A., Petoukhov, V., Schewe, J., & Schellnhuber, H. J. (2016). Abrupt monsoon transitions as seen in paleorecords can be explained by moisture-advection feedback. *Proceedings of the National Academy of Sciences*, *113*(17), E2348–E2349. https://doi.org/10.1073/pnas.1603130113

Levermann, A., Schewe, J., Petoukhov, V., & Held, H. (2009). Basic mechanism for abrupt monsoon transitions. *Proceedings of the National Academy of Sciences of the United States of America*, *106*(49), 20572–20577. https://doi.org/10.1073/pnas.0901414106

Lewkowicz, A. G., & Way, R. G. (2019). Extremes of summer climate trigger thousands of thermokarst landslides in a High Arctic environment. *Nature Communications*, *10*(1), 1–11. https://doi.org/10.1038/s41467-019-09314-7

Lhermitte, S., Sun, S., Shuman, C., Wouters, B., Pattyn, F., Wuite, J., et al. (2020). Damage accelerates ice shelf instability and mass loss in Amundsen Sea Embayment. *Proceedings of the National Academy of Sciences*, *117*(40), 24735–24741. https://doi.org/10.1073/pnas.1912890117

Li, C., Notz, D., Tietsche, S., & Marotzke, J. (2013). The transient versus the equilibrium response of sea ice to global warming. *Journal of Climate*, *26*(15), 5624–5636. https://doi.org/10.1175/JCLI-D-12-00492.1

Li, F., Lozier, M. S., Bacon, S., Bower, A. S., Cunningham, S. A., de Jong, M. F., et al. (2021). Subpolar North Atlantic western boundary density anomalies and the Meridional Overturning Circulation. *Nature Communications*, *12*(1), 3002. https://doi.org/10.1038/s41467-021-23350-2

Li, S., & Liu, W. (2022). Deciphering the migration of the intertropical convergence zone during the last deglaciation. *Geophysical Research Letters*, *49*(10), e2022GL098806. https://doi.org/10.1029/2022GL098806

Li, W., & Fu, R. (2004). Transition of the large-scale atmospheric and land surface conditions from the dry to the wet season over Amazonia as diagnosed by the ECMWF re-analysis. *Journal of Climate*, *17*(13), 2637–2651. https://doi.org/10.1175/1520-0442(2004)017<2637:TOTLAA>2.0.CO;2

Li, W., Fu, R., & Dickinson, R. E. (2006). Rainfall and its seasonality over the Amazon in the 21st century as assessed by the coupled models for the IPCC AR4. *Journal of Geophysical Research*, *111*(2), 1–14. https://doi.org/10.1029/2005JD006355

Li, W., Fu, R., Juárez, R. I. N., & Fernandes, K. (2008). Observed change of the standardized precipitation index, its potential cause and implications to future climate change in the Amazon region. *Philosophical Transactions of the Royal Society B: Biological Sciences*, *363*(1498), 1767–1772. https://doi.org/10.1098/rstb.2007.0022

Liang, X.-Z., & Wang, W.-C. (1998). Associations between China monsoon rainfall and tropospheric jets. *Quarterly Journal of the Royal Meteorological Society*, *124*(552), 2597–2623. https://doi.org/10.1002/qj.49712455204

Lin, J. L., Qian, T., & Shinoda, T. (2014). Stratocumulus clouds in Southeastern Pacific simulated by eight CMIP5-CFMIP global climate models. *Journal of Climate*, *27*(8), 3000–3022. https://doi.org/10.1175/JCLI-D-13-00376.1

Lin, X., Rogers, B. M., Sweeney, C., Chevallier, F., Arshinov, M., Dlugokencky, E., et al. (2020). Siberian and temperate ecosystems shape Northern Hemisphere atmospheric CO_2 seasonal amplification. *Proceedings of the National Academy of Sciences*, *117*(35), 21079–21087. https://doi.org/10.1073/pnas.1914135117

Little, C. M., Hu, A., Hughes, C. W., McCarthy, G. D., Piecuch, C. G., Ponte, R. M., & Thomas, M. D. (2019). The relationship between U.S. east coast sea level and the Atlantic meridional overturning circulation: A review. *Journal of Geophysical Research: Oceans*, *124*(9), 6435–6458. https://doi.org/10.1029/2019JC015152

Liu, W., & Fedorov, A. V. (2019). Global impacts of Arctic sea ice loss mediated by the Atlantic meridional overturning circulation. *Geophysical Research Letters*, *46*(2), 944–952. https://doi.org/10.1029/2018GL080602

Liu, W., & Fedorov, A. (2022). Interaction between Arctic sea ice and the Atlantic meridional overturning circulation in a warming climate. *Climate Dynamics*, *58*(5), 1811–1827. https://doi.org/10.1007/s00382-021-05993-5

Liu, W., Fedorov, A., & Sévellec, F. (2019). The mechanisms of the Atlantic meridional overturning circulation slowdown induced by Arctic sea ice decline. *Journal of Climate*, *32*(4), 977–996. https://doi.org/10.1175/JCLI-D-18-0231.1

Liu, W., Fedorov, A. V., Xie, S.-P., & Hu, S. (2020). Climate impacts of a weakened Atlantic meridional overturning circulation in a warming climate. *Science Advances*, *6*(26), eaaz4876. https://doi.org/10.1126/sciadv.aaz4876

Liu, W., & Liu, Z. (2013). A diagnostic indicator of the stability of the Atlantic meridional overturning circulation in CCSM3. *Journal of Climate*, *26*(6), 1926–1938. https://doi.org/10.1175/JCLI-D-11-00681.1

Liu, W., Liu, Z., & Brady, E. C. (2014). Why is the AMOC monostable in coupled general circulation models? *Journal of Climate*, *27*(6), 2427–2443. https://doi.org/10.1175/JCLI-D-13-00264.1

Liu, W., Xie, S.-P., Liu, Z., & Zhu, J. (2017). Overlooked possibility of a collapsed Atlantic Meridional Overturning Circulation in warming climate. *Science Advances*, *3*(1), e1601666. https://doi.org/10.1126/sciadv.1601666

Liu, Y., Moore, J. C., Cheng, X., Gladstone, R. M., Bassis, J. N., Liu, H., et al. (2015). Ocean-driven thinning enhances iceberg calving and retreat of Antarctic ice shelves. *Proceedings of the National Academy of Sciences of the United States of America*, *112*(11), 3263–3268. https://doi.org/10.1073/pnas.1415137112

Liu, Z., Ballantyne, A. P., & Cooper, L. A. (2019). Biophysical feedback of global forest fires on surface temperature. *Nature Communications*, *10*(1), 1–9. https://doi.org/10.1038/s41467-018-08237-z

Liu, Z., Kimball, J. S., Parazoo, N. C., Ballantyne, A. P., Wang, W. J., Madani, N., et al. (2020). Increased high-latitude photosynthetic carbon gain offset by respiration carbon loss during an anomalous warm winter to spring transition. *Global Change Biology*, *26*(2), 682–696. https://doi.org/10.1111/gcb.14863

Lohmann, J., & Ditlevsen, P. D. (2021). Risk of tipping the overturning circulation due to increasing rates of ice melt. *Proceedings of the National Academy of Sciences*, *118*(9), e2017989118. https://doi.org/10.1073/pnas.2017989118

Lord, N. S., Crucifix, M., Lunt, D. J., Thorne, M. C., Bounceur, N., Dowsett, H., et al. (2017). Emulation of long-term changes in global climate: Application to the late Pliocene and future. *Climate of the Past*, *13*(11), 1539–1571. https://doi.org/10.5194/cp-13-1539-2017

Lovejoy, T. E., & Nobre, C. (2018). Amazon tipping point. *Science Advances*, *4*(2), eaat2340. https://doi.org/10.1126/sciadv.aat2340

Lozier, M. S., Bacon, S., Bower, A. S., Cunningham, S. A., De Jong, M. F., De Steur, L., et al. (2017). Overturning in the Subpolar North Atlantic program: A new international ocean observing system. *Bulletin of the American Meteorological Society*, *98*(4), 737–752. https://doi.org/10.1175/BAMS-D-16-0057.1

Lozier, M. S., Li, F., Bacon, S., Bahr, F., Bower, A. S., Cunningham, S. A., et al. (2019). A sea change in our view of overturning in the subpolar North Atlantic. *Science*, *363*(6426), 516–521. https://doi.org/10.1126/science.aau6592

Lucht, W., Schaphoff, S., Erbrecht, T., Heyder, U., & Cramer, W. (2006). Terrestrial vegetation redistribution and carbon balance under climate change. *Carbon Balance and Management*, *1*(1), 1–7. https://doi.org/10.1186/1750-0680-1-6

Lynch-Stieglitz, J. (2017). The Atlantic meridional overturning circulation and abrupt climate change. *Annual Review of Marine Science*, *9*(1), 83–104. https://doi.org/10.1146/annurev-marine-010816-060415

Lyra, A. D. A., Chou, S. C., & Sampaio, G. D. O. (2016). Sensitivity of the Amazon biome to high resolution climate change projections. *Acta Amazonica*, *46*(2), 175–188. https://doi.org/10.1590/1809-4392201502225

Ma, L., Wang, B., & Zhang, X. (2020). Impact of seawater equation of state on the simulation of Atlantic meridional overturning circulation. *Climate Dynamics*, *54*(1), 1161–1178. https://doi.org/10.1007/s00382-019-05052-0

Ma, X., Liu, W., Allen, R. J., Huang, G., & Li, X. (2020). Dependence of regional ocean heat uptake on anthropogenic warming scenarios. *Science Advances*, *6*(45), eabc0303. https://doi.org/10.1126/sciadv.abc0303

MacDonald, G. M., Kremenetski, K. V., & Beilman, D. W. (2008). Climate change and the northern Russian treeline zone. *Philosophical Transactions of the Royal Society B: Biological Sciences*, *363*(1501), 2283–2299. https://doi.org/10.1098/rstb.2007.2200

MacDonald, G. M., Velichko, A. A., Kremenetski, C. V., Borisova, O. K., Goleva, A. A., Andreev, A. A., et al. (2000). Holocene treeline history and climate change across northern Eurasia. *Quaternary Research*, *53*(3), 302–311. https://doi.org/10.1006/qres.1999.2123

MacFerrin, M., Machguth, H., As, D. V., Charalampidis, C., Stevens, C. M., Heilig, A., et al. (2019). Rapid expansion of Greenland's low-permeability ice slabs. *Nature*, *573*(7774), 403–407. https://doi.org/10.1038/s41586-019-1550-3

Mack, M. C., Bret-Harte, M. S., Hollingsworth, T. N., Jandt, R. R., Schuur, E. A. G., Shaver, G. R., & Verbyla, D. L. (2011). Carbon loss from an unprecedented Arctic tundra wildfire. *Nature*, *475*(7357), 489–492. https://doi.org/10.1038/nature10283

Mack, M. C., Walker, X. J., Johnstone, J. F., Alexander, H. D., Melvin, A. M., Jean, M., & Miller, S. N. (2021). Carbon loss from boreal forest wildfires offset by increased dominance of deciduous trees. *Science*, *372*(6539), 280–283. https://doi.org/10.1126/science.abf3903

Maher, B. A. (2008). Holocene variability of the East Asian summer monsoon from Chinese cave records: A re-assessment. *The Holocene*, *18*(6), 861–866. https://doi.org/10.1177/0959683608095569

Maher, C. T., Dial, R. J., Pastick, N. J., Hewitt, R. E., Jorgenson, M. T., & Sullivan, P. F. (2021). The climate envelope of Alaska's northern treelines: Implications for controlling factors and future treeline advance. *Ecography*, *44*(11), 1710–1722. https://doi.org/10.1111/ecog.05597

Malhi, Y., Aragão, L. E. O. C., Metcalfe, D. B., Paiva, R., Quesada, C. A., Almeida, S., et al. (2009). Comprehensive assessment of carbon productivity, allocation and storage in three Amazonian forests. *Global Change Biology*, *15*(5), 1255–1274. https://doi.org/10.1111/j.1365-2486.2008.01780.x

Malhi, Y., Wood, D., Baker, T. R., Wright, J., Phillips, O. L., Cochrane, T., et al. (2006). The regional variation of aboveground live biomass in old-growth Amazonian forests. *Global Change Biology*, *12*(7), 1107–1138. https://doi.org/10.1111/j.1365-2486.2006.01120.x

Mann, D. H., Rupp, T. S., Olson, M. A., & Duffy, P. A. (2012). Is Alaska's boreal forest now crossing a major ecological threshold? *Arctic, Antarctic, and Alpine Research*, *44*(3), 319–331. https://doi.org/10.1657/1938-4246-44.3.319

Marchal, J., Cumming, S. G., & McIntire, E. J. B. (2020). Turning down the heat: Vegetation feedbacks limit fire regime responses to global warming. *Ecosystems*, *23*(1), 204–216. https://doi.org/10.1007/s10021-019-00398-2

Marengo, J. A., Nobre, C. A., Sampaio, G., Salazar, L. F., & Borma, L. S. (2011). Climate change in the Amazon Basin: Tipping points, changes in extremes, and impacts on natural and human systems. In *Tropical Rainforest Responses to Climatic Change* (pp. 259–283). https://doi.org/10.1007/978-3-642-05383-2_9

Martin-Español, A., Bamber, J. L., & Zammit-Mangion, A. (2017). Constraining the mass balance of East Antarctica. *Geophysical Research Letters*, *44*(9), 4168–4175. https://doi.org/10.1002/2017GL072937

Martin-StPaul, N., Delzon, S., & Cochard, H. (2017). Plant resistance to drought depends on timely stomatal closure. *Ecology Letters*, *20*(11), 1437–1447. https://doi.org/10.1111/ele.12851

Masson-Delmotte, V., Schulz, M., Abe-Ouchi, A., Beer, J., Ganopolski, A., González Rouco, J. F., et al. (2013). Information from paleoclimate archives. In *Climate change 2013: The physical science basis. Contribution of Working Group I to the Fifth Assessment Report of the Intergovernmental Panel on Climate Change*. https://doi.org/10.1017/CBO9781107415324.013

Massonnet, F., Fichefet, T., Goosse, H., Bitz, C. M., Philippon-Berthier, G., Holland, M. M., & Barriat, P. Y. (2012). Constraining projections of summer Arctic sea ice. *Cryosphere*, *6*(6), 1383–1394. https://doi.org/10.5194/tc-6-1383-2012

Mau, S., Blees, J., Helmke, E., Niemann, H., & Damm, E. (2013). Vertical distribution of methane oxidation and methanotrophic response to elevated methane concentrations in stratified waters of the Arctic fjord Storfjorden (Svalbard, Norway). *Biogeosciences*, *10*(10), 6267–6268. https://doi.org/10.5194/bg-10-6267-2013

McCarthy, G. D., Brown, P. J., Flagg, C. N., Goni, G., Houpert, L., Hughes, C. W., et al. (2020). Sustainable observations of the AMOC: Methodology and technology. *Reviews of Geophysics*, *58*(1), e2019RG000654. https://doi.org/10.1029/2019RG000654

McCarty, J. L., Smith, T. E. L., & Turetsky, M. R. (2020). Arctic fires re-emerging. *Nature Geoscience*, *13*(10), 658–660. https://doi.org/10.1038/s41561-020-00645-5

McClanahan, T. R., Darling, E. S., Maina, J. M., Muthiga, N. A., D'agata, S., Jupiter, S. D., et al. (2019). Temperature patterns and mechanisms influencing coral bleaching during the 2016 El Niño. *Nature Climate Change*, *9*(11), 845–851. https://doi.org/10.1038/s41558-019-0576-8

McGee, D., de Menocal, P. B., Winckler, G., Stuut, J. B. W., & Bradtmiller, L. I. (2013). The magnitude, timing and abruptness of changes in North African dust deposition over the last 20,000 yr. *Earth and Planetary Science Letters*, *371–372*, 163–176. https://doi.org/10.1016/j.epsl.2013.03.054

McGinnis, D. F., Greinert, J., Artemov, Y., Beaubien, S. E., & Wüest, A. (2006). Fate of rising methane bubbles in stratified waters: How much methane reaches the atmosphere? *Journal of Geophysical Research*, *111*(9), 1–15. https://doi.org/10.1029/2005JC003183

Mcguire, A. D., Anderson, L. G., Christensen, T. R., Scott, D., Laodong, G., Hayes, D. J., et al. (2009). Sensitivity of the carbon cycle in the Arctic to climate change. *Ecological Monographs*, *79*(4), 523–555. https://doi.org/10.1890/08-2025.1

McGuire, A. D., Lawrence, D. M., Koven, C., Clein, J. S., Burke, E., Chen, G., et al. (2018). Dependence of the evolution of carbon dynamics in the northern permafrost region on the trajectory of climate change. *Proceedings of the National Academy of Sciences of the United States of America*, *115*(15), 3882–3887. https://doi.org/10.1073/pnas.1719903115

McInerney, F. A., & Wing, S. L. (2011). The Paleocene-Eocene thermal maximum: A perturbation of carbon cycle, climate, and biosphere with implications for the future. *Annual Review of Earth and Planetary Sciences*, *39*(1), 489–516. https://doi.org/10.1146/annurev-earth-040610-133431

McMillan, M., Leeson, A., Shepherd, A., Briggs, K., Armitage, T. W. K., Hogg, A., et al. (2016). A high-resolution record of Greenland mass balance. *Geophysical Research Letters*, *43*(13), 7002–7010. https://doi.org/10.1002/2016GL069666

McSweeney, R. (2020). Explainer: Nine 'tipping points' that could be triggered by climate change—Carbon brief. Retrieved from https://www.carbonbrief.org/explainer-nine-tipping-points-that-could-be-triggered-by-climate-change

Mekonnen, Z. A., Riley, W. J., Randerson, J. T., Grant, R. F., & Rogers, B. M. (2019). Expansion of high-latitude deciduous forests driven by interactions between climate warming and fire. *Nature Plants*, *5*(9), 952–958. https://doi.org/10.1038/s41477-019-0495-8

Mellado, J. P. (2017). Cloud-top entrainment in stratocumulus clouds. *Annual Review of Fluid Mechanics*, *49*(1), 145–169. https://doi.org/10.1146/annurev-fluid-010816-060231

Menary, M. B., Jackson, L. C., & Lozier, M. S. (2020). Reconciling the relationship between the AMOC and Labrador Sea in OSNAP observations and climate models. *Geophysical Research Letters*, *47*(18), e2020GL089793. https://doi.org/10.1029/2020GL089793

Menary, M. B., Robson, J., Allan, R. P., Booth, B. B. B., Cassou, C., Gastineau, G., et al. (2020). Aerosol-forced AMOC changes in CMIP6 historical simulations. *Geophysical Research Letters*, *47*(14), e2020GL088166. https://doi.org/10.1029/2020GL088166

Menary, M. B., & Wood, R. A. (2018). An anatomy of the projected North Atlantic warming hole in CMIP5 models. *Climate Dynamics*, *50*(7–8), 3063–3080. https://doi.org/10.1007/s00382-017-3793-8

Mengel, M., & Levermann, A. (2014). Ice plug prevents irreversible discharge from East Antarctica. *Nature Climate Change*, *4*(6), 451–455. https://doi.org/10.1038/nclimate2226

Menviel, L., Timmermann, A., Mouchet, A., & Timm, O. (2008). Meridional reorganizations of marine and terrestrial productivity during Heinrich events. *Paleoceanography*, *23*(1). https://doi.org/10.1029/2007PA001445

Meredith, M., Sommerkorn, M., Cassotta, S., Derksen, C., Ekaykin, A., Hollowed, A., et al. (2019). Polar regions. In *IPCC Special Report on the Ocean and Cryosphere in a Changing Climate*. https://doi.org/10.1016/S1366-7017(01)00066-6

Mestdagh, T., Poort, J., & De Batist, M. (2017). The sensitivity of gas hydrate reservoirs to climate change: Perspectives from a new combined model for permafrost-related and marine settings. *Earth-Science Reviews*, *169*, 104–131. https://doi.org/10.1016/j.earscirev.2017.04.013

Mies, M., Francini-Filho, R. B., Zilberberg, C., Garrido, A. G., Longo, G. O., Laurentino, E., et al. (2020). South Atlantic coral reefs are major global warming refugia and less susceptible to bleaching. *Frontiers in Marine Science*, *7*, 514. https://doi.org/10.3389/fmars.2020.00514

Milkov, A. V. (2004). Global estimates of hydrate-bound gas in marine sediments: How much is really out there? *Earth-Science Reviews*, *66*(3–4), 183–197. https://doi.org/10.1016/j.earscirev.2003.11.002

Millar, J. R., Nicholls, Z. R., Friedlingstein, P., & Allen, M. R. (2017). A modified impulse-response representation of the global near-surface air temperature and atmospheric concentration response to carbon dioxide emissions. *Atmospheric Chemistry and Physics*, *17*(11), 7213–7228. https://doi.org/10.5194/acp-17-7213-2017

Miner, K. R., D'Andrilli, J., Mackelprang, R., Edwards, A., Malaska, M. J., Waldrop, M. P., & Miller, C. E. (2021). Emergent biogeochemical risks from Arctic permafrost degradation. *Nature Climate Change*, *11*(10), 809–819. https://doi.org/10.1038/s41558-021-01162-y

Miner, K. R., Turetsky, M. R., Malina, E., Bartsch, A., Tamminen, J., McGuire, A. D., et al. (2022). Permafrost carbon emissions in a changing Arctic. *Nature Reviews Earth & Environment*, *3*(1), 55–67. https://doi.org/10.1038/s43017-021-00230-3

Minshull, T. A., Marín-Moreno, H., Armstrong McKay, D. I., & Wilson, P. A. (2016). Mechanistic insights into a hydrate contribution to the Paleocene-Eocene carbon cycle perturbation from coupled thermohydraulic simulations. *Geophysical Research Letters*, *43*(16), 8637–8644. https://doi.org/10.1002/2016GL069676

Moat, B. I., Smeed, D. A., Frajka-Williams, E., Desbruyères, D. G., Beaulieu, C., Johns, W. E., et al. (2020). Pending recovery in the strength of the meridional overturning circulation at 26°N. *Ocean Science*, *16*(4), 863–874. https://doi.org/10.5194/os-16-863-2020

Mollica, N. R., Guo, W., Cohen, A. L., Huang, K. F., Foster, G. L., Donald, H. K., & Solow, A. R. (2018). Ocean acidification affects coral growth by reducing skeletal density. *Proceedings of the National Academy of Sciences of the United States of America*, *115*(8), 1754–1759. https://doi.org/10.1073/pnas.1712806115

Molnar, P., Boos, W. R., & Battisti, D. S. (2010). Orographic controls on climate and paleoclimate of Asia: Thermal and mechanical roles for the Tibetan Plateau. *Annual Review of Earth and Planetary Sciences*, *38*(1), 77–102. https://doi.org/10.1146/annurev-earth-040809-152456

Morlighem, M., Williams, C. N., Rignot, E., An, L., Arndt, J. E., Bamber, J. L., et al. (2017). BedMachine v3: Complete bed topography and ocean bathymetry mapping of Greenland from multibeam echo sounding combined with mass conservation. *Geophysical Research Letters*, *44*(21), 11051–11061. https://doi.org/10.1002/2017GL074954

Mostofa, K. M. G., Liu, C.-Q., Zhai, W., Minella, M., Vione, D., Gao, K., et al. (2016). Reviews and syntheses: Ocean acidification and its potential impacts on marine ecosystems. *Biogeosciences*, *13*(6), 1767–1786. https://doi.org/10.5194/bg-13-1767-2016

Mouginot, J., Rignot, E., Bjørk, A. A., van den Broeke, M., Millan, R., Morlighem, M., et al. (2019). Forty-six years of Greenland Ice Sheet mass balance from 1972 to 2018. *Proceedings of the National Academy of Sciences*, *116*(19), 9239–9244. https://doi.org/10.1073/pnas.1904242116

Moy, A. D., Howard, W. R., Bray, S. G., & Trull, T. W. (2009). Reduced calcification in modern Southern Ocean planktonic foraminifera. *Nature Geoscience*, *2*(4), 276–280. https://doi.org/10.1038/ngeo460

Muglia, J., Skinner, L. C., & Schmittner, A. (2018). Weak overturning circulation and high Southern Ocean nutrient utilization maximized glacial ocean carbon. *Earth and Planetary Science Letters*, *496*, 47–56. https://doi.org/10.1016/j.epsl.2018.05.038

Murakami, T., Chen, L.-X., & Xie, A. (1986). Relationship among seasonal cycles, low-frequency oscillations, and transient disturbances as revealed from outgoing longwave radiation data. *Monthly Weather Review*, *114*(8), 1456–1465. https://doi.org/10.1175/1520-0493(1986)114<1456:RASCLF>2.0.CO;2

Mykleby, P. M., Snyder, P. K., & Twine, T. E. (2017). Quantifying the trade-off between carbon sequestration and albedo in midlatitude and high-latitude North American forests. *Geophysical Research Letters*, *44*(5), 2493–2501. https://doi.org/10.1002/2016GL071459

Nam, C., Bony, S., Dufresne, J. L., & Chepfer, H. (2012). The too few, too bright tropical low-cloud problem in CMIP5 models. *Geophysical Research Letters*, *39*(21), L21801. https://doi.org/10.1029/2012GL053421

Natali, S. M., Holdren, J. P., Rogers, B. M., Treharne, R., Duffy, P. B., Pomerance, R., & MacDonald, E. (2021). Permafrost carbon feedbacks threaten global climate goals. *Proceedings of the National Academy of Sciences*, *118*(21), e2100163118. https://doi.org/10.1073/pnas.2100163118

National Research Council. (2013). Abrupt impacts of climate change: Anticipating surprises. https://doi.org/10.17226/18373

Nepstad, D. C., Stickler, C. M., Soares-Filho, B., & Merry, F. (2008). Interactions among Amazon land use, forests and climate: Prospects for a near-term forest tipping point. *Philosophical Transactions of the Royal Society B: Biological Sciences*, *363*(1498), 1737–1746. https://doi.org/10.1098/rstb.2007.0036

Nepstad, D. C., Tohver, I. M., Ray, D., Moutinho, P., & Cardinot, G. (2007). Mortality of large trees and lianas following experimental drought in an Amazon forest. *Ecology*, *88*(9), 2259–2269. https://doi.org/10.1890/06-1046.1

Nepstad, D. C., Veríssimo, A., Alencar, A., Nobre, C., Lima, E., Lefebvre, P., et al. (1999). Large-scale impoverishment of Amazonian forests by logging and fire. *Nature*, *398*(6727), 505–508. https://doi.org/10.1038/19066

Neumann, R. B., Moorberg, C. J., Lundquist, J. D., Turner, J. C., Waldrop, M. P., McFarland, J. W., et al. (2019). Warming effects of spring rainfall increase methane emissions from thawing permafrost. *Geophysical Research Letters*, *46*(3), 1393–1401. https://doi.org/10.1029/2018GL081274

Nghiem, S. V., Rigor, I. G., Perovich, D. K., Clemente-Colón, P., Weatherly, J. W., & Neumann, G. (2007). Rapid reduction of Arctic perennial sea ice. *Geophysical Research Letters*, *34*(19), 1–6. https://doi.org/10.1029/2007GL031138

Nicholson, S. E., & Grist, J. P. (2001). A conceptual model for understanding rainfall variability in the West African Sahel on interannual and interdecadal timescales. *International Journal of Climatology*, *21*(14), 1733–1757. https://doi.org/10.1002/joc.648

Nielsen, S. B., Jochum, M., Pedro, J. B., Eden, C., & Nuterman, R. (2019). Two-timescale carbon cycle response to an AMOC collapse. *Paleoceanography and Paleoclimatology*, *34*(4), 511–523. https://doi.org/10.1029/2018PA003481

Nitzbon, J., Westermann, S., Langer, M., Martin, L. C. P., Strauss, J., Laboor, S., & Boike, J. (2020). Fast response of cold ice-rich permafrost in northeast Siberia to a warming climate. *Nature Communications*, *11*(1), 2201. https://doi.org/10.1038/s41467-020-15725-8

Niyogi, D., Kishtawal, C., Tripathi, S., & Govindaraju, R. S. (2010). Observational evidence that agricultural intensification and land use change may be reducing the Indian summer monsoon rainfall. *Water Resources Research*, *46*(3), W03533. https://doi.org/10.1029/2008WR007082

Nobre, C. A., & Borma, L. D. S. (2009). "Tipping points" for the Amazon forest. *Current Opinion in Environmental Sustainability*, *1*(1), 28–36. https://doi.org/10.1016/j.cosust.2009.07.003

Nobre, C. A., Sampaio, G., Borma, L. S., Castilla-Rubio, J. C., Silva, J. S., & Cardoso, M. (2016). Land-use and climate change risks in the amazon and the need of a novel sustainable development paradigm. *Proceedings of the National Academy of Sciences of the United States of America*, *113*(39), 10759–10768. https://doi.org/10.1073/pnas.1605516113

Nobre, C. A., Sellers, P. J., & Shukla, J. (1991). Amazonian deforestation and regional climate change. *Journal of Climate*, *4*(10), 957–988. https://doi.org/10.1175/1520-0442(1991)004<0957:adarcc>2.0.co;2

Notz, D. (2009). The future of ice sheets and sea ice: Between reversible retreat and unstoppable loss. *Proceedings of the National Academy of Sciences of the United States of America*, *106*(49), 20590–20595. https://doi.org/10.1073/pnas.0902356106

Notz, D., & Community, S. (2020). Arctic sea ice in CMIP6. *Geophysical Research Letters*, *47*(10), e2019GL086749. https://doi.org/10.1029/2019GL086749

Notz, D., & Marotzke, J. (2012). Observations reveal external driver for Arctic sea-ice retreat. *Geophysical Research Letters*, *39*(8). https://doi.org/10.1029/2012GL051094

Notz, D., & Stroeve, J. (2016). Observed Arctic sea-ice loss directly follows anthropogenic C_O2 emission. *Science*, *354*(6313), 747–750. https://doi.org/10.1126/science.aag2345

Notz, D., & Stroeve, J. (2018). The trajectory towards a seasonally ice-free Arctic Ocean. *Current Climate Change Reports*, 4(4), 407–416. https://doi.org/10.1007/s40641-018-0113-2

Numaguti, A. (1995). Characteristics of 4-to-20-day-period disturbances observed in the equatorial Pacific during the TOGA COARE IOP. *Journal of the Meteorological Society of Japan. Ser. II*, *73*(2B), 353–377. https://doi.org/10.2151/jmsj1965.73.2B_353

Olefeldt, D., Goswami, S., Grosse, G., Hayes, D., Hugelius, G., Kuhry, P., et al. (2016). Circumpolar distribution and carbon storage of thermokarst landscapes. *Nature Communications*, *7*(1), 13043. https://doi.org/10.1038/ncomms13043

Oliveira, L. J. C., Costa, M. H., Soares-Filho, B. S., & Coe, M. T. (2013). Large-scale expansion of agriculture in Amazonia may be a no-win scenario. *Environmental Research Letters*, *8*(2), 024021. https://doi.org/10.1088/1748-9326/8/2/024021

Onarheim, I. H., Eldevik, T., Smedsrud, L. H., & Stroeve, J. C. (2018). Seasonal and regional manifestation of Arctic sea ice loss. *Journal of Climate*, *31*(12), 4917–4932. https://doi.org/10.1175/JCLI-D-17-0427.1

O'Neill, B., van Aalst, M., Zaiton Ibrahim, Z., Berrang Ford, L., Bhadwal, S., Buhaug, H., et al. (2022). Chapter 16: Key risks across sectors and regions. In *Climate change 2022: Impacts, adaptation, and vulnerability. Contribution of Working Group II to the Sixth Assessment Report of the Intergovernmental Panel on Climate Change*. Cambridge University Press.

Oppenheimer, M., Glavovic, B., Hinkel, J., van de Wal, R., Magnan, A. K., Abd-Elgawad, A., et al. (2019). Sea level rise and implications for low lying islands, coasts and communities. In *IPCC Special Report on the Ocean and Cryosphere in a Changing Climate*. https://doi.org/10.1126/science.aam6284

Orr, J. C., Fabry, V. J., Aumont, O., Bopp, L., Doney, S. C., Feely, R. A., et al. (2005). Anthropogenic ocean acidification over the twenty-first century and its impact on calcifying organisms. *Nature*, *437*(7059), 681–686. https://doi.org/10.1038/nature04095

Overland, J. E., Wang, M., Walsh, J. E., Christensen, J. H., Kattsov, V. M., & Chapman, W. L. (2011). Chapter 3: Climate model projections for the Arctic. *Snow, Water, Ice and Permafrost in the Arctic (SWIPA): Climate Change and the Cryosphere* (pp. 37–54).

Palviainen, M., Laurén, A., Pumpanen, J., Bergeron, Y., Bond-Lamberty, B., Larjavaara, M., et al. (2020). Decadal-scale recovery of carbon stocks after wildfires throughout the boreal forests. *Global Biogeochemical Cycles*, *34*(8), e2020GB006612. https://doi.org/10.1029/2020GB006612

Pan, L., Powell, E. M., Latychev, K., Mitrovica, J. X., Creveling, J. R., Gomez, N., et al. (2021). Rapid postglacial rebound amplifies global sea level rise following West Antarctic Ice Sheet collapse. *Science Advances*, *7*(18), eabf7787. https://doi.org/10.1126/sciadv.abf7787

Pan, Y., Birdsey, R. A., Fang, J., Houghton, R., Kauppi, P. E., Kurz, W. A., et al. (2011). A large and persistent carbon sink in the world's forests. *Science*, *333*(6045), 988–993. https://doi.org/10.1126/science.1201609

Paolo, F. S., Fricker, H. A., & Padman, L. (2015). Volume loss from Antarctic ice shelves is accelerating. *Science*, *348*(6232), 327–331. https://doi.org/10.1126/science.aaa0940

Parsons, L. A. (2020). Implications of CMIP6 projected drying trends for 21st century Amazonian drought risk. *Earth's Future*, *8*(10), e2020EF001608. https://doi.org/10.1029/2020EF001608

Parsons, L. A., Yin, J., Overpeck, J. T., Stouffer, R. J., & Malyshev, S. (2014). Influence of the Atlantic Meridional Overturning Circulation on the monsoon rainfall and carbon balance of the American tropics. *Geophysical Research Letters*, *41*(1), 146–151. https://doi.org/10.1002/2013GL058454

Pascale, S., Carvalho, L. M. V., Adams, D. K., Castro, C. L., & Cavalcanti, I. F. A. (2019). Current and future variations of the monsoons of the Americas in a warming climate. *Current Climate Change Reports*, *5*(3), 125–144. https://doi.org/10.1007/s40641-019-00135-w

Pastick, N. J., Jorgenson, M. T., Goetz, S. J., Jones, B. M., Wylie, B. K., Minsley, B. J., et al. (2019). Spatiotemporal remote sensing of ecosystem change and causation across Alaska. *Global Change Biology*, *25*(3), 1171–1189. https://doi.org/10.1111/gcb.14279

Past Interglacials Working Group of PAGES. (2016). Interglacials of the last 800,000 years. *Reviews of Geophysics*, *54*(1), 162–219. https://doi.org/10.1002/2015RG000482

Pattyn, F., Ritz, C., Hanna, E., Asay-Davis, X., DeConto, R., Durand, G., et al. (2018). The Greenland and Antarctic ice sheets under 1.5°C global warming. *Nature Climate Change*, *8*(12), 1053–1061. https://doi.org/10.1038/s41558-018-0305-8

Paul, S., Ghosh, S., Oglesby, R., Pathak, A., Chandrasekharan, A., & Ramsankaran, R. (2016). Weakening of Indian summer monsoon rainfall due to changes in land use land cover. *Scientific Reports*, *6*(1), 32177. https://doi.org/10.1038/srep32177

Paull, C. K., Caress, D. W., Thomas, H., Lundsten, E., Anderson, K., Gwiazda, R., et al. (2015). Seafloor geomorphic manifestations of gas venting and shallow subbottom gas hydrate occurrences. *Geosphere*, *11*(2), 491–513. https://doi.org/10.1130/GES01012.1

Pausata, F. S. R., Battisti, D. S., Nisancioglu, K. H., & Bitz, C. M. (2011). Chinese stalagmite δ^{18}O controlled by changes in the Indian monsoon during a simulated Heinrich event. *Nature Geoscience*, *4*(7), 474–480. https://doi.org/10.1038/ngeo1169

Payne, A. J., Nowicki, S., Abe-Ouchi, A., Agosta, C., Alexander, P., Albrecht, T., et al. (2021). Future sea level change under coupled model intercomparison project phase 5 and phase 6 scenarios from the Greenland and Antarctic ice sheets. *Geophysical Research Letters*, *48*(16), e2020GL091741. https://doi.org/10.1029/2020GL091741

Pearson, R. G., Phillips, S. J., Loranty, M. M., Beck, P. S. A., Damoulas, T., Knight, S. J., & Goetz, S. J. (2013). Shifts in Arctic vegetation and associated feedbacks under climate change. *Nature Climate Change*, *3*(7), 673–677. https://doi.org/10.1038/nclimate1858

Perovich, D. K., Light, B., Eicken, H., Jones, K. F., Runciman, K., & Nghiem, S. V. (2007). Increasing solar heating of the Arctic Ocean and adjacent seas, 1979–2005: Attribution and role in the ice-albedo feedback. *Geophysical Research Letters*, *34*(19), L19505. https://doi.org/10.1029/2007GL031480

Perry, C. T., Alvarez-Filip, L., Graham, N. A. J., Mumby, P. J., Wilson, S. K., Kench, P. S., et al. (2018). Loss of coral reef growth capacity to track future increases in sea level. *Nature*, *558*(7710), 396–400. https://doi.org/10.1038/s41586-018-0194-z

Peters, G. P., Andrew, R. M., Canadell, J. G., Friedlingstein, P., Jackson, R. B., Korsbakken, J. I., et al. (2020). Carbon dioxide emissions continue to grow amidst slowly emerging climate policies. *Nature Climate Change*, *10*(1), 3–6. https://doi.org/10.1038/s41558-019-0659-6

Petrenko, V. V., Smith, A. M., Schaefer, H., Riedel, K., Brook, E., Baggenstos, D., et al. (2017). Minimal geological methane emissions during the Younger Dryas-Preboreal abrupt warming event. *Nature*, *548*(7668), 443–446. https://doi.org/10.1038/nature23316

Phillips, O. L., Aragão, L. E. O. C., Lewis, S. L., Fisher, J. B., Lloyd, J., López-González, G., et al. (2009). Drought sensitivity of the Amazon rainforest. *Science*, *323*(5919), 1344–1347. https://doi.org/10.1126/science.1164033

Phillips, O. L., van der Heijden, G., Lewis, S. L., López-González, G., Aragão, L. E. O. C., Lloyd, J., et al. (2010). Drought–mortality relationships for tropical forests. *New Phytologist*, *187*(3), 631–646. https://doi.org/10.1111/j.1469-8137.2010.03359.x

Piao, S., Wang, X., Park, T., Chen, C., Lian, X., He, Y., et al. (2020). Characteristics, drivers and feedbacks of global greening. *Nature Reviews Earth & Environment*, *1*, 14–27. https://doi.org/10.1038/s43017-019-0001-x

Pickart, R. S., & Spall, M. A. (2007). Impact of Labrador Sea convection on the North Atlantic meridional overturning circulation. *Journal of Physical Oceanography*, *37*(9), 2207–2227. https://doi.org/10.1175/JPO3178.1

Piñero, E., Marquardt, M., Hensen, C., Haeckel, M., & Wallmann, K. (2013). Estimation of the global inventory of methane hydrates in marine sediments using transfer functions. *Biogeosciences*, *10*(2), 959–975. https://doi.org/10.5194/bg-10-959-2013

Pistone, K., Eisenman, I., & Ramanathan, V. (2019). Radiative heating of an ice-free Arctic Ocean. *Geophysical Research Letters*, *46*(13), 7474–7480. https://doi.org/10.1029/2019GL082914

Plumb, R. A., & Hou, A. Y. (1992). The response of a zonally symmetric atmosphere to subtropical thermal forcing: Threshold behavior. *Journal of Atmospheric Sciences*, *49*(19), 1790–1799. https://doi.org/10.1175/1520-0469(1992)049<1790:TROAZS>2.0.CO;2

Pollard, D., DeConto, R. M., & Alley, R. B. (2015). Potential Antarctic Ice Sheet retreat driven by hydrofracturing and ice cliff failure. *Earth and Planetary Science Letters*, *412*, 112–121. https://doi.org/10.1016/j.epsl.2014.12.035

Pörtner, H.-O., Roberts, D. C., Adams, H., Adler, C., Aldunce, P., Ali, E., et al. (2022). Climate change 2022: Impacts, adaptation and vulnerability. *IPCC Sixth Assessment Report*. Retrieved from https://www.ipcc.ch/report/ar6/wg2/

Pueyo, S., de Alencastro Graça, P. M. L., Barbosa, R. I., Cots, R., Cardona, E., & Fearnside, P. M. (2010). Testing for criticality in ecosystem dynamics: The case of Amazonian rainforest and savanna fire. *Ecology Letters*, *13*(7), 793–802. https://doi.org/10.1111/j.1461-0248.2010.01497.x

Putnam, H. M. (2021). Avenues of reef-building coral acclimatization in response to rapid environmental change. *Journal of Experimental Biology*, *224*(Suppl_1), jeb239319. https://doi.org/10.1242/jeb.239319

Qin, Y., Xiao, X., Wigneron, J.-P., Ciais, P., Brandt, M., Fan, L., et al. (2021). Carbon loss from forest degradation exceeds that from deforestation in the Brazilian Amazon. *Nature Climate Change*, *11*(5), 442–448. https://doi.org/10.1038/s41558-021-01026-5

Raftery, A. E., Zimmer, A., Frierson, D. M. W., Startz, R., & Liu, P. (2017). Less than 2°C warming by 2100 unlikely. *Nature Climate Change*, *7*(9), 637–641. https://doi.org/10.1038/nclimate3352

Rahmstorf, S. (1996). On the freshwater forcing and transport of the Atlantic thermohaline circulation. *Climate Dynamics*, *12*(12), 799–811. https://doi.org/10.1007/s003820050144

Rahmstorf, S. (2002). Ocean circulation and climate during the past 120,000 years. *Nature*, *419*(6903), 207–214. https://doi.org/10.1038/nature01090

Rahmstorf, S., Box, J. E., Feulner, G., Mann, M. E., Robinson, A., Rutherford, S., & Schaffernicht, E. J. (2015). Exceptional twentieth-century slowdown in Atlantic Ocean overturning circulation. *Nature Climate Change*, *5*(5), 475–480. https://doi.org/10.1038/nclimate2554

Rahmstorf, S., & England, M. H. (1997). On the influence of Southern Hemisphere winds on North Atlantic deep water flow. *Journal of Physical Oceanography*, *26*(1988), 2040–2054. https://doi.org/10.1175/1520-0485(1997)027<2040:ioshwo>2.0.co;2

Ramanathan, V., Chung, C., Kim, D., Bettge, T., Buja, L., Kiehl, J. T., et al. (2005). Atmospheric brown clouds: Impacts on South Asian climate and hydrological cycle. *Proceedings of the National Academy of Sciences of the United States of America*, *102*(15), 5326–5333. https://doi.org/10.1073/pnas.0500656102

Ramaswamy, V., Boucher, O., Haigh, J., Hauglustaine, D., Haywood, J., Myhre, G., et al. (2001). Radiative forcing of climate change. In D. J. Griggs, M. Noguer, P. J. van Der Linden, X. Dai, K. Maskell, & C. A. Johnson (Eds.), *Climate change 2001: The scientific basis. Contribution of Working Group I to the Third Assessment Report of the Intergovernmental Panel on Climate Change* (Vol. 350, p. 416). Cambridge University Press.

Rammig, A., Jupp, T., Thonicke, K., Tietjen, B., Heinke, J., Lucht, W., et al. (2015). Estimating the risk of Amazonian forest dieback. *New Phytologist*, *187*(3), 694–706. https://doi.org/10.1111/j.1469-8137.2010.03318.x

Ranasinghe, R., Ruane, A. C., Vautard, R., Arnell, N., Coppola, E., Cruz, F. A., et al. (2021). Chapter 12: Climate change information for regional impact and for risk assessment. In *Climate Change 2021: The Physical Science Basis. Contribution of Working Group I to the Sixth Assessment Report of the Intergovernmental Panel on Climate Change* (pp. 351–364).

Randerson, J. T., Liu, H., Flanner, M. G., Chambers, S. D., Jin, Y., Hess, P. G., et al. (2006). The impact of boreal forest fire on climate warming. *Science*, *314*(5802), 1130–1132. https://doi.org/10.1126/science.1132075

Rantanen, M., Karpechko, A. Y., Lipponen, A., Nordling, K., Hyvärinen, O., Ruosteenoja, K., et al. (2022). The Arctic has warmed nearly four times faster than the globe since 1979. *Communications Earth & Environment*, *3*(1), 168. https://doi.org/10.1038/s43247-022-00498-3

Rasmussen, D. J., Buchanan, M. K., Kopp, R. E., & Oppenheimer, M. (2020). A flood damage allowance framework for coastal protection with deep uncertainty in sea level rise. *Earth's Future*, *8*(3), 1–16. https://doi.org/10.1029/2019EF001340

Reeburgh, W. S. (2007). Oceanic methane biogeochemistry. https://doi.org/10.1021/cr050362v

Rees, W. G., Hofgaard, A., Boudreau, S., Cairns, D. M., Harper, K., Mamet, S., et al. (2020). Is subarctic forest advance able to keep pace with climate change? *Global Change Biology*, *26*(7), 3965–3977. https://doi.org/10.1111/gcb.15113

Riahi, K., van Vuuren, D. P., Kriegler, E., Edmonds, J., O'Neill, B. C., Fujimori, S., et al. (2017). The Shared Socioeconomic Pathways and their energy, land use, and greenhouse gas emissions implications: An overview. *Global Environmental Change*, *42*, 153–168. https://doi.org/10.1016/j.gloenvcha.2016.05.009

Ridley, J. K., Lowe, J. A., & Hewitt, H. T. (2012). How reversible is sea ice loss? *Cryosphere*, *6*(1), 193–198. https://doi.org/10.5194/tc-6-193-2012

Rignot, E., Mouginot, J., Morlighem, M., Seroussi, H., & Scheuchl, B. (2014). Widespread, rapid grounding line retreat of Pine Island, Thwaites, Smith, and Kohler glaciers, west Antarctica, from 1992 to 2011. *Geophysical Research Letters*, *41*(10), 3502–3509. https://doi.org/10.1002/2014GL060140

Rignot, E., Mouginot, J., Scheuchl, B., van den Broeke, M., van Wessem, M. J., & Morlighem, M. (2019). Four decades of Antarctic Ice Sheet mass balance from 1979–2017. *Proceedings of the National Academy of Sciences*, *116*(4), 1095–1103. https://doi.org/10.1073/pnas.1812883116

Ritchie, P. D. L., Clarke, J. J., Cox, P. M., & Huntingford, C. (2021). Overshooting tipping point thresholds in a changing climate. *Nature*, *592*(7855), 517–523. https://doi.org/10.1038/s41586-021-03263-2

Ritson-Williams, R., & Gates, R. D. (2020). Coral community resilience to successive years of bleaching in Kāneʻohe Bay, Hawaiʻi. *Coral Reefs*, *39*(3), 757–769. https://doi.org/10.1007/s00338-020-01944-4

Rivkina, E., Laurinavichius, K., McGrath, J., Tiedje, J., Shcherbakova, V., & Gilichinsky, D. (2004). Microbial life in permafrost. *Advances in Space Research*, *33*(8), 1215–1221. https://doi.org/10.1016/j.asr.2003.06.024

Roberts, C. D., Waters, J., Peterson, K. A., Palmer, M. D., McCarthy, G. D., Frajka-Williams, E., et al. (2013). Atmosphere drives recent interannual variability of the Atlantic meridional overturning circulation at 26.5°N. *Geophysical Research Letters*, *40*(19), 5164–5170. https://doi.org/10.1002/grl.50930

Roberts, M. J., Jackson, L. C., Roberts, C. D., Meccia, V., Docquier, D., Koenigk, T., et al. (2020). Sensitivity of the Atlantic meridional overturning circulation to model resolution in CMIP6 HighResMIP simulations and implications for future changes. *Journal of Advances in Modeling Earth Systems*, *12*(8), e2019MS002014. https://doi.org/10.1029/2019MS002014

Robinson, A., Calov, R., & Ganopolski, A. (2012). Multistability and critical thresholds of the Greenland ice sheet. *Nature Climate Change*, *2*(6), 429–432. https://doi.org/10.1038/nclimate1449

Rocha, J. C., Peterson, G., Bodin, Ö., & Levin, S. (2018). Cascading regime shifts within and across scales. *Science*, *362*(6421), 1379–1383. https://doi.org/10.1126/science.aat7850

Rogers, B. M., Soja, A. J., Goulden, M. L., & Randerson, J. T. (2015). Influence of tree species on continental differences in boreal fires and climate feedbacks. *Nature Geoscience*, *8*(3), 228–234. https://doi.org/10.1038/ngeo2352

Rolph, R. J., Feltham, D. L., & Schröder, D. (2020). Changes of the Arctic marginal ice zone during the satellite era. *The Cryosphere*, *14*(6), 1971–1984. https://doi.org/10.5194/tc-14-1971-2020

Romanou, A., Marshall, J., Kelley, M., & Scott, J. (2017). Role of the ocean's AMOC in setting the uptake efficiency of transient tracers. *Geophysical Research Letters*, *44*(11), 5590–5598. https://doi.org/10.1002/2017GL072972

Romanovsky, V., Isaksen, K., Drozdov, D., Anisimov, O., Instanes, A., Leibman, M., et al. (2017). Changing permafrost and its impacts. In *Snow, water, ice and permafrost in the Arctic*. SWIPA.

Romanovsky, V. E., Smith, S. L., Shiklomanov, N. I., Streletskiy, D. A., Isaksen, K., Kholodov, A. L., et al. (2017). Terrestrial permafrost. In J. Blunden & D. Arndt (Eds.), *State of the Climate in 2016*. Bulletin of the American Meterological Society.

Rosenblum, E., Fajber, R., Stroeve, J. C., Gille, S. T., Tremblay, L. B., & Carmack, E. C. (2021). Surface salinity under transitioning ice cover in the Canada Basin: Climate model biases linked to vertical distribution of fresh water. *Geophysical Research Letters*, *48*(21), e2021GL094739. https://doi.org/10.1029/2021GL094739

Ross, N., Bingham, R. G., Corr, H. F. J., Ferraccioli, F., Jordan, T. A., Le Brocq, A., et al. (2012). Steep reverse bed slope at the grounding line of the Weddell Sea sector in West Antarctica. *Nature Geoscience*, *5*(6), 393–396. https://doi.org/10.1038/ngeo1468

Rotstayn, L. D., & Lohmann, U. (2002). Tropical rainfall trends and the indirect aerosol effect. *Journal of Climate*, *15*(15), 2103–2116. https://doi.org/10.1175/1520-0442(2002)015<2103:TRTATI>2.0.CO;2

Roxy, M. K., Ritika, K., Terray, P., Murtugudde, R., Ashok, K., & Goswami, B. N. (2015). Drying of Indian subcontinent by rapid Indian Ocean warming and a weakening land-sea thermal gradient. *Nature Communications*, *6*(1), 7423. https://doi.org/10.1038/ncomms8423

Rudy, A. C. A., Lamoureux, S. F., Kokelj, S. V., Smith, I. R., & England, J. H. (2017). Accelerating thermokarst transforms ice-cored terrain triggering a downstream cascade to the ocean. *Geophysical Research Letters*, *44*(21), 11080–11087. https://doi.org/10.1002/2017GL074912

Ruppel, C. D. (2011). Methane hydrates and contemporary climate change. *Nature Eduction Knowledge*, *2*(12).

Ruppel, C. D., & Kessler, J. D. (2017). The interaction of climate change and methane hydrates. *Reviews of Geophysics*, *55*(1), 126–168. https://doi.org/10.1002/2016RG000534

Ruppel, C. D., & Waite, W. F. (2020). Timescales and processes of methane hydrate formation and breakdown, with application to geologic systems. *Journal of Geophysical Research: Solid Earth*, *125*(8), e2018JB016459. https://doi.org/10.1029/2018JB016459

Ryan, J. C., Smith, L. C., Van As, D., Cooley, S. W., Cooper, M. G., Pitcher, L. H., & Hubbard, A. (2019). Greenland Ice Sheet surface melt amplified by snowline migration and bare ice exposure. *Science Advances*, *5*(3), eaav3738. https://doi.org/10.1126/sciadv.aav3738

Saatchi, S., Asefi-Najafabady, S., Malhi, Y., Aragão, L. E. O. C., Anderson, L. O., Myneni, R. B., & Nemani, R. (2013). Persistent effects of a severe drought on Amazonian forest canopy. *Proceedings of the National Academy of Sciences*, *110*(2), 565–570. https://doi.org/10.1073/pnas.1204651110

Saatchi, S. S., Harris, N. L., Brown, S., Lefsky, M., Mitchard, E. T. A., Salas, W., et al. (2011). Benchmark map of forest carbon stocks in tropical regions across three continents. *Proceedings of the National Academy of Sciences of the United States of America*, *108*(24), 9899–9904. https://doi.org/10.1073/pnas.1019576108

Saha, S., Chakraborty, D., Paul, R. K., Samanta, S., & Singh, S. B. (2018). Disparity in rainfall trend and patterns among different regions: Analysis of 158 years' time series of rainfall dataset across India. *Theoretical and Applied Climatology*, *134*(1), 381–395. https://doi.org/10.1007/s00704-017-2280-9

Salati, E., Dall'Olio, A., Matsui, E., & Gat, J. R. (1979). Recycling of water in the Amazon Basin: An isotopic study. *Water Resources Research*, *15*(5), 1250–1258. https://doi.org/10.1029/WR015i005p01250

Salati, E., & Vose, P. B. (1984). Amazon Basin: A system in equilibrium. *Science*, *225*(4658), 129–138. https://doi.org/10.1126/science.225.4658.129

Salazar, L. F., & Nobre, C. A. (2010). Climate change and thresholds of biome shifts in Amazonia. *Geophysical Research Letters*, *37*(17). https://doi.org/10.1029/2010GL043538

Sampe, T., & Xie, S.-P. (2010). Large-scale dynamics of the Meiyu-Baiu rainband: Environmental forcing by the westerly jet. *Journal of Climate*, *23*(1), 113–134. https://doi.org/10.1175/2009JCLI3128.1

Sassen, R., Joye, S., Sweet, S. T., Defreitas, D. A., Milkov, A. V., & MacDonald, I. R. (1999). Thermogenic gas hydrates and hydrocarbon gases in complex chemosynthetic communities, Gulf of Mexico continental slope. *Organic Geochemistry*, *30*(7), 485–497. https://doi.org/10.1016/S0146-6380(99)00050-9

Saunois, M., Bousquet, P., Poulter, B., Peregon, A., Ciais, P., Canadell, J. G., et al. (2016). The global methane budget 2000–2012. *Earth System Science Data*, *8*(2), 697–751. https://doi.org/10.5194/essd-8-697-2016

Saunois, M., Stavert, A. R., Poulter, B., Bousquet, P., Canadell, J. G., Jackson, R. B., et al. (2020). The global methane budget 2000–2017. *Earth System Science Data*, *12*(3), 1561–1623. https://doi.org/10.5194/essd-12-1561-2020

Sayedi, S. S., Abbott, B. W., Thornton, B. F., Frederick, J. M., Vonk, J. E., Overduin, P., et al. (2020). Subsea permafrost carbon stocks and climate change sensitivity estimated by expert assessment. *Environmental Research Letters*, *15*(12), 124075. https://doi.org/10.1088/1748-9326/abcc29

Schädel, C., Bader, M. K.-F., Schuur, E. A. G., Biasi, C., Bracho, R., Čapek, P., et al. (2016). Potential carbon emissions dominated by carbon dioxide from thawed permafrost soils. *Nature Climate Change*, *6*(10), 950–953. https://doi.org/10.1038/nclimate3054

Schaefer, K., Zhang, T., Bruhwiler, L., & Barrett, A. P. (2011). Amount and timing of permafrost carbon release in response to climate warming. *Tellus B: Chemical and Physical Meteorology*, *63*(2), 168–180. https://doi.org/10.1111/j.1600-0889.2010.00527.x

Schaphoff, S., Heyder, U., Ostberg, S., Gerten, D., Heinke, J., & Lucht, W. (2013). Contribution of permafrost soils to the global carbon budget. *Environmental Research Letters*, *8*(1), 014026. https://doi.org/10.1088/1748-9326/8/1/014026

Schaphoff, S., Reyer, C. P. O., Schepaschenko, D., Gerten, D., & Shvidenko, A. (2016). Tamm review: Observed and projected climate change impacts on Russia's forests and its carbon balance. *Forest Ecology and Management*, *361*, 432–444. https://doi.org/10.1016/j.foreco.2015.11.043

Scheffer, M., Carpenter, S., Lenton, T., Bascompte, J., Brock, W., Dakos, V., et al. (2012). Anticipating critical transitions. *Science*, *338*(6105), 344–348. https://doi.org/10.1126/science.1225244

Scheffer, M., Hirota, M., Holmgren, M., Van Nes, E. H., & Chapin, F. S. (2012). Thresholds for boreal biome transitions. *Proceedings of the National Academy of Sciences of the United States of America*, *109*(52), 21384–21389. https://doi.org/10.1073/pnas.1219844110

Schewe, J., Levermann, A., & Cheng, H. (2012). A critical humidity threshold for monsoon transitions. *Climate of the Past*, 8(2), 535–544. https://doi.org/10.5194/cp-8-535-2012

Schleussner, C. F., Frieler, K., Meinshausen, M., Yin, J., & Levermann, A. (2011). Emulating Atlantic overturning strength for low emission scenarios: Consequences for sea-level rise along the North American east coast. *Earth System Dynamics*, *2*(2), 191–200. https://doi.org/10.5194/esd-2-191-2011

Schleussner, C. F., Lissner, T. K., Fischer, E. M., Wohland, J., Perrette, M., Golly, A., et al. (2016). Differential climate impacts for policy-relevant limits to global warming: The case of 1.5°C and 2°C. *Earth System Dynamics*, *7*(2), 327–351. https://doi.org/10.5194/esd-7-327-2016

Schneider, T., Bischoff, T., & Haug, G. H. (2014). Migrations and dynamics of the intertropical convergence zone. *Nature*, *513*(7516), 45–53. https://doi.org/10.1038/nature13636

Schneider, T., Kaul, C. M., & Pressel, K. G. (2019). Possible climate transitions from breakup of stratocumulus decks under greenhouse warming. *Nature Geoscience*, *12*(3), 164–168. https://doi.org/10.1038/s41561-019-0310-1

Schneider, T., Kaul, C. M., & Pressel, K. G. (2020). Solar geoengineering may not prevent strong warming from direct effects of CO_2 on stratocumulus cloud cover. *Proceedings of the National Academy of Sciences*, *117*(48), 30179–30185. https://doi.org/10.1073/pnas.2003730117

Schneider Von Deimling, T., Grosse, G., Strauss, J., Schirrmeister, L., Morgenstern, A., Schaphoff, S., et al. (2015). Observation-based modelling of permafrost carbon fluxes with accounting for deep carbon deposits and thermokarst activity. *Biogeosciences*, *12*(11), 3469–3488. https://doi.org/10.5194/bg-12-3469-2015

Schneider von Deimling, T., Meinshausen, M., Levermann, A., Huber, V., Frieler, K., Lawrence, D. M., & Brovkin, V. (2012). Estimating the near-surface permafrost-carbon feedback on global warming. *Biogeosciences*, *9*(2), 649–665. https://doi.org/10.5194/bg-9-649-2012

Schoof, C. (2007). Ice sheet grounding line dynamics: Steady states, stability, and hysteresis. *Journal of Geophysical Research*, *112*(F3), F03S28. https://doi.org/10.1029/2006JF000664

Schulz, H., von Rad, U., Erlenkeuser, H., & von Rad, U. (1998). Correlation between Arabian Sea and Greenland climate oscillations of the past 110,000 years. *Nature*, *393*(6680), 54–57. https://doi.org/10.1038/31750

Schuur, E. A. G., & Abbott, B. (2011). Climate change: High risk of permafrost thaw. *Nature*, *480*(7375), 32–33. https://doi.org/10.1038/480032a

Schuur, E. A. G., McGuire, A. D., Romanovsky, C., Schädel, C., & Mack, M. (2018). Chapter 11: Arctic and boreal carbon. In N. Cavallaro, G. Shrestha, R. Birdsey, M. A. Mayes, R. G. Najjar, S. C. Reed, et al. (Eds.), *Second State of the Carbon Cycle Report (SOCCR2): A Sustained Assessment Report*. https://doi.org/10.7930/SOCCR2.2018.Ch11

Schuur, E. A. G., McGuire, A. D., Schädel, C., Grosse, G., Harden, J. W., Hayes, D. J., et al. (2015). Climate change and the permafrost carbon feedback. *Nature*, *520*(7546), 171–179. https://doi.org/10.1038/nature14338

Schwarber, A. K., Smith, S. J., Hartin, C. A., Vega-Westhoff, B. A., & Sriver, R. (2019). Evaluating climate emulation: Fundamental impulse testing of simple climate models. *Earth System Dynamics*, *10*(4), 729–739. https://doi.org/10.5194/esd-10-729-2019

Schwietzke, S., Sherwood, O. A., Bruhwiler, L. M. P., Miller, J. B., Etiope, G., Dlugokencky, E. J., et al. (2016). Upward revision of global fossil fuel methane emissions based on isotope database. *Nature*, *538*(7623), 88–91. https://doi.org/10.1038/nature19797

Screen, J. A., Deser, C., Simmonds, I., & Tomas, R. (2014). Atmospheric impacts of Arctic sea-ice loss, 1979–2009: Separating forced change from atmospheric internal variability. *Climate Dynamics*, *43*(1–2), 333–344. https://doi.org/10.1007/s00382-013-1830-9

Screen, J. A., & Simmonds, I. (2010). The central role of diminishing sea ice in recent Arctic temperature amplification. *Nature*, *464*(7293), 1334–1337. https://doi.org/10.1038/nature09051

Seidl, R., Honkaniemi, J., Aakala, T., Aleinikov, A., Angelstam, P., Bouchard, M., et al. (2020). Globally consistent climate sensitivity of natural disturbances across boreal and temperate forest ecosystems. *Ecography*, *43*(7), 967–978. https://doi.org/10.1111/ecog.04995

Seneca Lindsey, D., & Dupont, T. K. (2012). Mechanical effect of mélange-induced buttressing on embayment-terminating glacier dynamics. *The Cryosphere Discussions*, *6*(5), 4123–4136. https://doi.org/10.5194/tcd-6-4123-2012

Sergienko, O. V., & Wingham, D. J. (2019). Grounding line stability in a regime of low driving and basal stresses. *Journal of Glaciology*, *65*(253), 833–849. https://doi.org/10.1017/jog.2019.53

Sergienko, O. V., & Wingham, D. J. (2022). Bed topography and marine ice-sheet stability. *Journal of Glaciology*, *68*(267), 124–138. https://doi.org/10.1017/jog.2021.79

Seroussi, H., Nowicki, S., Payne, A., Goelzer, H., Lipscomb, W., Abe Ouchi, A., et al. (2020). ISMIP6 Antarctica: A multi-model ensemble of the Antarctic ice sheet evolution over the 21st century. *The Cryosphere Discussions*, 1–54. https://doi.org/10.5194/tc-2019-324

Serreze, M. C., Barrett, A. P., Stroeve, J. C., Kindig, D. N., & Holland, M. M. (2009). The emergence of surface-based Arctic amplification. *Cryosphere*, *3*(1), 11–19. https://doi.org/10.5194/tc-3-11-2009

Seshadri, A. K. (2017). Energetics and monsoon bifurcations. *Climate Dynamics*, *48*(1), 561–576. https://doi.org/10.1007/s00382-016-3094-7

Shakhova, N., Semiletov, I., Leifer, I., Sergienko, V., Salyuk, A., Kosmach, D., et al. (2014). Ebullition and storm-induced methane release from the East Siberian Arctic Shelf. *Nature Geoscience*, *7*(1), 64–70. https://doi.org/10.1038/ngeo2007

Shanahan, T. M., McKay, N. P., Hughen, K. A., Overpeck, J. T., Otto-Bliesner, B., Heil, C. W., et al. (2015). The time-transgressive termination of the African Humid Period. *Nature Geoscience*, *8*(2), 140–144. https://doi.org/10.1038/ngeo2329

Shaw, R., Luo, Y., Cheong, T., Abdul Halim, S., Chaturvedi, S., Hashizume, M., et al. (2022). Chapter 10: Asia. In *Climate change 2022: Impacts, adaptation, and vulnerability. Contribution of Working Group II to the Sixth Assessment Report of the Intergovernmental Panel on Climate Change*. Cambridge University Press.

Shen, Z., Duan, A., Li, D., & Li, J. (2021). Assessment and ranking of climate models in Arctic sea ice cover simulation: From CMIP5 to CMIP6. *Journal of Climate*, *34*(9), 3609–3627. https://doi.org/10.1175/JCLI-D-20-0294.1

Shepherd, A., Wingham, D., & Rignot, E. (2004). Warm ocean is eroding West Antarctic ice sheet. *Geophysical Research Letters*, *31*(23), L23402. https://doi.org/10.1029/2004GL021106

Sherriff, R. L., Berg, E. E., & Miller, A. E. (2011). Climate variability and spruce beetle (*Dendroctonus rufipennis*) outbreaks in south-central and southwest Alaska. *Ecology*, *92*(7), 1459–1470. https://doi.org/10.1890/10-1118.1

Sherwood, S. C., Webb, M. J., Annan, J. D., Armour, K. C., Forster, P. M., Hargreaves, J. C., et al. (2020). An assessment of Earth's climate sensitivity using multiple lines of evidence. *Reviews of Geophysics*, *58*(4), e2019RG000678. https://doi.org/10.1029/2019RG000678

Shugart, H. H., Asner, G. P., Fischer, R., Huth, A., Knapp, N., Le Toan, T., & Shuman, J. K. (2015). Computer and remote-sensing infrastructure to enhance large-scale testing of individual-based forest models. *Frontiers in Ecology and the Environment*, *13*(9), 503–511. https://doi.org/10.1890/140327

Shukla, S. P., Puma, M. J., & Cook, B. I. (2014). The response of the South Asian Summer Monsoon circulation to intensified irrigation in global climate model simulations. *Climate Dynamics*, *42*(1), 21–36. https://doi.org/10.1007/s00382-013-1786-9

Shuman, J. K., Foster, A. C., Shugart, H. H., Hoffman-Hall, A., Krylov, A., Loboda, T., et al. (2017). Fire disturbance and climate change: Implications for Russian forests. *Environmental Research Letters*, *12*(3), 035003. https://doi.org/10.1088/1748-9326/aa5eed

Shuman, J. K., Tchebakova, N. M., Parfenova, E. I., Soja, A. J., Shugart, H. H., Ershov, D., & Holcomb, K. (2015). Forest forecasting with vegetation models across Russia. *Canadian Journal of Forest Research*, *45*(2), 175–184. https://doi.org/10.1139/cjfr-2014-0138

Shur, Y. L., & Jorgenson, M. T. (2007). Patterns of permafrost formation and degradation in relation to climate and ecosystems. *Permafrost and Periglacial Processes*, *18*(1), 7–19. https://doi.org/10.1002/ppp.582

Shvidenko, A. Z., Shchepashchenko, D. G., Vaganov, E. A., Sukhinin, A. I., Maksyutov, S. S., McCallum, I., & Lakyda, I. P. (2011). Impact of wildfire in Russia between 1998–2010 on ecosystems and the global carbon budget. *Doklady Earth Sciences*, *441*(2), 1678–1682. https://doi.org/10.1134/S1028334X11120075

Silbiger, N. J., Guadayol, Ò., Thomas, F. I. M., & Donahue, M. J. (2014). Reefs shift from net accretion to net erosion along a natural environmental gradient. *Marine Ecology Progress Series*, *515*, 33–44. https://doi.org/10.3354/meps10999

Silva, C. V. J., Aragão, L. E. O. C., Young, P. J., Espirito-Santo, F., Berenguer, E., Anderson, L. O., et al. (2020). Estimating the multi-decadal carbon deficit of burned Amazonian forests. *Environmental Research Letters*, *15*(11), 114023. https://doi.org/10.1088/1748-9326/abb62c

Silva Junior, C. H. L., Anderson, L. O., Silva, A. L., Almeida, C. T., Dalagnol, R., Pletsch, M. A. J. S., et al. (2019). Fire responses to the 2010 and 2015/2016 Amazonian droughts. *Frontiers in Earth Science*, *7*, 97. https://doi.org/10.3389/feart.2019.00097

Silva Junior, C. H. L., Aragão, L. E. O. C., Anderson, L. O., Fonseca, M. G., Shimabukuro, Y. E., Vancutsem, C., et al. (2020). Persistent collapse of biomass in Amazonian forest edges following deforestation leads to unaccounted carbon losses. *Science Advances*, *6*(40), eaaz8360. https://doi.org/10.1126/sciadv.aaz8360

Silva Junior, C. H. L., Pessôa, A. C. M., Carvalho, N. S., Reis, J. B. C., Anderson, L. O., & Aragão, L. E. O. C. (2021). The Brazilian Amazon deforestation rate in 2020 is the greatest of the decade. *Nature Ecology & Evolution*, *5*(2), 144–145. https://doi.org/10.1038/s41559-020-01368-x

Silvano, A., Rintoul, S. R., & Herraiz-Borreguero, L. (2016). Ocean-ice shelf interaction in East Antarctica. *Oceanography*, *29*(4), 130–143. https://doi.org/10.5670/oceanog.2016.105

Singh, D., Ghosh, S., Roxy, M. K., & McDermid, S. (2019). Indian summer monsoon: Extreme events, historical changes, and role of anthropogenic forcings. *Wiley Interdisciplinary Reviews: Climate Change*, *10*(2), 1–35. https://doi.org/10.1002/wcc.571

Singh, D., Tsiang, M., Rajaratnam, B., & Diffenbaugh, N. S. (2014). Observed changes in extreme wet and dry spells during the South Asian summer monsoon season. *Nature Climate Change*, *4*(6), 456–461. https://doi.org/10.1038/nclimate2208

Skarke, A., Ruppel, C., Kodis, M., Brothers, D., & Lobecker, E. (2014). Widespread methane leakage from the sea floor on the northern US Atlantic margin. *Nature Geoscience*, *7*(9), 657–661. https://doi.org/10.1038/ngeo2232

Slater, D. A., Felikson, D., Straneo, F., Goelzer, H., Little, C. M., Morlighem, M., et al. (2020). Twenty-first century ocean forcing of the Greenland ice sheet for modelling of sea level contribution. *The Cryosphere*, *14*(3), 985–1008. https://doi.org/10.5194/tc-14-985-2020

Slater, T., Hogg, A. E., & Mottram, R. (2020). Ice-sheet losses track high-end sea-level rise projections. *Nature Climate Change*, *10*(10), 879–881. https://doi.org/10.1038/s41558-020-0893-y

Smith, B., Fricker, H. A., Gardner, A. S., Medley, B., Nilsson, J., Paolo, F. S., et al. (2020). Pervasive ice sheet mass loss reflects competing ocean and atmosphere processes. *Science*, *368*(6496), 1239–1242. https://doi.org/10.1126/science.aaz5845

Smith, C., Forster, P., Allen, M., Leach, N., Millar, R., Passerello, G., & Regayre, L. (2017). FAIR v1.1: A simple emissions-based impulse response and carbon cycle model. *Geoscientific Model Development Discussions*, 1–45. https://doi.org/10.5194/gmd-2017-266

Smith, C. J., Forster, P. M., Allen, M., Leach, N., Millar, R. J., Passerello, G. A., & Regayre, L. A. (2018). FAIR v1.3: A simple emissions-based impulse response and carbon cycle model. *Geoscientific Model Development*, *11*(6), 2273–2297. https://doi.org/10.5194/gmd-11-2273-2018

Smith, C. J., Kramer, R. J., Myhre, G., Alterskjær, K., Collins, W., Sima, A., et al. (2020). Effective radiative forcing and adjustments in CMIP6 models. *Atmospheric Chemistry and Physics*, *20*(16), 9591–9618. https://doi.org/10.5194/acp-20-9591-2020

Smith, S. L., O'Neill, H. B., Isaksen, K., Noetzli, J., & Romanovsky, V. E. (2022). The changing thermal state of permafrost. *Nature Reviews Earth & Environment*, *3*(1), 10–23. https://doi.org/10.1038/s43017-021-00240-1

Soja, A. J., Tchebakova, N. M., French, N. H. F., Flannigan, M. D., Shugart, H. H., Stocks, B. J., et al. (2007). Climate-induced boreal forest change: Predictions versus current observations. *Global and Planetary Change*, *56*(3–4), 274–296. https://doi.org/10.1016/j.gloplacha.2006.07.028

Solomon, S., Plattner, G. K., Knutti, R., & Friedlingstein, P. (2009). Irreversible climate change due to carbon dioxide emissions. *Proceedings of the National Academy of Sciences of the United States of America*, *106*(6), 1704–1709. https://doi.org/10.1073/pnas.0812721106

Spalding, M., Burke, L., Wood, S. A., Ashpole, J., Hutchison, J., & zu Ermgassen, P. (2017). Mapping the global value and distribution of coral reef tourism. *Marine Policy*, *82*, 104–113. https://doi.org/10.1016/j.marpol.2017.05.014

Spalding, M. D., & Brown, B. E. (2015). Warm-water coral reefs and climate change. *Science*, *350*(6262), 769–771. https://doi.org/10.1126/science.aad0349

Sparrow, K., Kessler, J., Southon, J., Garcia-Tigreros, F., Schreiner, K., Ruppel, C., et al. (2022). Limited contribution of ancient methane to surface waters of the U.S. Beaufort Sea shelf. *Science Advances*, *4*(1), eaao4842. https://doi.org/10.1126/sciadv.aao4842

Sparrow, K. J., Kessler, J. D., Southon, J. R., Garcia-Tigreros, F., Schreiner, K. M., Ruppel, C. D., et al. (2018). Limited contribution of ancient methane to surface waters of the U.S. Beaufort Sea shelf. *Science Advances*, *4*(1), eaao4842. https://doi.org/10.1126/sciadv.aao4842

Spracklen, D. V., Arnold, S. R., & Taylor, C. M. (2012). Observations of increased tropical rainfall preceded by air passage over forests. *Nature*, *489*(7415), 282–285. https://doi.org/10.1038/nature11390

Srokosz, M. A., & Bryden, H. L. (2015). Observing the Atlantic Meridional Overturning Circulation yields a decade of inevitable surprises. *Science*, *348*(6241), 1255575. https://doi.org/10.1126/science.1255575

Staal, A., Fetzer, I., Wang-Erlandsson, L., Bosmans, J. H. C., Dekker, S. C., van Nes, E. H., et al. (2020). Hysteresis of tropical forests in the 21st century. *Nature Communications*, *11*(1), 4978. https://doi.org/10.1038/s41467-020-18728-7

Staal, A., Flores, B. M., Aguiar, A. P. D., Bosmans, J. H. C., Fetzer, I., & Tuinenburg, O. A. (2020). Feedback between drought and deforestation in the Amazon. *Environmental Research Letters*, *15*(4), 044024. https://doi.org/10.1088/1748-9326/ab738e

Steffen, W., Rockström, J., Richardson, K., Lenton, T. M., Folke, C., Liverman, D., et al. (2018). Trajectories of the Earth System in the Anthropocene. *Proceedings of the National Academy of Sciences of the United States of America*, *115*(33), 8252–8259. https://doi.org/10.1073/pnas.1810141115

Steneck, R. S., Arnold, S. N., Boenish, R., de León, R., Mumby, P. J., Rasher, D. B., & Wilson, M. W. (2019). Managing recovery resilience in coral reefs against climate-induced bleaching and hurricanes: A 15 year case study from Bonaire, Dutch Caribbean. *Frontiers in Marine Science*, *6*, 265. https://doi.org/10.3389/fmars.2019.00265

Stickler, C. M., Coe, M. T., Costa, M. H., Nepstad, D. C., McGrath, D. G., Dias, L. C. P., et al. (2013). Dependence of hydropower energy generation on forests in the Amazon Basin at local and regional scales. *Proceedings of the National Academy of Sciences of the United States of America*, *110*(23), 9601–9606. https://doi.org/10.1073/pnas.1215331110

Stocker, T. F. (2000). Past and future reorganizations in the climate system. *Quaternary Science Review*s, *19*(1), 301–319. https://doi.org/10.1016/S0277-3791(99)00067-0

Stocker, T. F. (2013). Chapter 1—The ocean as a component of the climate system. In G. Siedler, S. M. Griffies, J. Gould, & J. A. B. T.-I. G. Church (Eds.), *Ocean circulation and climate* (Vol. 103, pp. 3–30). https://doi.org/10.1016/B978-0-12-391851-2.00001-5

Stocker, T. F., & Schmittner, A. (1997). Influence of CO_2 emission rates on the stability of the thermohaline circulation. *Nature*, *388*(6645), 862–865. https://doi.org/10.1038/42224

Stocker, T. F., & Wright, D. G. (1991). Rapid transitions of the ocean's deep circulation induced by changes in surface water fluxes. *Nature*, *351*(6329), 729–732. https://doi.org/10.1038/351729a0

Stommel, H. (1961). Thermohaline convection with two stable regimes of flow. *Tellu*s, *13*(2), 224–230. https://doi.org/10.1111/j.2153-3490.1961.tb00079.x

Storlazzi, C. D., Reguero, B. G., Cole, A. D., Lowe, E., Shope, J. B., Gibbs, A. E., et al. (2019). Rigorously valuing the role of U.S. coral reefs in coastal hazard risk reduction. In *Open-File Report*. https://doi.org/10.3133/ofr20191027

Stralberg, D., Arseneault, D., Baltzer, J. L., Barber, Q. E., Bayne, E. M., Boulanger, Y., et al. (2020). Climate-change refugia in boreal North America: What, where, and for how long? *Frontiers in Ecology and the Environment*, *18*(5), 261–270. https://doi.org/10.1002/fee.2188

Stroeve, J., Barrett, A., Serreze, M., & Schweiger, A. (2014). Using records from submarine, aircraft and satellites to evaluate climate model simulations of Arctic sea ice thickness. *Cryosphere*, *8*(5), 1839–1854. https://doi.org/10.5194/tc-8-1839-2014

Stroeve, J., Holland, M. M., Meier, W., Scambos, T., & Serreze, M. (2007). Arctic sea ice decline: Faster than forecast. *Geophysical Research Letters*, *34*(9), L09501. https://doi.org/10.1029/2007GL029703

Stroeve, J., Liston, G. E., Buzzard, S., Zhou, L., Mallett, R., Barrett, A., et al. (2020). A Lagrangian snow evolution system for sea ice applications (SnowModel-LG): Part II—Analyses. *Journal of Geophysical Research: Oceans*, *125*(10), e2019JC015900. https://doi.org/10.1029/2019JC015900

Stroeve, J., & Notz, D. (2018). Changing state of Arctic sea ice across all seasons. *Environmental Research Letters*, *13*(10), 103001. https://doi.org/10.1088/1748-9326/aade56

Stroeve, J. C., Kattsov, V., Barrett, A., Serreze, M., Pavlova, T., Holland, M., & Meier, W. N. (2012). Trends in Arctic sea ice extent from CMIP5, CMIP3 and observations. *Geophysical Research Letters*, *39*(16), 1–7. https://doi.org/10.1029/2012GL052676

Stroeve, J. C., Serreze, M. C., Holland, M. M., Kay, J. E., Malanik, J., & Barrett, A. P. (2012). The Arctic's rapidly shrinking sea ice cover: A research synthesis. *Climatic Change*, *110*(3–4), 1005–1027. https://doi.org/10.1007/s10584-011-0101-1

Sturm, M., & Massom, R. A. (2016). Snow in the sea ice system: Friend or foe? In *Sea ice* (3rd ed.). https://doi.org/10.1002/9781118778371.ch3

Sully, S., Burkepile, D. E., Donovan, M. K., Hodgson, G., & van Woesik, R. (2019). A global analysis of coral bleaching over the past two decades. *Nature Communications*, *10*(1), 1264. https://doi.org/10.1038/s41467-019-09238-2

Sultan, B., & Janicot, S. (2003). The West African monsoon dynamics. Part II: The "preonset" and "onset" of the summer monsoon. *Journal of Climate*, *16*(21), 3407–3427. https://doi.org/10.1175/1520-0442(2003)016<3407:TWAMDP>2.0.CO;2

Sun, S., Pattyn, F., Simon, E. G., Albrecht, T., Cornford, S., Calov, R., et al. (2020). Antarctic ice sheet response to sudden and sustained ice-shelf collapse (ABUMIP). *Journal of Glaciology*, *66*(260), 891–904. https://doi.org/10.1017/jog.2020.67

Takahashi, T., Sutherland, S. C., Wanninkhof, R., Sweeney, C., Feely, R. A., Chipman, D. W., et al. (2009). Climatological mean and decadal change in surface ocean pCO₂, and net sea–air CO₂ flux over the global oceans. *Deep Sea Research Part II: Topical Studies in Oceanography*, *56*(8), 554–577. https://doi.org/10.1016/j.dsr2.2008.12.009

Takemura, T., Nozawa, T., Emori, S., Nakajima, T. Y., & Nakajima, T. (2005). Simulation of climate response to aerosol direct and indirect effects with aerosol transport-radiation model. *Journal of Geophysical Research*, *110*(D2), D02202. https://doi.org/10.1029/2004JD005029

Talento, S., & Ganopolski, A. (2021). Reduced-complexity model for the impact of anthropogenic CO₂ emissions on future glacial cycles. *Earth System Dynamics*, *12*(4), 1275–1293. https://doi.org/10.5194/esd-12-1275-2021

Tan, Z., Schneider, T., Teixeira, J., & Pressel, K. G. (2017). Large-eddy simulation of subtropical cloud-topped boundary layers: 2. Cloud response to climate change. *Journal of Advances in Modeling Earth Systems*, *9*(1), 19–38. https://doi.org/10.1002/2016MS000804

Tape, K., Sturm, M., & Racine, C. (2006). The evidence for shrub expansion in Northern Alaska and the Pan-Arctic. *Global Change Biology*, *12*(4), 686–702. https://doi.org/10.1111/j.1365-2486.2006.01128.x

Taylor, C. M., Belušić, D., Guichard, F., Parker, D. J., Vischel, T., Bock, O., et al. (2017). Frequency of extreme Sahelian storms tripled since 1982 in satellite observations. *Nature*, *544*(7651), 475–478. https://doi.org/10.1038/nature22069

The IMBIE Team. (2018). Mass balance of the Antarctic ice sheet from 1992 to 2017. *Nature*, *558*(7709), 219–222. https://doi.org/10.1098/rsta.2006.1792

The IMBIE Team. (2020). Mass balance of the Greenland ice sheet from 1992 to 2018. *Nature*, *579*(7798), 233–239. https://doi.org/10.1038/s41586-019-1855-2

Thomas, Z. A., Jones, R. T., Turney, C. S. M., Golledge, N., Fogwill, C., Bradshaw, C. J. A., et al. (2020). Tipping elements and amplified polar warming during the Last Interglacial. *Quaternary Science Reviews*, *233*, 106222. https://doi.org/10.1016/j.quascirev.2020.106222

Thomas, R. H., & Bentley, C. R. (1978). A model for Holocene retreat of the West Antarctic ice sheet. *Quaternary Research*, *10*(2), 150–170. https://doi.org/10.1016/0033-5894(78)90098-4

Thornalley, D. J. R., Oppo, D. W., Ortega, P., Robson, J. I., Brierley, C. M., Davis, R., et al. (2018). Anomalously weak Labrador Sea convection and Atlantic overturning during the past 150 years. *Nature*, *556*(7700), 227–230. https://doi.org/10.1038/s41586-018-0007-4

Thornton, B. F., Geibel, M. C., Crill, P. M., Humborg, C., & Mörth, C.-M. (2016). Methane fluxes from the sea to the atmosphere across the Siberian shelf seas. *Geophysical Research Letters*, *43*(11), 5869–5877. https://doi.org/10.1002/2016GL068977

Thornton, B. F., Prytherch, J., Andersson, K., Brooks, I. M., Salisbury, D., Tjernström, M., & Crill, P. M. (2020). Shipborne eddy covariance observations of methane fluxes constrain Arctic sea emissions. *Science Advances*, *6*(5), eaay7934. https://doi.org/10.1126/sciadv.aay7934

Tietsche, S., Notz, D., Jungclaus, J. H., & Marotzke, J. (2011). Recovery mechanisms of Arctic summer sea ice. *Geophysical Research Letters*, *38*(2), L02707. https://doi.org/10.1029/2010GL045698

Timmermans, M.-L., Ladd, C., & Wood, K. (2017). Sea surface temperatue. In J. Richter-Menge, J. E. Overland, J. T. Mathis, & E. Osborne (Eds.), *Arctic Report Card 2017*.

Tohjima, Y., Zeng, J., Shirai, T., Niwa, Y., Ishidoya, S., Taketani, F., et al. (2020). Estimation of CH₄ emissions from the East Siberian Arctic Shelf based on atmospheric observations aboard the R/V Mirai during fall cruises from 2012 to 2017. *Polar Science*, *27*, 100571. https://doi.org/10.1016/j.polar.2020.100571

Topál, D., Ding, Q., Mitchell, J., Baxter, I., Herein, M., Haszpra, T., et al. (2020). An internal atmospheric process determining summertime Arctic sea ice melting in the next three decades: Lessons learned from five large ensembles and multiple CMIP5 climate simulations. *Journal of Climate*, *33*(17), 7431–7454. https://doi.org/10.1175/JCLI-D-19-0803.1

Trenberth, K. E., Stepaniak, D. P., & Caron, J. M. (2000). The global monsoon as seen through the divergent atmospheric circulation. *Journal of Climate*, *13*(22), 3969–3993. https://doi.org/10.1175/1520-0442(2000)013<3969:TGMAST>2.0.CO;2

Trisos, C., Adelekan, I., Totin, E., Ayanlade, A., Efitre, J., Gemeda, A., et al. (2022). Chapter 9: Africa. In *Climate change 2022: Impacts, adaptation, and vulnerability. Contribution of Working Group II to the Sixth Assessment Report of the Intergovernmental Panel on Climate Change*. Retrieved from https://www.ipcc.ch/report/ar6/wg2/

Turetsky, M. R., Abbott, B., Jones, M., Walter Anthony, K. M., Olefeldt, D., Schuur, E. A. G., et al. (2020). Carbon release through abrupt permafrost thaw. *Nature Geoscience*, *13*(2), 138–143. https://doi.org/10.1038/s41561-019-0526-0

Turetsky, M. R., Jones, M. C., Walter Anthony, K., Olefeldt, D., Schuur, E. A. G., Koven, C., et al. (2019). Permafrost collapse is accelerating carbon release. *Nature*, *569*(7754), 32–24. https://doi.org/10.1038/d41586-019-01313-4

Turner, A. G., & Annamalai, H. (2012). Climate change and the South Asian summer monsoon. *Nature Climate Change*, 2(8), 587–595. https://doi.org/10.1038/nclimate1495

Turner, M. G., Calder, W. J., Cumming, G. S., Hughes, T. P., Jentsch, A., LaDeau, S. L., et al. (2020). Climate change, ecosystems and abrupt change: Science priorities. *Philosophical Transactions of the Royal Society B: Biological Sciences*, *375*(1794), 20190105. https://doi.org/10.1098/rstb.2019.0105

Ulfsbo, A., Cassar, N., Korhonen, M., van Heuven, S., Hoppema, M., Kattner, G., & Anderson, L. G. (2014). Late summer net community production in the central Arctic Ocean using multiple approaches. *Global Biogeochemical Cycles*, *28*(10), 1129–1148. https://doi.org/10.1002/2014GB004833

US Forest Service. (2019). Forest health conditions in Alaska—2019. Retrieved from http://forestry.alaska.gov/pdfs/2003_fhp_CONDRPT_web_final.pdf

Valentine, D. L., Blanton, D. C., Reeburgh, W. S., & Kastner, M. (2001). Water column methane oxidation adjacent to an area of active hydrate dissociation, Eel River Basin. *Geochimica et Cosmochimica Acta*, *65*(16), 2633–2640. https://doi.org/10.1016/S0016-7037(01)00625-1

van den Broeke, M. R., Enderlin, E. M., Howat, I. M., Kuipers Munneke, P., Noël, B. P. Y., van de Berg, W. J., et al. (2016). On the recent contribution of the Greenland ice sheet to sea level change. *The Cryosphere*, *10*(5), 1933–1946. https://doi.org/10.5194/tc-10-1933-2016

van der Zande, R. M., Achlatis, M., Bender-Champ, D., Kubicek, A., Dove, S., & Hoegh-Guldberg, O. (2020). Paradise lost: End-of-century warming and acidification under business-as-usual emissions have severe consequences for symbiotic corals. *Global Change Biology*, *26*(4), 2203–2219. https://doi.org/10.1111/gcb.14998

Vavrus, S. J., Holland, M. M., Jahn, A., Bailey, D. A., & Blazey, B. A. (2012). Twenty-first-century Arctic climate change in CCSM4. *Journal of Climate*, *25*(8), 2696–2710. https://doi.org/10.1175/JCLI-D-11-00220.1

Velicogna, I., Sutterley, T. C., & Van Den Broeke, M. R. (2014). Regional acceleration in ice mass loss from Greenland and Antarctica using GRACE time-variable gravity data. *Geophysical Research Letters*, *41*(22), 8130–8137. https://doi.org/10.1002/2014GL061052

Veraverbeke, S., Rogers, B. M., Goulden, M. L., Jandt, R. R., Miller, C. E., Wiggins, E. B., & Randerson, J. T. (2017). Lightning as a major driver of recent large fire years in North American boreal forests. *Nature Climate Change*, *7*(7), 529–534. https://doi.org/10.1038/nclimate3329

Veron, J. E. N., Hoegh-Guldberg, O., Lenton, T. M., Lough, J. M., Obura, D. O., Pearce-Kelly, P., et al. (2009). The coral reef crisis: The critical importance of <350 ppm CO₂. *Marine Pollution Bulletin*, *58*(10), 1428–1436. https://doi.org/10.1016/j.marpolbul.2009.09.009

Victoria, R. L., Martinelli, L. A., Moraes, J. M., Ballester, M. V., Krusche, A. V., Pellegrino, G., et al. (1998). Surface air temperature variations in the amazon region and its borders during this century. *Journal of Climate*, *11*(5), 1105–1110. https://doi.org/10.1175/1520-0442(1998)011<1105:satvit>2.0.co;2

Voigt, C., Marushchak, M. E., Abbott, B. W., Biasi, C., Elberling, B., Siciliano, S. D., et al. (2020). Nitrous oxide emissions from permafrost-affected soils. *Nature Reviews Earth & Environment*, *1*(8), 420–434. https://doi.org/10.1038/s43017-020-0063-9

Vonk, J. E., Mann, P. J., Davydov, S., Davydova, A., Spencer, R. G. M., Schade, J., et al. (2013). High biolability of ancient permafrost carbon upon thaw. *Geophysical Research Letters*, *40*(11), 2689–2693. https://doi.org/10.1002/grl.50348

Wadhams, P. (2012). Arctic ice cover, ice thickness and tipping points. *Ambio*, *41*(1), 23–33. https://doi.org/10.1007/s13280-011-0222-9

Wagner, F. H., Hérault, B., Bonal, D., Stahl, C., Anderson, L. O., Baker, T. R., et al. (2016). Climate seasonality limits leaf carbon assimilation and wood productivity in tropical forests. *Biogeosciences*, *13*(8), 2537–2562. https://doi.org/10.5194/bg-13-2537-2016

Wagner, F. H., Hérault, B., Rossi, V., Hilker, T., Maeda, E. E., Sanchez, A., et al. (2017). Climate drivers of the Amazon forest greening. *PLoS One*, *12*(7), e0180932. https://doi.org/10.1371/journal.pone.0180932

Wagner, T. J. W., & Eisenman, I. (2015). How climate model complexity influences sea ice stability. *Journal of Climate*, *28*(10), 3998–4014. https://doi.org/10.1175/jcli-d-14-00654.1

Walker, A. P., Hanson, P. J., De Kauwe, M. G., Medlyn, B. E., Zaehle, S., Asao, S., et al. (2014). Comprehensive ecosystem model-data synthesis using multiple data sets at two temperate forest free-air CO_2 enrichment experiments: Model performance at ambient CO_2 concentration. *Journal of Geophysical Research: Biogeosciences*, *119*(5), 937–964. https://doi.org/10.1002/2013JG002553

Walker, X. J., Baltzer, J. L., Cumming, S. G., Day, N. J., Ebert, C., Goetz, S., et al. (2019). Increasing wildfires threaten historic carbon sink of boreal forest soils. *Nature*, *572*(7770), 520–523. https://doi.org/10.1038/s41586-019-1474-y

Wallmann, K., Riedel, M., Hong, W. L., Patton, H., Hubbard, A., Pape, T., et al. (2018). Gas hydrate dissociation off Svalbard induced by isostatic rebound rather than global warming. *Nature Communications*, *9*(1), 83. https://doi.org/10.1038/s41467-017-02550-9

Walsh, J. E., Overland, J. E., Groisman, P. Y., & Rudolf, B. (2011). Ongoing climate change in the Arctic. *Ambio*, *40*(Suppl 1), 6–16. https://doi.org/10.1007/s13280-011-0211-z

Walsh, M. G., De Smalen, A. W., & Mor, S. M. (2018). Climatic influence on anthrax suitability in warming northern latitudes. *Scientific Reports*, *8*(1), 9269. https://doi.org/10.1038/s41598-018-27604-w

Walter Anthony, K., Schneider von Deimling, T., Nitze, I., Frolking, S., Emond, A., Daanen, R., et al. (2018). 21st-century modeled permafrost carbon emissions accelerated by abrupt thaw beneath lakes. *Nature Communications*, *9*(1), 3262. https://doi.org/10.1038/s41467-018-05738-9

Wang, B., Jin, C., & Liu, J. (2020). Understanding future change of global monsoons projected by CMIP6 models. *Journal of Climate*, *33*(15), 6471–6489. https://doi.org/10.1175/JCLI-D-19-0993.1

Wang, B., Jun, I., Socolofsky, S. A., DiMarco, S. F., & Kessler, J. D. (2020). Dynamics of gas bubbles from a submarine hydrocarbon seep within the hydrate stability zone. *Geophysical Research Letters*, *47*(18), e2020GL089256. https://doi.org/10.1029/2020GL089256

Wang, J. A., Baccini, A., Farina, M., Randerson, J. T., & Friedl, M. A. (2021). Disturbance suppresses the aboveground carbon sink in North American boreal forests. *Nature Climate Change*, *11*(5), 435–441. https://doi.org/10.1038/s41558-021-01027-4

Wang, J. A., Sulla-Menashe, D., Woodcock, C. E., Sonnentag, O., Keeling, R. F., & Friedl, M. A. (2019). Extensive land cover change across Arctic–Boreal Northwestern North America from disturbance and climate forcing. *Global Change Biology*, *26*(2), 807–822. https://doi.org/10.1111/gcb.14804

Wang, X., Auler, A. S., Edwards, R. L., Cheng, H., Cristalli, P. S., Smart, P. L., et al. (2004). Wet periods in northeastern Brazil over the past 210 kyr linked to distant climate anomalies. *Nature*, *432*(7018), 740–743. https://doi.org/10.1038/nature03067

Wang, Y., Cheng, H., Edwards, R. L., Kong, X., Shao, X., Chen, S., et al. (2008). Millennial- and orbital-scale changes in the East Asian monsoon over the past 224,000 years. *Nature*, *451*(7182), 1090–1093. https://doi.org/10.1038/nature06692

Wang, Y. J., Cheng, H., Edwards, R. L., An, Z. S., Wu, J. Y., Shen, C.-C., & Dorale, J. A. (2001). A high-resolution absolute-dated late Pleistocene monsoon record from Hulu cave, China. *Science*, *294*(5550), 2345–2348. https://doi.org/10.1126/science.1064618

Way, R. G., Lewkowicz, A. G., & Zhang, Y. (2018). Characteristics and fate of isolated permafrost patches in coastal Labrador, Canada. *Cryosphere*, *12*(8), 2667–2688. https://doi.org/10.5194/tc-12-2667-2018

WCRP Global Sea Level Budget Group. (2018). Global sea-level budget 1993–present. *Earth System Science Data*, *10*(3), 1551–1590. https://doi.org/10.5194/essd-10-1551-2018

Weatherdon, L. V., Magnan, A. K., Rogers, A. D., Sumaila, U. R., & Cheung, W. W. L. (2016). Observed and projected impacts of climate change on marine fisheries, aquaculture, coastal tourism, and human health: An update. *Frontiers in Marine Science*, *3*, 48. https://doi.org/10.3389/fmars.2016.00048

Webster, M. A., Rigor, I. G., Nghiem, S. V., Kurtz, N. T., Farrell, S. L., Perovich, D. K., & Sturm, M. (2014). Interdecadal changes in snow depth on Arctic sea ice. *Journal of Geophysical Research: Oceans*, *119*(8), 5395–5406. https://doi.org/10.1002/2014JC009985

Webster, P. J. (2004). The Elementary Hadley Circulation. In H. F. Diaz & R. S. Bradley (Eds.), *The Hadley circulation: Present, past and future*. https://doi.org/10.1007/978-1-4020-2944-8_2

Weertman, J. (1974). Stability of the junction of an ice sheet and an ice shelf. *Journal of Glaciology*, *13*(67), 3–11. https://doi.org/10.3189/s0022143000023327

Weijer, W., Cheng, W., Drijfhout, S. S., Fedorov, A. V., Hu, A., Jackson, L. C., et al. (2019). Stability of the Atlantic Meridional Overturning Circulation: A review and synthesis. *Journal of Geophysical Research: Oceans*, *124*(8), 5336–5375. https://doi.org/10.1029/2019JC015083

Weijer, W., Cheng, W., Garuba, O. A., Hu, A., & Nadiga, B. T. (2020). CMIP6 models predict significant 21st century decline of the Atlantic meridional overturning circulation. *Geophysical Research Letters*, *47*(12), e2019GL086075. https://doi.org/10.1029/2019GL086075

Wernberg, T., Bennett, S., Babcock, R. C., De Bettignies, T., Cure, K., Depczynski, M., et al. (2015). Climate-driven regime shift of a temperate marine ecosystem. *Science*, *353*(6295), 169–172. https://doi.org/10.1126/science.aad8745

Westbrook, G. K., Thatcher, K. E., Rohling, E. J., Piotrowski, A. M., Pälike, H., Osborne, A. H., et al. (2009). Escape of methane gas from the seabed along the West Spitsbergen continental margin. *Geophysical Research Letters*, *36*(15), L15608. https://doi.org/10.1029/2009GL039191

Wheeler, M. C., & McBride, J. L. (2005). Australian-Indonesian monsoon. In W. K. M. Lau & D. E. Waliser (Eds.), *Intraseasonal variability in the atmosphere-ocean climate system*. https://doi.org/10.1007/3-540-27250-X_5

Wilcox, E. J., Keim, D., de Jong, T., Walker, B., Sonnentag, O., Sniderhan, A. E., et al. (2019). Tundra shrub expansion may amplify permafrost thaw by advancing snowmelt timing. *Arctic Science*, *5*(4), 202–217. https://doi.org/10.1139/as-2018-0028

Wilkerson, J., Dobosy, R., Sayres, D. S., Healy, C., Dumas, E., Baker, B., & Anderson, J. G. (2019). Permafrost nitrous oxide emissions observed on a landscape scale using the airborne eddy-covariance method. *Atmospheric Chemistry and Physics*, *19*(7), 4257–4268. https://doi.org/10.5194/acp-19-4257-2019

Willis, J. K. (2010). Can in situ floats and satellite altimeters detect long-term changes in Atlantic Ocean overturning? *Geophysical Research Letters*, *37*(6). https://doi.org/10.1029/2010GL042372

Winton, M. (2006). Does the Arctic sea ice have a tipping point? *Geophysical Research Letters*, *33*(23), L23504. https://doi.org/10.1029/2006GL028017

Winton, M. (2011). Do climate models underestimate the sensitivity of Northern Hemisphere sea ice cover? *Journal of Climate*, *24*(15), 3924–3934. https://doi.org/10.1175/2011JCLI4146.1

Wise, M. G., Dowdeswell, J. A., Jakobsson, M., & Larter, R. D. (2017). Evidence of marine ice-cliff instability in Pine Island Bay from iceberg-keel plough marks. *Nature*, *550*(7677), 506–510. https://doi.org/10.1038/nature24458

Wisser, D., Marchenko, S., Talbot, J., Treat, C., & Frolking, S. (2011). Soil temperature response to 21st century global warming: The role of and some implications for peat carbon in thawing permafrost soils in North America. *Earth System Dynamics*, *2*(1), 121–138. https://doi.org/10.5194/esd-2-121-2011

Wittmann, A. C., & Pörtner, H.-O. (2013). Sensitivities of extant animal taxa to ocean acidification. *Nature Climate Change*, *3*(11), 995–1001. https://doi.org/10.1038/nclimate1982

Wood, R. (2012). Stratocumulus clouds. *Monthly Weather Review*, *140*(8), 2373–2423. https://doi.org/10.1175/MWR-D-11-00121.1

Woodroffe, C. D., & Webster, J. M. (2014). Coral reefs and sea-level change. *Marine Geology*, *352*, 248–267. https://doi.org/10.1016/j.margeo.2013.12.006

Wotton, B. M., Flannigan, M. D., & Marshall, G. A. (2017). Potential climate change impacts on fire intensity and key wildfire suppression thresholds in Canada. *Environmental Research Letters*, *12*(9), 095003. https://doi.org/10.1088/1748-9326/aa7e6e

Wouters, B., Martin-Español, A., Helm, V., Flament, T., Van Wessem, J. M., Ligtenberg, S. R. M., et al. (2015). Dynamic thinning of glaciers on the Southern Antarctic Peninsula. *Science*, *348*(6237), 899–903. https://doi.org/10.1126/science.aaa5727

Wright, J. S., Fu, R., Worden, J. R., Chakraborty, S., Clinton, N. E., Risi, C., et al. (2017). Rainforest-initiated wet season onset over the southern Amazon. *Proceedings of the National Academy of Sciences of the United States of America*, *114*(32), 8481–8486. https://doi.org/10.1073/pnas.1621516114

Wu, C., Venevsky, S., Sitch, S., Yang, Y., Wang, M., Wang, L., & Gao, Y. (2017). Present-day and future contribution of climate and fires to vegetation composition in the boreal forest of China. *Ecosphere*, *8*(8), e01917. https://doi.org/10.1002/ecs2.1917

Wunderling, N., Donges, J. F., Kurths, J., & Winkelmann, R. (2021). Interacting tipping elements increase risk of climate domino effects under global warming. *Earth System Dynamics*, *12*(2), 601–619. https://doi.org/10.5194/esd-12-601-2021

Wunderling, N., Willeit, M., Donges, J. F., & Winkelmann, R. (2020). Global warming due to loss of large ice masses and Arctic summer sea ice. *Nature Communications*, *11*(1), 5177. https://doi.org/10.1038/s41467-020-18934-3

Wunsch, C. (2005). The total meridional heat flux and its oceanic and atmospheric partition. *Journal of Climate*, *18*(21), 4374–4380. https://doi.org/10.1175/JCLI3539.1

Wyatt, A. S. J., Leichter, J. J., Toth, L. T., Miyajima, T., Aronson, R. B., & Nagata, T. (2020). Heat accumulation on coral reefs mitigated by internal waves. *Nature Geoscience*, *13*(1), 28–34. https://doi.org/10.1038/s41561-019-0486-4

Xie, S.-P., & Saiki, N. (1999). Abrupt onset and slow seasonal evolution of summer monsoon in an idealized GCM simulation. *Journal of the Meteorological Society of Japan. Ser. II*, *77*(4), 949–968. https://doi.org/10.2151/jmsj1965.77.4_949

Yanagiya, K., & Furuya, M. (2020). Post-wildfire surface deformation near Batagay, Eastern Siberia, detected by L-band and C-band InSAR. *Journal of Geophysical Research: Earth Surface*, *125*(7), e2019JF005473. https://doi.org/10.1029/2019JF005473

Yanai, M. (1964). Formation of tropical cyclones. *Reviews of Geophysics*, *2*(2), 367–414. https://doi.org/10.1029/RG002i002p00367

Yeager, S. G., Karspeck, A. R., & Danabasoglu, G. (2015). Predicted slowdown in the rate of Atlantic sea ice loss. *Geophysical Research Letters*, *42*(24), 10704–10713. https://doi.org/10.1002/2015GL065364

Yin, J., & Goddard, P. B. (2013). Oceanic control of sea level rise patterns along the East Coast of the United States. *Geophysical Research Letters*, *40*(20), 5514–5520. https://doi.org/10.1002/2013GL057992

Yin, J., Schlesinger, M. E., & Stouffer, R. J. (2009). Model projections of rapid sea-level rise on the northeast coast of the United States. *Nature Geoscience*, *2*(4), 262–266. https://doi.org/10.1038/ngeo462

Zalles, V., Hansen, M. C., Potapov, P. V., Parker, D., Stehman, S. V., Pickens, A. H., et al. (2021). Rapid expansion of human impact on natural land in South America since 1985. *Science Advances*, *7*(14), eabg1620. https://doi.org/10.1126/sciadv.abg1620

Zatsepina, O. Y., & Buffett, B. A. (1998). Thermodynamic conditions for the stability of gas hydrate in the seafloor. *Journal of Geophysical Research*, *103*(B10), 24127–24139. https://doi.org/10.1029/98jb02137

Zeebe, R. E., Ridgwell, A., & Zachos, J. C. (2016). Anthropogenic carbon release rate unprecedented during the past 66 million years. *Nature Geoscience*, *9*(4), 325–329. https://doi.org/10.1038/ngeo2681

Zeng, N., Dickinson, R. E., & Zeng, X. (1996). Climatic impact of Amazon deforestation—A mechanistic model study. *Journal of Climate*, *9*(4), 859–883. https://doi.org/10.1175/1520-0442(1996)009<0859:CIOADM>2.0.CO;2

Zhang, X., He, J., Zhang, J., Polyakov, I., Gerdes, R., Inoue, J., & Wu, P. (2013). Enhanced poleward moisture transport and amplified northern high-latitude wetting trend. *Nature Climate Change*, *3*(1), 47–51. https://doi.org/10.1038/nclimate1631

Zhao, J., & Johns, W. (2014). Wind-forced interannual variability of the Atlantic meridional overturning circulation at 26.5°N. *Journal of Geophysical Research: Oceans*, *119*(4), 2403–2419. https://doi.org/10.1002/2013JC009407

Zickfeld, K., Knopf, B., Petoukhov, V., & Schellnhuber, H. J. (2005). Is the Indian summer monsoon stable against global change? *Geophysical Research Letters*, *32*(15), L15707. https://doi.org/10.1029/2005GL022771

Zickfeld, K., Solomon, S., & Gilford, D. M. (2017). Centuries of thermal sea-level rise due to anthropogenic emissions of short-lived greenhouse gases. *Proceedings of the National Academy of Sciences of the United States of America*, *114*(4), 657–662. https://doi.org/10.1073/pnas.1612066114

Zolkos, S., & Tank, S. E. (2020). Experimental evidence that permafrost thaw history and mineral composition shape abiotic carbon cycling in thermokarst-affected stream networks. *Frontiers in Earth Science*, *8*, 152. https://doi.org/10.3389/feart.2020.00152

Zou, D., Zhao, L., Sheng, Y., Chen, J., Hu, G., Wu, T., et al. (2017). A new map of permafrost distribution on the Tibetan Plateau. *The Cryosphere*, *11*(6), 2527–2542. https://doi.org/10.5194/tc-11-2527-2017

Zou, S., Lozier, M. S., Li, F., Abernathey, R., & Jackson, L. (2020). Density-compensated overturning in the Labrador Sea. *Nature Geoscience*, *13*(2), 121–126. https://doi.org/10.1038/s41561-019-0517-1